THEORETICAL AND EXPERIMENTAL STUDY OF FLUX SELECTORS

BY

LOUIS-PHILIPPE BOIVIN

SUBMITTED IN PARTIAL FULFILLMENT OF THE

REQUIREMENTS FOR THE DEGREE OF

DOCTOR OF PHILOSOPHY

DEPARTMENT OF PHYSICS

FACULTY OF PURE AND APPLIED SCIENCE

UNIVERSITY OF OTTAWA

OTTAWA, CANADA

1969

ACKNOWLEDGMENTS

The successful completion of this work would not have been possible without the help of many persons. I wish to express my gratitude to my supervisor, Prof. Lansraux, for his constant interest and guidance for the project which he suggested to me. Also, I wish to thank the National Research Council, for authorizing me to use the laboratory facilities, and the members of the Physics Division, for their generous help; in particular, I am grateful for the assistance given to me by the Design Office, the Machine Shop, the Optical Shop, and the Diffraction Optics Section; sincere thanks go to Mr. M. Ranger, who made and assembled most of the equipment used in the experimental part of this work. I want to thank also the staff of the Computation Centre of the University of Ottawa for helpful suggestions. Special thanks go to my father, who has generously taken upon him the task of typing this thesis. I gratefully acknowledge the financial assistance given to me during the past four years by the National Research Council.

STATEMENT OF ORIGINALITY

The author claims originality for the following aspects of the present work:

(1) The introduction and calculation of the amplitude filter $T(x,M)$.

(2) The calculation of the diffraction patterns, encircled energy curves, and modulation transfer functions associated with the amplitude filters $T(x,5)$ and $T(x,M)$ for all the cases studied in chap. 3; the diffraction patterns and encircled energy curves associated with amplitude filter $T(x,5)$, for the cases $\phi(x) = 0$, πx^2, $2\pi x^2$, πx^4, $2\pi x^4$ where calculated independently and earlier by Lansraux, using a different method.

(3) The introduction and calculation of flux selectors 1a-A4-H, 1b-A4-H, 2-A5... series, 1a-B4-H, and those corresponding to all the other types of zone division; calculation of flux selectors 2-A2-H.

(4) The calculation of the diffraction patterns formed by the above flux selectors.

(5) The investigation by means of ray tracing of certain properties of axicons.

(6) The use of photo-etching to make flux selectors.

(7) The production of high-quality flux selectors having a relatively large number of rings.

(8) The approach used in the analysis of the distortion introduced in the image of a plane object by a thin, aberration-free lens.

(9) Certain aspects of the method used for the determination of the thickness of a thin film bounded by air on one side and by an opaque metallic layer on the other.

ABSTRACT

In previous work, Lansraux has studied amplitude filters and the diffraction patterns formed by them: he has restricted his study to aberration-free optical systems, correctly focussed, having rotational symmetry, and in the case of a point source located on the optical axis. In particular, he has determined [7, 18] the pupil transmission T(x,Wm) (= amplitude filter) such that the encircled energy factor for a given normalized radius Wm in the diffraction pattern is an absolute maximum; he has done these calculations for values of Wm from 0 to 10 in steps of .5. The quasi-impossibility of making satisfactory amplitude filters has led Lansraux to introduce flux selectors to replace the former in optical systems: The flux selector consists essentially of a series of alternately light transmitting and opaque concentric annuli (or rings), whose radii are calculated such that the flux selector forms as much as possible the same diffraction pattern as the amplitude filter.

The purpose of our work was to extend the studies done by Lansraux on amplitude filters and flux selectors, and to make improved flux selectors.

We have determined the amplitude filter T(x,M) such that in the range W= 0 to 10, its encircled energy curve is the best approximation, in the least square sense, to the envelope curve for the absolute maxima of the encircled energy factors determined by Lansraux. The pupils T(x,5) and T(x,M) were selected as the most interesting ones for further study.
We have calculated the diffraction patterns formed by these two amplitude filters, their corresponding encircled energy factors and their modulation transfer functions. We have considered the following cases:1)aberration-free optical systems, with and without defect of focus 2) optical systems

having spherical aberration, with and without defect of focus. For comparison purposes, we have done the same calculations for the case of a uniformly transmitting pupil.

Using the T(x,5) amplitude filter, we have made a thorough study of 10 annuli flux selectors in order to select the best type for practical realization. This study has shown that the best flux selector for most purpose is of an equizonal type. We have calculated the 50 zone flux selectors of this type corresponding to the amplitude filters T(x,5) and T(x,M), and then proceeded to the practical realization of these.

In order to do this, we have used a photo-etching process. The latter is described in detail in our work; it essentially involves three steps: the production of a mask (negative); contact printing of this mask onto a lens coated with layers of copper and photo-sensitive emulsion; and finally, developping and etching of the photo resist image.

The masks were produced by photographic reduction of large scale models of the flux selectors. They are accurate to within 1 or 2 microns on the radii of all the rings. The positive reproduction of these masks on the copper-coated lens by means of photoetching are also accurate to within 1 or 2 microns.

A preliminary qualitative experimental study of the effects of these flux selectors in optical systems was made and the results are in good agreement with the theoretical calculations.

TABLE OF CONTENTS

Part A - Theoretical Work

	Page
Introduction	1
I Pupil Transmission $T(x,W_m)$ Maximizing the Encircled Energy Factor for a Given Value of W_m.	4
II Pupil Transmission $T(x,M)$ Optimizing the Encircled Energy Factor for a Given Range of W.	9
III Calculation of the Diffraction Patterns, Encircled Energy Factors, and Modulation Transfer Functions Associated with the Amplitude Filters $T(x,5)$ and $T(x,M)$.	17
Introduction	17
A Method of Calculation	17
B Calculation of Diffraction Patterns	18
C Calculation of Encircled Energy Factors	19
D Calculation of Modulation Transfer Functions	22
E Results	24
F Discussion	26
Conclusions	34
IV Flux Selectors: What They Are, Why They Are Needed, and How They Are Calculated.	35
V Investigation and Comparison of Various Types of Flux Selectors.	42
A Preliminary Remarks	42
B Classification of Flux Selectors	46
C Discussion of the Various Flux Selectors Calculated	48
Conclusions	61

Part B - Experimental Work

	Page
Introduction	65
I Production of the Negative	68
(a) Glass Cone or Axicon Method	70
(b) Photographic Reduction Method	74
(1) Construction of the lucite (plexiglass) model	74
(2) Optical system used for photographic reduction	75
(3) Photographic plates used	78
(4) Light source	79
(5) Measurements on the negatives	82
II Photo-Etching Process	84
(1) Coating the Work with a Metallic Layer	84
(2) Coating the Metallized Surface with Photo-Etching Emulsion	86
(3) Contact Printing	90
(4) Development and Etching of the Photoresist Image	93
III Experimental Work Done with the Flux Selectors	94
References	102
Appendix A - Distortion Introduced in the Image of a Plane Object Formed by a Thin Lens when the Object Is Not Perpendicular to the Optical Axis	103
Appendix B - Channelled Spectrum Formed by a Collimated Beam of White Light Reflected from a Thin Film Bounded on One Side by Air and on the Other by an Opaque Metallic Coating	106
Appendix C - Computer Programs	109
Errata	

PART A - THEORETICAL WORK

Introduction:

Ever since the introduction of lenses and mirrors, scientists have tried to improve the quality of images formed by optical systems. One of the biggest difficulties in such endeavours lies in finding a good criterion of image quality. As a result, there are today many criteria being used, some of these being more suitable for a given problem than others. A short review of the most usual criteria will now be given.

(a) Resolution criterion:

The latter essentially equates the imaging quality of an optical system with its ability to resolve fine details in the object under study. The two best known resolution criteria, that due to Rayleigh[1] and that due to Sparrow[2] , essentially imply the same thing, i.e., that the best optical system is that in which the diffraction pattern corresponding to an ideal point or line has the narrowest central maximum. Much work has been done in order to find hyper-resolving optical systems. It has been found that by modifying the light distribution in the exit pupil of an optical system, improved resolution is possible, but at the cost of a decrease in the amplitude at the center of the diffraction pattern, and an increase in the amplitude of the secondary maxima. (Wilkins 1950[3]). Furthermore, if only non phase changing pupils are to be used, the best that can be done theoretically is an increase in resolution by a factor of 1.6 (Gal'Pern[4] and Wilkins[5]). As a result, such resolution improving techniques are used in practice to obtain gains in resolution of no more than 25% (or less).

(b) Amplitude filtering (Apodisation)

In apodisation, a special case of amplitude filtering, one modifies the light distribution in the exit pupil of an optical system in order to minimize,in the diffraction pattern,the amplitude of the rings relative to the central spot. As a result, the diameter of the central spot is almost invariably increased relative to that in the Airy pattern. The two principal criteria of apodisation which have been used are the maximum encircled energy factor and the minimum spreading factor. The latter is defined as L(W)= ratio of the energy outside a radius W to the intensity on axis in the observation plane. The problem is then to find a pupil function which will minimize L(W). This problem has been studied by P. Jacquinot and Mme B. Roizen-Dossier and Fousse et al[6] . The encircled energy factor, or something close to it, has been considered by several authors. In the form considered by Lansraux, it is defined as follows: E (W) = ratio of energy inside a circle of radius W in the diffraction pattern to the total energy. Lansraux[7] has studied the following problem: For a given value of W, what is the pupil transmission T(x,W) such that E(W) is an absolute maximum? He has solved this problem for various values of W and has shown some very interesting properties of these so-called amplitude filters. He has also introduced the concept of flux selectors, which are grating-like pupils calculated to have the same effect as the amplitude filters, and has calculated a few simple cases.

It was the purpose of the work described in this thesis to comple Lansraux's work along the following lines:

1) To calculate new amplitude filters based on a more general criterion.
2) To investigate fully the effects of the above amplitude filters in optical systems.
3) To investigate the different types of flux selectors possible and to determine the best type.
4) To produce flux selectors and observe their effects in optical systems.

(c) Modulation Transfer Functions (MTF)

In certain problems, the quality of an optical system is assessed from its MTF. In the case of an object incoherently illuminated, the MTF is defined as the Fourier transform of the intensity distribution in the diffraction pattern corresponding to a point source on the optical axis in the object plane. If O represents the illumination in the object, and O' the illumination in the image, then it can be shown that

$$MTF = F[\ O'\ ]\ /\ F[\ O\ ]$$

where F[ ] denotes Fourier transformation. The MTF, F[O], and F[O'] will be functions, in general, of two parameters referred to as spatial frequencies. F[O] is called the spatial frequency spectrum of the object, and F[O'] the spatial frequency spectrum of the image. Thus, the MTF represents how the optical system transmits the object spatial frequencies. Using the MTF as a quality criterion, then, one would define the perfect optical system as one for which the MTF is unity (or a constant) for all spatial frequencies. However, MTF studies have shown, for example, that:

1) Although the spatial frequency spectrum of an object can be infinite, that of the image is always limited, and the limit frequency, which can be associated with the resolving power of the optical system, depends only on the contour of the pupil and not on its light distribution.
2) Apodising pupils generally increase the MTF for low frequencies, while decreasing it for high frequencies.
3) Resolution-improving pupils have the opposite effect to the above.

It is difficult to state what type of MTFis best in practice, because this depends very much on the type of object under study.

CHAPTER I

PUPIL TRANSMISSION T(x,Wm) MAXIMIZING THE ENCIRCLED ENERGY FACTOR FOR A GIVEN VALUE OF Wm.

A summary of the theoretical study done by Lansraux on the problem of amplitude filters will now be given. This theoretical study has been the basis of our work.

Let us consider a monochromatic point source P on the optical axis z of a lens (Fig A1-1). Let Q be the conjugate point of P.

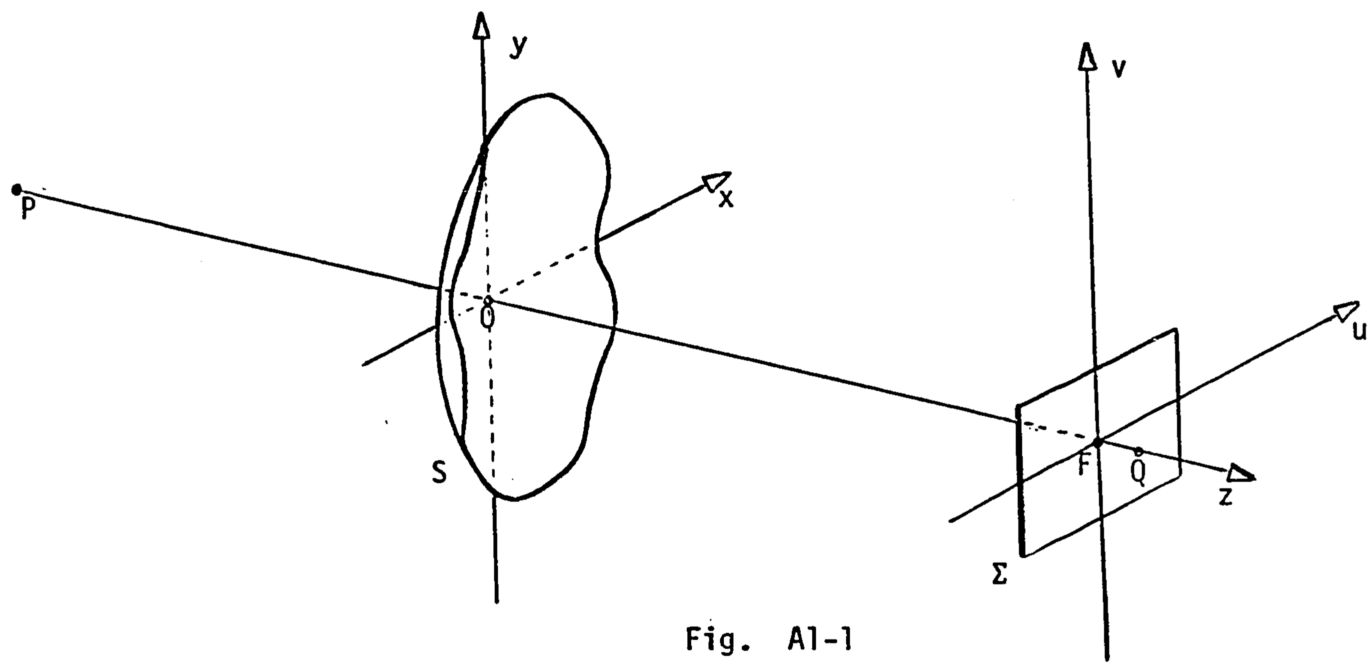

Fig. A1-1

Let Ω be the wavefront emerging from the exit pupil, and intersecting the axis at point O. Ω is spherical only when the optical system is aberration-free and when amplitude filtering does not introduce a non-uniform phase. In the general case, theseconditions are not met, but Ω is nonetheless almost spherical; let S be a spherical surface through O with which Ω almost coincides and which has its center of curvature at a point F. S is called a sphere of reference. Consider a plane of observation Σ normal to axis z at pt F. Introduce cartesian coord. systems (x,y) and (u,v) normal to z at O and F resp. Then, it can be shown[8] that the complex amplitude at a point (u,v) of Σ is given by:

$$\text{A1-1} \quad g(u,v) = M \iint_S T(x,y) e^{i\phi(x,y)} e^{-i2\pi n(ux+vy)/\lambda OF} \, dxdy$$

where M= normalization constant, λ = wavelength of light (in vacuum), n= refractive index

T (x,y) represents the pupil transmission or amplitude filtering

$\phi(x,y) = \psi(x,y) + \tau(x,y) + \alpha(x^2+y^2)$ in which $\psi(x,y)$ represents the lens aberration, $\tau(x,y)$ " the phase associated with amplitude filtering, $\alpha(x^2+y^2)$ " the defect of focus $[\alpha = \pi n(1/OF - 1/OQ)/\lambda]$

We now make the following co-ordinate transformation: $X = x\sqrt{n/\lambda OF}$.

$Y = y\sqrt{n/\lambda OF}$, $U = u\sqrt{n/\lambda \cdot OF}$, $V = v\sqrt{n/\lambda \cdot OF}$, so that A1-1 becomes

$$\text{A1-2} \quad g'(U,V) = M' \iint_{S'} T'(X,Y) e^{i\phi'(X,Y)} e^{-i2\pi(UX+VY)} \, dXdY$$

We shall limit our studies to systems having rotational symmetry about the optical axis; i.e., if we change to polar co-ordinates and put $X = r\cos\theta$, $Y = r\sin\theta$, $U = \rho\cos\phi$, $V = \rho\sin\phi$, then A1-2 becomes:

$$g''(\rho) = M' \int_0^R r\, T''(r) e^{i\phi''(r)} \int_0^{2\pi} e^{-i2\pi r\rho\cos(\theta-\phi)} \, d\theta dr$$

where R is the radius of the edge of the exit pupil. Now,

$$\int_0^{2\pi} e^{-i2\pi r\rho\cos(\theta-\phi)} \, d\theta = 2\pi Jo(2\pi r\rho). \quad \text{Therefore,}$$

$$g''(\rho) = 2\pi M' \int_0^R r\, T''(r)\, e^{i\phi''(r)} Jo(2\pi r\rho)\, dr$$

Making again a co-ordinate transformation, we put $x=r/R$ $W=2\pi R\rho$; from now on, only these parameters will be used since they are valid for all pupils. We have then $g'''(W) = \pi R^2 M' \int_0^1 T'''(x)e^{i\phi'''(x)} Jo(Wx)dx^2$

Putting $g'''(W) = A(W)$, re-defining the constant M, and dropping the primes for convenience on T''' and ϕ''' , we have

A1-3 $A(W) = M\int_0^1 T(x)\, e^{i\phi(x)}\, Jo(Wx)\, dx^2$ for an optical system having rotational symmetry. If $T(x) \equiv 1$, and if $\phi(x) \equiv 0$, then A1-3 becomes

$$A(W) = M\int_0^1 Jo(Wx)\, dx^2 = 2MJ_1(W)/W$$

, and if we put M=1 for unit amplitude at the center of the diffraction pattern, we have the well-known Airy pattern: $A(W)= 2\,J_1(W)/W$ A1-4 . See Fig. A5-1

The problem of determining the type of function T(x) such that the diffraction pattern is improved according to some criterion has been dealt with by many authors. P. Jacquinot and B. Roizen-Dossier[6] have given an excellent review of the work done on this subject and the reader is referred to that paper for a comparison of the various approaches to the problem as well as their relative merits. Lansraux has chosen as criterion of image quality the encircled energy factor: the latter is defined as the ratio of the amount of energy inside a circle of "radius" W(centered on optical axis) to the total amount of energy in the diffraction pattern. Analytically this can be written:

A1-5 $$E(W) = \int_0^W I(W)\, d(W^2) \Big/ \int_0^\infty I(W)d(W^2)$$

Where $I(W)=|A(W)|^2$

For certain values of Wm selected a-priori, Lansraux has determined the functions T(x,Wm) which make E(Wm) an absolute maximum, in the case of an aberration free optical system correctly focussed. The method of calculation is outlined below.

Lansraux has shown that any pupil transmission making E(W) an absolute extremum must be real[7]. Hence, $\tau(x)$ is zero. Also, Lansraux has shown that any pupil T(x) can be expressed as a Taylor expansion in $1-x^2$ of the form

$$T(x) = \sum_{p=1}^{\infty} pk_p(1-x^2)^{p-1}$$

Lansraux has also shown that finite expansions (n terms) may be used. Expressing T(x) in the form

A1-6 $$T(x) = \sum_{p=1}^{n} pk_p^n(1-x^2)^{p-1}$$

, E(W) becomes, by substitution of A1-6 and A1-3 into A1-5

$$E_n(W) = \sum_{p=1}^{n}\sum_{q=1}^{n} k_p^n\, k_q^n\, a_p^q(W) \Big/ \sum_{p=1}^{n}\sum_{q=1}^{n} k_p^n\, k_q^n\, a_p^q(\infty)$$

where $a_p^q = \int_0^W L_p(W)L_q(W)\, d(W^2)$ and L_k is defined by $L_k(W) = 2^k k!\, J_k(W) / W^k$

The coefficients k_p^n are determined by requiring that all the $\partial E_n(W)/\partial k_p^n$ be zero for an extremum. The above conditions yield an homogeneous system of linear equations; the determinant Δ of this system must be zero in order that a non-trivial solution exist. This determinant is an n^{th} degree polynomial in $E_n(w)$ and involves only the numbers a_p^q; whence, the values of $E_n(W)$ satisfying the equation $\Delta=0$ can be determined; the largest of these roots is chosen as the appropiate one. Then, going back to the system of equation, the coefficients k_p^n can be determined; Lansraux performed the above calculations for different values of Wm, and, in each case, for several orders n. After having studied the results, he has reached the following conclusions:

(1) The function $T(x,Wm)$ corresponding to $W=5$ gives the best diffraction pattern for general purposes.

(2) For that particular function, the expansion of order 10 is the one which can be calculated most accurately (with the computer (I.B.M. 1620) used in performing the calculations). Note: Although theoretically the higher the order, the more accurate the results, it is found that in practice, because of cumulative errors introduced in making the calculations with a computer, the accuracy deteriorates with increasing n beyond a certain order n_c (10 here).

Consequently, the function $T(x,5)$ calculated for $n=n_c=10$ was selected for our work. The coefficients k_p^{10} are known to about 12 significant figures. Fig. A1-2 shows the variation of $T(x,5)$ with x. The diffraction pattern formed by $T(x,5)$ is given in Figures A3-1 and A5-2. (The calculation of this diffraction pattern will be considered below.)

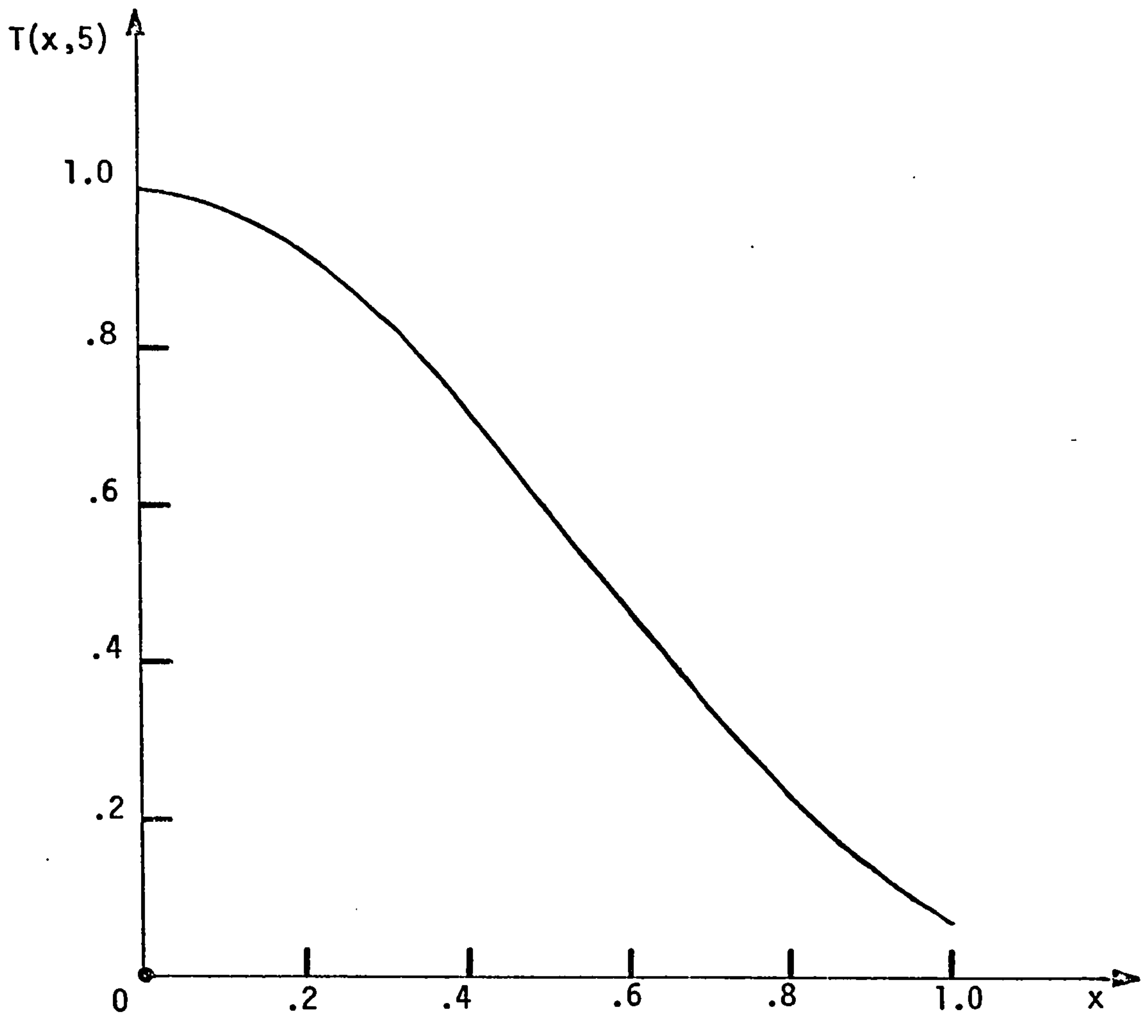

Fig. A1-2 Curve of normalized amplitude T(x,5)

$$T(x,5) = \sum_{1}^{10} pk_p(1 - x^2)^{p-1} \text{ , where}$$

$k_1 = 0.06824715$ $\quad$ $k_2 = 0.14641643$

$k_3 = 0.11796662$ $\quad$ $k_4 = 0.05032501$

$k_5 = 0.01334284$ $\quad$ $k_6 = 0.00241714$

$k_7 = 0.00031704$ $\quad$ $k_8 = 0.00003288$

$k_9 = 0.00000198$ $\quad$ $k_{10} = 0.00000029$

CHAPTER II

PUPIL TRANSMISSION T(x,M) OPTIMIZING THE ENCIRCLED ENERGY FACTOR FOR A GIVEN RANGE OF W.

In the preceding chapter, we have considered the following problem: what is the pupil transmission T(x,Wm) which, for a given value of Wm, yields the absolute maximum encircled energy factor Em(Wm). We denote by E(W,Wm) the encircled energy curve associated with T(x,Wm); hence, E(Wm,Wm) = Em(Wm). The envelope M(W) to the curves E(W,Wm) is the locus of the extrema E(Wm,Wm); it represents, in the context of encircled energy factors, the limit of performance of optical systems[7]. In this chapter, we shall study the following problem: consider a finite interval ΔW in the image plane. What is the pupil transmission T(x,M) whose encircled energycurve E(W) is "closest", in the interval ΔW, to the envelope curve M(W)? We must first define what we mean by one curve being the "closest" one to another curve: consider the sum

$$\text{A2-1} \qquad S= \sum_{i=o}^{m} [M(Wi) - E(Wi)]^{\ell} = \sum_{i=o}^{m} D^{\ell}$$

where the sum is evaluated for m equidistant points in the interval ΔW. Then, for a given m and ℓ, the curve, represented by the function E(W), for which S is a minimum is the closest (or best approximation) to M(W) in the interval ΔW. We have chosen to minimize the sum of D^{ℓ} at discrete points inside ΔW rather than minimize the integral of D^{ℓ} over ΔW because M(W) is known only at certain discrete values of W, and because this considerable simplifies the mathematics. For the same reasons, we have chosen the interval ΔW to be the closed interval 0 to 10 (the values of M(W) being unknown beyond that). The values of Wi chosen were the values

0 to 10 in steps of 1. The choice of ℓ is not so easy to make. Suppose T(x), hence E(W), is defined in terms of n variables k_j^n, as in the preceding chapter; i.e.,

$$T(x) = \sum_{p=1}^{n} p k_p^n (1-x^2)^{p-1}$$

Then, the requirement for minimizing S is

$$\frac{\partial S}{\partial k_j^n} = 0 \qquad j=1,n$$

or

$$\text{A2-2} \quad \sum_{i=o}^{m} - \ell \, [M(Wi) - E(Wi)]^{\ell-1} \; \frac{\partial E(Wi)}{\partial k_j^n} = 0$$

If we choose $\ell = 1$, then this reduces to

$$\sum_{i=o}^{m} \frac{\partial E(Wi)}{\partial k_j^n} = 0 \qquad j = 1, n$$

This can be expressed as a set of homogeneous linear equations involving the n parameters k_j^n and the sum Σ E(Wi), and can be solved directly for these unknowns, as in the preceding chapter. We see, however, that the solution is independent of the values M(Wi): This is not satisfactory from the theoretical point of view, and because of this, we have decided not to consider the case $\ell = 1$.

The case $\ell = 2$ is the classical least square approximation case. Although the cases for $\ell \geqslant 3$ are also acceptable mathematically (since $M(Wi) - E(Wi) \geqslant 0$), they were not considered because they are much more complicated to solve, and also, they give too much weight to the terms in A2-1 corresponding to small values of W.

We wish, therefore, to find a set of parameters $\{ k_j^n \}$ such that

A2-3 $$S(\{k_j^n\}) = \sum_{i=1}^{m} [M(Wi) - E(\{ k_j^n \},Wi)]^2$$

(Wi = 0 to 10 in steps of 1)

is a minimum. We shall determine the solution for $n = 5$. Henceforth, we shall drop the "n" superscript on k_j^n in order to avoid confusion. Requirement A2-2 for a minimum gives:

A2-4 $$\frac{\partial S}{\partial k_j} = \sum_{i=1}^{m} [M(Wi) - E(\{ k_j\} , Wi)] \frac{\partial E}{\partial k_j} = 0$$

$j = 1, n$

From the preceding chapter, we have

A2-5 $$E(\{k_j\} , Wi) = \frac{\sum_{p=1}^{n} \sum_{q=1}^{n} k_p \; k_q \; a_p^q \; (Wi)}{\sum_{p=1}^{n} \sum_{q=1}^{n} k_p \; k_q \; a_p^q \; (\infty)}$$

from which:

A2-6 $$\frac{\partial E}{\partial k_j} = \frac{2 \sum_{q=1}^{n} k_q \; [a_j^q (Wi) - E(\{k_j\} , Wi) \; a_j^q (\infty)]}{\sum_{p=1}^{n} \sum_{q=1}^{n} k_p \; k_q \; a_p^q \; (\infty)}$$

Substituting both of these expressions in A2-4 gives a very complicated set of simultaneous non-linear equations. Rather than attempt an analytical solution, we have preferred to use numerical methods on an IBM computer.

One method of solution considered was the following: S, as given by A2-3, is a function of 5 independent variables k_j; at the minimum point,

$$\text{A2-7} \qquad \frac{\partial S}{\partial k_j} = 0 \quad \text{for all } j .$$

Let us denote by $\{\bar{k}_j\}$ the values of k_j corresponding to the minimum. A2-7 implies that if we allow S to vary about the minimum position with respect to only one parameter k_j, we shall obtain a minimum for the value $k_j = \bar{k}_j$, this being the case for all the parameters in the group. Suppose now that we have a series of parameters $\{ {}^{o}k_j \}$ not equal to the $\{\bar{k}_j\}$, and that we allow S to vary with respect to, say, the first of these, ${}^{o}k_1$. If the $\{{}^{o}k_j\}$ are sufficiently close to the $\{\bar{k}_j\}$, we can expect S to obtain its minimum value for a value of ${}^{1}k_1$ which is closer to $\bar{k}_1$ than ${}^{o}k_1$ was. We have

$$S({}^{1}k_1 , {}^{o}k_2 \ldots\ldots) < S({}^{o}k_1 , {}^{o}k_2 , \ldots\ldots)$$

so that the series of parameters ${}^{1}k_1$, ${}^{o}k_2$, ...
is closer to the $\{ \bar{k}_j \}$ than the $\{ {}^{o}k_j \}$ series; then, we replace ${}^{o}k_1$ by ${}^{1}k_1$, and repeat the variation process with respect to ${}^{o}k_2$, until we find a ${}^{1}k_2$ such that S is a minimum, replace ${}^{o}k_2$ by ${}^{1}k_2$, and continue the process for the other 3 parameters, after which the procedure is re-initiated with ${}^{1}k_1$. If this iterative procedure converges, one should reach a point where no further change is produced in the parameters with successive iterations. In order to accelerate convergence, the $\{{}^{o}k_j\}$ were chosen as follows: Consider the sum S for the two points W=0 and 1. The function T(x) which minimizes this sum must be close to the function T(x, .5) which yields the absolute maximum value of E(.5) for W= .5. This function T(x, .5)

has been calculated by Lansraux[7]. Its parameters should therefore be a good initial choice for the solution of the above problem for W=0 and 1. Once this problem has been solved, using the method outlined above, its solution serves as a good approximate solution to the problem of minimizing S for W = 0, 1 and 2. This procedure is repeated, increasing W by 1 each time, until the desired solution for the interval W = 0 to 10 is obtained.

This method was tried out, and the convergence was found to be very slow; for example, in the case W = 0 to 10, after 400 iterations (when S reached the value 2.9429×10^{-3}), convergence was not yet achieved since S changed by 10^{-7} from one iteration to the next (whereas it would have to change by less than 10^{-16} for termination of the iterations, where 10^{-16} represents about the ultimate precision of the computer).

Another method was sought which would converge faster than the above method. Fletcher and Powell[9] have described a rapid descent method for minimization of a function of several variables for which the gradient can be computed for any value of the variables. This method is incorporated in a subroutine available in the IBM program library. The user must provide a subroutine which calculates the function value and the gradient vector for any value of the variables: The subroutine which we have prepared determines S and $\frac{\partial S}{\partial K_j}$ (equations A2-3 and A2-4).

$E(W)$ and $\frac{\partial E(W)}{\partial k_j}$ are calculated from equations A2-5 and A2-6.

The $a_p^q(\infty)$, $a_p^q(W)$ and $M(W)$ have been calculated by Lansraux (unpublished work) to a high degree of precision (≃ 22 significant digits). When the IBM subroutine is used, it is necessary to provide an estimate of the minimum function value, as well as an initial choice for the parameters k_j. We have not used the results of the preceding method as input data to this second method in order to have a completely independent solution. However, we have proceeded as we did for the first method, starting with a minimization of S for W = 0 and 1, and increasing W by 1 at each step until the required minimization of S for W = 0 to 10 was achieved. The calculations using this second method converge rapidly, and less than 400 iterations were required in each case. The precision in the minimum values of S is about $\pm 10^{-16}$. For the solution we are interested in, ie, the case W = 0 to 10, the value of S found was $2.94288... \times 10^{-3}$ The precision in the parameters $\overline{k}_j$ of the function T(x) (≡ T(x,M)) is about $\pm 10^{-10}$ in absolute value. Consequently, since

A2-8 $$T(x,M) = \sum_{p=1}^{5} p\,\overline{k}_p\,(1-x^2)^{p-1}$$

the maximum error in T(x,M) due to errors in the parameters $\overline{k}_p$ is

$$\Delta T_{max} \leqslant \left\{ \Sigma \left|\frac{\partial T}{\partial \overline{k}_p}\right| \left| \Delta \overline{k}_p \right| \right\}_{x=o}$$

$$\Delta T_{max} \leqslant \sum_{p=1}^{5} p \left| \Delta \overline{k}_p \right| < 5\, \Sigma \left| \Delta \overline{k}_p \right|$$

ie $\Delta T_{max} < 2.5 \times 10^{-9}$

Hence, we quote $\pm 10^{-8}$ as a very safe error limit on the function T(x,M) calculated.

When we compare the solutions produced by the two methods, we find that they agree with each other: the results of the first method would probably be equal to those of the second if the number of iterations was greatly increased: for example, the solutions minimizing S over the W intervals (0,1) , (0,2), etc..., and (0,10) by the first method agree to about 5 significant digits (in the value of S) in all cases with those produced by the second method, and the functions T(x) corresponding to each case are the same, within 1% max error, for both methods.

Thus, we can conclude that the two methods give the same solution, but the second method converges much faster. Since these two completely independent methods appear to converge, in all cases considered, to the same solution, we conclude that there is only one solution for a given set of points W.

CONCLUSIONS

In this chapter, we have solved the problem of finding a pupil function T(x,M) whose encircled energy curve minimizes the sum

$$S = \sum_{i=1}^{m} [M(W_i) - E(W_i)]^2$$

for the values W = 0 to 10 in steps of 1, and where $M(W_i)$ is the absolute maximum encircled energy factor for $W=W_i$. (See fig. A2-1 for the results of the calculations: the parameters $\overline{K}_j$, and the graph representing T(x,M).)

We have supposed T(x,M) to be a real function of the type defined by equa. A2-8. This raises two questions:

1) could there exist a complex function T(x) which would be a better solution than the real T(x,M) ?

2) in the case of a real $T(x,M)$, the $n=5$ solution is an approximation to the limit solution when $n \to \infty$; is this approximation good ?

The answer to question 1) is not as easy to determine as it was in the case of maximizing $E(W)$ for a given W: in that case, it has been shown that[7] in order to have an absolute maximum $E(W)$, $T(x)$ must be real; for a small interval of W, we could use the same argument as in the above to show that the solution must be a real $T(x,M)$; however, for an extended interval of W, as we have used, this is not obvious, although it seems very probable. In our work, we are not concerned with complex pupils, since these are more difficult to realize in practice, so that this problem is not important to us at the present.

In order to answer question 2), one would have to solve the problem for higher values of n. We shall do this at a later date. However, for the present, we can make the following observations: The function $T(x,M)$ which we have determined is very similar to the function $T(x,3.5)$ which optimizes the encircled energy factor for $W = 3.5$[7], and which Lansraux has determined for various values of n. He has shown that the solution $T(x,3.5)$ (and the other $T(x,W_m)$ as well) for $n = 5$ are very close to the limit solutions when $n \to \infty$. Since the problem we have considered is similar to the one considered by Lansraux, and since the solution to our problem is indeed very close to one of the pupils calculated by him, we expect that our solution for $n = 5$ is a good approximation to the limit solution as $n \to \infty$.

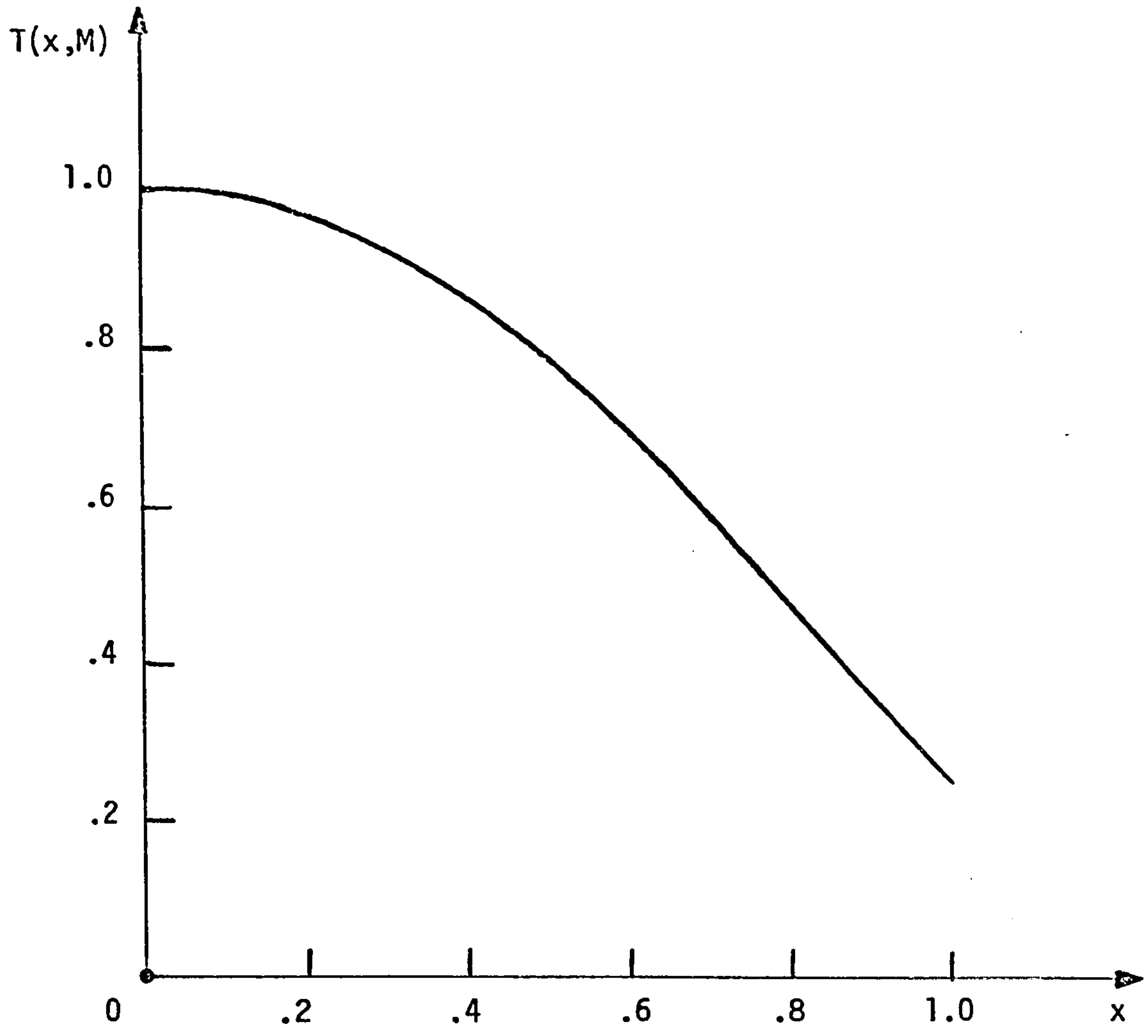

Fig. A2-1 Curve of normalized amplitude T(x,M)

$$T(x,M) = \sum_{1}^{5} pk_p(1 - x^2)^{p-1} \text{ ,where}$$

$k_1 = 0.24562193$ $k_2 = 0.22997469$

$k_3 = 0.17294407$ $k_4 = -0.0531986$

$k_5 = -0.00232175$

CHAPTER III

CALCULATION OF THE DIFFRACTION PATTERNS, ENCIRCLED ENERGY FACTORS, AND MODULATION TRANSFER FUNCTIONS ASSOCIATED WITH AMPLITUDE FILTERS T(x,5) AND T(x,M).

INTRODUCTION:

In this chapter, we shall compare the diffraction patterns and encircled energy factors corresponding to the different amplitude filters discussed in the preceding chapters with those corresponding to a uniformly transmitting pupil. We shall consider the following cases:

1) aberration-free optical systems, correctly focussed;
2) aberration-free optical systems, with defect of focus;
3) optical systems with spherical aberration of the 3rd order and defect of focus.

In view of the importance modulation transfer functions have taken in certain methods of image assessments, we shall also give the transfer functions corresponding to the above cases.

A- METHOD OF CALCULATION:

All the calculations in this chapter have made use of Gauss's method of numerical integration. Since this method is well known, it willnot be described here. For information, one can refer to Berezin and Zhidkov's book on computing methods[10].

Suppose the integral to be evaluated is

$$\int_a^b f(x)\,dx$$

First, the transformation of variables from x to x' given by

$$x = \left(\frac{b-a}{2}\right) x' + \frac{a+b}{2} \qquad \text{A3-1}$$

is done to change the range of integration from (a,b) to (-1, 1); the integral above becomes

$$\left(\frac{b-a}{2}\right)\int_{-1}^{+1} f'(x')\,dx'$$

Applying Gauss's method, this integral is approximated as follows:-

A3-2 $$\int_{-1}^{+1} f'(x')\,dx' \approx \sum_{i=1}^{n} C_i\ f'(y_i)$$

where the weights C_i and the abscissae y_i (which are the roots of Legendre's polynomial of degree n) are known and can be obtained from tables. Gauss's method was used because of its great accuracy (for a given n) compared to other common integration methods. It can be shown[10], for example, that exact results will be obtained for an arbitrary polynomial integrand of any degree up to 2n-1.

B- CALCULATION OF DIFFRACTION PATTERNS:

From chapter 1, the amplitude in the diffraction pattern formed by a pupil T(x) is

A3-3 $$A(W) = M\int_0^1 T(x)e^{i\phi(x)}\ Jo(Wx)\ dx^2$$

where T(x) is real, and where all phase terms (defect of focus, aberrations) are included in $\phi(x)$. M is a normalization constant: in order to compare the diffraction patterns corresponding to different functions T(x), we normalize A(W) so that A(o) = 1 when $\phi(x) = 0$; the constant M is then

A3-4 $$M = 1 \Big/ 2\int_0^1 x\,T(x)\,dx$$

Re-writing A3-3 in a form suitable for the application of Gauss's method, we have

$$\text{A3-5}\quad A(W)=\frac{M}{2}\int_{-1}^{+1}(u+1)T\left(\frac{u+1}{2}\right)\cos\,\phi\left(\frac{u+1}{2}\right)Jo\left[W\frac{(u+1)}{2}\right]du$$

$$+\frac{Mi}{2}\int_{-1}^{+1}(u+1)T\left(\frac{u+1}{2}\right)\sin\phi\left(\frac{u+1}{2}\right)Jo\left[W\frac{(u+1)}{2}\right]du$$

$$=\frac{M}{2}\sum_{i=1}^{n}C_i\,(y_i+1)T\left(\frac{y_i+1}{2}\right)\cos\phi\left(\frac{y_i+1}{2}\right)Jo\left[W\frac{(y_i+1)}{2}\right]$$

$$+\frac{Mi}{2}\sum C_i\,(y_i+1)T\left(\frac{y_i+1}{2}\right)\sin\phi\left(\frac{y_i+1}{2}\right)Jo\left[W\frac{(y_i+1)}{2}\right]\qquad\text{,and}$$

$$\text{A3-6}\quad M = 1\Big/\frac{1}{2}\sum_{i=1}^{n}C_i\;(y_i+1)\;T\left(\frac{y_i+1}{2}\right)$$

The values of C_i and y_i are obtained from tables. An IBM 360 computer was used to perform the calculations. A value of n = 24 was selected in order to have an accuracy of about $\pm 10^{-7}$ in calculations. The functions cos and sin are calculated by means of built-in subroutines in the computer. The functions T(x) which we have considered are easy to calculate since they are obtained (see chapters 1 and 2) in a polynomial form. The function Jo was calculated by means of a subroutine which we have developped and the method of this calculation will be described later in chapter 5. To determine the accuracy of the calculations, the latter were repeated in several cases for n = 16. It was found that these values differed from those of the n = 24 case by less than 10^{-7}. As a result, we can quote this value as a reasonable measure of accuracy.

C- CALCULATION OF ENCIRCLED ENERGY FACTORS:

The encircled energy factor is defined as

$$\text{A3-7}\quad E(W) = \frac{\int_0^W |A(W)|^2 dW^2}{\int_0^\infty |A(W)|^2 dW^2}$$

The denominator can be evaluated by making use of Plancherel's theorem

$$\int_0^\infty |A(W)|^2 \, dW^2 = 4\int_0^1 |T(x)|^2 \, dx^2$$

This relationship is a mathematical expression of the principle of conservation of energy. For evaluation by Gauss' method, we re-write the above as

$$\int_0^\infty |A(W)|^2 \, dW^2 = 2 \sum_{i=1}^{n} C_i \, (y_i+1) \, T^2 \, \frac{(y_i+1)}{2}$$

REMARK:

The factor 4 in the above relationship results from the type of normalization of the functions T(x) and A(W): here, in order to simplify the calculations, the normalization constant M in A3-3 is put equal to 1. With this choice of M, the factor 4 in the conservation of energy relationship above is valid for any pupil T(x); in particular it is valid for $T(x)\equiv 1$. This can easily be verified as follows: From A3-3, we have $A(W) = 2J_1(W) / W$ so that the l.h.s. of the relationship gives[11]

$$\int_0^\infty |A(W)|^2 \, dW^2 = 4 \, [Jo^2(W)+J_1{}^2(W)]_0^\infty = 4$$

On the other hand, the r.h.s. gives

$$4\int_0^1 T^2 \, (x) \, dx^2 = 4\int_0^1 dx^2 = 4 \,, \quad \text{which}$$

agrees with the l.h.s.

The numerator in A3-7 can be written

$$2\int_0^W W\left[\int_0^1 T(u)e^{i\phi(u)} Jo(Wu)du^2\right]\left[\int_0^1 T(v)e^{-i\phi(v)} Jo(Wv)dv^2\right] dW$$

$$= 8\int_0^W\int_0^1\int_0^1 uvT(u)T(v)e^{i[\phi(u)-\phi(v)]}Jo(Wu)Jo(Wv)WdudvdW \quad \text{A3-8}$$

This integral can be decomposed into a real part and an imaginary part; the latter one is equal to zero by reason of symmetry. Consequently, the integral reduces to:

$$8\int_0^W\int_0^1\int_0^1 uvT(u)T(v)\cos[\phi(u)-\phi(v)]WJo(Wu)Jo(Wv)du\,dv\,dW$$

$$= 8\int_0^1\int_0^1 uv\,T(u)T(v)\cos[\phi(u)-\phi(v)]\int_0^W WJo(Wu)Jo(Wv)dW$$

The inner integral involving W is a well-known Lommel integral whose value is

$$\frac{W}{u^2-v^2}[\,u\,Jo(Wv)\,J_1(Wu) - vJo(Wu)J_1(Wv)]$$

Therefore, the numerator can be re-written for evaluation by Gauss's method:-

A3-9

$$W\sum_{j=1}^{m}\sum_{i=1}^{n} C_i\,C_j\,(y_i+1)(y_j+1)\,T\left(\frac{y_i+1}{2}\right)T\left(\frac{y_j+1}{2}\right)\cos\left[\phi\left(\frac{y_i+1}{2}\right)-\phi\left(\frac{y_j+1}{2}\right)\right]\left[(y_i+1)Jo\left[W\frac{(y_j+1)}{2}\right]J_1\left[W\frac{(y_i+1)}{2}\right]-(y_j+1)Jo\left[W\frac{(y_i+1)}{2}\right]J_1\left[W\frac{(y_j+1)}{2}\right]\right]\Bigg/(y_i+1)^2-(y_j+1)^2$$

The calculations were done on an IBM 360. n and m were chosen to be 24 and 16 resp. (They were chose different to avoid the possibility of getting a zero denominator in A3-9.) The accuracy was checked as before and the max. error found to be about 10^{-7} at $W = 25$.

D- CALCULATION OF MODULATION TRANSFER FUNCTIONS-

If one is dealing with pupils having rotational symmetry about the optical axis, then the modulation transfer function (MTF), which we shall denote by G, will be a function of only one parameter, which we shall call s (for spatial frequency). Furthermore, it can be shown that[12]

$$\text{A3-10} \qquad G(s) = \iint_A T(r)e^{i\phi(r)}\left[T(r')e^{i\phi(r')}\right]^* r\,dr\,d\theta$$

where $r'^2 = r^2 + s^2 - 2sr\cos\theta$

The diagram below explains the symbols.

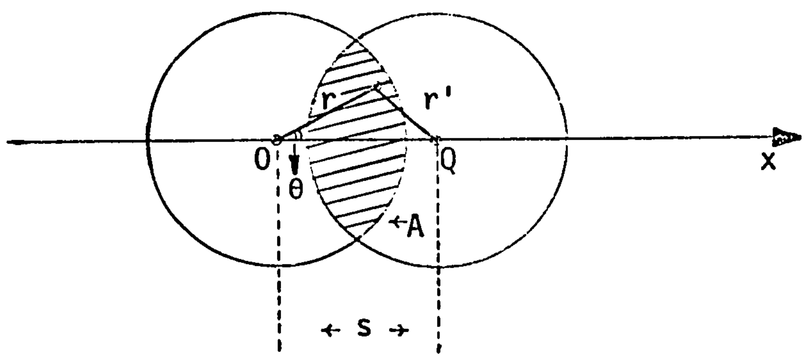

G(s) is the convolution of the pupil $T(r)e^{i\phi(r)}$ with its complex conjugate $\left[T(r')e^{i\phi(r')}\right]^*$, shifted a distance s along the x-axis. Since T(r) is real, A3-10 can be re-written as

$$\iint_A T(r)T(r')e^{i[\phi(r)-\phi(r')]}\,r\,dr\,d\theta = \iint_A T(r)T(r')\cos[\phi(r)-\phi(r')]\,r\,dr\,d\theta$$

$$+i\iint_A T(r)T(r')\sin[\phi(r)-\phi(r')]\,r\,dr\,d\theta$$

For reasons of symmetry, the imaginary part of the above integral vanishes, and the real part can be re-written as an integral over the first quadrant A' of the common area of the two pupils T(r) and T(r'). Thus, we have

A3-11 $$G(s) = 4\iint_{A'} T(r)T(r')\cos[\phi(r) - \phi(r')]\, r\,dr\,d\theta$$

The limits of integration are $(0, \cos^{-1}\frac{s}{2r})$ for θ (inner integral) and $(s/2\ ,\ 1)$ for r. Since inverse cosines are not easily calculated by a computer, the inner integral is modified by the transformation of variables $\cos\theta = u$: A3-11 then becomes

A3-12 $$G(s) = 4\int_{s/2}^{1} rT(r)\left[\int_{s/2r}^{1} \frac{T(r')\cos[\phi(r) - \phi(r')]}{\sqrt{1-u^2}}\,du\right]dr$$

with $r'^2 = r^2 + s^2 - 2sru.$

This integral is to be evaluated by Gauss's method, and hence must be further transformed in order to have the proper limits:

A3-13

$$G(s) = \frac{(2-s)^2}{8}\int_{-1}^{1} (x+1)T(r)\left[\int_{-1}^{1} \frac{T(r')\cos[\phi(r) - \phi(r')]}{\sqrt{1-u^2}}\,dy\right]dx$$

where
$$r = \frac{(2-s)x}{4} + \frac{2+s}{4}$$
$$u = \frac{(2r-s)y}{4r} + \frac{2r+s}{4r}$$
$$r'^2 = r^2+s^2 - 2sru$$

Hence, the integral can be directly calculated by Gauss' method. Note that s can take values from 0 to 2 inclusively. Beyond $s = 2$, $G(s) \equiv 0$. The calculations were done on the IBM 360. The accuracy was checked as before, and the max. error found to be about $\pm.001$.

E - RESULTS

The cases studied were the following:

1) aberration-free optical systems, correctly focussed: $\phi(x)=0$

2) aberration-free optical systems, with defect of focus:

$\phi(x) = \pi/2\ x^2\ ,\ \pi x^2\ ,\ 3\pi/2\ x^2\ ,\ 2\pi x^2$

3) optical systems with spherical aberration and defect of focus: $\phi(x)=$

πx^4	
$\pi x^4 - \pi/2\ x^2$	(diffraction patterns only)
$\pi x^4 - \pi\ x^2$	
$\pi x^4 - 3\pi/2\ x^2$	(" " ")
$\pi x^4 - 2\pi x^2$	
$2\pi x^4$	
$2\pi x^4 - \pi x^2$	(" " ")
$2\pi x^4 - 2\pi x^2$	
$2\pi x^4 - 3\pi x^2$	(" " ")
$2\pi x^4 - 4\pi x^2$	

The results of the calculations described above are given in the following pages. The curves were drawn by an IBM plotter. For the diffraction patterns and the encircled energy factors, tables of numerical values, accurate to 5 decimal places, are also given.

REMARKS

a) When $\phi(x) \neq 0$, the amplitudes in the diffraction patterns formed by the three pupils $T(x) \equiv 1$, $T(x, 5)$ and $T(x,M)$ will be complex: in the associated tables of numerical values, we have given the real parts (AR), the imaginary parts (AI), and the moduli A $(= \sqrt{AR^2 + AI^2})$ of these complex amplitudes. The curves show the variation of A with W.

b) In all cases, the curves corresponding to the uniformly transmitting pupil ($T(x) \equiv 1.0$) are drawn in black ink, those corresponding to the $T(x,5)$ amplitude filter are drawn in red ink, and those corresponding to the $T(x,M)$ amplitude filter are drawn in green ink.

c) The MTF curves were plotted with 21 points (at an interval of .1 in $\tilde{s}$). The encircled energy factors, and most of the diffraction patterns were plotted with 51 points at intervals of .5 in W. The plotter uses parabolic interpolation to draw the curves. Because of this, a small error was introduced in the curves corresponding to the diffraction patterns, where the latter has cusps or angular minima. It was necessary to increase the number of points used in certain cases in order to eliminate or reduce this error. The diffraction patterns corresponding to the following cases were drawn with 251 points (at an interval of W of .1):

1) $\phi(x) = 0$

2) $\phi(x) = \pi x^4 - \pi x^2$

3) $\phi(x) = 2\pi x^4 - 4\pi x^2$

d) Precision of the curves:-

The precision in the tracing of the curves was estimated to be about $\pm.005$ on the average, with a maximum error of $\pm.01$ (usually encountered at some of the minima in the curves corresponding to the diffraction patterns).

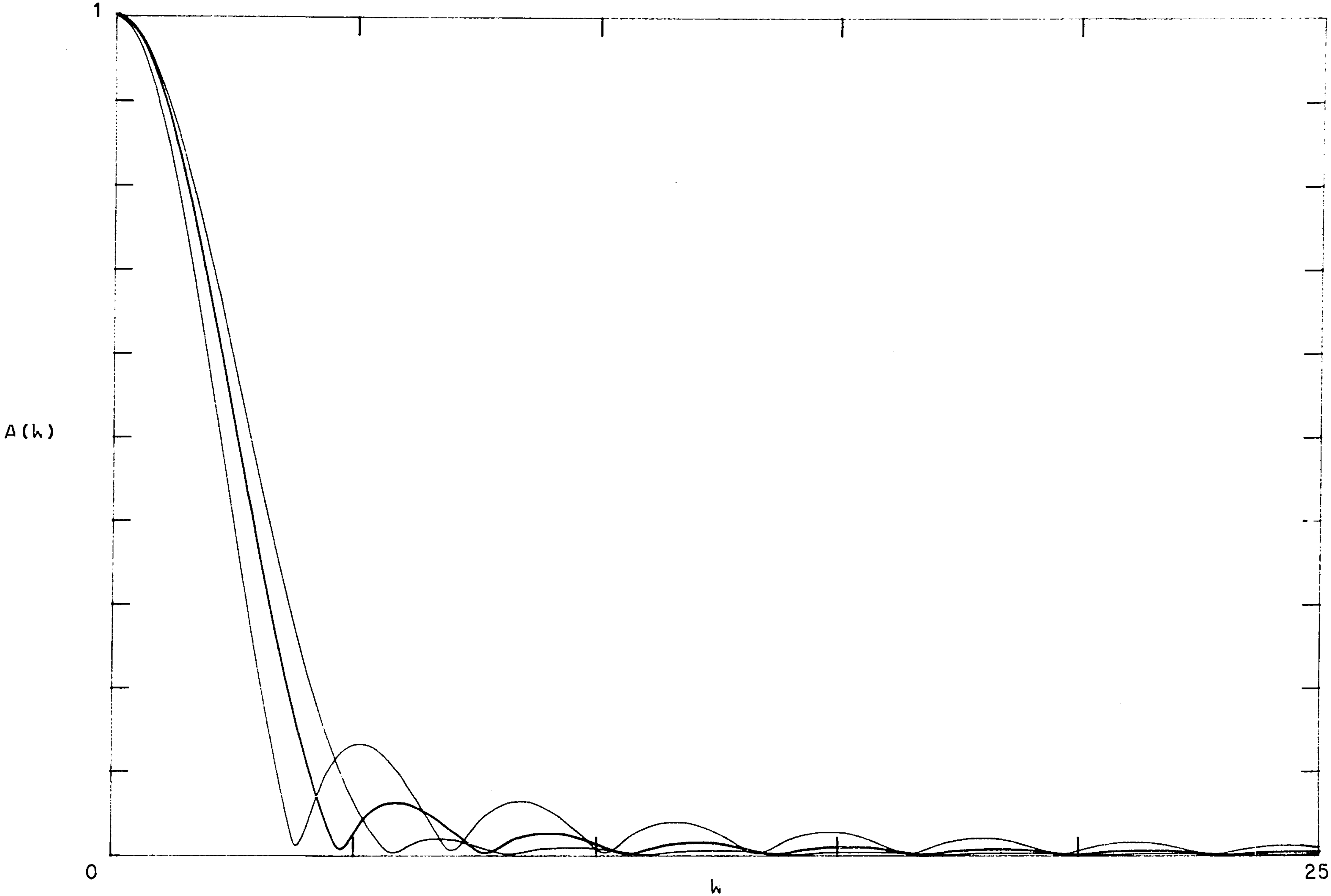

Fig. A3-1 Diffraction patterns formed by the pupils $T(x)=1, T(x,5), T(x,M)$ for the case $\phi(x) = 0$

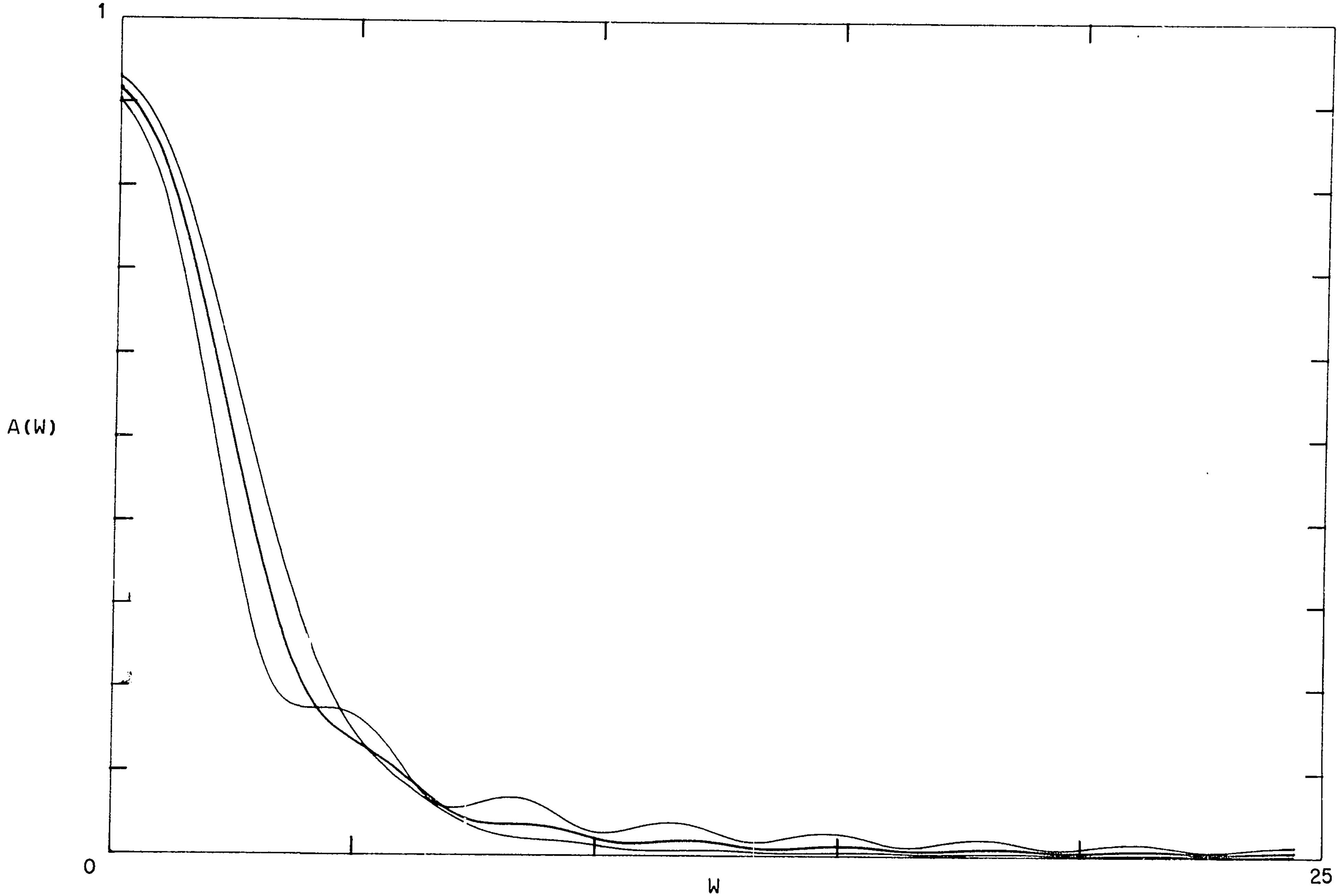

Fig. A3-2 Diffraction patterns formed by the pupils $T(x)=1, T(x,5), T(x,M)$ for the case $\phi(x)=.5\pi x^2$

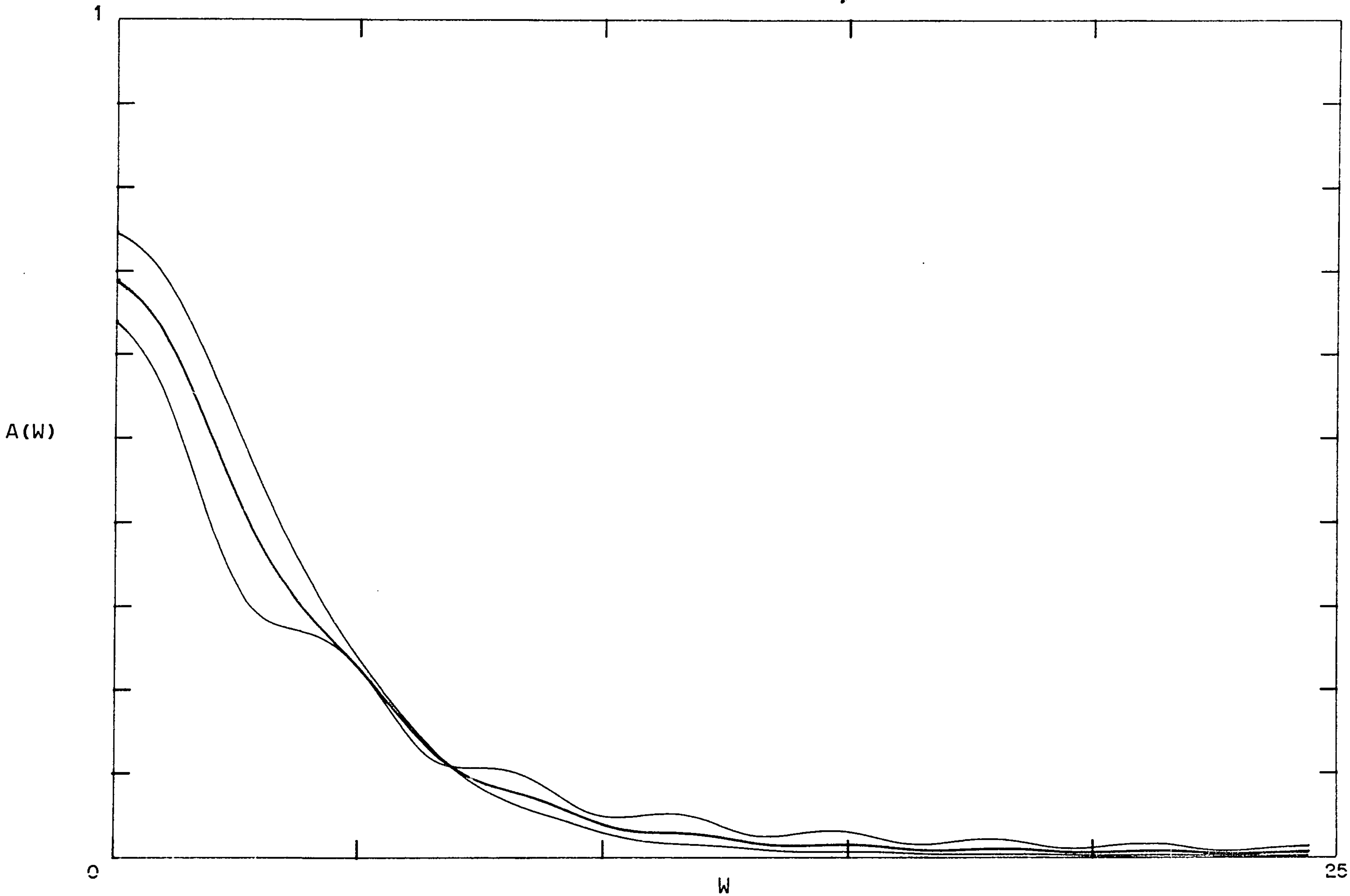

Fig. A3-3 Diffraction patterns formed by the pupils $T(x)=1, T(x,5), T(x,M)$ for the case $\phi(x) = \pi x^2$

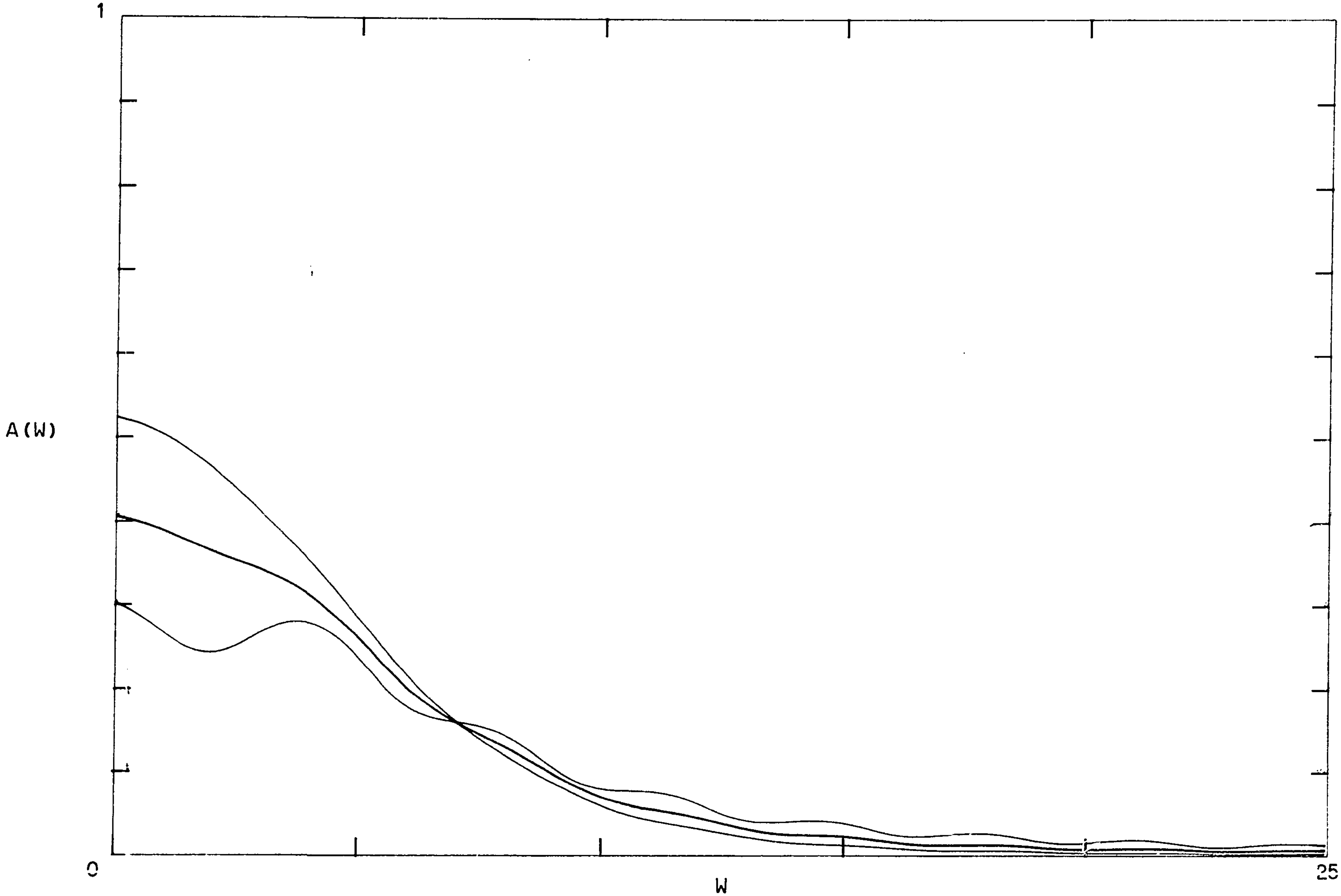

Fig. A3-4 Diffraction patterns formed by the pupils $T(x)=1, T(x,5), T(x,M)$ for the case $\phi(x)=1.5\pi x^2$

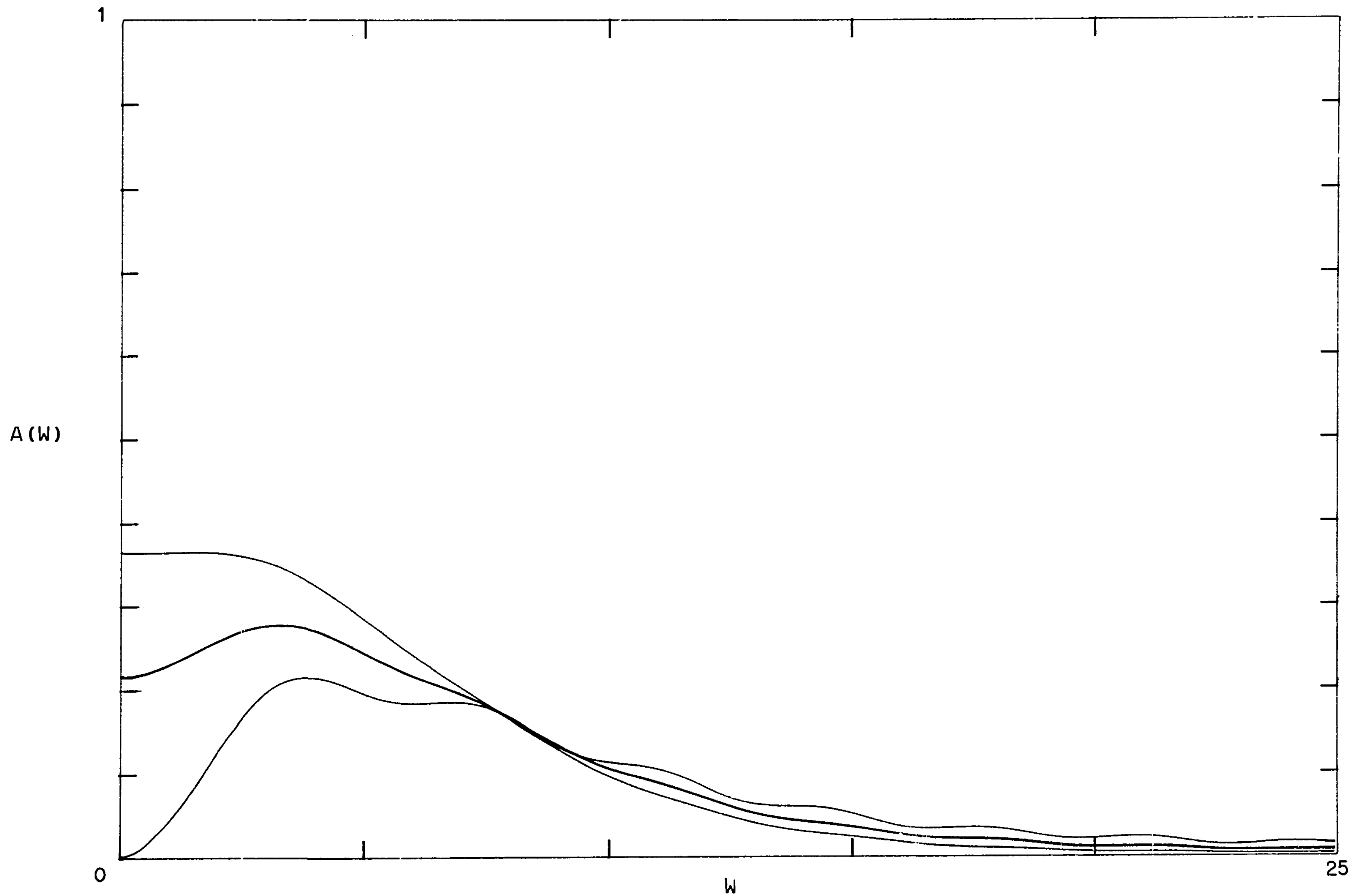

Fig. A3-5 Diffraction patterns formed by the pupils $T(x)=1, T(x,5), T(x,M)$ for the case $\phi(x)= 2\pi x^2$

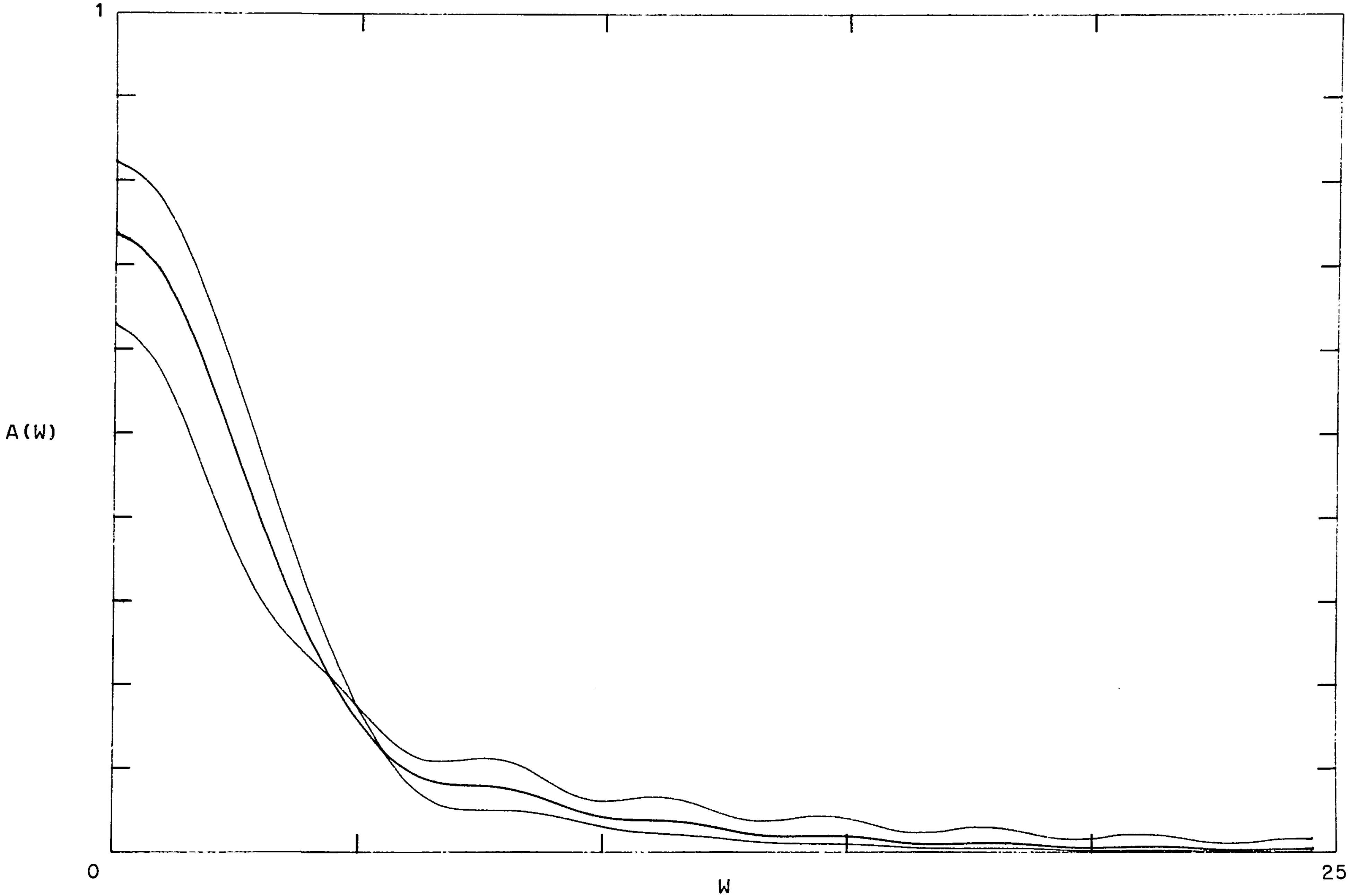

Fig. A3-6 Diffraction patterns formed by the pupils $T(x)=1$, $T(x,5)$, $T(x,M)$ for the case $\phi(x)=\pi x^4$

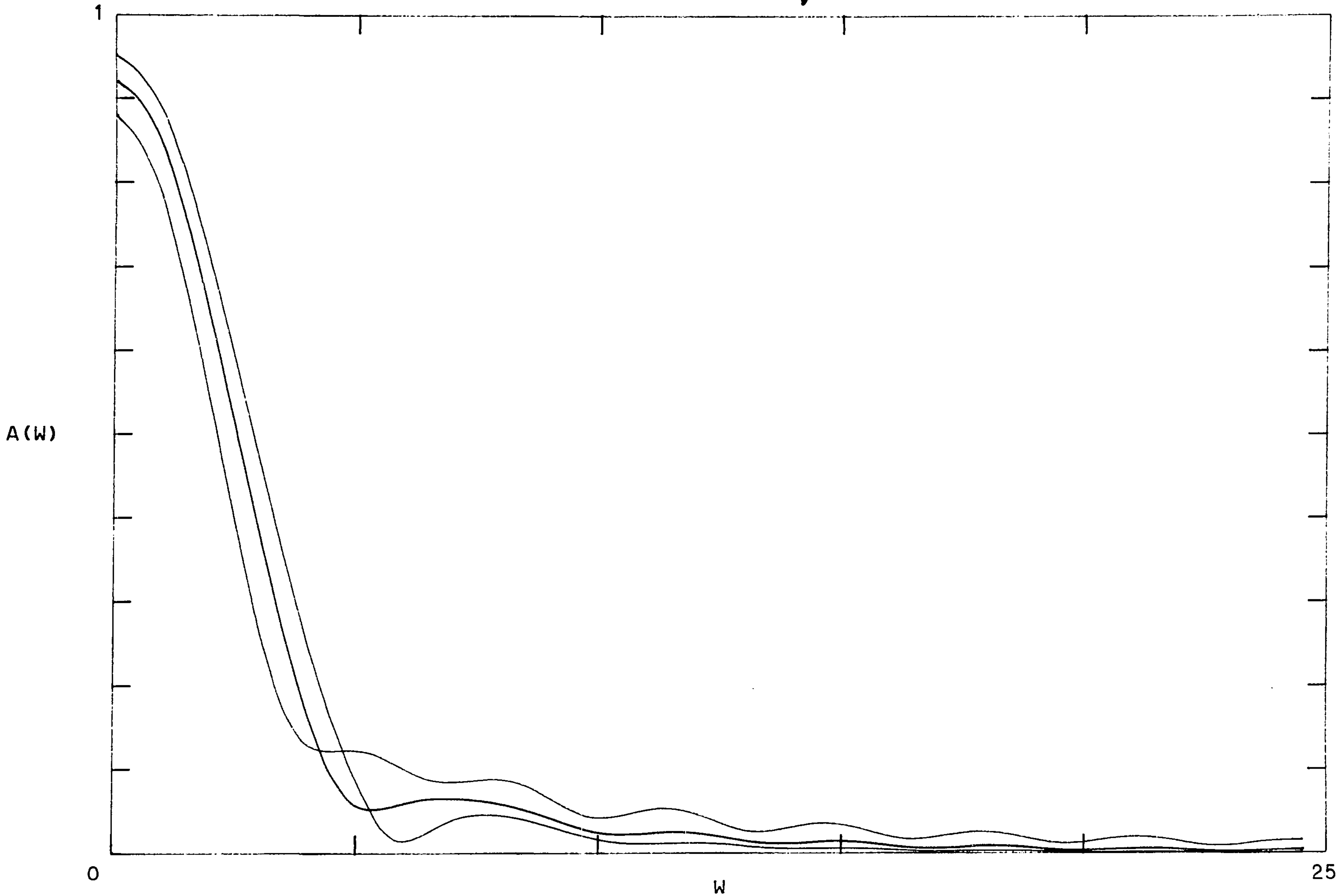

Fig. A3-7 Diffraction patterns formed by the pupils $T(x)=1, T(x,5), T(x,M)$ for the case $\phi(x)=\pi x^4 - 5\pi x^2$

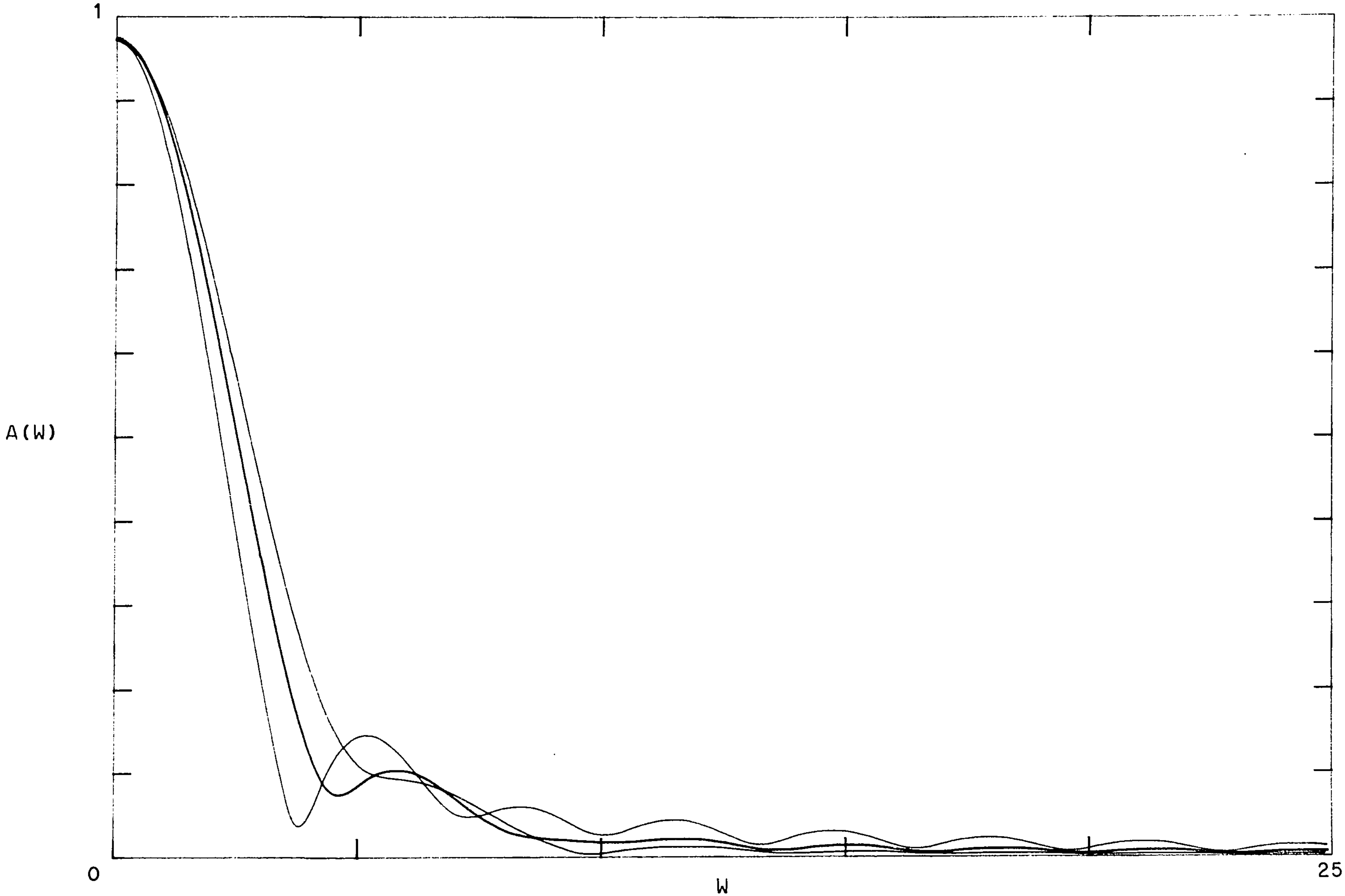

Fig. A3-8 Diffraction patterns formed by the pupils $T(x)=1, T(x,5), T(x,M)$ for the case $\phi(x)=\pi x^4 - \pi x^2$

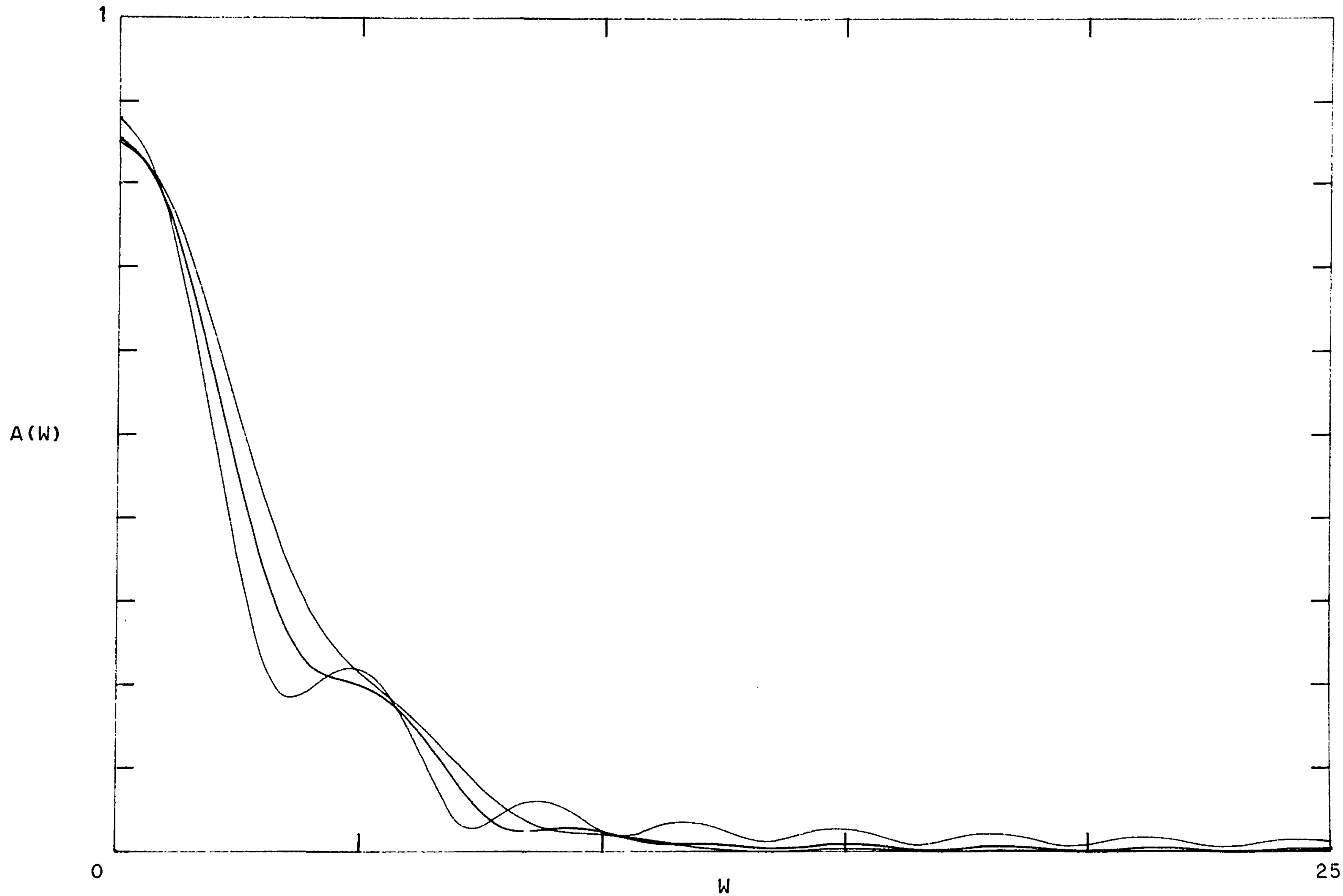

Fig. A3-9 Diffraction patterns formed by the pupils $T(x)=1, T(x,5), T(x,M)$ for the case $\phi(x)=\pi x^4-1.5\pi x^2$

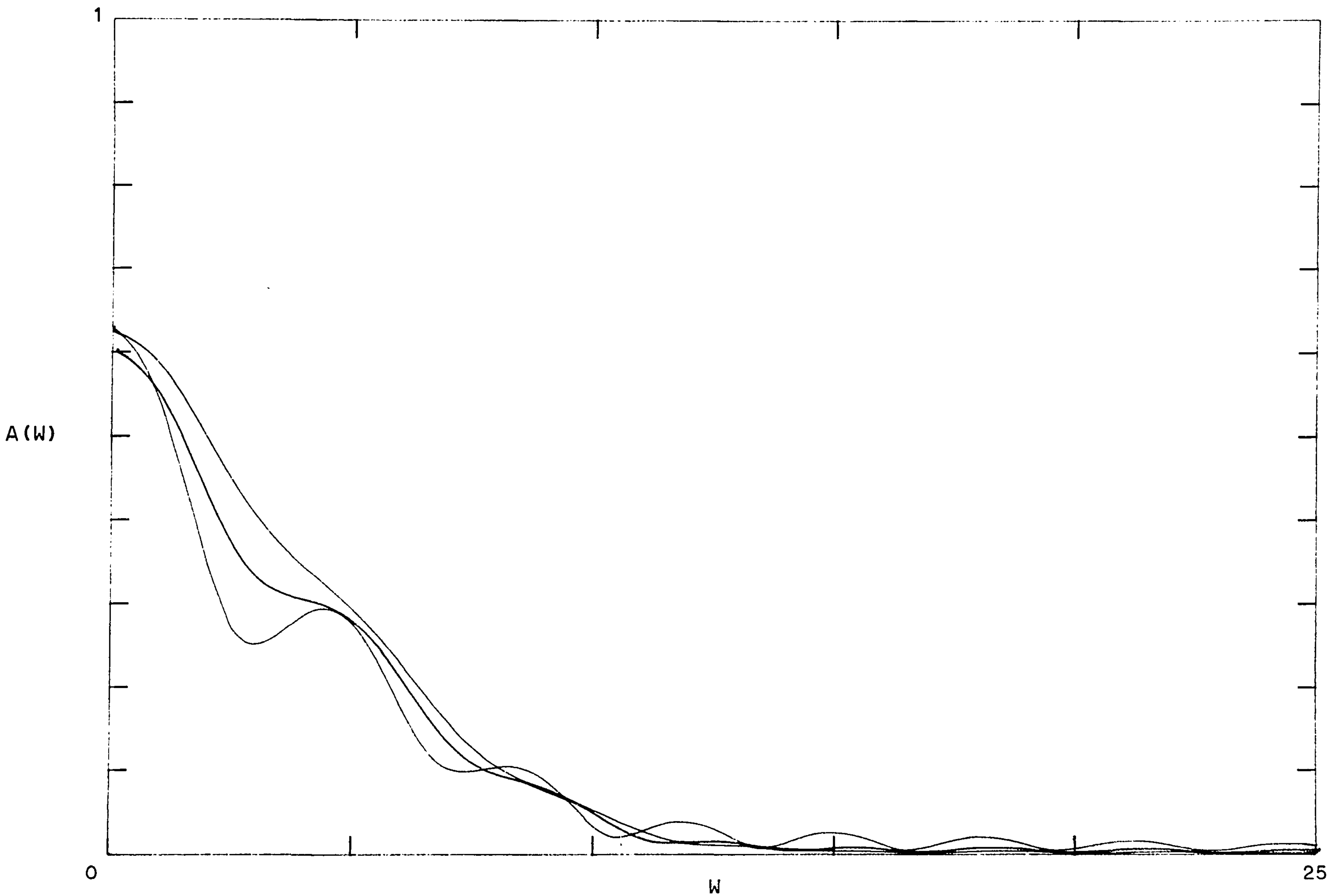

Fig. A3-10 Diffraction patterns formed by the pupils T(x)=1,T(x,5),T(x,M) for the case $\phi(x)=\pi x^4-2\pi x^2$

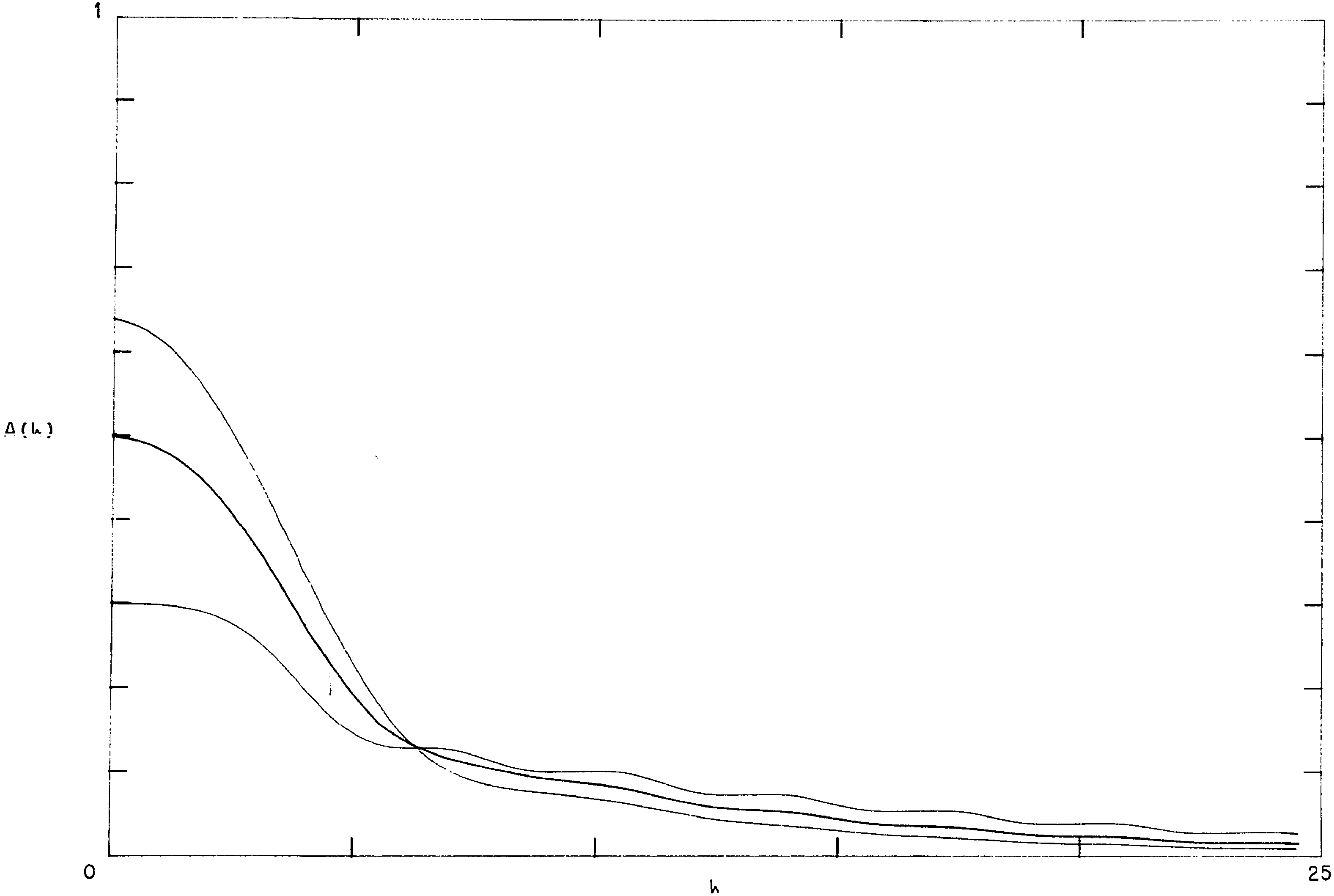

Fig. A3-11 Diffraction patterns formed by the pupils $T(x)=1, T(x,5), T(x,M)$ for the case $\phi(x)= 2\pi x^4$

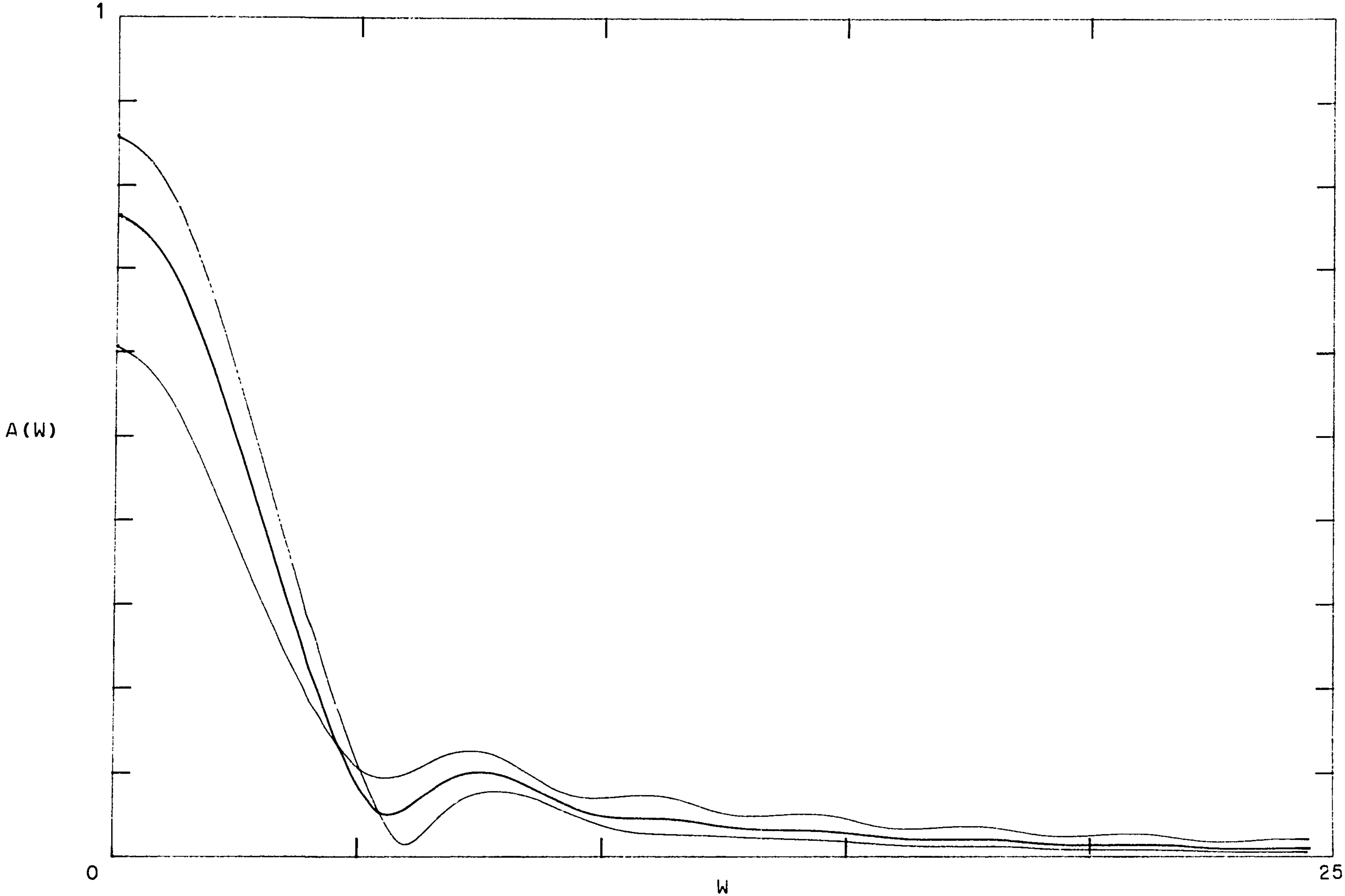

Fig. A3-12 Diffraction patterns formed by the pupils $T(x)=1, T(x,5), T(x,M)$ for the case $\phi(x)=2\pi x^4-\pi x^2$

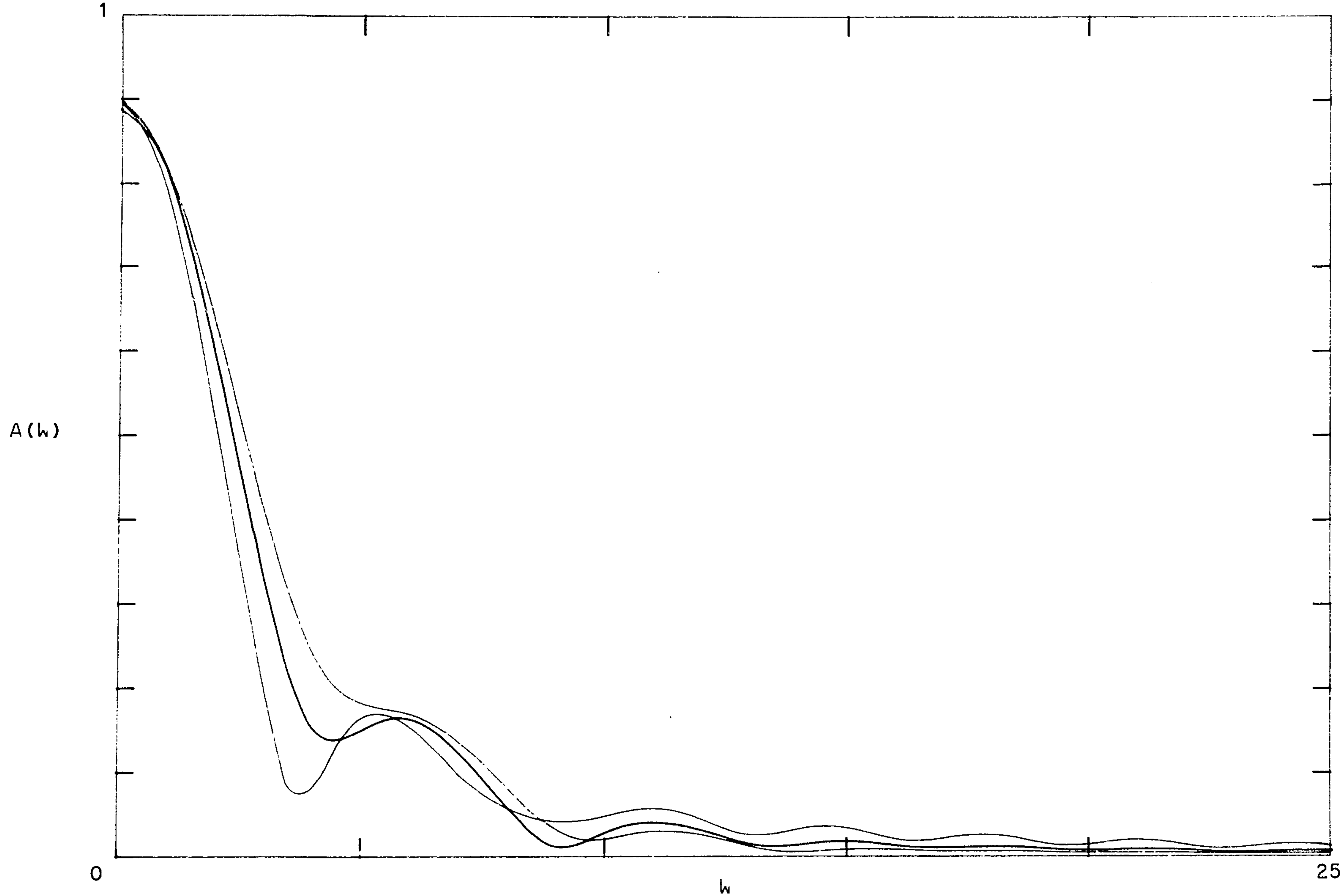

Fig. A3-13 Diffraction patterns formed by the pupils $T(x)=1, T(x,5), T(x,M)$ for the case $\phi(x)=2\pi x^4-2\pi x^2$

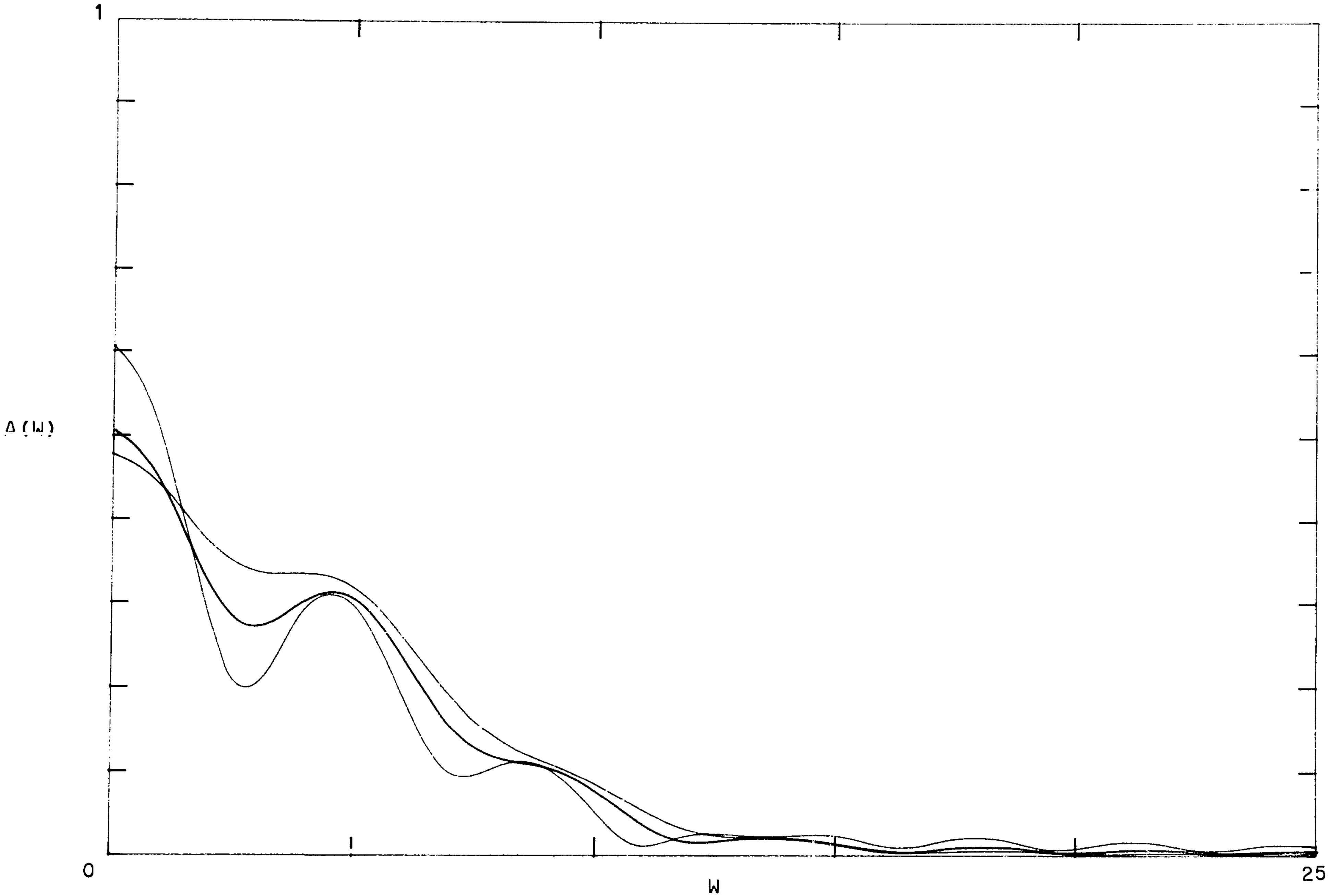

Fig. A3-14 Diffraction patterns formed by the pupils T(x)=1, T(x,5), T(x,M) for the case $\phi(x)=2\pi x^4-3\pi x^2$

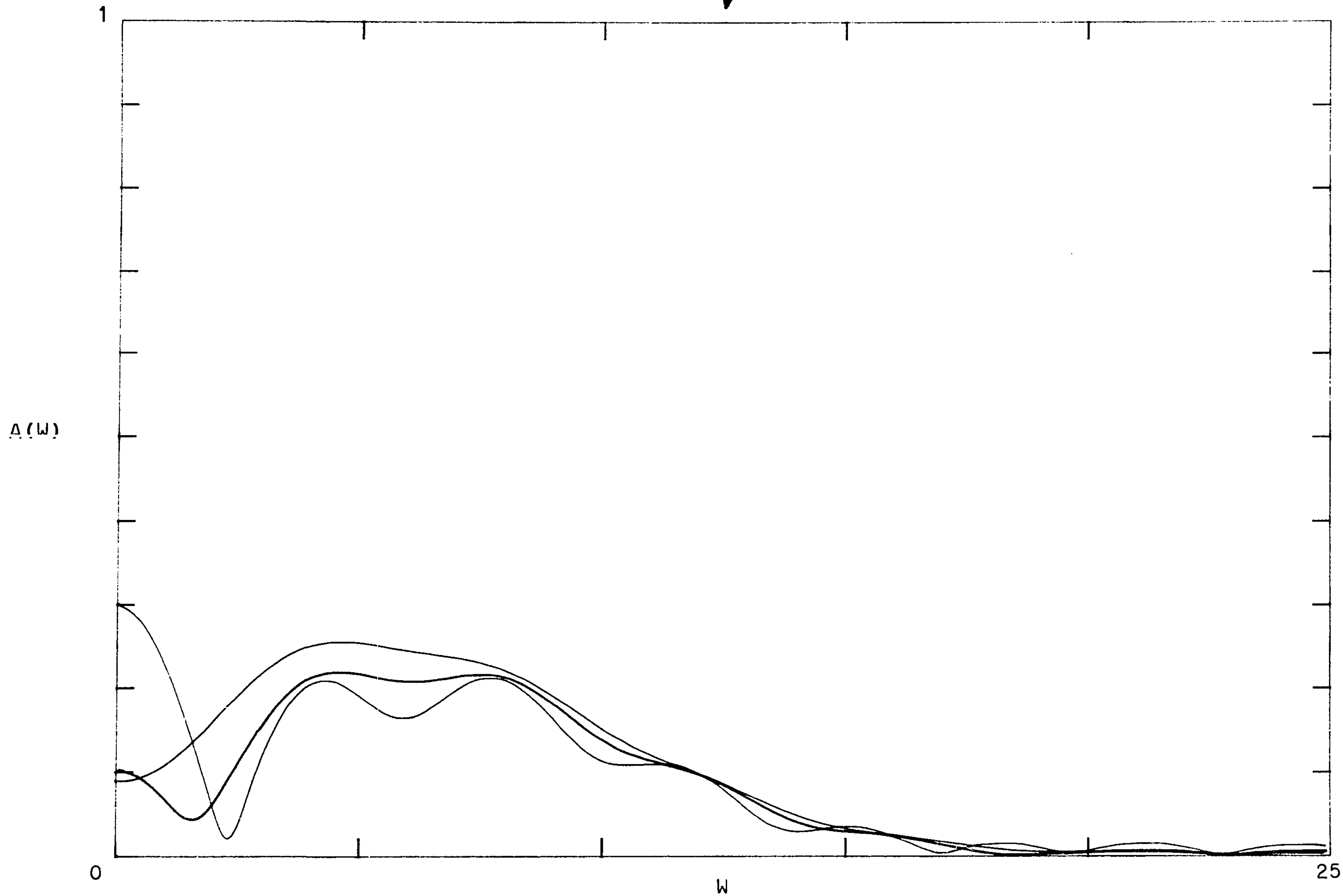

Fig. A3-15 Diffraction patterns formed by the pupils $T(x)=1, T(x,5), T(x,M)$ for the case $\phi(x)=2\pi x^4-4\pi x^2$

Table A3-1a Diffraction pattern formed by the pupil $T(x)=1$ for the case $\phi(x) = 0$

(AR= real part of amplitude, AI= imaginary part of amplitude, A= modulus of amplitude)

W	AR	AI	A	W	AR	AI	A
0.0	1.00000	0.0	1.00000	0.5	0.96907	0.0	0.96907
1.0	0.88010	0.0	0.88010	1.5	0.74392	0.0	0.74392
2.0	0.57672	0.0	0.57672	2.5	0.39768	0.0	0.39768
3.0	0.22604	0.0	0.22604	3.5	0.07850	0.0	0.07850
4.0	-0.03302	0.0	0.03302	4.5	-0.10269	0.0	0.10269
5.0	-0.13103	0.0	0.13103	5.5	-0.12416	0.0	0.12416
6.0	-0.09223	0.0	0.09223	6.5	-0.04734	0.0	0.04734
7.0	-0.00134	0.0	0.00134	7.5	0.03607	0.0	0.03607
8.0	0.05866	0.0	0.05866	8.5	0.06426	0.0	0.06426
9.0	0.05451	0.0	0.05451	9.5	0.03395	0.0	0.03395
10.0	0.00869	0.0	0.00869	10.5	-0.01502	0.0	0.01502
11.0	-0.03214	0.0	0.03214	11.5	-0.03972	0.0	0.03972
12.0	-0.03724	0.0	0.03724	12.5	-0.02648	0.0	0.02648
13.0	-0.01082	0.0	0.01082	13.5	0.00564	0.0	0.00564
14.0	0.01905	0.0	0.01905	14.5	0.02668	0.0	0.02668
15.0	0.02735	0.0	0.02735	15.5	0.02158	0.0	0.02158
16.0	0.01130	0.0	0.01130	16.5	-0.00070	0.0	0.00070
17.0	-0.01149	0.0	0.01149	17.5	-0.01868	0.0	0.01868
18.0	-0.02089	0.0	0.02089	18.5	-0.01801	0.0	0.01801
19.0	-0.01113	0.0	0.01113	19.5	-0.00214	0.0	0.00214
20.0	0.00668	0.0	0.00668	20.5	0.01329	0.0	0.01329
21.0	0.01630	0.0	0.01630	21.5	0.01524	0.0	0.01524
22.0	0.01065	0.0	0.01065	22.5	0.00384	0.0	0.00384
23.0	-0.00344	0.0	0.00344	23.5	-0.00944	0.0	0.00944
24.0	-0.01284	0.0	0.01284	24.5	-0.01298	0.0	0.01298
25.0	-0.01003	0.0	0.01003				

Table A3-1b Diffraction pattern formed by the pupil T(x,5) for the case $\phi(x) = 0$

(AR= real part of amplitude, AI= imaginary part of amplitude, A= modulus of amplitude)

W	AR	AI	A	W	AR	AI	A
0.0	1.00000	0.0	1.00000	0.5	0.98056	0.0	0.98056
1.0	0.92406	0.0	0.92406	1.5	0.83569	0.0	0.83569
2.0	0.72339	0.0	0.72339	2.5	0.59685	0.0	0.59685
3.0	0.46630	0.0	0.46630	3.5	0.34140	0.0	0.34140
4.0	0.23014	0.0	0.23014	4.5	0.13813	0.0	0.13813
5.0	0.06825	0.0	0.06825	5.5	0.02062	0.0	0.02062
6.0	-0.00695	0.0	0.00695	6.5	-0.01837	0.0	0.01837
7.0	-0.01840	0.0	0.01840	7.5	-0.01195	0.0	0.01195
8.0	-0.00329	0.0	0.00329	8.5	0.00437	0.0	0.00437
9.0	0.00912	0.0	0.00912	9.5	0.01033	0.0	0.01033
10.0	0.00844	0.0	0.00844	10.5	0.00454	0.0	0.00454
11.0	0.00003	0.0	0.00003	11.5	-0.00382	0.0	0.00382
12.0	-0.00613	0.0	0.00613	12.5	-0.00654	0.0	0.00654
13.0	-0.00520	0.0	0.00520	13.5	-0.00269	0.0	0.00269
14.0	0.00022	0.0	0.00022	14.5	0.00275	0.0	0.00275
15.0	0.00432	0.0	0.00432	15.5	0.00464	0.0	0.00464
16.0	0.00376	0.0	0.00376	16.5	0.00203	0.0	0.00203
17.0	-0.00005	0.0	0.00005	17.5	-0.00193	0.0	0.00193
18.0	-0.00317	0.0	0.00317	18.5	-0.00352	0.0	0.00352
19.0	-0.00297	0.0	0.00297	19.5	-0.00173	0.0	0.00173
20.0	-0.00016	0.0	0.00016	20.5	0.00133	0.0	0.00133
21.0	0.00238	0.0	0.00238	21.5	0.00278	0.0	0.00278
22.0	0.00246	0.0	0.00246	22.5	0.00157	0.0	0.00157
23.0	0.00035	0.0	0.00035	23.5	-0.00088	0.0	0.00088
24.0	-0.00181	0.0	0.00181	24.5	-0.00224	0.0	0.00224
25.0	-0.00210	0.0	0.00210				

Table A3-1c Diffraction pattern formed by the pupil T(x,M) for the case $\phi(x) = 0$

(AR= real part of amplitude, AI= imaginary part of amplitude, A= modulus of amplitude)

W	AR	AI	A	W	AR	AI	A
0.0	1.00000	0.0	1.00000	0.5	0.97580	0.0	0.97580
1.0	0.90579	0.0	0.90579	1.5	0.79735	0.0	0.79735
2.0	0.66166	0.0	0.66166	2.5	0.51211	0.0	0.51211
3.0	0.36261	0.0	0.36261	3.5	0.22572	0.0	0.22572
4.0	0.11125	0.0	0.11125	4.5	0.02523	0.0	0.02523
5.0	-0.03046	0.0	0.03046	5.5	-0.05780	0.0	0.05780
6.0	-0.06190	0.0	0.06190	6.5	-0.04977	0.0	0.04977
7.0	-0.02905	0.0	0.02905	7.5	-0.00676	0.0	0.00676
8.0	0.01166	0.0	0.01166	8.5	0.02294	0.0	0.02294
9.0	0.02606	0.0	0.02606	9.5	0.02200	0.0	0.02200
10.0	0.01311	0.0	0.01311	10.5	0.00238	0.0	0.00238
11.0	-0.00730	0.0	0.00730	11.5	-0.01378	0.0	0.01378
12.0	-0.01597	0.0	0.01597	12.5	-0.01394	0.0	0.01394
13.0	-0.00873	0.0	0.00873	13.5	-0.00198	0.0	0.00198
14.0	0.00451	0.0	0.00451	14.5	0.00920	0.0	0.00920
15.0	0.01117	0.0	0.01117	15.5	0.01023	0.0	0.01023
16.0	0.00689	0.0	0.00689	16.5	0.00219	0.0	0.00219
17.0	-0.00263	0.0	0.00263	17.5	-0.00639	0.0	0.00639
18.0	-0.00830	0.0	0.00830	18.5	-0.00804	0.0	0.00804
19.0	-0.00586	0.0	0.00586	19.5	-0.00244	0.0	0.00244
20.0	0.00132	0.0	0.00132	20.5	0.00449	0.0	0.00449
21.0	0.00635	0.0	0.00635	21.5	0.00655	0.0	0.00655
22.0	0.00515	0.0	0.00515	22.5	0.00261	0.0	0.00261
23.0	-0.00040	0.0	0.00040	23.5	-0.00312	0.0	0.00312
24.0	-0.00492	0.0	0.00492	24.5	-0.00543	0.0	0.00543
25.0	-0.00460	0.0	0.00460				

Table A3-2a Diffraction pattern formed by the pupil T(x)=1 for the case $\phi(x) = .5\pi x^2$

(AR= real part of amplitude,AI= imaginary part of amplitude,A= modulus of amplitude)

W	AR	AI	A	W	AR	AI	A
0.0	0.63662	0.63662	0.90032	0.5	0.62228	0.61158	0.87250
1.0	0.58064	0.53980	0.79280	1.5	0.51568	0.43084	0.67197
2.0	0.43346	0.29889	0.52652	2.5	0.34141	0.16059	0.37729
3.0	0.24740	0.03243	0.24951	3.5	0.15883	-0.07167	0.17425
4.0	0.08187	-0.14228	0.16415	4.5	0.02080	-0.17562	0.17685
5.0	-0.02226	-0.17362	0.17505	5.5	-0.04736	-0.14317	0.15080
6.0	-0.05647	-0.09450	0.11009	6.5	-0.05299	-0.03920	0.06591
7.0	-0.04109	0.01182	0.04276	7.5	-0.02507	0.05008	0.05601
8.0	-0.00879	0.07071	0.07125	8.5	0.00482	0.07281	0.07297
9.0	0.01394	0.05911	0.06073	9.5	0.01797	0.03498	0.03932
10.0	0.01733	0.00705	0.01871	10.5	0.01322	-0.01821	0.02251
11.0	0.00721	-0.03580	0.03652	11.5	0.00092	-0.04297	0.04298
12.0	-0.00430	-0.03952	0.03975	12.5	-0.00758	-0.02756	0.02858
13.0	-0.00859	-0.01077	0.01377	13.5	-0.00753	0.00653	0.00996
14.0	-0.00499	0.02041	0.02101	14.5	-0.00177	0.02810	0.02816
15.0	0.00132	0.02851	0.02855	15.5	0.00363	0.02229	0.02258
16.0	0.00477	0.01150	0.01245	16.5	0.00467	-0.00096	0.00476
17.0	0.00353	-0.01206	0.01256	17.5	0.00174	-0.01937	0.01945
18.0	-0.00019	-0.02154	0.02154	18.5	-0.00183	-0.01848	0.01857
19.0	-0.00283	-0.01133	0.01168	19.5	-0.00307	-0.00209	0.00371
20.0	-0.00257	0.00694	0.00740	20.5	-0.00154	0.01366	0.01375
21.0	-0.00028	0.01668	0.01668	21.5	0.00090	0.01555	0.01557
22.0	0.00175	0.01083	0.01097	22.5	0.00209	0.00387	0.00440
23.0	0.00192	-0.00355	0.00404	23.5	0.00132	-0.00964	0.00973
24.0	0.00047	-0.01307	0.01308	24.5	-0.00040	-0.01319	0.01319
25.0	-0.00109	-0.01017	0.01022				

Table A3-2b Diffraction pattern formed by the pupil T(x,5) for the case $\phi(x) = .5\pi x^2$

(AR= real part of amplitude,AI= imaginary part of amplitude,A= modulus of amplitude)

W	AR	AI	A	W	AR	AI	A
0.0	0.82184	0.43280	0.92884	0.5	0.80914	0.42000	0.91165
1.0	0.77198	0.38304	0.86178	1.5	0.71311	0.32595	0.78407
2.0	0.63681	0.25484	0.68591	2.5	0.54842	0.17708	0.57630
3.0	0.45383	0.10026	0.46477	3.5	0.35892	0.03129	0.36029
4.0	0.26903	-0.02447	0.27014	4.5	0.18848	-0.06376	0.19897
5.0	0.12035	-0.08561	0.14769	5.5	0.06628	-0.09127	0.11280
6.0	0.02652	-0.08374	0.08784	6.5	0.00014	-0.06716	0.06716
7.0	-0.01477	-0.04606	0.04837	7.5	-0.02064	-0.02468	0.03217
8.0	-0.02017	-0.00637	0.02115	8.5	-0.01592	0.00673	0.01728
9.0	-0.01010	0.01381	0.01711	9.5	-0.00438	0.01529	0.01590
10.0	0.00016	0.01247	0.01247	10.5	0.00301	0.00717	0.00777
11.0	0.00416	0.00124	0.00434	11.5	0.00391	-0.00373	0.00541
12.0	0.00276	-0.00676	0.00730	12.5	0.00124	-0.00746	0.00757
13.0	-0.00018	-0.00610	0.00610	13.5	-0.00120	-0.00335	0.00356
14.0	-0.00167	-0.00012	0.00167	14.5	-0.00161	0.00272	0.00316
15.0	-0.00115	0.00451	0.00465	15.5	-0.00050	0.00494	0.00497
16.0	0.00015	0.00408	0.00408	16.5	0.00065	0.00227	0.00236
17.0	0.00089	0.00008	0.00089	17.5	0.00087	-0.00192	0.00210
18.0	0.00063	-0.00325	0.00331	18.5	0.00028	-0.00365	0.00366
19.0	-0.00009	-0.00311	0.00311	19.5	-0.00039	-0.00185	0.00189
20.0	-0.00054	-0.00023	0.00059	20.5	-0.00054	0.00132	0.00143
21.0	-0.00041	0.00242	0.00246	21.5	-0.00019	0.00285	0.00285
22.0	0.00005	0.00254	0.00254	22.5	0.00024	0.00163	0.00165
23.0	0.00036	0.00038	0.00052	23.5	0.00037	-0.00087	0.00095
24.0	0.00029	-0.00183	0.00186	24.5	0.00015	-0.00228	0.00229
25.0	-0.00001	-0.00215	0.00215				

Table A3-2c Diffraction pattern formed by the pupil T(x,M) for the case $\phi(x) = .5\pi x^2$

(AR= real part of amplitude,AI= imaginary part of amplitude,A= modulus of amplitude)

W	AR	AI	A	W	AR	AI	A
0.0	0.74938	0.52105	0.91272	0.5	0.73558	0.50338	0.89133
1.0	0.69534	0.45253	0.82963	1.5	0.63202	0.37461	0.73470
2.0	0.55078	0.27881	0.61733	2.5	0.45802	0.17603	0.49068
3.0	0.36069	0.07734	0.36889	3.5	0.26553	-0.00755	0.26563
4.0	0.17845	-0.07155	0.19225	4.5	0.10397	-0.11092	0.15203
5.0	0.04495	-0.12556	0.13336	5.5	0.00241	-0.11861	0.11864
6.0	-0.02427	-0.09569	0.09872	6.5	-0.03710	-0.06370	0.07372
7.0	-0.03904	-0.02970	0.04905	7.5	-0.03348	0.00029	0.03348
8.0	-0.02380	0.02200	0.03241	8.5	-0.01295	0.03344	0.03586
9.0	-0.00321	0.03477	0.03492	9.5	0.00401	0.02801	0.02829
10.0	0.00810	0.01630	0.01820	10.5	0.00921	0.00317	0.00974
11.0	0.00795	-0.00820	0.01142	11.5	0.00524	-0.01560	0.01645
12.0	0.00204	-0.01801	0.01812	12.5	-0.00083	-0.01568	0.01571
13.0	-0.00282	-0.00989	0.01028	13.5	-0.00369	-0.00247	0.00444
14.0	-0.00350	0.00459	0.00577	14.5	-0.00250	0.00969	0.01000
15.0	-0.00111	0.01184	0.01189	15.5	0.00030	0.01087	0.01088
16.0	0.00138	0.00737	0.00750	16.5	0.00194	0.00243	0.00311
17.0	0.00194	-0.00262	0.00327	17.5	0.00148	-0.00658	0.00674
18.0	0.00072	-0.00858	0.00861	18.5	-0.00009	-0.00834	0.00834
19.0	-0.00077	-0.00610	0.00615	19.5	-0.00117	-0.00257	0.00282
20.0	-0.00124	0.00131	0.00180	20.5	-0.00100	0.00457	0.00468
21.0	-0.00054	0.00649	0.00651	21.5	-0.00002	0.00671	0.00671
22.0	0.00045	0.00529	0.00531	22.5	0.00076	0.00269	0.00280
23.0	0.00085	-0.00038	0.00093	23.5	0.00073	-0.00316	0.00324
24.0	0.00044	-0.00500	0.00502	24.5	0.00008	-0.00552	0.00552
25.0	-0.00026	-0.00468	0.00469				

Table A3-3a Diffraction pattern formed by the pupil $T(x)=1$ for the case $\phi(x) = \pi x^2$

(AR= real part of amplitude,AI= imaginary part of amplitude,A= modulus of amplitude)

W	AR	AI	A	W	AR	AI	A
0.0	0.0	0.63662	0.63662	0.5	0.01247	0.61691	0.61704
1.0	0.04757	0.55995	0.56196	1.5	0.09882	0.47194	0.48218
2.0	0.15674	0.36232	0.39477	2.5	0.21054	0.24245	0.32111
3.0	0.25013	0.12419	0.27927	3.5	0.26785	0.01840	0.26848
4.0	0.25981	-0.06638	0.26815	4.5	0.22650	-0.12478	0.25860
5.0	0.17263	-0.15507	0.23206	5.5	0.10616	-0.15901	0.19119
6.0	0.03681	-0.14128	0.14599	6.5	-0.02568	-0.10853	0.11152
7.0	-0.07319	-0.06828	0.10009	7.5	-0.10061	-0.02775	0.10437
8.0	-0.10646	0.00707	0.10669	8.5	-0.09291	0.03212	0.09830
9.0	-0.06512	0.04558	0.07949	9.5	-0.03012	0.04775	0.05646
10.0	0.00468	0.04071	0.04098	10.5	0.03280	0.02766	0.04291
11.0	0.04984	0.01220	0.05131	11.5	0.05404	-0.00232	0.05409
12.0	0.04634	-0.01333	0.04822	12.5	0.02993	-0.01941	0.03567
13.0	0.00936	-0.02031	0.02236	13.5	-0.01052	-0.01680	0.01982
14.0	-0.02556	-0.01039	0.02759	14.5	-0.03310	-0.00292	0.03323
15.0	-0.03237	0.00389	0.03260	15.5	-0.02445	0.00872	0.02596
16.0	-0.01188	0.01086	0.01610	16.5	0.00207	0.01029	0.01049
17.0	0.01413	0.00752	0.01601	17.5	0.02176	0.00350	0.02204
18.0	0.02367	-0.00073	0.02368	18.5	0.01995	-0.00420	0.02038
19.0	0.01194	-0.00626	0.01348	19.5	0.00185	-0.00663	0.00688
20.0	-0.00783	-0.00546	0.00954	20.5	-0.01489	-0.00319	0.01523
21.0	-0.01792	-0.00047	0.01793	21.5	-0.01653	0.00203	0.01665
22.0	-0.01136	0.00377	0.01197	22.5	-0.00391	0.00446	0.00593
23.0	0.00394	0.00404	0.00564	23.5	0.01031	0.00274	0.01067
24.0	0.01382	0.00094	0.01386	24.5	0.01385	-0.00088	0.01387
25.0	0.01060	-0.00232	0.01085				

Table A3-3b Diffraction pattern formed by the pupil T(x,5) for the case $\phi(x) = \pi x^2$

(AR= real part of amplitude,AI= imaginary part of amplitude,A= modulus of amplitude)

W	AR	AI	A	W	AR	AI	A
0.0	0.45203	0.59070	0.74381	0.5	0.45201	0.57648	0.73256
1.0	0.45141	0.53513	0.70010	1.5	0.44871	0.47039	0.65008
2.0	0.44171	0.38800	0.58792	2.5	0.42807	0.29506	0.51991
3.0	0.40576	0.19922	0.45203	3.5	0.37362	0.10786	0.38888
4.0	0.33164	0.02731	0.33276	4.5	0.28117	-0.03769	0.28368
5.0	0.22478	-0.08440	0.24011	5.5	0.16602	-0.11215	0.20035
6.0	0.10886	-0.12222	0.16367	6.5	0.05720	-0.11742	0.13061
7.0	0.01433	-0.10160	0.10261	7.5	-0.01756	-0.07908	0.08100
8.0	-0.03761	-0.05404	0.06584	8.5	-0.04631	-0.03010	0.05523
9.0	-0.04540	-0.00992	0.04647	9.5	-0.03745	0.00490	0.03777
10.0	-0.02549	0.01385	0.02901	10.5	-0.01247	0.01737	0.02138
11.0	-0.00088	0.01653	0.01656	11.5	0.00756	0.01281	0.01488
12.0	0.01207	0.00774	0.01433	12.5	0.01270	0.00265	0.01298
13.0	0.01026	-0.00146	0.01037	13.5	0.00597	-0.00405	0.00721
14.0	0.00117	-0.00500	0.00514	14.5	-0.00295	-0.00455	0.00542
15.0	-0.00556	-0.00315	0.00639	15.5	-0.00633	-0.00135	0.00647
16.0	-0.00539	0.00036	0.00540	16.5	-0.00323	0.00160	0.00360
17.0	-0.00056	0.00219	0.00226	17.5	0.00190	0.00213	0.00285
18.0	0.00358	0.00156	0.00390	18.5	0.00417	0.00071	0.00423
19.0	0.00365	-0.00017	0.00365	19.5	0.00227	-0.00085	0.00242
20.0	0.00046	-0.00122	0.00130	20.5	-0.00129	-0.00123	0.00178
21.0	-0.00256	-0.00093	0.00273	21.5	-0.00309	-0.00045	0.00312
22.0	-0.00280	0.00008	0.00280	22.5	-0.00185	0.00051	0.00192
23.0	-0.00051	0.00077	0.00092	23.5	0.00085	0.00080	0.00117
24.0	0.00190	0.00064	0.00200	24.5	0.00241	0.00033	0.00243
25.0	0.00229	-0.00002	0.00229				

Table A3-3c Diffraction pattern formed by the pupil T(x,M) for the case $\phi(x) = \pi x^2$

(AR= real part of amplitude,AI= imaginary part of amplitude,A= modulus of amplitude)

W	AR	AI	A	W	AR	AI	A
0.0	0.26649	0.62968	0.68374	0.5	0.27095	0.61265	0.66989
1.0	0.28318	0.56326	0.63044	1.5	0.29993	0.48638	0.57143
2.0	0.31645	0.38946	0.50182	2.5	0.32745	0.28158	0.43187
3.0	0.32805	0.17242	0.37060	3.5	0.31477	0.07108	0.32269
4.0	0.28619	-0.01488	0.28657	4.5	0.24329	-0.08020	0.25616
5.0	0.18932	-0.12232	0.22540	5.5	0.12932	-0.14144	0.19165
6.0	0.06924	-0.14018	0.15635	6.5	0.01503	-0.12299	0.12390
7.0	-0.02831	-0.09538	0.09950	7.5	-0.05751	-0.06310	0.08538
8.0	-0.07139	-0.03137	0.07798	8.5	-0.07099	-0.00429	0.07112
9.0	-0.05919	0.01551	0.06119	9.5	-0.04012	0.02699	0.04835
10.0	-0.01838	0.03052	0.03563	10.5	0.00174	0.02762	0.02767
11.0	0.01697	0.02043	0.02656	11.5	0.02542	0.01132	0.02783
12.0	0.02677	0.00245	0.02688	12.5	0.02210	-0.00460	0.02257
13.0	0.01346	-0.00889	0.01613	13.5	0.00337	-0.01023	0.01077
14.0	-0.00576	-0.00903	0.01072	14.5	-0.01208	-0.00612	0.01354
15.0	-0.01461	-0.00248	0.01482	15.5	-0.01334	0.00096	0.01337
16.0	-0.00907	0.00348	0.00971	16.5	-0.00319	0.00470	0.00568
17.0	0.00273	0.00460	0.00535	17.5	0.00732	0.00344	0.00809
18.0	0.00965	0.00167	0.00979	18.5	0.00941	-0.00021	0.00941
19.0	0.00693	-0.00174	0.00714	19.5	0.00302	-0.00262	0.00400
20.0	-0.00127	-0.00275	0.00303	20.5	-0.00487	-0.00221	0.00534
21.0	-0.00699	-0.00121	0.00709	21.5	-0.00725	-0.00005	0.00725
22.0	-0.00575	0.00097	0.00583	22.5	-0.00297	0.00163	0.00339
23.0	0.00032	0.00183	0.00185	23.5	0.00329	0.00156	0.00364
24.0	0.00527	0.00095	0.00535	24.5	0.00584	0.00018	0.00584
25.0	0.00496	-0.00055	0.00499				

Table A3-4a Diffraction pattern formed by the pupil T(x)=1 for the case $\phi(x) = 1.5\pi x^2$

(AR= real part of amplitude,AI= imaginary part of amplitude,A= modulus of amplitude)

W	AR	AI	A	W	AR	AI	A
0.0	-0.21221	0.21221	0.30011	0.5	-0.19632	0.21492	0.29108
1.0	-0.15085	0.22181	0.26825	1.5	-0.08210	0.22949	0.24373
2.0	0.00054	0.23316	0.23316	2.5	0.08593	0.22778	0.24345
3.0	0.16287	0.20929	0.26519	3.5	0.22168	0.17569	0.28286
4.0	0.25558	0.12769	0.28571	4.5	0.26151	0.06885	0.27042
5.0	0.24038	0.00513	0.24044	5.5	0.19677	-0.05610	0.20461
6.0	0.13797	-0.10730	0.17478	6.5	0.07279	-0.14215	0.15970
7.0	0.01013	-0.15665	0.15698	7.5	-0.04231	-0.14992	0.15578
8.0	-0.07910	-0.12428	0.14732	8.5	-0.09765	-0.08488	0.12938
9.0	-0.09828	-0.03875	0.10564	9.5	-0.08393	0.00645	0.08418
10.0	-0.05936	0.04378	0.07375	10.5	-0.03018	0.06813	0.07452
11.0	-0.00190	0.07706	0.07708	11.5	0.02098	0.07095	0.07399
12.0	0.03555	0.05283	0.06368	12.5	0.04079	0.02750	0.04920
13.0	0.03743	0.00062	0.03744	13.5	0.02762	-0.02252	0.03563
14.0	0.01431	-0.03790	0.04051	14.5	0.00064	-0.04345	0.04345
15.0	-0.01070	-0.03926	0.04069	15.5	-0.01788	-0.02736	0.03268
16.0	-0.02015	-0.01112	0.02302	16.5	-0.01785	0.00555	0.01869
17.0	-0.01216	0.01907	0.02262	17.5	-0.00479	0.02687	0.02729
18.0	0.00247	0.02787	0.02798	18.5	0.00812	0.02255	0.02397
19.0	0.01117	0.01272	0.01693	19.5	0.01134	0.00098	0.01138
20.0	0.00899	-0.00985	0.01334	20.5	0.00496	-0.01744	0.01813
21.0	0.00035	-0.02035	0.02036	21.5	-0.00375	-0.01834	0.01872
22.0	-0.00649	-0.01227	0.01388	22.5	-0.00744	-0.00386	0.00838
23.0	-0.00660	0.00478	0.00815	23.5	-0.00435	0.01164	0.01243
24.0	-0.00137	0.01527	0.01533	24.5	0.00160	0.01507	0.01516
25.0	0.00388	0.01136	0.01201				

Table A3-4b Diffraction pattern formed by the pupil T(x,5) for the case $\phi(x) = 1.5\pi x^2$

(AR= real part of amplitude,AI= imaginary part of amplitude,A= modulus of amplitude)

W	AR	AI	A	W	AR	AI	A
0.0	0.18065	0.48975	0.52201	0.5	0.18687	0.48312	0.51800
1.0	0.20455	0.46335	0.50650	1.5	0.23086	0.43094	0.48888
2.0	0.26157	0.38676	0.46691	2.5	0.29162	0.33227	0.44210
3.0	0.31590	0.26954	0.41526	3.5	0.32991	0.20133	0.38650
4.0	0.33047	0.13103	0.35549	4.5	0.31604	0.06241	0.32215
5.0	0.28701	-0.00059	0.28701	5.5	0.24552	-0.05433	0.25146
6.0	0.19516	-0.09583	0.21742	6.5	0.14044	-0.12314	0.18678
7.0	0.08616	-0.13561	0.16067	7.5	0.03680	-0.13399	0.13895
8.0	-0.00407	-0.12033	0.12039	8.5	-0.03411	-0.09773	0.10351
9.0	-0.05242	-0.06994	0.08741	9.5	-0.05954	-0.04087	0.07221
10.0	-0.05715	-0.01407	0.05885	10.5	-0.04777	0.00766	0.04838
11.0	-0.03431	0.02257	0.04107	11.5	-0.01962	0.03011	0.03594
12.0	-0.00610	0.03082	0.03141	12.5	0.00452	0.02613	0.02652
13.0	0.01132	0.01803	0.02129	13.5	0.01417	0.00867	0.01661
14.0	0.01361	-0.00001	0.01361	14.5	0.01061	-0.00656	0.01247
15.0	0.00633	-0.01019	0.01200	15.5	0.00191	-0.01080	0.01097
16.0	-0.00176	-0.00890	0.00907	16.5	-0.00414	-0.00539	0.00679
17.0	-0.00503	-0.00133	0.00520	17.5	-0.00460	0.00228	0.00513
18.0	-0.00323	0.00471	0.00571	18.5	-0.00141	0.00560	0.00577
19.0	0.00035	0.00499	0.00500	19.5	0.00168	0.00325	0.00366
20.0	0.00235	0.00095	0.00254	20.5	0.00234	-0.00128	0.00267
21.0	0.00177	-0.00292	0.00342	21.5	0.00087	-0.00365	0.00375
22.0	-0.00009	-0.00340	0.00340	22.5	-0.00088	-0.00233	0.00249
23.0	-0.00134	-0.00079	0.00155	23.5	-0.00141	0.00080	0.00162
24.0	-0.00112	0.00205	0.00233	24.5	-0.00060	0.00268	0.00275
25.0	-0.0	0.00260	0.00260				

Table A3-4c Diffraction pattern formed by the pupil T(x,M) for the case $\phi(x) = 1.5\pi x^2$

(AR= real part of amplitude,AI= imaginary part of amplitude,A= modulus of amplitude)

W	AR	AI	A	W	AR	AI	A
0.0	-0.00393	0.40303	0.40305	0.5	0.00651	0.39912	0.39917
1.0	0.03634	0.38711	0.38881	1.5	0.08129	0.36630	0.37521
2.0	0.13495	0.33587	0.36197	2.5	0.18970	0.29532	0.35100
3.0	0.23781	0.24492	0.34138	3.5	0.27255	0.18608	0.33002
4.0	0.28908	0.12147	0.31357	4.5	0.28510	0.05496	0.29034
5.0	0.26103	-0.00876	0.26118	5.5	0.21992	-0.06478	0.22926
6.0	0.16679	-0.10863	0.19905	6.5	0.10794	-0.13700	0.17441
7.0	0.04991	-0.14825	0.15643	7.5	-0.00137	-0.14275	0.14276
8.0	-0.04135	-0.12281	0.12958	8.5	-0.06739	-0.09238	0.11435
9.0	-0.07888	-0.05647	0.09701	9.5	-0.07719	-0.02036	0.07983
10.0	-0.06517	0.01114	0.06611	10.5	-0.04659	0.03442	0.05792
11.0	-0.02552	0.04746	0.05388	11.5	-0.00562	0.05004	0.05035
12.0	0.01028	0.04360	0.04479	12.5	0.02050	0.03081	0.03701
13.0	0.02461	0.01501	0.02883	13.5	0.02325	-0.00044	0.02326
14.0	0.01786	-0.01276	0.02195	14.5	0.01030	-0.02015	0.02263
15.0	0.00245	-0.02200	0.02214	15.5	-0.00413	-0.01887	0.01932
16.0	-0.00841	-0.01221	0.01483	16.5	-0.01000	-0.00396	0.01076
17.0	-0.00913	0.00387	0.00991	17.5	-0.00644	0.00965	0.01160
18.0	-0.00285	0.01239	0.01272	18.5	0.00070	0.01190	0.01192
19.0	0.00345	0.00870	0.00936	19.5	0.00493	0.00385	0.00626
20.0	0.00504	-0.00134	0.00521	20.5	0.00396	-0.00563	0.00688
21.0	0.00213	-0.00813	0.00840	21.5	0.00008	-0.00844	0.00844
22.0	-0.00170	-0.00670	0.00691	22.5	-0.00282	-0.00352	0.00451
23.0	-0.00313	0.00022	0.00314	23.5	-0.00266	0.00359	0.00446
24.0	-0.00162	0.00581	0.00603	24.5	-0.00032	0.00647	0.00648
25.0	0.00090	0.00552	0.00559				

Table A3-5a Diffraction pattern formed by the pupil T(x)=1 for the case $\phi(x) = 2\pi x^2$

(AR= real part of amplitude,AI= imaginary part of amplitude,A= modulus of amplitude)

W	AR	AI	A	W	AR	AI	A
0.0	-0.0	0.0	0.0	0.5	0.00005	0.00979	0.00979
1.0	0.00076	0.03736	0.03737	1.5	0.00365	0.07758	0.07767
2.0	0.01070	0.12293	0.12339	2.5	0.02370	0.16475	0.16645
3.0	0.04356	0.19479	0.19960	3.5	0.06976	0.20659	0.21805
4.0	0.10010	0.19661	0.22062	4.5	0.13090	0.16481	0.21047
5.0	0.15747	0.11466	0.19479	5.5	0.17497	0.05253	0.18268
6.0	0.17933	-0.01335	0.17983	6.5	0.16814	-0.07429	0.18382
7.0	0.14128	-0.12249	0.18699	7.5	0.10111	-0.15229	0.18280
8.0	0.05225	-0.16093	0.16920	8.5	0.00088	-0.14890	0.14890
9.0	-0.04624	-0.11965	0.12828	9.5	-0.08297	-0.07893	0.11451
10.0	-0.10476	-0.03367	0.11004	10.5	-0.10950	0.00914	0.10988
11.0	-0.09778	0.04358	0.10705	11.5	-0.07279	0.06564	0.09802
12.0	-0.03965	0.07372	0.08371	12.5	-0.00449	0.06859	0.06873
13.0	0.02670	0.05306	0.05940	13.5	0.04907	0.03130	0.05820
14.0	0.05974	0.00794	0.06026	14.5	0.05813	-0.01274	0.05951
15.0	0.04595	-0.02750	0.05355	15.5	0.02668	-0.03464	0.04372
16.0	0.00479	-0.03402	0.03436	16.5	-0.01522	-0.02699	0.03098
17.0	-0.02963	-0.01585	0.03360	17.5	-0.03620	-0.00339	0.03636
18.0	-0.03450	0.00776	0.03536	18.5	-0.02577	0.01558	0.03011
19.0	-0.01259	0.01899	0.02278	19.5	0.00182	0.01793	0.01802
20.0	0.01425	0.01325	0.01946	20.5	0.02226	0.00644	0.02318
21.0	0.02455	-0.00080	0.02456	21.5	0.02116	-0.00688	0.02225
22.0	0.01338	-0.01065	0.01710	22.5	0.00332	-0.01159	0.01206
23.0	-0.00657	-0.00986	0.01185	23.5	-0.01409	-0.00617	0.01538
24.0	-0.01776	-0.00155	0.01783	24.5	-0.01706	0.00287	0.01729
25.0	-0.01249	0.00613	0.01392				

Table A3-5b Diffraction pattern formed by the pupil T(x,5) for the case $\phi(x) = 2\pi x^2$

(AR= real part of amplitude, AI= imaginary part of amplitude, A= modulus of amplitude)

W	AR	AI	A	W	AR	AI	A
0.0	0.10137	0.34829	0.36274	0.5	0.10540	0.34760	0.36322
1.0	0.11717	0.34504	0.36439	1.5	0.13569	0.33931	0.36544
2.0	0.15939	0.32853	0.36515	2.5	0.18612	0.31068	0.36217
3.0	0.21332	0.28414	0.35530	3.5	0.23815	0.24803	0.34385
4.0	0.25775	0.20266	0.32788	4.5	0.26950	0.14958	0.30822
5.0	0.27131	0.09159	0.28635	5.5	0.26192	0.03240	0.26391
6.0	0.24107	-0.02375	0.24224	6.5	0.20967	-0.07268	0.22191
7.0	0.16972	-0.11082	0.20270	7.5	0.12419	-0.13566	0.18392
8.0	0.07666	-0.14612	0.16500	8.5	0.03096	-0.14263	0.14595
9.0	-0.00930	-0.12708	0.12742	9.5	-0.04117	-0.10251	0.11047
10.0	-0.06272	-0.07268	0.09600	10.5	-0.07325	-0.04153	0.08420
11.0	-0.07331	-0.01269	0.07440	11.5	-0.06461	0.01095	0.06553
12.0	-0.04967	0.02756	0.05681	12.5	-0.03150	0.03646	0.04818
13.0	-0.01308	0.03808	0.04026	13.5	0.00300	0.03376	0.03389
14.0	0.01487	0.02541	0.02944	14.5	0.02157	0.01517	0.02638
15.0	0.02310	0.00505	0.02365	15.5	0.02025	-0.00338	0.02053
16.0	0.01439	-0.00909	0.01703	16.5	0.00716	-0.01174	0.01375
17.0	0.00015	-0.01155	0.01155	17.5	-0.00536	-0.00919	0.01064
18.0	-0.00861	-0.00559	0.01027	18.5	-0.00938	-0.00171	0.00953
19.0	-0.00797	0.00163	0.00814	19.5	-0.00508	0.00388	0.00639
20.0	-0.00157	0.00481	0.00506	20.5	0.00168	0.00449	0.00480
21.0	0.00400	0.00324	0.00515	21.5	0.00501	0.00151	0.00524
22.0	0.00469	-0.00023	0.00469	22.5	0.00329	-0.00160	0.00365
23.0	0.00128	-0.00235	0.00268	23.5	-0.00077	-0.00243	0.00255
24.0	-0.00239	-0.00192	0.00306	24.5	-0.00324	-0.00104	0.00340
25.0	-0.00320	-0.00004	0.00320				

Table A3-5c Diffraction pattern formed by the pupil T(x,M) for the case $\phi(x) = 2\pi x^2$

(AR= real part of amplitude,AI= imaginary part of amplitude,A= modulus of amplitude)

W	AR	AI	A	W	AR	AI	A
0.0	0.01537	0.21209	0.21264	0.5	0.01898	0.21537	0.21620
1.0	0.02968	0.22423	0.22619	1.5	0.04709	0.23592	0.24057
2.0	0.07043	0.24642	0.25628	2.5	0.09842	0.25121	0.26980
3.0	0.12916	0.24613	0.27796	3.5	0.16011	0.22820	0.27877
4.0	0.18827	0.19624	0.27195	4.5	0.21036	0.15121	0.25906
5.0	0.22329	0.09614	0.24311	5.5	0.22461	0.03576	0.22744
6.0	0.21290	-0.02415	0.21426	6.5	0.18817	-0.07767	0.20357
7.0	0.15200	-0.11955	0.19338	7.5	0.10744	-0.14604	0.18130
8.0	0.05870	-0.15535	0.16607	8.5	0.01064	-0.14791	0.14829
9.0	-0.03194	-0.12618	0.13016	9.5	-0.06494	-0.09425	0.11446
10.0	-0.08554	-0.05717	0.10288	10.5	-0.09263	-0.02013	0.09479
11.0	-0.08690	0.01220	0.08776	11.5	-0.07072	0.03640	0.07953
12.0	-0.04764	0.05055	0.06946	12.5	-0.02188	0.05444	0.05867
13.0	0.00242	0.04936	0.04942	13.5	0.02181	0.03772	0.04357
14.0	0.03400	0.02256	0.04081	14.5	0.03816	0.00696	0.03879
15.0	0.03487	-0.00644	0.03546	15.5	0.02589	-0.01582	0.03034
16.0	0.01374	-0.02032	0.02453	16.5	0.00115	-0.02010	0.02014
17.0	-0.00944	-0.01612	0.01868	17.5	-0.01630	-0.00984	0.01904
18.0	-0.01866	-0.00288	0.01889	18.5	-0.01673	0.00326	0.01704
19.0	-0.01152	0.00754	0.01377	19.5	-0.00461	0.00941	0.01048
20.0	0.00231	0.00894	0.00923	20.5	0.00774	0.00662	0.01018
21.0	0.01069	0.00326	0.01117	21.5	0.01082	-0.00024	0.01082
22.0	0.00845	-0.00312	0.00901	22.5	0.00440	-0.00483	0.00653
23.0	-0.00022	-0.00518	0.00518	23.5	-0.00428	-0.00429	0.00606
24.0	-0.00692	-0.00254	0.00737	24.5	-0.00766	-0.00045	0.00768
25.0	-0.00652	0.00146	0.00668				

Table A3-6a Diffraction pattern formed by the pupil T(x)=1 for the case $\phi(x) = \pi x^4$

(AR= real part of amplitude, AI= imaginary part of amplitude, A= modulus of amplitude)

W	AR	AI	A	W	AR	AI	A
0.0	0.37398	0.50485	0.62829	0.5	0.37391	0.48517	0.61253
1.0	0.37277	0.42863	0.56805	1.5	0.36811	0.34234	0.50269
2.0	0.35654	0.23700	0.42812	2.5	0.33466	0.12529	0.35734
3.0	0.30009	0.02008	0.30076	3.5	0.25223	-0.06743	0.26109
4.0	0.19280	-0.12911	0.23204	4.5	0.12582	-0.16093	0.20428
5.0	0.05711	-0.16321	0.17291	5.5	-0.00658	-0.14026	0.14041
6.0	-0.05872	-0.09939	0.11544	6.5	-0.09414	-0.04958	0.10639
7.0	-0.10996	0.00005	0.10996	7.5	-0.10615	0.04162	0.11402
8.0	-0.08553	0.06960	0.11027	8.5	-0.05327	0.08140	0.09728
9.0	-0.01599	0.07744	0.07907	9.5	0.01944	0.06073	0.06377
10.0	0.04704	0.03604	0.05926	10.5	0.06274	0.00888	0.06336
11.0	0.06494	-0.01556	0.06678	11.5	0.05466	-0.03326	0.06399
12.0	0.03513	-0.04198	0.05474	12.5	0.01100	-0.04139	0.04283
13.0	-0.01258	-0.03294	0.03526	13.5	-0.03106	-0.01935	0.03659
14.0	-0.04130	-0.00395	0.04149	14.5	-0.04206	0.01001	0.04324
15.0	-0.03412	0.01998	0.03954	15.5	-0.01994	0.02454	0.03162
16.0	-0.00304	0.02347	0.02367	16.5	0.01282	0.01775	0.02189
17.0	0.02440	0.00912	0.02605	17.5	0.02965	-0.00027	0.02965
18.0	0.02802	-0.00839	0.02925	18.5	0.02047	-0.01371	0.02464
19.0	0.00914	-0.01547	0.01797	19.5	-0.00318	-0.01371	0.01408
20.0	-0.01373	-0.00923	0.01655	20.5	-0.02034	-0.00330	0.02061
21.0	-0.02187	0.00266	0.02203	21.5	-0.01838	0.00735	0.01979
22.0	-0.01104	0.00991	0.01484	22.5	-0.00179	0.01002	0.01017
23.0	0.00715	0.00790	0.01066	23.5	0.01380	0.00427	0.01444
24.0	0.01680	0.00007	0.01680	24.5	0.01575	-0.00370	0.01618
25.0	0.01117	-0.00627	0.01281				

Table A3-6b Diffraction pattern formed by the pupil T(x,5) for the case $\phi(x) = \pi x^4$

(AR= real part of amplitude, AI= imaginary part of amplitude, A= modulus of amplitude)

W	AR	AI	A	W	AR	AI	A
0.0	0.75596	0.32928	0.82456	0.5	0.74733	0.31847	0.81236
1.0	0.72174	0.28725	0.77680	1.5	0.68009	0.23906	0.72088
2.0	0.62391	0.17914	0.64912	2.5	0.55542	0.11383	0.56697
3.0	0.47752	0.04972	0.48010	3.5	0.39369	-0.00715	0.39376
4.0	0.30792	-0.05201	0.31228	4.5	0.22439	-0.08189	0.23887
5.0	0.14719	-0.09583	0.17563	5.5	0.07992	-0.09488	0.12405
6.0	0.02539	-0.08173	0.08558	6.5	-0.01472	-0.06022	0.06200
7.0	-0.04002	-0.03472	0.05298	7.5	-0.05145	-0.00942	0.05230
8.0	-0.05110	0.01215	0.05252	8.5	-0.04196	0.02757	0.05021
9.0	-0.02750	0.03570	0.04506	9.5	-0.01120	0.03668	0.03835
10.0	0.00385	0.03172	0.03195	10.5	0.01534	0.02272	0.02741
11.0	0.02194	0.01192	0.02497	11.5	0.02334	0.00145	0.02339
12.0	0.02020	-0.00700	0.02138	12.5	0.01383	-0.01236	0.01855
13.0	0.00594	-0.01428	0.01547	13.5	-0.00174	-0.01309	0.01321
14.0	-0.00780	-0.00961	0.01238	14.5	-0.01132	-0.00492	0.01234
15.0	-0.01199	-0.00015	0.01199	15.5	-0.01011	0.00376	0.01078
16.0	-0.00642	0.00619	0.00892	16.5	-0.00195	0.00692	0.00718
17.0	0.00228	0.00608	0.00650	17.5	0.00541	0.00412	0.00681
18.0	0.00693	0.00163	0.00712	18.5	0.00673	-0.00079	0.00678
19.0	0.00507	-0.00265	0.00572	19.5	0.00249	-0.00364	0.00441
20.0	-0.00032	-0.00368	0.00370	20.5	-0.00273	-0.00291	0.00399
21.0	-0.00423	-0.00161	0.00452	21.5	-0.00459	-0.00015	0.00459
22.0	-0.00386	0.00114	0.00402	22.5	-0.00231	0.00198	0.00305
23.0	-0.00039	0.00227	0.00230	23.5	0.00143	0.00200	0.00246
24.0	0.00274	0.00131	0.00304	24.5	0.00328	0.00041	0.00330
25.0	0.00300	-0.00047	0.00303				

Table A3-6c Diffraction pattern formed by the pupil T(x,M) for the case $\phi(x) = \pi x^4$

(AR= real part of amplitude,AI= imaginary part of amplitude,A= modulus of amplitude)

W	AR	AI	A	W	AR	AI	A
0.0	0.61403	0.41249	0.73972	0.5	0.60785	0.39781	0.72645
1.0	0.58926	0.35552	0.68820	1.5	0.55817	0.29057	0.62928
2.0	0.51472	0.21049	0.55610	2.5	0.45952	0.12425	0.47602
3.0	0.39398	0.04113	0.39613	3.5	0.32053	-0.03058	0.32198
4.0	0.24259	-0.08457	0.25691	4.5	0.16445	-0.11724	0.20196
5.0	0.09083	-0.12799	0.15694	5.5	0.02638	-0.11901	0.12190
6.0	-0.02497	-0.09481	0.09804	6.5	-0.06051	-0.06129	0.08613
7.0	-0.07925	-0.02484	0.08305	7.5	-0.08201	0.00870	0.08247
8.0	-0.07135	0.03476	0.07937	8.5	-0.05118	0.05060	0.07197
9.0	-0.02617	0.05544	0.06131	9.5	-0.00109	0.05040	0.05041
10.0	0.01997	0.03797	0.04290	10.5	0.03406	0.02148	0.04027
11.0	0.03979	0.00441	0.04004	11.5	0.03736	-0.01019	0.03872
12.0	0.02835	-0.02019	0.03481	12.5	0.01534	-0.02460	0.02899
13.0	0.00129	-0.02357	0.02361	13.5	-0.01098	-0.01822	0.02127
14.0	-0.01935	-0.01027	0.02191	14.5	-0.02269	-0.00168	0.02275
15.0	-0.02097	0.00578	0.02175	15.5	-0.01517	0.01084	0.01865
16.0	-0.00697	0.01287	0.01464	16.5	0.00165	0.01193	0.01205
17.0	0.00885	0.00868	0.01239	17.5	0.01328	0.00411	0.01391
18.0	0.01432	-0.00062	0.01434	18.5	0.01212	-0.00452	0.01294
19.0	0.00750	-0.00688	0.01018	19.5	0.00173	-0.00742	0.00762
20.0	-0.00382	-0.00628	0.00734	20.5	-0.00793	-0.00392	0.00885
21.0	-0.00985	-0.00103	0.00990	21.5	-0.00935	0.00171	0.00950
22.0	-0.00676	0.00372	0.00772	22.5	-0.00287	0.00464	0.00546
23.0	0.00133	0.00441	0.00460	23.5	0.00485	0.00321	0.00582
24.0	0.00696	0.00144	0.00710	24.5	0.00727	-0.00046	0.00728
25.0	0.00587	-0.00203	0.00621				

Table A3-7a Diffraction pattern formed by the pupil $T(x)=1$ for the case $\phi(x) = \pi x^4 - .5\pi x^2$

(AR= real part of amplitude,AI= imaginary part of amplitude,A= modulus of amplitude)

W	AR	AI	A	W	AR	AI	A
0.0	0.85300	0.20639	0.87762	0.5	0.82994	0.19340	0.85218
1.0	0.76327	0.15657	0.77916	1.5	0.66017	0.10195	0.66800
2.0	0.53155	0.03839	0.53293	2.5	0.39051	-0.02401	0.39125
3.0	0.25070	-0.07570	0.26188	3.5	0.12451	-0.10928	0.16567
4.0	0.02165	-0.12075	0.12267	4.5	-0.05188	-0.11003	0.12164
5.0	-0.09425	-0.08082	0.12415	5.5	-0.10759	-0.03975	0.11469
6.0	-0.09728	0.00497	0.09741	6.5	-0.07083	0.04510	0.08397
7.0	-0.03656	0.07388	0.08243	7.5	-0.00227	0.08714	0.08716
8.0	0.02577	0.08388	0.08775	8.5	0.04359	0.06624	0.07930
9.0	0.04973	0.03886	0.06311	9.5	0.04510	0.00778	0.04577
10.0	0.03242	-0.02077	0.03850	10.5	0.01544	-0.04164	0.04441
11.0	-0.00185	-0.05163	0.05166	11.5	-0.01605	-0.04997	0.05249
12.0	-0.02484	-0.03827	0.04563	12.5	-0.02731	-0.01998	0.03383
13.0	-0.02389	0.00045	0.02389	13.5	-0.01613	0.01856	0.02459
14.0	-0.00621	0.03078	0.03140	14.5	0.00356	0.03513	0.03531
15.0	0.01119	0.03143	0.03337	15.5	0.01542	0.02127	0.02627
16.0	0.01581	0.00743	0.01747	16.5	0.01281	-0.00673	0.01447
17.0	0.00747	-0.01809	0.01957	17.5	0.00122	-0.02440	0.02443
18.0	-0.00450	-0.02470	0.02511	18.5	-0.00853	-0.01943	0.02122
19.0	-0.01021	-0.01023	0.01445	19.5	-0.00946	0.00052	0.00947
20.0	-0.00672	0.01028	0.01229	20.5	-0.00283	0.01693	0.01716
21.0	0.00125	0.01919	0.01923	21.5	0.00460	0.01689	0.01750
22.0	0.00656	0.01087	0.01270	22.5	0.00684	0.00279	0.00739
23.0	0.00556	-0.00536	0.00772	23.5	0.00317	-0.01170	0.01212
24.0	0.00030	-0.01490	0.01490	24.5	-0.00234	-0.01442	0.01460
25.0	-0.00419	-0.01061	0.01141				

Table A3-7b Diffraction pattern formed by the pupil T(x,5) for the case $\phi(x) = \pi x^4 - .5\pi x^2$

(AR= real part of amplitude,AI= imaginary part of amplitude,A= modulus of amplitude)

W	AR	AI	A	W	AR	AI	A
0.0	0.95369	-0.00927	0.95373	0.5	0.93640	-0.01230	0.93648
1.0	0.88603	-0.02081	0.88627	1.5	0.80682	-0.03313	0.80750
2.0	0.70534	-0.04685	0.70690	2.5	0.58968	-0.05920	0.59265
3.0	0.46859	-0.06762	0.47344	3.5	0.35053	-0.07013	0.35748
4.0	0.24284	-0.06576	0.25159	4.5	0.15107	-0.05469	0.16066
5.0	0.07858	-0.03817	0.08736	5.5	0.02648	-0.01836	0.03222
6.0	-0.00627	0.00211	0.00662	6.5	-0.02237	0.02053	0.03037
7.0	-0.02565	0.03464	0.04311	7.5	-0.02041	0.04292	0.04753
8.0	-0.01084	0.04482	0.04611	8.5	-0.00049	0.04079	0.04079
9.0	0.00803	0.03215	0.03314	9.5	0.01323	0.02081	0.02466
10.0	0.01466	0.00886	0.01713	10.5	0.01275	-0.00175	0.01287
11.0	0.00854	-0.00953	0.01279	11.5	0.00330	-0.01369	0.01408
12.0	-0.00171	-0.01416	0.01426	12.5	-0.00553	-0.01155	0.01281
13.0	-0.00759	-0.00694	0.01028	13.5	-0.00778	-0.00160	0.00794
14.0	-0.00638	0.00323	0.00715	14.5	-0.00395	0.00660	0.00769
15.0	-0.00116	0.00802	0.00810	15.5	0.00137	0.00744	0.00757
16.0	0.00314	0.00528	0.00615	16.5	0.00393	0.00221	0.00451
17.0	0.00373	-0.00097	0.00385	17.5	0.00275	-0.00353	0.00447
18.0	0.00132	-0.00497	0.00514	18.5	-0.00018	-0.00510	0.00511
19.0	-0.00140	-0.00404	0.00428	19.5	-0.00212	-0.00215	0.00302
20.0	-0.00226	0.00004	0.00226	20.5	-0.00186	0.00199	0.00272
21.0	-0.00110	0.00328	0.00346	21.5	-0.00019	0.00367	0.00367
22.0	0.00064	0.00315	0.00322	22.5	0.00122	0.00194	0.00229
23.0	0.00143	0.00037	0.00148	23.5	0.00129	-0.00116	0.00173
24.0	0.00087	-0.00228	0.00243	24.5	0.00029	-0.00276	0.00278
25.0	-0.00029	-0.00255	0.00256				

Table A3-7c Diffraction pattern formed by the pupil $T(x,M)$ for the case $\phi(x) = \pi x^4 - .5\pi x^2$

(AR= real part of amplitude, AI= imaginary part of amplitude, A= modulus of amplitude)

W	AR	AI	A	W	AR	AI	A
0.0	0.92014	0.06860	0.92269	0.5	0.89998	0.06209	0.90212
1.0	0.84145	0.04370	0.84258	1.5	0.75010	0.01659	0.75028
2.0	0.63443	-0.01461	0.63459	2.5	0.50480	-0.04460	0.50677
3.0	0.37224	-0.06838	0.37847	3.5	0.24711	-0.08209	0.26039
4.0	0.13803	-0.08366	0.16140	4.5	0.05101	-0.07311	0.08915
5.0	-0.01096	-0.05252	0.05366	5.5	-0.04795	-0.02554	0.05433
6.0	-0.06270	0.00329	0.06279	6.5	-0.05991	0.02935	0.06671
7.0	-0.04539	0.04876	0.06662	7.5	-0.02513	0.05903	0.06416
8.0	-0.00448	0.05938	0.05955	8.5	0.01249	0.05076	0.05227
9.0	0.02331	0.03557	0.04253	9.5	0.02718	0.01713	0.03212
10.0	0.02475	-0.00104	0.02477	10.5	0.01773	-0.01581	0.02376
11.0	0.00837	-0.02502	0.02639	11.5	-0.00104	-0.02779	0.02780
12.0	-0.00862	-0.02450	0.02598	12.5	-0.01318	-0.01668	0.02126
13.0	-0.01429	-0.00652	0.01571	13.5	-0.01231	0.00359	0.01283
14.0	-0.00815	0.01157	0.01415	14.5	-0.00300	0.01600	0.01628
15.0	0.00192	0.01638	0.01650	15.5	0.00564	0.01312	0.01428
16.0	0.00756	0.00734	0.01053	16.5	0.00756	0.00058	0.00758
17.0	0.00592	-0.00555	0.00811	17.5	0.00324	-0.00977	0.01029
18.0	0.00024	-0.01133	0.01134	18.5	-0.00238	-0.01016	0.01043
19.0	-0.00410	-0.00677	0.00792	19.5	-0.00468	-0.00216	0.00515
20.0	-0.00413	0.00252	0.00484	20.5	-0.00272	0.00619	0.00677
21.0	-0.00088	0.00810	0.00815	21.5	0.00093	0.00796	0.00802
22.0	0.00230	0.00597	0.00640	22.5	0.00299	0.00275	0.00406
23.0	0.00291	-0.00087	0.00304	23.5	0.00218	-0.00400	0.00455
24.0	0.00102	-0.00595	0.00604	24.5	-0.00024	-0.00636	0.00637
25.0	-0.00131	-0.00524	0.00540				

Table A3-8a Diffraction pattern formed by the pupil T(x)=1 for the case $\phi(x) = \pi x^4 - \pi x^2$

(AR= real part of amplitude, AI= imaginary part of amplitude, A= modulus of amplitude)

W	AR	AI	A	W	AR	AI	A
0.0	0.84184	-0.48759	0.97285	0.5	0.81581	-0.47250	0.94276
1.0	0.74102	-0.42890	0.85619	1.5	0.62679	-0.36162	0.72363
2.0	0.48708	-0.27794	0.56080	2.5	0.33826	-0.18667	0.38635
3.0	0.19670	-0.09691	0.21927	3.5	0.07635	-0.01695	0.07821
4.0	-0.01307	0.04675	0.04854	4.5	-0.06718	0.09024	0.11250
5.0	-0.08710	0.11240	0.14220	5.5	-0.07870	0.11479	0.13918
6.0	-0.05111	0.10116	0.11334	6.5	-0.01487	0.07672	0.07815
7.0	0.02002	0.04724	0.05131	7.5	0.04575	0.01816	0.04923
8.0	0.05776	-0.00615	0.05808	8.5	0.05510	-0.02286	0.05966
9.0	0.04013	-0.03088	0.05064	9.5	0.01754	-0.03076	0.03541
10.0	-0.00686	-0.02429	0.02524	10.5	-0.02753	-0.01407	0.03091
11.0	-0.04033	-0.00286	0.04043	11.5	-0.04323	0.00691	0.04378
12.0	-0.03657	0.01349	0.03897	12.5	-0.02269	0.01609	0.02781
13.0	-0.00530	0.01482	0.01574	13.5	0.01148	0.01056	0.01559
14.0	0.02403	0.00466	0.02448	14.5	0.03000	-0.00140	0.03004
15.0	0.02869	-0.00631	0.02937	15.5	0.02104	-0.00918	0.02296
16.0	0.00935	-0.00968	0.01345	16.5	-0.00342	-0.00802	0.00872
17.0	-0.01430	-0.00483	0.01509	17.5	-0.02098	-0.00099	0.02100
18.0	-0.02229	0.00259	0.02244	18.5	-0.01838	0.00515	0.01909
19.0	-0.01054	0.00628	0.01226	19.5	-0.00087	0.00588	0.00594
20.0	0.00826	0.00422	0.00928	20.5	0.01480	0.00181	0.01491
21.0	0.01743	-0.00074	0.01744	21.5	0.01581	-0.00284	0.01606
22.0	0.01061	-0.00408	0.01137	22.5	0.00329	-0.00427	0.00539
23.0	-0.00432	-0.00347	0.00554	23.5	-0.01041	-0.00197	0.01060
24.0	-0.01367	-0.00017	0.01368	24.5	-0.01352	0.00149	0.01360
25.0	-0.01019	0.00265	0.01053				

Table A3-8b Diffraction pattern formed by the pupil T(x,5) for the case $\phi(x) = \pi x^4 - \pi x^2$

(AR= real part of amplitude,AI= imaginary part of amplitude,A= modulus of amplitude)

W	AR	AI	A	W	AR	AI	A
0.0	0.85676	-0.45657	0.97082	0.5	0.84099	-0.44584	0.95186
1.0	0.79515	-0.41464	0.89677	1.5	0.72350	-0.36579	0.81071
2.0	0.63247	-0.30362	0.70157	2.5	0.52990	-0.23347	0.57905
3.0	0.42405	-0.16109	0.45361	3.5	0.32261	-0.09200	0.33548
4.0	0.23192	-0.03094	0.23398	4.5	0.15631	0.01860	0.15741
5.0	0.09789	0.05459	0.11209	5.5	0.05659	0.07660	0.09523
6.0	0.03051	0.08558	0.09085	6.5	0.01650	0.08364	0.08525
7.0	0.01081	0.07364	0.07443	7.5	0.00976	0.05872	0.05952
8.0	0.01025	0.04192	0.04315	8.5	0.01012	0.02580	0.02771
9.0	0.00827	0.01223	0.01476	9.5	0.00459	0.00228	0.00513
10.0	-0.00027	-0.00377	0.00378	10.5	-0.00528	-0.00627	0.00820
11.0	-0.00936	-0.00603	0.01113	11.5	-0.01166	-0.00409	0.01236
12.0	-0.01180	-0.00147	0.01189	12.5	-0.00987	0.00098	0.00992
13.0	-0.00643	0.00267	0.00696	13.5	-0.00230	0.00335	0.00406
14.0	0.00162	0.00305	0.00346	14.5	0.00456	0.00203	0.00499
15.0	0.00603	0.00065	0.00606	15.5	0.00591	-0.00070	0.00595
16.0	0.00443	-0.00171	0.00474	16.5	0.00209	-0.00220	0.00303
17.0	-0.00046	-0.00212	0.00217	17.5	-0.00262	-0.00159	0.00306
18.0	-0.00392	-0.00078	0.00400	18.5	-0.00415	0.00008	0.00415
19.0	-0.00337	0.00080	0.00346	19.5	-0.00185	0.00124	0.00222
20.0	-0.00003	0.00132	0.00132	20.5	0.00164	0.00109	0.00197
21.0	0.00277	0.00064	0.00285	21.5	0.00315	0.00010	0.00315
22.0	0.00273	-0.00040	0.00276	22.5	0.00169	-0.00074	0.00184
23.0	0.00032	-0.00086	0.00092	23.5	-0.00102	-0.00077	0.00128
24.0	-0.00202	-0.00051	0.00209	24.5	-0.00246	-0.00016	0.00247
25.0	-0.00228	0.00019	0.00229				

Table A3-8c Diffraction pattern formed by the pupil T(x,M) for the case $\phi(x) = \pi x^4 - \pi x^2$

(AR= real part of amplitude,AI= imaginary part of amplitude,A= modulus of amplitude)

W	AR	AI	A	W	AR	AI	A
0.0	0.84410	-0.48291	0.97247	0.5	0.82426	-0.47002	0.94885
1.0	0.76689	-0.43264	0.88051	1.5	0.67816	-0.37447	0.77468
2.0	0.56736	-0.30120	0.64235	2.5	0.44559	-0.21972	0.49681
3.0	0.32425	-0.13735	0.35215	3.5	0.21359	-0.06096	0.22212
4.0	0.12140	0.00379	0.12146	4.5	0.05229	0.05303	0.07448
5.0	0.00741	0.08494	0.08526	5.5	-0.01530	0.09976	0.10093
6.0	-0.02033	0.09958	0.10163	6.5	-0.01357	0.08779	0.08883
7.0	-0.00125	0.06854	0.06855	7.5	0.01117	0.04608	0.04742
8.0	0.01971	0.02421	0.03122	8.5	0.02232	0.00584	0.02307
9.0	0.01881	-0.00727	0.02017	9.5	0.01060	-0.01452	0.01798
10.0	0.00007	-0.01634	0.01634	10.5	-0.01012	-0.01397	0.01725
11.0	-0.01765	-0.00901	0.01981	11.5	-0.02102	-0.00318	0.02126
12.0	-0.01984	0.00206	0.01994	12.5	-0.01474	0.00571	0.01581
13.0	-0.00717	0.00730	0.01023	13.5	0.00100	0.00688	0.00695
14.0	0.00797	0.00492	0.00937	14.5	0.01234	0.00214	0.01253
15.0	0.01345	-0.00072	0.01347	15.5	0.01139	-0.00299	0.01177
16.0	0.00694	-0.00426	0.00815	16.5	0.00137	-0.00440	0.00460
17.0	-0.00396	-0.00353	0.00530	17.5	-0.00785	-0.00199	0.00810
18.0	-0.00954	-0.00022	0.00955	18.5	-0.00885	0.00136	0.00895
19.0	-0.00614	0.00242	0.00660	19.5	-0.00222	0.00280	0.00357
20.0	0.00190	0.00249	0.00313	20.5	0.00524	0.00165	0.00550
21.0	0.00708	0.00053	0.00710	21.5	0.00710	-0.00057	0.00713
22.0	0.00544	-0.00141	0.00562	22.5	0.00260	-0.00183	0.00318
23.0	-0.00065	-0.00178	0.00190	23.5	-0.00352	-0.00132	0.00376
24.0	-0.00537	-0.00061	0.00540	24.5	-0.00581	0.00018	0.00581
25.0	-0.00483	0.00084	0.00491				

Table A3-9a Diffraction pattern formed by the pupil T(x)=1 for the case $\phi(x) = \pi x^4 - 1.5\pi x^2$

(AR= real part of amplitude,AI= imaginary part of amplitude,A= modulus of amplitude)

W	AR	AI	A	W	AR	AI	A
0.0	0.20639	-0.85300	0.87762	0.5	0.20664	-0.82328	0.84882
1.0	0.20707	-0.73787	0.76637	1.5	0.20686	-0.60739	0.64165
2.0	0.20478	-0.44778	0.49238	2.5	0.19948	-0.27778	0.34199
3.0	0.18981	-0.11628	0.22260	3.5	0.17502	0.02047	0.17621
4.0	0.15498	0.12094	0.19658	4.5	0.13028	0.17963	0.22190
5.0	0.10223	0.19733	0.22223	5.5	0.07262	0.18035	0.19442
6.0	0.04358	0.13899	0.14566	6.5	0.01723	0.08540	0.08712
7.0	-0.00460	0.03150	0.03183	7.5	-0.02063	-0.01302	0.02439
8.0	-0.03027	-0.04191	0.05170	8.5	-0.03369	-0.05299	0.06280
9.0	-0.03175	-0.04789	0.05746	9.5	-0.02583	-0.03112	0.04044
10.0	-0.01759	-0.00880	0.01967	10.5	-0.00874	0.01281	0.01551
11.0	-0.00077	0.02862	0.02863	11.5	0.00524	0.03561	0.03599
12.0	0.00872	0.03316	0.03428	12.5	0.00960	0.02288	0.02482
13.0	0.00828	0.00803	0.01154	13.5	0.00549	-0.00747	0.00927
14.0	0.00205	-0.01993	0.02003	14.5	-0.00120	-0.02672	0.02675
15.0	-0.00362	-0.02676	0.02701	15.5	-0.00485	-0.02062	0.02118
16.0	-0.00482	-0.01023	0.01131	16.5	-0.00372	0.00167	0.00408
17.0	-0.00195	0.01221	0.01236	17.5	0.00002	0.01906	0.01906
18.0	0.00173	0.02093	0.02100	18.5	0.00284	0.01778	0.01800
19.0	0.00319	0.01071	0.01117	19.5	0.00279	0.00166	0.00325
20.0	0.00182	-0.00713	0.00736	20.5	0.00056	-0.01361	0.01362
21.0	-0.00069	-0.01645	0.01646	21.5	-0.00165	-0.01522	0.01531
22.0	-0.00213	-0.01049	0.01070	22.5	-0.00208	-0.00359	0.00415
23.0	-0.00158	0.00371	0.00403	23.5	-0.00076	0.00968	0.00971
24.0	0.00014	0.01299	0.01299	24.5	0.00092	0.01303	0.01306
25.0	0.00142	0.00998	0.01008				

Table A3-9b Diffraction pattern formed by the pupil T(x,5) for the case $\phi(x) = \pi x^4 - 1.5\pi x^2$

(AR= real part of amplitude,AI= imaginary part of amplitude,A= modulus of amplitude)

W	AR	AI	A	W	AR	AI	A
0.0	0.47051	-0.70884	0.85078	0.5	0.46746	-0.69121	0.83444
1.0	0.45829	-0.64007	0.78722	1.5	0.44306	-0.56043	0.71441
2.0	0.42186	-0.45992	0.62409	2.5	0.39494	-0.34782	0.52627
3.0	0.36274	-0.23391	0.43162	3.5	0.32597	-0.12733	0.34996
4.0	0.28561	-0.03554	0.28781	4.5	0.24291	0.03636	0.24561
5.0	0.19934	0.08599	0.21710	5.5	0.15650	0.11367	0.19343
6.0	0.11600	0.12197	0.16832	6.5	0.07928	0.11513	0.13978
7.0	0.04754	0.09818	0.10909	7.5	0.02161	0.07622	0.07923
8.0	0.00188	0.05367	0.05370	8.5	-0.01174	0.03382	0.03580
9.0	-0.01973	0.01861	0.02712	9.5	-0.02293	0.00866	0.02451
10.0	-0.02242	0.00348	0.02269	10.5	-0.01937	0.00186	0.01946
11.0	-0.01493	0.00228	0.01510	11.5	-0.01009	0.00331	0.01062
12.0	-0.00564	0.00387	0.00684	12.5	-0.00209	0.00340	0.00399
13.0	0.00032	0.00185	0.00188	13.5	0.00160	-0.00040	0.00165
14.0	0.00192	-0.00276	0.00336	14.5	0.00157	-0.00462	0.00488
15.0	0.00087	-0.00550	0.00557	15.5	0.00011	-0.00522	0.00522
16.0	-0.00050	-0.00388	0.00391	16.5	-0.00082	-0.00184	0.00201
17.0	-0.00084	0.00039	0.00093	17.5	-0.00061	0.00230	0.00238
18.0	-0.00024	0.00348	0.00349	18.5	0.00016	0.00372	0.00373
19.0	0.00048	0.00305	0.00309	19.5	0.00065	0.00171	0.00183
20.0	0.00065	0.00007	0.00065	20.5	0.00050	-0.00145	0.00154
21.0	0.00025	-0.00251	0.00252	21.5	-0.00002	-0.00287	0.00287
22.0	-0.00026	-0.00251	0.00252	22.5	-0.00041	-0.00156	0.00161
23.0	-0.00044	-0.00030	0.00053	23.5	-0.00037	0.00095	0.00101
24.0	-0.00022	0.00188	0.00189	24.5	-0.00003	0.00230	0.00230
25.0	0.00014	0.00213	0.00214				

Table A3-9c Diffraction pattern formed by the pupil $T(x,M)$ for the case $\phi(x) = \pi x^4 - 1.5\pi x^2$

(AR= real part of amplitude,AI= imaginary part of amplitude;A= modulus of amplitude)

W	AR	AI	A	W	AR	AI	A
0.0	0.35151	-0.77931	0.85492	0.5	0.34975	-0.75665	0.83358
1.0	0.34433	-0.69120	0.77222	1.5	0.33498	-0.59015	0.67860
2.0	0.32130	-0.46436	0.56469	2.5	0.30295	-0.32687	0.44567
3.0	0.27975	-0.19110	0.33879	3.5	0.25187	-0.06916	0.26119
4.0	0.21986	0.02963	0.22185	4.5	0.18474	0.09966	0.20991
5.0	0.14789	0.13946	0.20328	5.5	0.11100	0.15137	0.18771
6.0	0.07584	0.14076	0.15989	6.5	0.04412	0.11487	0.12305
7.0	0.01728	0.08150	0.08331	7.5	-0.00371	0.04779	0.04793
8.0	-0.01838	0.01924	0.02660	8.5	-0.02685	-0.00082	0.02686
9.0	-0.02978	-0.01136	0.03188	9.5	-0.02824	-0.01338	0.03125
10.0	-0.02356	-0.00927	0.02532	10.5	-0.01716	-0.00210	0.01729
11.0	-0.01034	0.00515	0.01155	11.5	-0.00418	0.01018	0.01101
12.0	0.00058	0.01175	0.01177	12.5	0.00360	0.00975	0.01039
13.0	0.00486	0.00503	0.00699	13.5	0.00464	-0.00094	0.00474
14.0	0.00341	-0.00652	0.00736	14.5	0.00170	-0.01033	0.01047
15.0	0.0	-0.01154	0.01154	15.5	-0.00131	-0.01003	0.01011
16.0	-0.00202	-0.00633	0.00665	16.5	-0.00209	-0.00148	0.00256
17.0	-0.00162	0.00332	0.00369	17.5	-0.00082	0.00694	0.00699
18.0	0.00006	0.00863	0.00863	18.5	0.00082	0.00816	0.00820
19.0	0.00129	0.00579	0.00593	19.5	0.00139	0.00223	0.00263
20.0	0.00117	-0.00158	0.00196	20.5	0.00069	-0.00474	0.00479
21.0	0.00012	-0.00653	0.00653	21.5	-0.00041	-0.00664	0.00665
22.0	-0.00079	-0.00516	0.00522	22.5	-0.00094	-0.00254	0.00271
23.0	-0.00086	0.00052	0.00101	23.5	-0.00059	0.00325	0.00331
24.0	-0.00021	0.00504	0.00504	24.5	0.00018	0.00550	0.00551
25.0	0.00049	0.00462	0.00465				

Table A3-10a Diffraction pattern formed by the pupil T(x)=1 for the case $\phi(x) = \pi x^4 - 2\pi x^2$

(AR= real part of amplitude,AI= imaginary part of amplitude,A= modulus of amplitude)

W	AR	AI	A	W	AR	AI	A
0.0	-0.37398	-0.50486	0.62828	0.5	-0.35089	-0.49328	0.60535
1.0	-0.28497	-0.45956	0.54074	1.5	-0.18572	-0.40657	0.44698
2.0	-0.06722	-0.33879	0.34539	2.5	0.05408	-0.26174	0.26727
3.0	0.16201	-0.18149	0.24328	3.5	0.24315	-0.10394	0.26444
4.0	0.28875	-0.03432	0.29078	4.5	0.29584	0.02333	0.29676
5.0	0.26731	0.06646	0.27545	5.5	0.21107	0.09408	0.23109
6.0	0.13838	0.10678	0.17479	6.5	0.06175	0.10643	0.12305
7.0	-0.00717	0.09585	0.09612	7.5	-0.05939	0.07836	0.09833
8.0	-0.08984	0.05739	0.10660	8.5	-0.09770	0.03604	0.10413
9.0	-0.08608	0.01680	0.08771	9.5	-0.06096	0.00139	0.06098
10.0	-0.02975	-0.00932	0.03117	10.5	0.00026	-0.01525	0.01525
11.0	0.02322	-0.01697	0.02876	11.5	0.03566	-0.01546	0.03887
12.0	0.03681	-0.01192	0.03869	12.5	0.02841	-0.00750	0.02938
13.0	0.01396	-0.00322	0.01433	13.5	-0.00220	0.00023	0.00221
14.0	-0.01597	0.00247	0.01616	14.5	-0.02431	0.00343	0.02455
15.0	-0.02583	0.00329	0.02604	15.5	-0.02085	0.00241	0.02099
16.0	-0.01120	0.00118	0.01127	16.5	0.00038	-0.00004	0.00039
17.0	0.01098	-0.00096	0.01102	17.5	0.01815	-0.00145	0.01821
18.0	0.02047	-0.00148	0.02052	18.5	0.01776	-0.00114	0.01780
19.0	0.01104	-0.00058	0.01106	19.5	0.00220	0.00003	0.00220
20.0	-0.00654	0.00054	0.00657	20.5	-0.01312	0.00084	0.01315
21.0	-0.01615	0.00091	0.01617	21.5	-0.01514	0.00075	0.01516
22.0	-0.01061	0.00044	0.01062	22.5	-0.00386	0.00008	0.00386
23.0	0.00338	-0.00026	0.00339	23.5	0.00936	-0.00049	0.00938
24.0	0.01276	-0.00057	0.01277	24.5	0.01292	-0.00052	0.01293
25.0	0.01000	-0.00035	0.01001				

Table A3-10b Diffraction pattern formed by the pupil T(x,5) for the case $\phi(x) = \pi x^4 - 2\pi x^2$

(AR= real part of amplitude, AI= imaginary part of amplitude, A= modulus of amplitude)

W	AR	AI	A	W	AR	AI	A
0.0	0.08014	-0.61822	0.62339	0.5	0.08893	-0.60690	0.61338
1.0	0.11399	-0.57374	0.58496	1.5	0.15166	-0.52112	0.54274
2.0	0.19640	-0.45274	0.49350	2.5	0.24168	-0.37326	0.44468
3.0	0.28092	-0.28794	0.40228	3.5	0.30841	-0.20209	0.36873
4.0	0.32011	-0.12070	0.34211	4.5	0.31416	-0.04796	0.31780
5.0	0.29102	0.01293	0.29130	5.5	0.25329	0.06004	0.26031
6.0	0.20525	0.09265	0.22519	6.5	0.15208	0.11128	0.18844
7.0	0.09914	0.11739	0.15366	7.5	0.05122	0.11321	0.12425
8.0	0.01190	0.10137	0.10206	8.5	-0.01673	0.08464	0.08628
9.0	-0.03422	0.06565	0.07403	9.5	-0.04155	0.04664	0.06246
10.0	-0.04076	0.02934	0.05022	10.5	-0.03452	0.01492	0.03761
11.0	-0.02556	0.00395	0.02587	11.5	-0.01629	-0.00349	0.01666
12.0	-0.00846	-0.00773	0.01146	12.5	-0.00302	-0.00935	0.00983
13.0	-0.00018	-0.00908	0.00908	13.5	0.00049	-0.00762	0.00764
14.0	-0.00024	-0.00564	0.00564	14.5	-0.00148	-0.00362	0.00391
15.0	-0.00247	-0.00189	0.00311	15.5	-0.00271	-0.00063	0.00278
16.0	-0.00208	0.00014	0.00209	16.5	-0.00075	0.00048	0.00089
17.0	0.00090	0.00051	0.00103	17.5	0.00240	0.00037	0.00242
18.0	0.00334	0.00016	0.00335	18.5	0.00351	-0.00001	0.00351
19.0	0.00286	-0.00011	0.00287	19.5	0.00160	-0.00012	0.00161
20.0	0.00005	-0.00007	0.00009	20.5	-0.00140	0.00002	0.00140
21.0	-0.00241	0.00010	0.00241	21.5	-0.00277	0.00015	0.00278
22.0	-0.00244	0.00016	0.00245	22.5	-0.00154	0.00014	0.00155
23.0	-0.00033	0.00008	0.00034	23.5	0.00089	0.00001	0.00089
24.0	0.00181	-0.00005	0.00181	24.5	0.00223	-0.00009	0.00223
25.0	0.00208	-0.00011	0.00209				

Table A3-10c Diffraction pattern formed by the pupil T(x,M) for the case $\phi(x) = \pi x^4 - 2\pi x^2$

(AR= real part of amplitude,AI= imaginary part of amplitude,A= modulus of amplitude)

W	AR	AI	A	W	AR	AI	A
0.0	-0.12300	-0.58783	0.60056	0.5	-0.10852	-0.57589	0.58603
1.0	-0.06714	-0.54100	0.54515	1.5	-0.00474	-0.48586	0.48588
2.0	0.06990	-0.41469	0.42054	2.5	0.14647	-0.33276	0.36357
3.0	0.21466	-0.24592	0.32643	3.5	0.26569	-0.16003	0.31016
4.0	0.29353	-0.08041	0.30434	4.5	0.29565	-0.01144	0.29587
5.0	0.27318	0.04383	0.27668	5.5	0.23052	0.08375	0.24527
6.0	0.17443	0.10815	0.20524	6.5	0.11284	0.11816	0.16338
7.0	0.05356	0.11595	0.12772	7.5	0.00315	0.10438	0.10442
8.0	-0.03394	0.08661	0.09302	8.5	-0.05579	0.06577	0.08624
9.0	-0.06298	0.04462	0.07718	9.5	-0.05812	0.02537	0.06342
10.0	-0.04517	0.00950	0.04616	10.5	-0.02853	-0.00221	0.02862
11.0	-0.01225	-0.00965	0.01560	11.5	0.00061	-0.01323	0.01324
12.0	0.00837	-0.01371	0.01606	12.5	0.01076	-0.01203	0.01614
13.0	0.00870	-0.00915	0.01262	13.5	0.00391	-0.00591	0.00708
14.0	-0.00163	-0.00294	0.00336	14.5	-0.00616	-0.00063	0.00619
15.0	-0.00847	0.00084	0.00851	15.5	-0.00815	0.00151	0.00829
16.0	-0.00551	0.00155	0.00572	16.5	-0.00145	0.00117	0.00187
17.0	0.00286	0.00062	0.00293	17.5	0.00629	0.00009	0.00629
18.0	0.00802	-0.00029	0.00802	18.5	0.00772	-0.00046	0.00773
19.0	0.00558	-0.00044	0.00560	19.5	0.00224	-0.00028	0.00226
20.0	-0.00142	-0.00006	0.00142	20.5	-0.00450	0.00015	0.00450
21.0	-0.00630	0.00029	0.00631	21.5	-0.00648	0.00034	0.00649
22.0	-0.00509	0.00030	0.00510	22.5	-0.00257	0.00019	0.00257
23.0	0.00041	0.00004	0.00042	23.5	0.00311	-0.00009	0.00311
24.0	0.00489	-0.00019	0.00490	24.5	0.00539	-0.00023	0.00540
25.0	0.00457	-0.00021	0.00457				

Table A3-11a. Diffraction pattern formed by the pupil T(x)=1 for the case $\phi(x) = 2\pi x^4$

(AR= real part of amplitude,AI= imaginary part of amplitude,A= modulus of amplitude)

W	AR	AI	A	W	AR	AI	A
0.0	0.24413	0.17171	0.29846	0.5	0.24411	0.17165	0.29842
1.0	0.24391	0.17080	0.29777	1.5	0.24305	0.16733	0.29508
2.0	0.24073	0.15874	0.28836	2.5	0.23592	0.14262	0.27568
3.0	0.22738	0.11737	0.25589	3.5	0.21386	0.08289	0.22936
4.0	0.19429	0.04088	0.19854	4.5	0.16806	-0.00517	0.16814
5.0	0.13524	-0.05036	0.14431	5.5	0.09682	-0.08924	0.13167
6.0	0.05474	-0.11666	0.12886	6.5	0.01185	-0.12879	0.12933
7.0	-0.02836	-0.12386	0.12706	7.5	-0.06220	-0.10263	0.12001
8.0	-0.08633	-0.06832	0.11009	8.5	-0.09827	-0.02622	0.10171
9.0	-0.09695	0.01724	0.09847	9.5	-0.08294	0.05547	0.09978
10.0	-0.05853	0.08286	0.10144	10.5	-0.02747	0.09572	0.09958
11.0	0.00554	0.09282	0.09298	11.5	0.03554	0.07558	0.08352
12.0	0.05812	0.04771	0.07520	12.5	0.07014	0.01452	0.07163
13.0	0.07020	-0.01811	0.07250	13.5	0.05890	-0.04474	0.07397
14.0	0.03870	-0.06129	0.07249	14.5	0.01347	-0.06573	0.06710
15.0	-0.01222	-0.05829	0.05956	15.5	-0.03391	-0.04127	0.05341
16.0	-0.04805	-0.01854	0.05150	16.5	-0.05261	0.00533	0.05287
17.0	-0.04736	0.02589	0.05398	17.5	-0.03390	0.03967	0.05218
18.0	-0.01524	0.04473	0.04725	18.5	0.00483	0.04091	0.04120
19.0	0.02243	0.02975	0.03726	19.5	0.03441	0.01403	0.03716
20.0	0.03887	-0.00282	0.03897	20.5	0.03545	-0.01745	0.03951
21.0	0.02538	-0.02724	0.03723	21.5	0.01109	-0.03071	0.03265
22.0	-0.00430	-0.02777	0.02810	22.5	-0.01764	-0.01960	0.02637
23.0	-0.02640	-0.00831	0.02767	23.5	-0.02913	0.00355	0.02934
24.0	-0.02569	0.01354	0.02904	24.5	-0.01723	0.01981	0.02625
25.0	-0.00584	0.02141	0.02219				

Table A3-11b Diffraction pattern formed by the pupil T(x,5) for the case $\phi(x) = 2\pi x^4$

(AR= real part of amplitude,AI= imaginary part of amplitude,A= modulus of amplitude)

W	AR	AI	A	W	AR	AI	A
0.0	0.56367	0.29903	0.63808	0.5	0.56040	0.29309	0.63242
1.0	0.55048	0.27554	0.61559	1.5	0.53366	0.24724	0.58815
2.0	0.50959	0.20964	0.55103	2.5	0.47800	0.16477	0.50560
3.0	0.43883	0.11520	0.45370	3.5	0.39239	0.06395	0.39757
4.0	0.33953	0.01429	0.33983	4.5	0.28165	-0.03045	0.28329
5.0	0.22075	-0.06725	0.23077	5.5	0.15933	-0.09366	0.18481
6.0	0.10019	-0.10813	0.14741	6.5	0.04626	-0.11022	0.11953
7.0	0.00020	-0.10070	0.10070	7.5	-0.03578	-0.08152	0.08902
8.0	-0.06027	-0.05556	0.08197	8.5	-0.07282	-0.02633	0.07743
9.0	-0.07402	0.00247	0.07406	9.5	-0.06546	0.02742	0.07097
10.0	-0.04958	0.04582	0.06751	10.5	-0.02937	0.05600	0.06323
11.0	-0.00800	0.05749	0.05804	11.5	0.01153	0.05105	0.05234
12.0	0.02678	0.03845	0.04686	12.5	0.03611	0.02218	0.04238
13.0	0.03890	0.00501	0.03922	13.5	0.03549	-0.01043	0.03699
14.0	0.02712	-0.02203	0.03494	14.5	0.01563	-0.02849	0.03249
15.0	0.00317	-0.02945	0.02962	15.5	-0.00819	-0.02546	0.02675
16.0	-0.01675	-0.01781	0.02445	16.5	-0.02143	-0.00823	0.02296
17.0	-0.02190	0.00143	0.02195	17.5	-0.01857	0.00949	0.02085
18.0	-0.01243	0.01478	0.01931	18.5	-0.00488	0.01672	0.01741
19.0	0.00260	0.01539	0.01561	19.5	0.00868	0.01145	0.01437
20.0	0.01243	0.00594	0.01377	20.5	0.01341	0.00008	0.01341
21.0	0.01176	-0.00501	0.01278	21.5	0.00808	-0.00847	0.01171
22.0	0.00329	-0.00986	0.01039	22.5	-0.00158	-0.00916	0.00930
23.0	-0.00556	-0.00678	0.00877	23.5	-0.00799	-0.00337	0.00867
24.0	-0.00855	0.00026	0.00855	24.5	-0.00732	0.00337	0.00806
25.0	-0.00475	0.00541	0.00720				

Table A3-1c Diffraction pattern formed by the pupil T(x,M) for the case $\phi(x) = 2\pi x^4$

(AR= real part of amplitude,AI= imaginary part of amplitude,A= modulus of amplitude)

W	AR	AI	A	W	AR	AI	A
0.0	0.41575	0.27557	0.49878	0.5	0.41420	0.27100	0.49498
1.0	0.40936	0.25730	0.48350	1.5	0.40067	0.23459	0.46429
2.0	0.38732	0.20325	0.43741	2.5	0.36839	0.16412	0.40330
3.0	0.34306	0.11871	0.36302	3.5	0.31078	0.06934	0.31843
4.0	0.27155	0.01907	0.27222	4.5	0.22600	-0.02850	0.22779
5.0	0.17553	-0.06956	0.18881	5.5	0.12230	-0.10059	0.15836
6.0	0.06909	-0.11890	0.13751	6.5	0.01906	-0.12302	0.12449
7.0	-0.02456	-0.11310	0.11574	7.5	-0.05888	-0.09093	0.10833
8.0	-0.08172	-0.05978	0.10125	8.5	-0.09195	-0.02402	0.09504
9.0	-0.08971	0.01150	0.09045	9.5	-0.07646	0.04214	0.08730
10.0	-0.05482	0.06411	0.08435	10.5	-0.02830	0.07506	0.08022
11.0	-0.00083	0.07434	0.07434	11.5	0.02377	0.06304	0.06737
12.0	0.04230	0.04376	0.06086	12.5	0.05263	0.02014	0.05635
13.0	0.05394	-0.00379	0.05407	13.5	0.04684	-0.02428	0.05276
14.0	0.03316	-0.03844	0.05077	14.5	0.01564	-0.04463	0.04729
15.0	-0.00257	-0.04268	0.04276	15.5	-0.01845	-0.03380	0.03850
16.0	-0.02957	-0.02021	0.03582	16.5	-0.03449	-0.00478	0.03482
17.0	-0.03294	0.00963	0.03432	17.5	-0.02578	0.02060	0.03300
18.0	-0.01479	0.02654	0.03039	18.5	-0.00229	0.02696	0.02706
19.0	0.00934	0.02239	0.02426	19.5	0.01804	0.01422	0.02297
20.0	0.02248	0.00437	0.02290	20.5	0.02223	-0.00513	0.02281
21.0	0.01776	-0.01252	0.02173	21.5	0.01032	-0.01663	0.01958
22.0	0.00162	-0.01703	0.01711	22.5	-0.00653	-0.01406	0.01550
23.0	-0.01259	-0.00866	0.01527	23.5	-0.01553	-0.00216	0.01568
24.0	-0.01506	0.00401	0.01559	24.5	-0.01157	0.00868	0.01446
25.0	-0.00605	0.01105	0.01260				

Table A3-12a Diffraction pattern formed by the pupil $T(x)=1$ for the case $\phi(x) = 2\pi x^4 - \pi x^2$

(AR= real part of amplitude,AI= imaginary part of amplitude,A modulus of amplitude)

W	AR	AI	A	W	AR	AI	A
0.0	0.57897	0.17270	0.60418	0.5	0.56994	0.16023	0.59204
1.0	0.54314	0.12481	0.55730	1.5	0.49945	0.07213	0.50463
2.0	0.44049	0.01056	0.44062	2.5	0.36885	-0.05022	0.37226
3.0	0.28817	-0.10088	0.30531	3.5	0.20310	-0.13394	0.24329
4.0	0.11911	-0.14498	0.18764	4.5	0.04203	-0.13327	0.13974
5.0	-0.02265	-0.10176	0.10425	5.5	-0.07041	-0.05646	0.09025
6.0	-0.09845	-0.00529	0.09859	6.5	-0.10615	0.04331	0.11465
7.0	-0.09527	0.08184	0.12560	7.5	-0.06979	0.10491	0.12600
8.0	-0.03537	0.11007	0.11561	8.5	0.00150	0.09800	0.09801
9.0	0.03446	0.07220	0.08001	9.5	0.05828	0.03820	0.06968
10.0	0.06961	0.00244	0.06965	10.5	0.06751	-0.02891	0.07344
11.0	0.05342	-0.05102	0.07387	11.5	0.03080	-0.06112	0.06844
12.0	0.00443	-0.05881	0.05897	12.5	-0.02057	-0.04596	0.05035
13.0	-0.03965	-0.02614	0.04750	13.5	-0.04971	-0.00383	0.04986
14.0	-0.04953	0.01653	0.05221	14.5	-0.03992	0.03129	0.05073
15.0	-0.02346	0.03828	0.04490	15.5	-0.00387	0.03700	0.03720
16.0	0.01479	0.02861	0.03221	16.5	0.02890	0.01553	0.03281
17.0	0.03601	0.00084	0.03602	17.5	0.03524	-0.01237	0.03735
18.0	0.02737	-0.02163	0.03488	18.5	0.01454	-0.02549	0.02935
19.0	-0.00023	-0.02374	0.02374	19.5	-0.01374	-0.01732	0.02211
20.0	-0.02327	-0.00803	0.02462	20.5	-0.02714	0.00194	0.02721
21.0	-0.02495	0.01046	0.02705	21.5	-0.01761	0.01589	0.02372
22.0	-0.00707	0.01743	0.01881	22.5	0.00419	0.01513	0.01569
23.0	0.01368	0.00985	0.01686	23.5	0.01949	0.00300	0.01972
24.0	0.02062	-0.00382	0.02097	24.5	0.01713	-0.00914	0.01942
25.0	0.01012	-0.01198	0.01568				

Table A3-12b Diffraction pattern formed by the pupil T(x,5) for the case $\phi(x) = 2\pi x^4 - \pi x^2$

(AR= real part of amplitude,AI= imaginary part of amplitude,A modulus of amplitude)

W	AR	AI	A	W	AR	AI	A
0.0	0.85350	-0.07692	0.85696	0.5	0.84050	-0.07969	0.84427
1.0	0.80237	-0.08737	0.80711	1.5	0.74155	-0.09818	0.74803
2.0	0.66198	-0.10954	0.67098	2.5	0.56869	-0.11847	0.58090
3.0	0.46750	-0.12220	0.48321	3.5	0.36452	-0.11863	0.38333
4.0	0.26566	-0.10672	0.28629	4.5	0.17617	-0.08674	0.19637
5.0	0.10022	-0.06023	0.11693	5.5	0.04057	-0.02975	0.05031
6.0	-0.00163	0.00145	0.00218	6.5	-0.02682	0.02999	0.04023
7.0	-0.03688	0.05285	0.06445	7.5	-0.03488	0.06782	0.07626
8.0	-0.02456	0.07382	0.07780	8.5	-0.00994	0.07101	0.07171
9.0	0.00523	0.06072	0.06095	9.5	0.01790	0.04516	0.04857
10.0	0.02598	0.02704	0.03750	10.5	0.02852	0.00918	0.02996
11.0	0.02571	-0.00602	0.02640	11.5	0.01863	-0.01680	0.02509
12.0	0.00901	-0.02233	0.02408	12.5	-0.00117	-0.02267	0.02271
13.0	-0.01005	-0.01873	0.02125	13.5	-0.01618	-0.01193	0.02011
14.0	-0.01879	-0.00400	0.01921	14.5	-0.01778	0.00342	0.01811
15.0	-0.01376	0.00904	0.01647	15.5	-0.00780	0.01207	0.01436
16.0	-0.00120	0.01231	0.01236	16.5	0.00472	0.01012	0.01116
17.0	0.00893	0.00627	0.01091	17.5	0.01085	0.00173	0.01099
18.0	0.01037	-0.00251	0.01067	18.5	0.00788	-0.00565	0.00970
19.0	0.00410	-0.00723	0.00831	19.5	-0.00006	-0.00714	0.00714
20.0	-0.00370	-0.00562	0.00673	20.5	-0.00615	-0.00315	0.00691
21.0	-0.00703	-0.00037	0.00704	21.5	-0.00632	0.00211	0.00666
22.0	-0.00435	0.00382	0.00579	22.5	-0.00166	0.00451	0.00481
23.0	0.00110	0.00416	0.00430	23.5	0.00333	0.00296	0.00446
24.0	0.00460	0.00129	0.00478	24.5	0.00473	-0.00046	0.00475
25.0	0.00381	-0.00189	0.00425				

Table A3-12c Diffraction pattern formed by the pupil T(x,M) for the case $\phi(x) = 2\pi x^4 - \pi x^2$

(AR= real part of amplitude,AI= imaginary part of amplitude,A modulus of amplitude)

W	AR	AI	A	W	AR	AI	A
0.0	0.76009	0.01942	0.76033	0.5	0.74755	0.01302	0.74766
1.0	0.71069	-0.00506	0.71070	1.5	0.65175	-0.03158	0.65252
2.0	0.57435	-0.06181	0.57767	2.5	0.48328	-0.09028	0.49164
3.0	0.38421	-0.11178	0.40014	3.5	0.28330	-0.12218	0.30852
4.0	0.18677	-0.11914	0.22153	4.5	0.10031	-0.10254	0.14345
5.0	0.02865	-0.07438	0.07971	5.5	-0.02497	-0.03849	0.04588
6.0	-0.05907	0.00015	0.05907	6.5	-0.07412	0.03627	0.08252
7.0	-0.07239	0.06513	0.09738	7.5	-0.05767	0.08329	0.10131
8.0	-0.03477	0.08907	0.09562	8.5	-0.00884	0.08277	0.08324
9.0	0.01529	0.06645	0.06819	9.5	0.03373	0.04355	0.05509
10.0	0.04401	0.01819	0.04762	10.5	0.04528	-0.00551	0.04562
11.0	0.03832	-0.02415	0.04529	11.5	0.02522	-0.03547	0.04352
12.0	0.00893	-0.03869	0.03971	12.5	-0.00729	-0.03446	0.03522
13.0	-0.02055	-0.02460	0.03205	13.5	-0.02871	-0.01167	0.03099
14.0	-0.03079	0.00155	0.03083	14.5	-0.02701	0.01259	0.02980
15.0	-0.01863	0.01967	0.02710	15.5	-0.00769	0.02200	0.02331
16.0	0.00349	0.01975	0.02005	16.5	0.01274	0.01394	0.01888
17.0	0.01847	0.00615	0.01947	17.5	0.01992	-0.00183	0.02000
18.0	0.01722	-0.00843	0.01917	18.5	0.01133	-0.01249	0.01686
19.0	0.00374	-0.01351	0.01402	19.5	-0.00384	-0.01166	0.01228
20.0	-0.00984	-0.00766	0.01247	20.5	-0.01319	-0.00257	0.01344
21.0	-0.01343	0.00243	0.01365	21.5	-0.01079	0.00632	0.01251
22.0	-0.00610	0.00842	0.01040	22.5	-0.00054	0.00849	0.00851
23.0	0.00462	0.00676	0.00819	23.5	0.00832	0.00378	0.00913
24.0	0.00986	0.00033	0.00987	24.5	0.00910	-0.00281	0.00952
25.0	0.00640	-0.00499	0.00811				

Table A3-13a Diffraction pattern formed by the pupil T(x)=1 for the case $\phi(x) = 2\pi x^4 - 2\pi x^2$

(AR= real part of amplitude,AI= imaginary part of amplitude,A= modulus of amplitude)

W	AR	AI	A	W	AR	AI	A
0.0	0.43826	-0.77989	0.89460	0.5	0.42473	-0.75575	0.86693
1.0	0.38610	-0.68608	0.78726	1.5	0.32787	-0.57871	0.66514
2.0	0.25815	-0.44550	0.51489	2.5	0.18624	-0.30065	0.35365
3.0	0.12103	-0.15881	0.19968	3.5	0.06959	-0.03321	0.07711
4.0	0.03605	0.06605	0.07524	4.5	0.02111	0.13298	0.13465
5.0	0.02222	0.16622	0.16770	5.5	0.03428	0.16870	0.17215
6.0	0.05082	0.14683	0.15537	6.5	0.06534	0.10917	0.12723
7.0	0.07260	0.06496	0.09742	7.5	0.06954	0.02269	0.07315
8.0	0.05571	-0.01108	0.05680	8.5	0.03320	-0.03244	0.04642
9.0	0.00604	-0.04032	0.04077	9.5	-0.02082	-0.03623	0.04178
10.0	-0.04252	-0.02357	0.04861	10.5	-0.05537	-0.00676	0.05578
11.0	-0.05754	0.00978	0.05837	11.5	-0.04935	0.02239	0.05419
12.0	-0.03310	0.02882	0.04389	12.5	-0.01253	0.02840	0.03104
13.0	0.00803	0.02201	0.02342	13.5	0.02458	0.01164	0.02720
14.0	0.03420	-0.00008	0.03420	14.5	0.03562	-0.01058	0.03716
15.0	0.02931	-0.01781	0.03430	15.5	0.01733	-0.02062	0.02694
16.0	0.00272	-0.01891	0.01910	16.5	-0.01117	-0.01351	0.01753
17.0	-0.02140	-0.00595	0.02222	17.5	-0.02606	0.00198	0.02614
18.0	-0.02459	0.00857	0.02604	18.5	-0.01778	0.01259	0.02179
19.0	-0.00756	0.01347	0.01545	19.5	0.00356	0.01137	0.01191
20.0	0.01305	0.00704	0.01482	20.5	0.01890	0.00166	0.01898
21.0	0.02008	-0.00351	0.02039	21.5	0.01666	-0.00738	0.01822
22.0	0.00971	-0.00923	0.01339	22.5	0.00105	-0.00886	0.00892
23.0	-0.00726	-0.00657	0.00979	23.5	-0.01334	-0.00306	0.01369
24.0	-0.01597	0.00080	0.01599	24.5	-0.01477	0.00411	0.01533
25.0	-0.01026	0.00619	0.01198				

Table A3-13b Diffraction pattern formed by the pupil T(x,5) for the case $\phi(x) = 2\pi x^4 - 2\pi x^2$

(AR= real part of amplitude,AI= imaginary part of amplitude,A= modulus of amplitude)

W	AR	AI	A	W	AR	AI	A
0.0	0.48942	-0.73910	0.88645	0.5	0.48294	-0.72229	0.86887
1.0	0.46414	-0.67339	0.81785	1.5	0.43481	-0.59682	0.73842
2.0	0.39765	-0.49937	0.63835	2.5	0.35583	-0.38937	0.52746
3.)	0.31257	-0.27576	0.41682	3.5	0.27069	-0.16712	0.31812
4.0	0.23228	-0.07074	0.24281	4.5	0.19849	0.00803	0.19865
5.0	0.16954	0.06615	0.18199	5.5	0.14485	0.10301	0.17774
6.0	0.12330	0.12016	0.17217	6.5	0.10360	0.12088	0.15921
7.0	0.08461	0.10949	0.13838	7.5	0.06560	0.09071	0.11194
8.0	0.04640	0.06899	0.08314	8.5	0.02744	0.04801	0.05530
9.0	0.00961	0.03036	0.03184	9.5	-0.00597	0.01741	0.01840
10.0	-0.01818	0.00941	0.02047	10.5	-0.02618	0.00570	0.02680
11.0	-0.02963	0.00507	0.03006	11.5	-0.02875	0.00607	0.02938
12.0	-0.02429	0.00736	0.02538	12.5	-0.01746	0.00797	0.01919
13.0	-0.00967	0.00736	0.01215	13.5	-0.00229	0.00548	0.00594
14.0	0.00352	0.00266	0.00441	14.5	0.00707	-0.00053	0.00709
15.0	0.00814	-0.00343	0.00883	15.5	0.00700	-0.00551	0.00891
16.0	0.00431	-0.00643	0.00774	16.5	0.00091	-0.00613	0.00619
17.0	-0.00230	-0.00478	0.00530	17.5	-0.00463	-0.00277	0.00539
18.0	-0.00563	-0.00056	0.00565	18.5	-0.00522	0.00139	0.00540
19.0	-0.00364	0.00273	0.00455	19.5	-0.00137	0.00327	0.00354
20.0	0.00102	0.00302	0.00318	20.5	0.00296	0.00214	0.00366
21.0	0.00407	0.00091	0.00417	21.5	0.00416	-0.00036	0.00417
22.0	0.00330	-0.00138	0.00357	22.5	0.00176	-0.00196	0.00264
23.0	-0.00004	-0.00203	0.00203	23.5	-0.00168	-0.00163	0.00234
24.0	-0.00279	-0.00090	0.00293	24.5	-0.00316	-0.00006	0.00316
25.0	-0.00276	0.00071	0.00285				

Table A3-13c Diffraction pattern formed by the pupil T(x,M) for the case $\phi(x) = 2\pi x^4 - 2\pi x^2$

(AR= real part of amplitude, AI= imaginary part of amplitude, A= modulus of amplitude)

W	AR	AI	A	W	AR	AI	A
0.0	0.44601	-0.77375	0.89309	0.5	0.43722	-0.75345	0.87112
1.0	0.41192	-0.69461	0.80756	1.5	0.37315	-0.60312	0.70922
2.0	0.32544	-0.48797	0.58654	2.5	0.27403	-0.36009	0.45250
3.0	0.22405	-0.23099	0.32180	3.5	0.17978	-0.11142	0.21151
4.0	0.14400	-0.01014	0.14436	4.5	0.11775	0.06697	0.13546
5.0	0.10033	0.11728	0.15434	5.5	0.08963	0.14144	0.16745
6.0	0.08271	0.14289	0.16510	6.5	0.07650	0.12705	0.14830
7.0	0.06840	0.10040	0.12148	7.5	0.05680	0.06942	0.08970
8.0	0.04138	0.03973	0.05736	8.5	0.02302	0.01546	0.02773
9.0	0.00360	-0.00105	0.00375	9.5	-0.01450	-0.00933	0.01724
10.0	-0.02891	-0.01039	0.03072	10.5	-0.03782	-0.00633	0.03835
11.0	-0.04032	0.00030	0.04032	11.5	-0.03659	0.00703	0.03726
12.0	-0.02785	0.01191	0.03029	12.5	-0.01609	0.01382	0.02121
13.0	-0.00366	0.01253	0.01305	13.5	0.00716	0.00858	0.01118
14.0	0.01463	0.00307	0.01495	14.5	0.01781	-0.00267	0.01801
15.0	0.01665	-0.00741	0.01823	15.5	0.01199	-0.01026	0.01578
16.0	0.00525	-0.01082	0.01202	16.5	-0.00189	-0.00920	0.00940
17.0	-0.00783	-0.00598	0.00985	17.5	-0.01139	-0.00200	0.01156
18.0	-0.01203	0.00186	0.01217	18.5	-0.00990	0.00480	0.01100
19.0	-0.00572	0.00634	0.00854	19.5	-0.00061	0.00632	0.00635
20.0	0.00420	0.00493	0.00648	20.5	0.00766	0.00264	0.00811
21.0	0.00910	0.00006	0.00910	21.5	0.00836	-0.00224	0.00866
22.0	0.00578	-0.00376	0.00690	22.5	0.00209	-0.00428	0.00476
23.0	-0.00180	-0.00378	0.00419	23.5	-0.00497	-0.00249	0.00556
24.0	-0.00676	-0.00077	0.00681	24.5	-0.00686	0.00093	0.00692
25.0	-0.00536	0.00226	0.00582				

Table A3-14a Diffraction pattern formed by the pupil T(x)=1 for the case $\phi(x) = 2\pi x^4 - 3\pi x^2$

(AR= real part of amplitude,AI= imaginary part of amplitude,A= modulus of amplitude)

W	AR	AI	A	W	AR	AI	A
0.0	-0.57896	-0.17271	0.60418	0.5	-0.55213	-0.17450	0.57905
1.0	-0.47518	-0.17926	0.50787	1.5	-0.35824	-0.18521	0.40329
2.0	-0.21642	-0.18978	0.28784	2.5	-0.06747	-0.19009	0.20171
3.0	0.07083	-0.18354	0.19673	3.5	0.18332	-0.16835	0.24889
4.0	0.25947	-0.14392	0.29671	4.5	0.29461	-0.11107	0.31485
5.0	0.29016	-0.07195	0.29895	5.5	0.25283	-0.02980	0.25459
6.0	0.19314	0.01154	0.19348	6.5	0.12331	0.04819	0.13239
7.0	0.05521	0.07681	0.09460	7.5	-0.00152	0.09509	0.09510
8.0	-0.04074	0.10203	0.10986	8.5	-0.06032	0.09809	0.11515
9.0	-0.06189	0.08501	0.10515	9.5	-0.04999	0.06554	0.08243
10.0	-0.03074	0.04294	0.05281	10.5	-0.01044	0.02047	0.02298
11.0	0.00571	0.00098	0.00579	11.5	0.01448	-0.01354	0.01983
12.0	0.01498	-0.02210	0.02670	12.5	0.00848	-0.02475	0.02616
13.0	-0.00221	-0.02244	0.02254	13.5	-0.01355	-0.01671	0.02151
14.0	-0.02224	-0.00938	0.02413	14.5	-0.02595	-0.00220	0.02604
15.0	-0.02379	0.00346	0.02405	15.5	-0.01641	0.00679	0.01776
16.0	-0.00567	0.00759	0.00947	16.5	0.00582	0.00619	0.00850
17.0	0.01543	0.00335	0.01579	17.5	0.02109	-0.00003	0.02109
18.0	0.02175	-0.00304	0.02196	18.5	0.01756	-0.00502	0.01827
19.0	0.00978	-0.00561	0.01127	19.5	0.00039	-0.00482	0.00484
20.0	-0.00838	-0.00299	0.00890	20.5	-0.01458	-0.00063	0.01460
21.0	-0.01697	0.00167	0.01705	21.5	-0.01525	0.00340	0.01563
22.0	-0.01011	0.00421	0.01095	22.5	-0.00295	0.00401	0.00498
23.0	0.00444	0.00294	0.00532	23.5	0.01031	0.00132	0.01040
24.0	0.01340	-0.00045	0.01341	24.5	0.01316	-0.00196	0.01330
25.0	0.00983	-0.00288	0.01024				

Table A3-14b Diffraction pattern formed by the pupil T(x,5) for the case $\phi(x) = 2\pi x^4 - 3\pi x^2$

(AR= real part of amplitude,AI= imaginary part of amplitude,A= modulus of amplitude)

W	AR	AI	A	W	AR	AI	A
0.0	-0.20103	-0.43282	0.47723	0.5	-0.18738	-0.42926	0.46837
1.0	-0.14802	-0.41851	0.44392	1.5	-0.08748	-0.40048	0.40992
2.0	-0.01262	-0.37506	0.37527	2.5	0.06827	-0.34233	0.34907
3.0	0.14656	-0.30268	0.33630	3.5	0.21438	-0.25693	0.33463
4.0	0.26552	-0.20640	0.33631	4.5	0.29610	-0.15292	0.33325
5.0	0.30486	-0.09872	0.32045	5.5	0.29311	-0.04631	0.29675
6.0	0.26426	0.00178	0.26426	6.5	0.22317	0.04325	0.22732
7.0	0.17540	0.07624	0.19125	7.5	0.12634	0.09956	0.16085
8.0	0.08062	0.11279	0.13865	8.5	0.04160	0.11635	0.12356
9.0	0.01117	0.11137	0.11193	9.5	-0.01022	0.09960	0.10012
10.0	-0.02330	0.08316	0.08636	10.5	-0.02961	0.06428	0.07077
11.0	-0.03105	0.04509	0.05475	11.5	-0.02953	0.02738	0.04028
12.0	-0.02662	0.01247	0.02940	12.5	-0.02340	0.00109	0.02342
13.0	-0.02041	-0.00653	0.02143	13.5	-0.01776	-0.01067	0.02072
14.0	-0.01529	-0.01193	0.01940	14.5	-0.01271	-0.01113	0.01690
15.0	-0.00981	-0.00911	0.01339	15.5	-0.00655	-0.00665	0.00933
16.0	-0.00307	-0.00432	0.00530	16.5	0.00029	-0.00250	0.00252
17.0	0.00314	-0.00133	0.00341	17.5	0.00511	-0.00076	0.00516
18.0	0.00596	-0.00065	0.00599	18.5	0.00565	-0.00077	0.00570
19.0	0.00437	-0.00091	0.00446	19.5	0.00245	-0.00094	0.00263
20.0	0.00036	-0.00077	0.00085	20.5	-0.00146	-0.00043	0.00152
21.0	-0.00266	0.00003	0.00266	21.5	-0.00305	0.00048	0.00309
22.0	-0.00264	0.00083	0.00277	22.5	-0.00160	0.00100	0.00189
23.0	-0.00026	0.00096	0.00100	23.5	0.00105	0.00074	0.00128
24.0	0.00200	0.00039	0.00204	24.5	0.00240	0.0	0.00240
25.0	0.00218	-0.00034	0.00221				

Table A3-14c Diffraction pattern formed by the pupil T(x,M) for the case $\phi(x) = 2\pi x^4 - 3\pi x^2$

(AR= real part of amplitude,AI= imaginary part of amplitude,A= modulus of amplitude)

W	AR	AI	A	W	AR	AI	A
0.0	-0.38219	-0.32764	0.50341	0.5	-0.36305	-0.32609	0.48799
1.0	-0.30797	-0.32117	0.44496	1.5	-0.22364	-0.31215	0.38400
2.0	-0.12015	-0.29802	0.32133	2.5	-0.00952	-0.27775	0.27791
3.0	0.09597	-0.25063	0.26837	3.5	0.18539	-0.21649	0.28502
4.0	0.25059	-0.17595	0.30619	4.5	0.28705	-0.13045	0.31530
5.0	0.29422	-0.08223	0.30549	5.5	0.27518	-0.03405	0.27728
6.0	0.23589	0.01105	0.23615	6.5	0.18399	0.05016	0.19071
7.0	0.12756	0.08085	0.15103	7.5	0.07387	0.10150	0.12554
8.0	0.02849	0.11149	0.11507	8.5	-0.00527	0.11122	0.11135
9.0	-0.02645	0.10211	0.10548	9.5	-0.03616	0.08631	0.09358
10.0	-0.03698	0.06641	0.07601	10.5	-0.03221	0.04512	0.05544
11.0	-0.02513	0.02490	0.03538	11.5	-0.01839	0.00768	0.01994
12.0	-0.01366	-0.00528	0.01464	12.5	-0.01149	-0.01350	0.01772
13.0	-0.01149	-0.01719	0.02067	13.5	-0.01263	-0.01713	0.02128
14.0	-0.01368	-0.01443	0.01988	14.5	-0.01355	-0.01033	0.01704
15.0	-0.01163	-0.00598	0.01308	15.5	-0.00790	-0.00225	0.00822
16.0	-0.00292	0.00031	0.00293	16.5	0.00241	0.00155	0.00287
17.0	0.00702	0.00161	0.00720	17.5	0.01001	0.00085	0.01004
18.0	0.01083	-0.00027	0.01083	18.5	0.00943	-0.00132	0.00952
19.0	0.00625	-0.00196	0.00655	19.5	0.00209	-0.00205	0.00293
20.0	-0.00208	-0.00159	0.00261	20.5	-0.00535	-0.00074	0.00540
21.0	-0.00707	0.00027	0.00708	21.5	-0.00699	0.00117	0.00708
22.0	-0.00526	0.00176	0.00555	22.5	-0.00243	0.00192	0.00310
23.0	0.00077	0.00166	0.00183	23.5	0.00356	0.00106	0.00371
24.0	0.00531	0.00028	0.00531	24.5	0.00567	-0.00048	0.00569
25.0	0.00466	-0.00106	0.00478				

Table A3-15a Diffraction pattern formed by the pupil $T(x)=1$ for the case $\phi(x) = 2\pi x^4 - 4\pi x^2$

(AR= real part of amplitude,AI= imaginary part of amplitude,A= modulus of amplitude)

W	AR	AI	A	W	AR	AI	A
0.0	0.24413	0.17171	0.29846	0.5	0.22909	0.16109	0.28006
1.0	0.18661	0.13049	0.22771	1.5	0.12406	0.08360	0.14960
2.0	0.05227	0.02600	0.05838	2.5	-0.01645	-0.03554	0.03917
3.0	-0.07048	-0.09392	0.11742	3.5	-0.10093	-0.14258	0.17469
4.0	-0.10316	-0.17632	0.20428	4.5	-0.07750	-0.19189	0.20695
5.0	-0.02908	-0.18828	0.19051	5.5	0.03322	-0.16677	0.17005
6.0	0.09839	-0.13064	0.16355	6.5	0.15531	-0.08464	0.17688
7.0	0.19468	-0.03432	0.19768	7.5	0.21048	0.01470	0.21100
8.0	0.20094	0.05743	0.20898	8.5	0.16851	0.09006	0.19106
9.0	0.11923	0.11032	0.16244	9.5	0.06146	0.11762	0.13271
10.0	0.00426	0.11291	0.11299	10.5	-0.04423	0.09841	0.10789
11.0	-0.07807	0.07719	0.10978	11.5	-0.09438	0.05264	0.10807
12.0	-0.09350	0.02806	0.09762	12.5	-0.07862	0.00617	0.07886
13.0	-0.05481	-0.01107	0.05591	13.5	-0.02795	-0.02265	0.03597
14.0	-0.00349	-0.02847	0.02868	14.5	0.01449	-0.02917	0.03257
15.0	0.02388	-0.02594	0.03526	15.5	0.02464	-0.02024	0.03189
16.0	0.01858	-0.01351	0.02297	16.5	0.00861	-0.00702	0.01111
17.0	-0.00194	-0.00166	0.00255	17.5	-0.01019	0.00206	0.01039
18.0	-0.01422	0.00405	0.01479	18.5	-0.01346	0.00451	0.01420
19.0	-0.00859	0.00388	0.00942	19.5	-0.00127	0.00264	0.00293
20.0	0.00638	0.00127	0.00650	20.5	0.01231	0.00013	0.01231
21.0	0.01507	-0.00058	0.01508	21.5	0.01409	-0.00080	0.01411
22.0	0.00977	-0.00062	0.00979	22.5	0.00329	-0.00019	0.00330
23.0	-0.00367	0.00030	0.00368	23.5	-0.00945	0.00069	0.00947
24.0	-0.01271	0.00086	0.01274	24.5	-0.01282	0.00080	0.01284
25.0	-0.00991	0.00054	0.00992				

Table A3-15b Diffraction pattern formed by the pupil T(x,5) for the case $\phi(x) = 2\pi x^4 - 4\pi x^2$

(AR= real part of amplitude, AI= imaginary part of amplitude, A= modulus of amplitude)

W	AR	AI	A	W	AR	AI	A
0.0	0.03316	-0.08132	0.08782	0.5	0.03133	-0.08698	0.09245
1.0	0.02647	-0.10318	0.10653	1.5	0.02042	-0.12773	0.12935
2.0	0.01580	-0.15724	0.15804	2.5	0.01547	-0.18761	0.18825
3.0	0.02191	-0.21450	0.21561	3.5	0.03670	-0.23386	0.23672
4.0	0.06003	-0.24246	0.24978	4.5	0.09057	-0.23824	0.25488
5.0	0.12559	-0.22055	0.25380	5.5	0.16128	-0.19020	0.24937
6.0	0.19330	-0.14934	0.24427	6.5	0.21748	-0.10119	0.23987
7.0	0.23043	-0.04963	0.23571	7.5	0.23005	0.00124	0.23005
8.0	0.21588	0.04754	0.22105	8.5	0.18916	0.08605	0.20781
9.0	0.15259	0.11447	0.19075	9.5	0.10995	0.13160	0.17149
10.0	0.06553	0.13741	0.15224	10.5	0.02354	0.13287	0.13494
11.0	-0.01249	0.11981	0.12046	11.5	-0.04006	0.10059	0.10828
12.0	-0.05796	0.07782	0.09703	12.5	-0.06627	0.05404	0.08551
13.0	-0.06616	0.03148	0.07327	13.5	-0.05961	0.01185	0.06078
14.0	-0.04898	-0.00373	0.04912	14.5	-0.03660	-0.01476	0.03946
15.0	-0.02446	-0.02131	0.03244	15.5	-0.01400	-0.02389	0.02769
16.0	-0.00600	-0.02330	0.02406	16.5	-0.00061	-0.02049	0.02050
17.0	0.00248	-0.01641	0.01659	17.5	0.00385	-0.01190	0.01250
18.0	0.00419	-0.00761	0.00869	18.5	0.00410	-0.00398	0.00571
19.0	0.00398	-0.00122	0.00416	19.5	0.00398	0.00062	0.00403
20.0	0.00410	0.00165	0.00442	20.5	0.00415	0.00204	0.00463
21.0	0.00397	0.00200	0.00444	21.5	0.00340	0.00172	0.00381
22.0	0.00242	0.00134	0.00277	22.5	0.00114	0.00098	0.00150
23.0	-0.00025	0.00069	0.00073	23.5	-0.00148	0.00047	0.00155
24.0	-0.00233	0.00032	0.00235	24.5	-0.00264	0.00021	0.00265
25.0	-0.00237	0.00012	0.00237				

Table A3-15c Diffraction pattern formed by the pupil T(x,M) for the case $\phi(x) = 2\pi x^4 - 4\pi x^2$

(AR= real part of amplitude,AI= imaginary part of amplitude,A= modulus of amplitude)

W	AR	AI	A	W	AR	AI	A
0.0	0.08888	0.04867	0.10133	0.5	0.08242	0.04040	0.09179
1.0	0.06440	0.01663	0.06651	1.5	0.03860	-0.01970	0.04334
2.0	0.01053	-0.06408	0.06494	2.5	-0.01359	-0.11104	0.11187
3.0	-0.02805	-0.15479	0.15731	3.5	-0.02866	-0.18994	0.19210
4.0	-0.01364	-0.21220	0.21264	4.5	0.01610	-0.21877	0.21936
5.0	0.05697	-0.20873	0.21637	5.5	0.10337	-0.18302	0.21019
6.0	0.14857	-0.14428	0.20710	6.5	0.18588	-0.09648	0.20943
7.0	0.20970	-0.04437	0.21434	7.5	0.21643	0.00710	0.21655
8.0	0.20503	0.05335	0.21186	8.5	0.17705	0.09070	0.19893
9.0	0.13634	0.11667	0.17944	9.5	0.08829	0.13017	0.15729
10.0	0.03894	0.13152	0.13717	10.5	-0.00596	0.12222	0.12236
11.0	-0.04185	0.10467	0.11273	11.5	-0.06591	0.08182	0.10507
12.0	-0.07729	0.05671	0.09587	12.5	-0.07705	0.03215	0.08349
13.0	-0.06768	0.01043	0.06848	13.5	-0.05258	-0.00690	0.05303
14.0	-0.03531	-0.01904	0.04011	14.5	-0.01901	-0.02594	0.03216
15.0	-0.00595	-0.02813	0.02875	15.5	0.00271	-0.02658	0.02672
16.0	0.00691	-0.02249	0.02353	16.5	0.00746	-0.01705	0.01861
17.0	0.00569	-0.01133	0.01268	17.5	0.00308	-0.00614	0.00687
18.0	0.00086	-0.00200	0.00218	18.5	-0.00017	0.00088	0.00089
19.0	0.00020	0.00251	0.00252	19.5	0.00170	0.00311	0.00354
20.0	0.00369	0.00297	0.00473	20.5	0.00542	0.00241	0.00593
21.0	0.00626	0.00171	0.00649	21.5	0.00585	0.00107	0.00594
22.0	0.00419	0.00059	0.00423	22.5	0.00164	0.00031	0.00167
23.0	-0.00121	0.00020	0.00123	23.5	-0.00371	0.00019	0.00372
24.0	-0.00529	0.00021	0.00530	24.5	-0.00561	0.00021	0.00562
25.0	-0.00466	0.00016	0.00466				

Fig. A3-16 Curves of encircled energy factors associated with the pupils $T(x)=1, T(x,5)$, and $T(x,M)$ for the cases:

(a) $\phi(x) = 0$

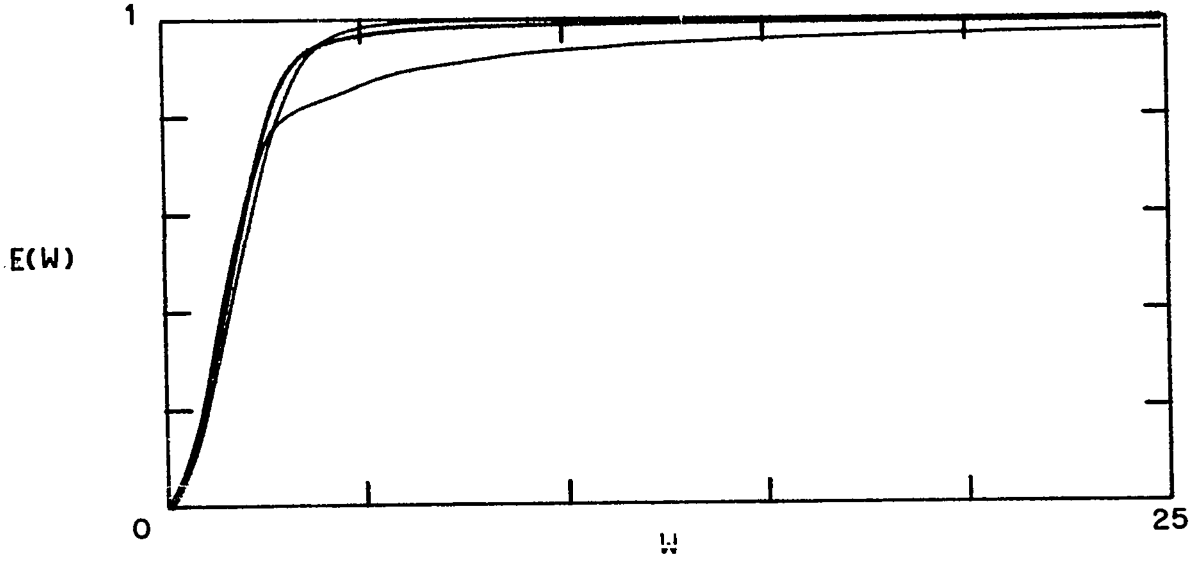

(b) $\phi(x) = \pi x^2$

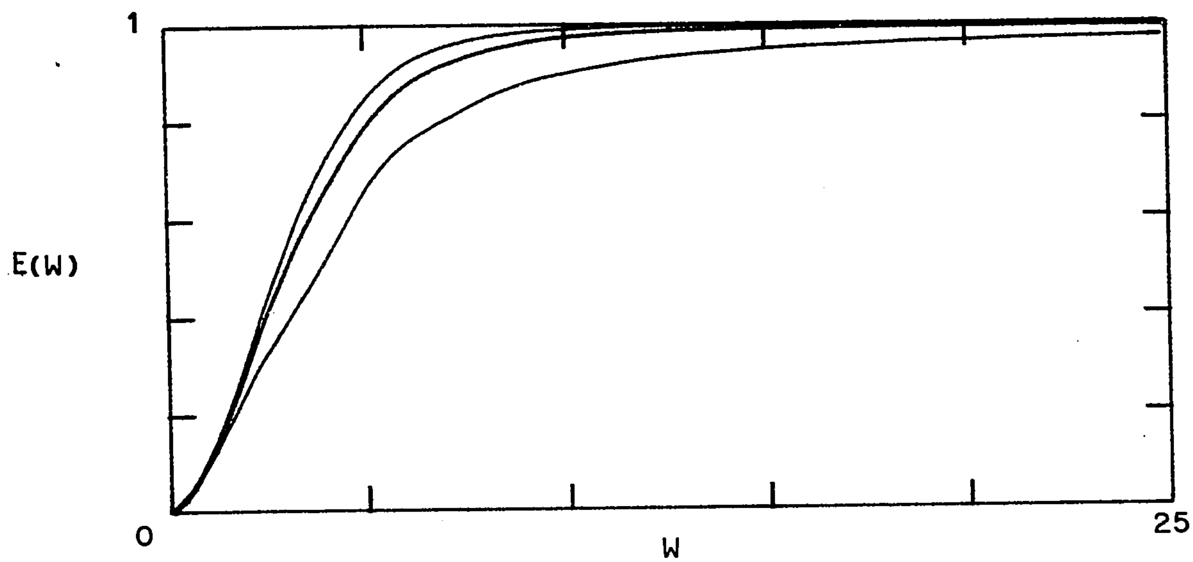

(c) $\phi(x) = 2\pi x^2$

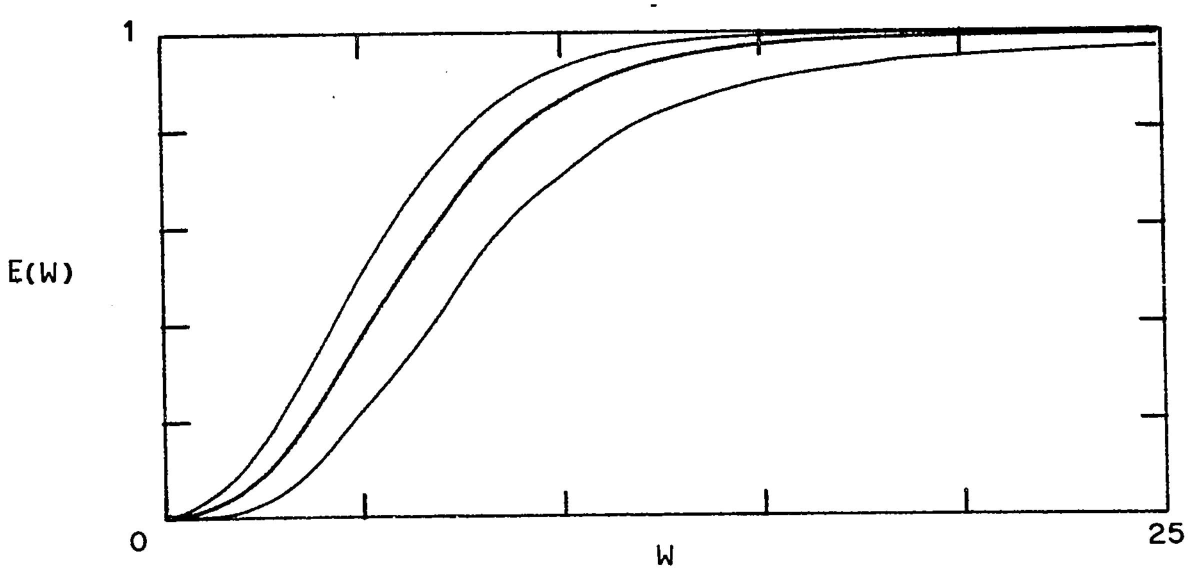

Fig. A3-17 Curves of encircled energy factors associated with the pupils T(x)=1, T(x,5), and T(x,M) for the cases:

(a) $\phi(x) = \pi x^4$

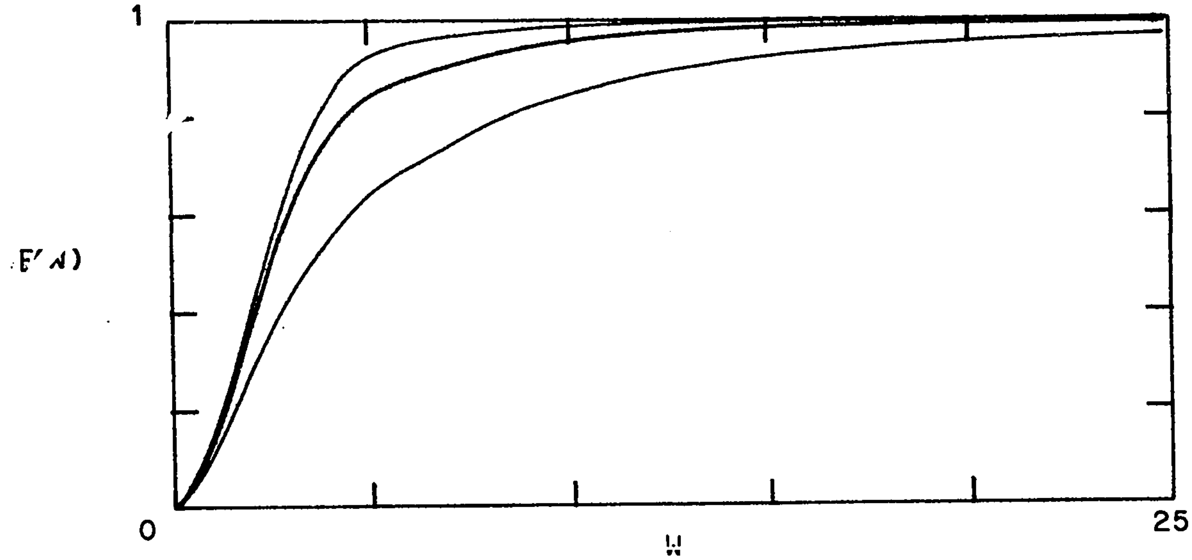

(b) $\phi(x) = \pi x^4 - \pi x^2$

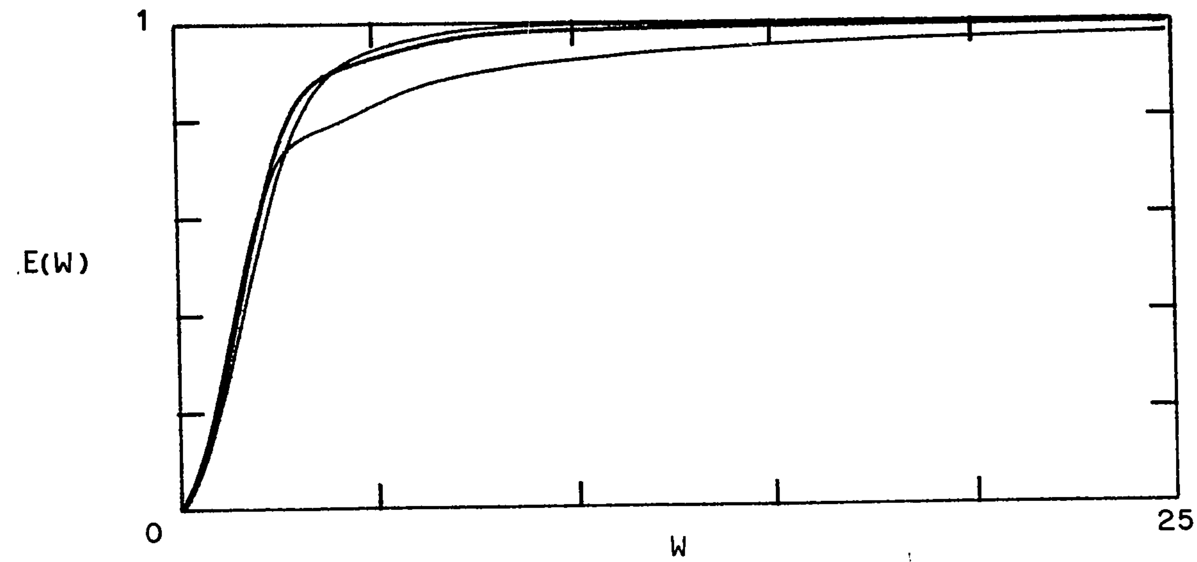

(c) $\phi(x) = \pi x^4 - 2\pi x^2$

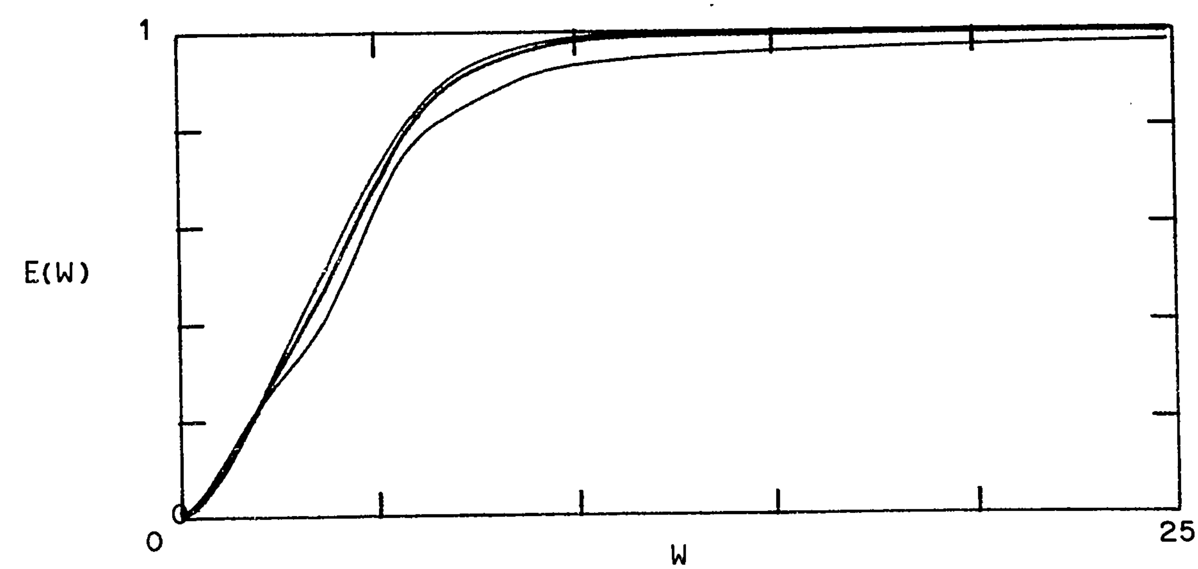

Fig. A3-18 Curves of encircled energy factors associated with the pupils T(x)=1,T(x,5), and T(x,M) for the cases:

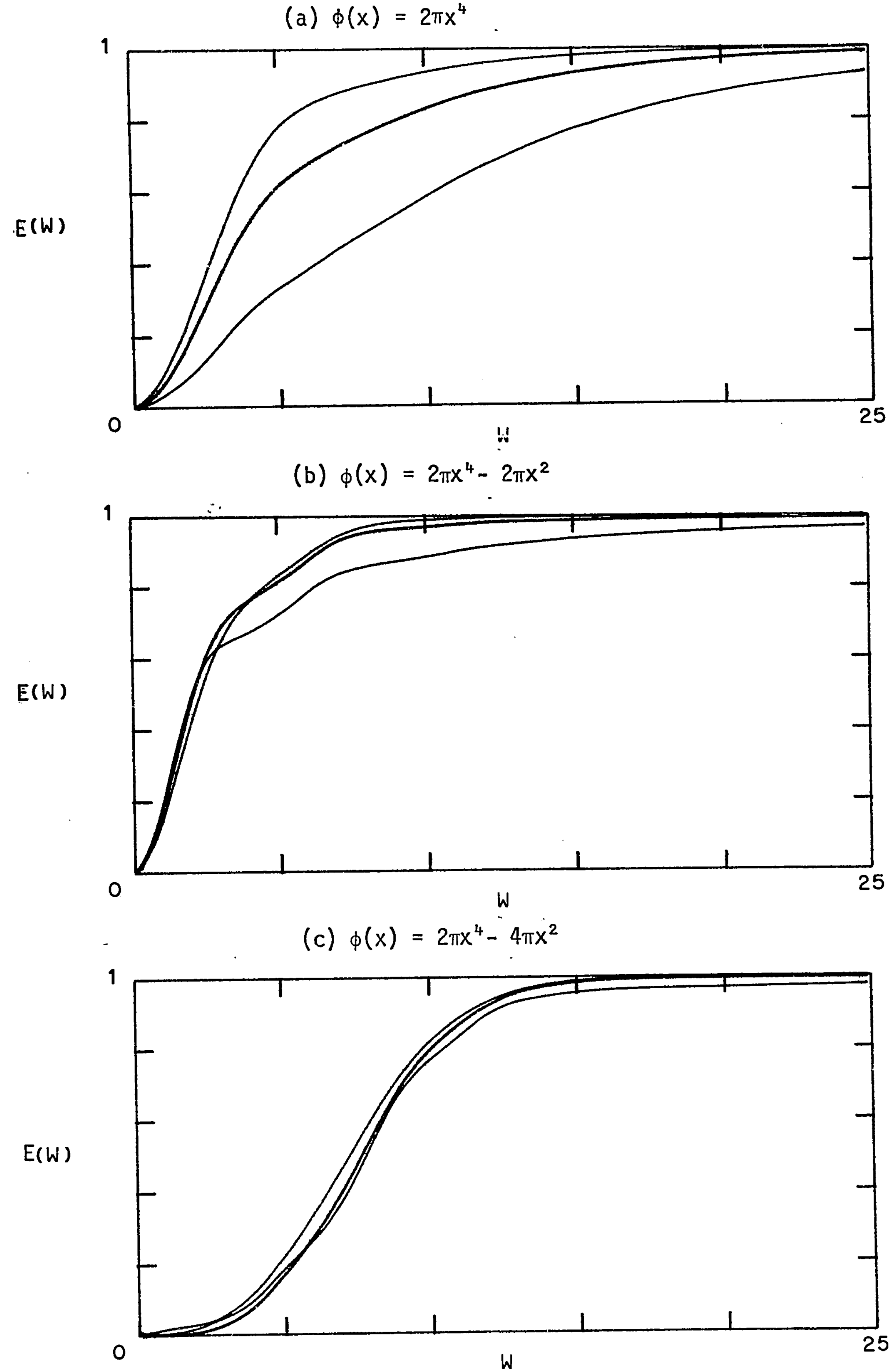

OTTAWA, ONTARIO, CANADA.

Table A3-16

Encircled energy factors associated with the pupils T(x)=1, T(x,5), and T(x,M) for the cases:

	$\phi(x) = 0$			$\phi(x) = \pi x^2$			$\phi(x) = 2\pi x^2$		
W	T(X)=1	T(X,5)	T(X,M)	T(X)=1	T(X,5)	T(X,M)	T(X)=1	T(X,5)	T(X,M)
0.5	0.06058	0.04256	0.05332	0.02456	0.02365	0.02503	0.0	0.00572	0.00251
1.0	0.22083	0.16061	0.19835	0.08966	0.09043	0.09427	0.00012	0.02295	0.01054
1.5	0.42674	0.32851	0.39633	0.17460	0.18925	0.19278	0.00122	0.05196	0.02545
2.0	0.61726	0.51292	0.59960	0.25811	0.30547	0.30256	0.00580	0.09243	0.04914
2.5	0.75056	0.68282	0.76860	0.32906	0.42501	0.40915	0.01792	0.14415	0.08332
3.0	0.81741	0.81735	0.88320	0.38961	0.53735	0.50516	0.04141	0.20567	0.12952
3.5	0.83663	0.90898	0.94440	0.44967	0.63664	0.58977	0.07740	0.27472	0.18392
4.0	0.83791	0.96183	0.96762	0.51721	0.72097	0.66533	0.12304	0.34924	0.24629
4.5	0.84386	0.98665	0.97210	0.59159	0.79075	0.73355	0.17274	0.42292	0.31191
5.0	0.86115	0.99534	0.97240	0.66383	0.84710	0.79378	0.22149	0.49579	0.37736
6.0	0.90075	0.99723	0.97972	0.76395	0.92413	0.88182	0.31470	0.62255	0.50136
7.0	0.90993	0.99788	0.98652	0.80747	0.96341	0.92665	0.42448	0.73965	0.61949
8.0	0.91548	0.99827	0.98714	0.84811	0.98108	0.95118	0.54745	0.82761	0.72645
9.0	0.93156	0.99836	0.98996	0.88778	0.99020	0.96960	0.64179	0.88052	[illegible]
10.0	0.93763	0.99868	0.99087	0.90405	0.99495	0.97354	0.70570	0.93120	0.86318
11.0	0.93944	0.99877	0.99106	0.91431	0.99673	0.98338	0.76853	0.95729	0.90455
12.0	0.94780	0.99884	0.99196	0.93023	0.99763	0.98717	0.82285	0.97448	0.93612
13.0	0.95224	0.99900	0.99296	0.93841	0.99834	0.98990	0.85339	0.98466	0.95520
14.0	0.95294	0.99905	0.99307	0.94163	0.99861	0.99072	0.87670	0.99017	0.96648
15.0	0.95773	0.99909	0.99358	0.94516	0.99876	0.99185	0.90161	0.99369	0.97610
16.0	0.96124	0.99920	0.99425	0.95432	0.99897	0.99301	0.91666	0.99596	0.98234
17.0	0.96161	0.99922	0.99434	0.95564	0.99906	0.99331	0.92512	0.99703	0.98542
18.0	0.96448	0.99925	0.99464	0.95967	0.99911	0.99381	0.93630	0.99778	0.98817
19.0	0.96733	0.99932	0.99513	0.96336	0.99922	0.99448	0.94458	0.99835	0.99046
20.0	0.96764	0.99935	0.99521	0.96412	0.99926	0.99466	0.94816	0.99864	0.99142

Table A3-17

Encircled energy factors associated with the pupils $T(x)=1$, $T(x,5)$, and $T(x,M)$ for the cases:

W	$\phi(x) = \pi x^4$			$\phi(x) = \pi x^4 - \pi x^2$			$\phi(x) = \pi x^4 - 2\pi x^2$		
	T(X)=1	T(X,5)	T(X,M)	T(X)=1	T(X,5)	T(X,M)	T(X)=1	T(X,5)	T(X,M)
0.5	0.02406	0.02907	0.02936	0.05734	0.04011	0.05042	0.02378	0.01659	0.01923
1.0	0.08934	0.11126	0.11134	0.20900	0.15132	0.18751	0.03530	0.06371	0.07162
1.5	0.17873	0.23288	0.22978	0.40386	0.30939	0.37449	0.16130	0.17220	0.14404
2.0	0.27306	0.37530	0.36390	0.59408	0.48289	0.56623	0.22934	0.21353	0.22216
2.5	0.35911	0.51950	0.49449	0.71003	0.64272	0.72540	0.28072	0.29910	0.29497
3.0	0.43269	0.65006	0.60831	0.77305	0.76958	0.83328	0.32369	0.38423	0.36755
3.5	0.49611	0.75745	0.69938	0.79122	0.85694	0.89144	0.37534	0.46763	0.43878
4.0	0.55280	0.83827	0.76759	0.79316	0.90921	0.91511	0.44832	0.54958	0.51598
4.5	0.60341	0.89402	0.81613	0.80092	0.93692	0.92310	0.54143	0.62983	0.59905
5.0	0.64576	0.92921	0.84928	0.82127	0.95135	0.92934	0.64007	0.70640	0.68558
6.0	0.70104	0.96027	0.88627	0.87156	0.96938	0.95278	0.78485	0.83480	0.82925
7.0	0.73932	0.96973	0.90805	0.89281	0.98541	0.97463	0.83343	0.91540	0.90557
8.0	0.78695	0.97689	0.93009	0.90266	0.99467	0.98252	0.87555	0.95660	0.94278
9.0	0.82654	0.98418	0.94905	0.91688	0.99715	0.98467	0.91956	0.97891	0.97012
10.0	0.84707	0.98906	0.95989	0.92332	0.99733	0.98603	0.93794	0.99180	0.98671
11.0	0.86813	0.99188	0.96748	0.92870	0.99758	0.98745	0.94035	0.99712	0.99098
12.0	0.89039	0.99405	0.97434	0.93905	0.99817	0.98962	0.94937	0.99839	0.99198
13.0	0.90289	0.99554	0.97949	0.94407	0.99859	0.99098	0.95368	0.99881	0.99330
14.0	0.91228	0.99639	0.98229	0.94614	0.99868	0.99136	0.95425	0.99908	0.99366
15.0	0.92526	0.99715	0.98548	0.95226	0.99881	0.99231	0.95830	0.99917	0.99392
16.0	0.93313	0.99777	0.98782	0.95631	0.99899	0.99321	0.96159	0.99921	0.99434
17.0	0.93749	0.99808	0.98396	0.95730	0.99905	0.99343	0.96195	0.99922	0.99441
18.0	0.94485	0.99836	0.99040	0.96094	0.99911	0.99391	0.96468	0.99925	0.99471
19.0	0.95039	0.99865	0.99172	0.96418	0.99921	0.99452	0.96745	0.99933	0.99515
20.0	0.95265	0.99879	0.99227	0.96480	0.99925	0.99467	0.96776	0.99935	0.99523

Table A3-18

Encircled energy factors associated with the pupils T(x)=1, T(x,5), and T(x,M) for the cases:

	$\phi(x) = 2\pi x^4$			$\phi(x) = 2\pi x^4 - 2\pi x^2$			$\phi(x) = 2\pi x^4 - 4\pi x^2$		
W	T(X)=1	T(X,5)	T(X,M)	T(X)=1	T(X,5)	T(X,M)	T(X)=1	T(X,5)	T(X,M)
0.5	0.00557	0.01751	0.01349	0.04848	0.03343	0.04251	0.00523	0.00035	0.00051
1.0	0.02224	0.06821	0.05272	0.17672	0.12601	0.15795	0.01732	0.00164	0.00152
1.5	0.04972	0.14681	0.11408	0.34142	0.25731	0.31496	0.02850	0.00468	0.00229
2.0	0.08702	0.24535	0.19183	0.49355	0.40108	0.47527	0.03337	0.01100	0.00329
2.5	0.13187	0.35435	0.27874	0.59947	0.53346	0.60763	0.03392	0.02283	0.00725
3.0	0.18057	0.46413	0.36697	0.65205	0.63939	0.69721	0.03876	0.04248	0.01946
3.5	0.22851	0.56625	0.44939	0.66733	0.71489	0.74695	0.05701	0.07152	0.04059
4.0	0.27144	0.65463	0.52076	0.67099	0.76523	0.77164	0.09170	0.11038	0.07466
4.5	0.30701	0.72608	0.57862	0.68344	0.80029	0.78872	0.13753	0.15760	0.11844
5.0	0.33567	0.78036	0.62338	0.71172	0.82959	0.81046	0.18489	0.21110	0.16795
6.0	0.38446	0.84680	0.68484	0.78977	0.88965	0.87593	0.26645	0.32962	0.27457
7.0	0.43941	0.87995	0.72928	0.84248	0.94592	0.93702	0.37048	0.45941	0.39994
8.0	0.49189	0.90092	0.76772	0.86356	0.97853	0.96406	0.53361	0.59640	0.55187
9.0	0.53658	0.91868	0.80143	0.87305	0.98828	0.96790	0.68590	0.72291	0.69713
10.0	0.58395	0.93525	0.83308	0.88181	0.99330	0.96942	0.77217	0.81994	0.80045
11.0	0.63514	0.94975	0.86237	0.89779	0.99236	0.97590	0.83462	0.88685	0.87016
12.0	0.67546	0.96071	0.88525	0.91408	0.99567	0.98265	0.89991	0.93382	0.92535
13.0	0.70821	0.96858	0.90282	0.92063	0.99730	0.98526	0.93874	0.96555	0.96321
14.0	0.74464	0.97501	0.91917	0.92592	0.99754	0.98614	0.94894	0.98309	0.98036
15.0	0.77696	0.98030	0.93324	0.93541	0.99779	0.98810	0.95657	0.99118	0.98728
16.0	0.79969	0.98418	0.94343	0.94112	0.99820	0.98975	0.96407	0.99538	0.99205
17.0	0.82272	0.98722	0.95221	0.94401	0.99843	0.99047	0.96548	0.99779	0.99454
18.0	0.84607	0.98984	0.96043	0.94970	0.99861	0.99146	0.96644	0.99878	0.99500
19.0	0.86209	0.99180	0.96640	0.95402	0.99879	0.99241	0.96815	0.99901	0.99502
20.0	0.87581	0.99322	0.97098	0.95570	0.99888	0.99280	0.96842	0.99913	0.99513

Fig. A3-19

MTF curves associated with the pupils $T(x)=1, T(x,5)$, $T(x,M)$ for the cases:

(a) $\phi(x)=0$

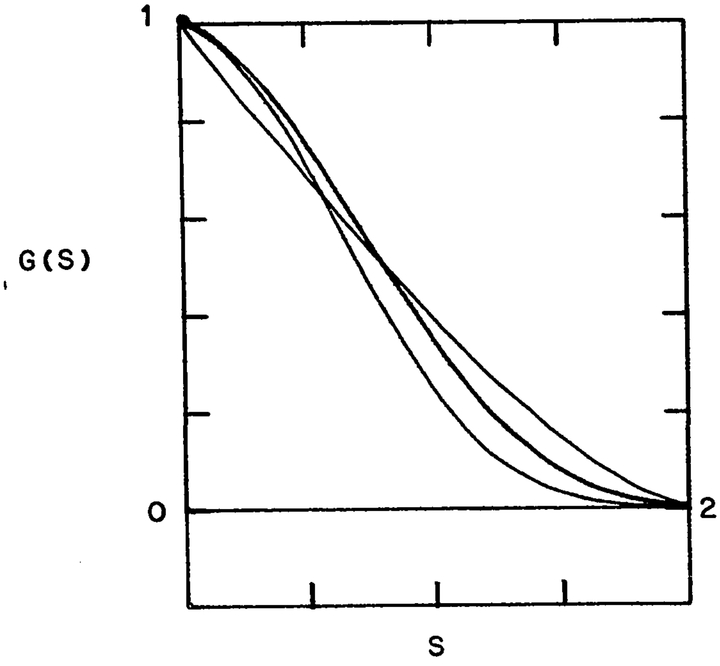

(b) $\phi(x)=\pi x^2$

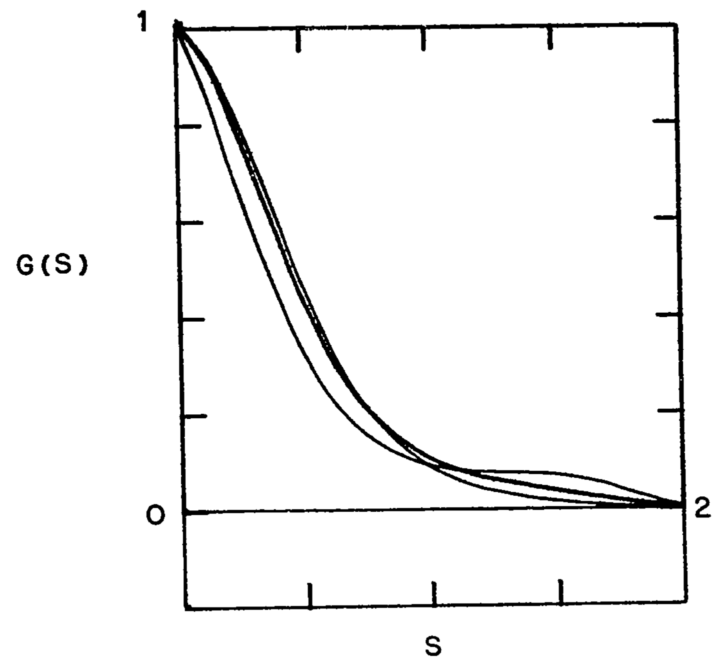

(c) $\phi(x)=2\pi x^2$

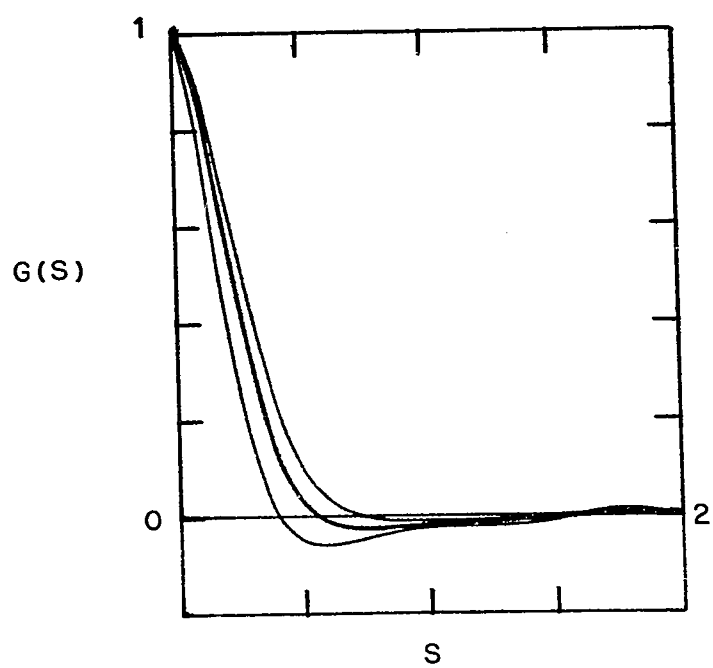

Fig. A3-20

MTF curves associated with the pupils $T(x)=1, T(x,5)$, $T(x,M)$ for the cases:

(a) $\phi(x) = \pi x^4$

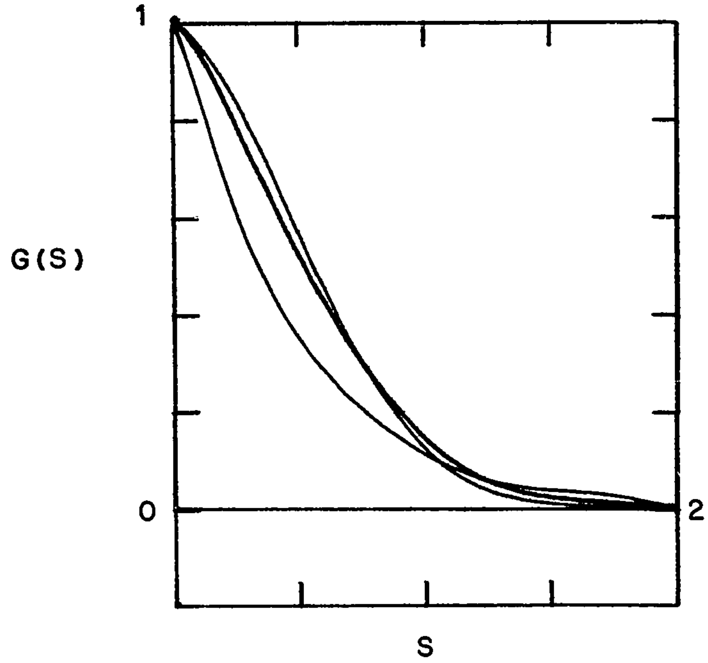

(b) $\phi(x) = \pi x^4 - \pi x^2$

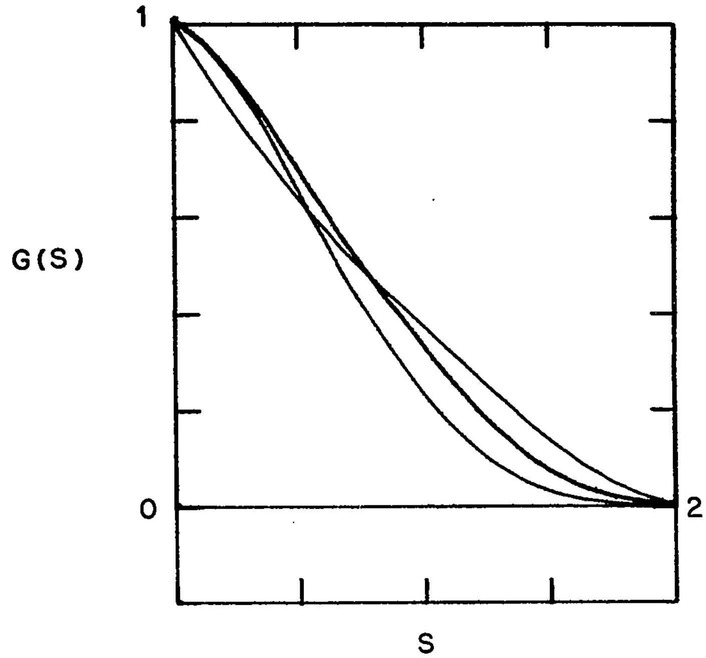

(c) $\phi(x) = \pi x^4 - 2\pi x^2$

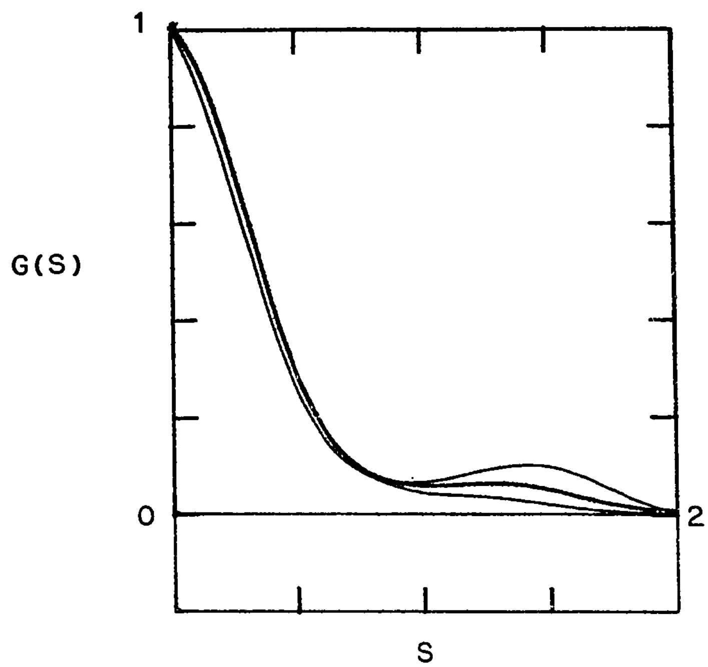

Fig. A3-21

MTF curves associated with the pupils T(x)=1, T(x,5), T(x,M) for the cases:

(a) $\phi(x)=2\pi x^4$

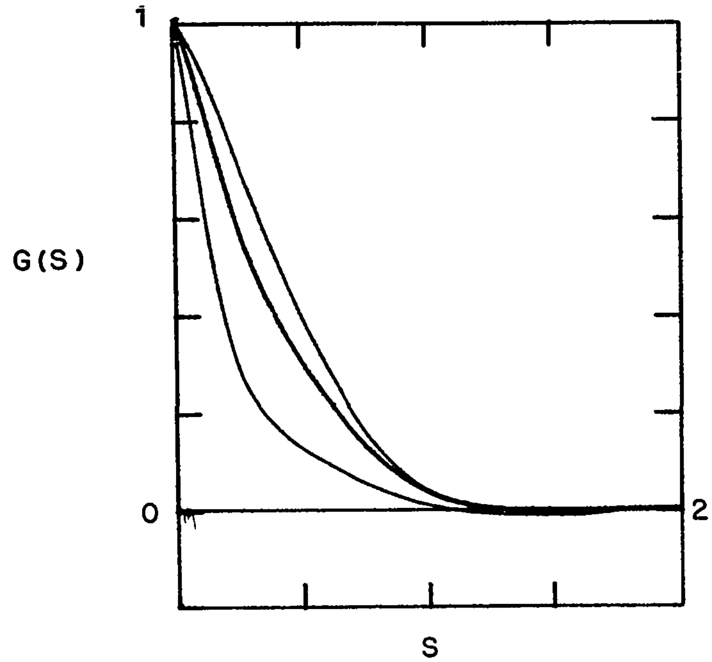

(b) $\phi(x)=2\pi x^4 - 2\pi x^2$

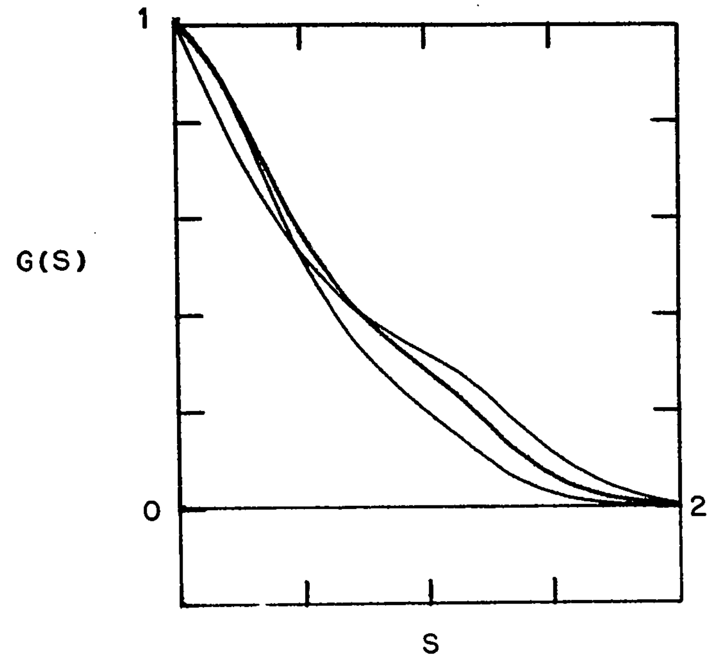

(c) $\phi(x)=2\pi x^4 - 4\pi x^2$

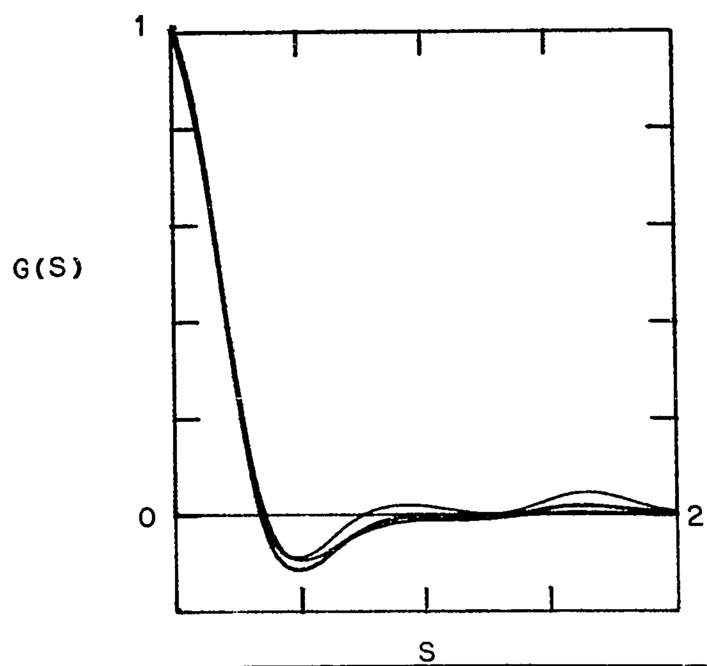

F- DISCUSSION:-

a) Diffraction Patterns:- Figs A3-1 to A3-15
Tables A3-1 to A3-15

Consider first the diffraction patterns corresponding to the aberration-free case and to the defect of focus cases. In the former case, we note that the filters T(x,5) and T(x,M) form diffraction patterns in which the central spot is wider than that of the Airy pattern, but in which the amplitude of the secondary maxima has been greatly reduced: the radius of the central spot corresponding to T(x,5) is about 5.8, that corresponding to T(x,M) is about 4.7, whereas for the Airy pattern it is 3.8. As defect of focus increases, the diffraction patterns corresponding to the three cases evolve roughly in the same way: ie, the amplitude of the central maximum drops, the diameter of the central spot increases, the minima are no longer zero, and the amplitude of the secondary maxima increases. However, we note that the central amplitude drops fastest for the T(x)=1 case, next comes the T(x,M) filter, and the T(x,5) filter last. Furthermore, the amplitude of the secondary maxima is always much greater for $T(x)\equiv 1$ than for the other two cases. As far as comparing the diameters of the central spots is concerned, this is neither easy nor very meaningful, because the first minimum is either very different from zero, or almost inexistant; also, the central amplitudes corresponding to the different amplitude filters are different. Another approach would be to define the "width" of the central spot using Sparrow's criterion[2] : according to this criterion, two incoherent point sources, of equal brightness, will be just resolved when the second derivative of the total illumination in the image vanishes at the center of the pattern. It can be shown that this implies

$$\frac{d^2 \, |A(W)|^2}{dW^2} = 0 \qquad W=Wo$$

where 2Wo is the Sparrow limit of resolution. In other words, the limit of resolution, in this sense, is twice the distance from the center of the pattern to the first inflection point on the intensity vs W curve; hence, this distance, or width, would serve as a criterion of quality for a diffraction pattern. However, we do not think that this criterion is any better than the previous one in assessing the relative merits of diffraction patterns: consider, for example, the diffraction patterns corresponding to $\phi(x)=1.5\pi x^2$. From the curve corresponding to $T(x)=1$, it is obvious that the intensity vs W curve would have its first inflection point at about .95, hence Sparrow's limit of resolution would be about 1.9. Inspection of the curve indicates that this is very unlikely, since the first minimum is a shallow dip, and the intensity decreases only slowly past that point. However, let us look more closely at the Rayleigh criterion: according to the latter, two incoherent point sources will be just resolved when the centre of one diffraction pattern coincides with the first minimum of the other. In this case, if the first minimum is zero, then the intensity at the center of the resulting pattern is about 80% of that in the adjacent maxima. Of course, when the first minimum is different from zero, the Rayleigh criterion is not directly applicable; in such cases, it is usually assumed that the two point sources will be just resolved if the intensity at the center of the pattern is about 80% of the intensity in the adjacent maxima. If 2δ represents the resolution limit in this generalized Rayleigh criterion, then the conditions stated above can be expressed as $\dfrac{2A^2(\delta)}{A^2(o) + A^2(2\delta)} = .8$

When the first minimum is close to zero, then we have that $A^2(\delta) \simeq .4\,A^2(o)$; i.e., the "Rayleigh" limit is almost equal to the half intensity width, or half-width, of the diffraction pattern. The half-width is $2\delta h$, where $A^2(\delta h) = .5\,A^2(o)$.

On the other hand, when the first minimum is very different from zero, not only is the "Rayleigh" resolution limit difficult to determine, but also it becomes quite meaningless. Consider for example the case when the first minimum is about $.7A^2(o)$: it is obvious that in this case, it is impossible to define the Rayleigh limit as above. In cases such as this, the half-width is a more convenient basis of comparison of diffraction patterns, and we shall use it in the analysis that follows. Since the curves represent amplitude versus W, we shall consider the width $\delta$where $A(\delta) = .7A(o)$.

If we determine these half-widths for the cases considered above, we find that as the defect of focus increases, the half-widths of the diffraction patterns corresponding to the three pupils increase, as we would expect, but their relative differences decrease, until at a position roughly between those corresponding to $\phi(x) = \pi x^2$ and $\phi(x) = 1.5\pi x^2$, the three half-widths are the same. Beyond that, the half-width of the diffraction pattern corresponding to $T(x,5)$ is the least, then comes that corresponding to $T(x,M)$, and finally the case $T(x) \equiv 1$ has the greatest half-width. If we further increase the defect of focus, then we can no longer speak of half-widths, because the diffraction patterns begin to show a central minimum (which can result in images having contrast reversals or spurious resolution). Note that at

$\phi(x) = 2\pi x^2$, the intensity at the center has dropped to zero in the case of $T(x)\equiv 1$, whereas for $T(x,5)$ there is no dip at all at the center, and for $T(x,M)$, there is a small dip.

We next consider the case of spherical aberration with and without defect of focus. Let us write $\phi(x) = \alpha x^4 - \beta x^2$. We recall that $\phi(x)$ gives the departure of the wavefront emerging from the exit pupil of the optical system from the reference sphere centered in the observation plane. Suppose $\beta=0$; by extension of the aberration-free case, we shall say that there is no defect of focus. When spherical aberration is present ($\alpha \neq o$), this position corresponds to the paraxial focus, because for rays very near the optical axis, $\alpha x^4 \approx 0$, hence there is no aberration for these rays, and they are correctly focussed in the image plane.
Suppose now that $\beta = 2\alpha$: we have

$$\phi(x) = \alpha(x^4-2x^2)$$

$$\partial\phi/\partial x = 4\alpha x(x^2-1)$$

Thus, $\partial\phi/\partial x = 0$ when $x = 1$, which means that at the edge of the pupil, the wavefront is tangent to the reference sphere. Since the rays of light (ie, the direction of propagation of the waves) are perpendicular to the wavefront (Malus-Dupin theorem), this means that rays of light at the edge of the pupil will be correctly focussed at the center of curvature of the reference sphere, in the observation plane. This position is called the marginal focus. At a point halfway between the paraxial focus and the marginal focus, (i.e., when $\beta = \alpha$), $\phi(x) = \alpha(x^4 - x^2)$ and we see that $\phi(x)$ is 0 at $x = 0$ and $x = 1$. This position corresponds roughly to that of the circle of least confusion in geometrical optics.

If we study the diffraction patterns formed by the three pupils when spherical aberration is present, we note that:

1) The best diffraction patterns are formed when $\phi(x) = \pi x^4 - \pi x^2$ or $2\pi x^4 - 2\pi x^2$(i.e.,$\alpha=\beta$). In these cases, the diffraction patterns resemble those formed in the aberration-free case, and as far as the relative merits of the 3 pupils are concerned, the same comments which were made in the preceding section can be applied here.

2) For a small defect of focus (around the paraxial focus), the pupils T(x,5) and T(x,M) improve the diffraction pattern: they produce a greater amplitude at the center of the pattern, and they considerably reduce the amplitude of the secondary maxima. From these points of view, the T(x,5) pupil is the best. As far as half-widths are concerned, the $T(x)\equiv 1$ case has the least, but the differences between the three cases are relatively smaller than in the aberration-free case.

3) When the defect of focus is large,i.e.,beyond $\beta=\alpha$, the filters bring little improvement to the diffraction patterns (especially in the presence of large spherical aberration), except in the far field ($W > 15$) , where the amplitudes of the maxima are reduced.

b) Encircled Energy factors: Fig. A3-16 to A3-18
and Tables A3-16 to A3-18

In all the cases studied, it can be seen readily from the curves that the amplitude filters T(x,5) and T(x,M) concentrate more energy towards the center of the diffraction pattern than the uniformly transmitting pupil T(x) = 1.

In the case of defect of focus, both the T(x,5) and T(x,M) curves are markedly better than those corresponding to $T(x)\equiv 1$, and it appears that the T(x,5) filter is the best one to use for moderate to large defect of focus; for a small defect of focus, or no defect of focus, the T(x,M) filter gives the best performance up to about W=4, after which the T(x,5) filter becomes preferable.

The curves for spherical aberration plus defect of focus show that optimum concentration of energy is achieved, for the 3 pupils, when the observation plane is roughly midway between the paraxial focus and the marginal focus: i.e., in the cases $\phi(x) = \pi x^4 - \pi x^2$ and $\phi(x) = 2\pi x^4 - 2\pi x^2$. Around this optimum position, the T(x,M) filter gives the best results below about W = 4, whereas above this value, the T(x,5) filter is best. As one moves away from this optimum position towards either the marginal or the paraxial focus, the T(x,5) filter gives the best results for all values of W. Note in particular the spectacular improvement at the paraxial focus.

c) Modulation Transfer Functions: Figs A3-19 to A3-21

We shall first consider the case of an aberration-free optical system, without and with defect of focus. In the former case, note that the filters T(x,5) and T(x,M) behave like typical apodisers, i.e., they improve the low-frequency response of the optical system, but the high frequency response is considerably decreased. We shall call "cross-over frequency" the spatial frequency at which the MTF curve of pupil T(x,5) or T(x,M) intersects that of pupil $T(x)\equiv 1$. For T(x,5), the cross-over frequency is at about s = .56, whereas it is at about s = .80 for T(x,M). As we increase the defect of focus, the cross-over frequencies for both T(x,5) and T(x,M) increase to a greater value of s ; that is, the filters T(x,5) and T(x,M) improve the response of the system for a greater range of spatial frequencies. (Note: a small negative value for the MTF is better than a large negative value, because negative values imply spurious resolution and contrast reversals). For example, in the case where the defect of focus is $2\pi x^2$, the three curves intersect at a value of s of about 1.6, so that the two filters T(x,5) and T(x,M) improve the response of the system over that of the pupil $T(x)\equiv 1$ for $0 \leqslant s \leqslant 1.6$ and the pupil $T(x)\equiv 1.0$ has a slightly better response for $1.6 < s \leqslant 2$. Note also that for small -to- moderate defect of focus, the filter T(x,M) is superior to the T(x,5) filter throughout the range of s, whereas beyond a position roughly midway between those corresponding to πx^2 and $2\pi x^2$, the reverse is true.

For the case of spherical aberration plus defect of focus, we note the following:

1) At the paraxial focus, both amplitude filters greatly improve the MTF for a range of s which is quite extended: for example, when $\alpha=\pi$, the

cross-over frequencies are 1.04 and 1.25 for T(x,5) and T(x,M) resp. When $\alpha = 2\pi$, the improvement is achieved throughout the range of s. We note that for $\alpha=\pi$, the T(x,5) filter is better than the T(x,M) filter for $s \leqslant .75$, and the reverse is true beyond that value, whereas for $\alpha = 2\pi$, T(x,5) is better throughout the range of s.

2) When $\alpha = \beta$, i.e., at a position midway between the paraxial and marginal foci, the MTF curves are very close to the ones corresponding to the aberration-free case ($\alpha=\beta=0$), and the same observations as for that case apply. We note also that, as in the case of diffraction patterns and encircled energy factors, it is at this position that, for all pupils considered, the over all response of the system is best.

3) Finally, as we approach the marginal focus, the MTF of the three pupils are almost the same at low frequencies, whereas at high frequencies, the $T(x)\equiv 1$ pupil has a slightly better response than the T(x,5) and T(x,M) pupils.

CONCLUSIONS:

From the foregoing discussion, we can draw the following conclusions about the effect of the amplitude filters T(x,5) and T(x,M) in optical systems:

1) Lenses equipped with these amplitude filters will form images having in general a much better overall contrast and lower background than unfiltered lenses, except when the object contains very fine detail.

2) The depth of focus in filtered systems will be greater than that of unfiltered systems of the same numerical aperture. The T(x,M) filter is preferable in systems where the depth of focus required is relatively small, and where images have very fine details; on the other hand, the T(x,5) filter is preferable when maximum defocussing tolerance is required or/and when resolution of very fine details is not required as much as good image contrast.

3) When spherical aberration is present in a lens, the best image is formed at a position of the observation plane corresponding to $\alpha=\beta$; in this case, the amplitude filters improve the image as in 1). The filters also improve the depth of focus for a defocussing towards the paraxial focus. Filtered lenses can be used over a wider range of apertures than unfiltered ones before spherical aberration seriously deteriorates the image. Also, the position of the best image ($\alpha=\beta$) changes as the aperture of a lens is changed. This requires re-focussing. With filtered lenses, this re-focussing is greatly reduced (with the same aperture). Finally, we note that when spherical aberration is present, the T(x,5) filter gives better results than the T(x,M) filter.

CHAPTER IV

FLUX SELECTORS: WHAT THEY ARE, WHY THEY ARE NEEDED, AND HOW THEY ARE CALCULATED

It is very difficult to make a good amplitude filter, and all efforts to do so have failed. The reason for this is that the main methods available so far require the use of either photographic emulsions, neutral density glasses, or metallic coatings of variable thickness to produce the required variation in light transmission: but photographic emulsions and neutral glasses produce scattering of light, whereas the metal films introduce phase variations in the light beam, and both these effects are detrimental to the resulting diffraction pattern.

The so-called "flux-selector" was introduced by Lansraux to avoid these difficulties. In the derivation below, we follow his treatment of the problem. Consider equation A1-3 which gives the diffraction pattern produced by T(x). In the aberration-free case, the contribution dA to A(W) of an infinitesimal annular element extending from x-dx/2 to x+dx/2 is $MT(x)J_0(Wx)d(x^2)$. Since $d(x^2)$ is proportional to the area dS of the element considered, we put $Md(x^2) = M'dS$. Now, inside the element dS, one can find elements dS' such that T(x)dS=dS'. We can then write dA as $M'T(x)J_0(Wx)dS$ or as $M'J_0(Wx)dS'$. But this last expression represents the contribution (to the diffraction pattern) of an element of a perfectly transmitting pupil, the element being situated at the same radius x, and having a smaller area than dS. Hence, associated with each infinitesimal annular area dS of the pupil T(x) is a smaller annular area dS' of a perfectly transmitting pupil such that the contributions of dS and dS' to the diffraction pattern are the same and such that dS'/dS = T(x). Hence, the infinite set of perfectly transmitting annuli dS' can replace the pupil T(x). We can apply the same idea, and generalize it slightly, to the case where the area segments considered are finite. Suppose we divide the pupil T(x) into N zones, and denote the upper and lower boundary of each zone by x_n and x'_n resp. Since the zones are all contiguous to one another, it is obvious that $x_n = x'_{n-1}$. For each pair (x_n, x'_n), we wish to associate a pair (r_n, r'_n) such that

$$\text{A4-7} \quad \int_{r_n}^{r'_n} J_0(Wx)d(x^2) = C\int_{x_n}^{x'_n} T(x)J_0(Wx)d(x^2) \quad \underline{\text{for all } W}$$

C is here a constant, as yet undetermined. If $C \leqslant 1$, we expect (r_n, r'_n) to be inside (x_n, x'_n), i.e., $r_n > x_n$ and $r'_n < x'_n$. The left hand side of A4-7 represents the diffraction pattern formed by a perfectly transmitting annulus having radii r_n and r'_n. Therefore, if A4-7 is satisfied for all N zones, the set of N annuli (r_n, r'_n), the separation between two successive annuli being opaque, can replace the transmission function T(x), and give the same diffraction pattern (apart from a constant multiple C) as T(x). This set of annuli constitutes the flux selector (abbreviation F.S.). It can already be seen that many different types of F.S. can exist, depending on the choice of the zone division (x_n, x'_n).

Given a zone division, the calculation of the F.S. radii from A4-7 is not simple, since it involves the solution of an integral relationship; furthermore, it is expected that there is no solution which is absolutely independent of W. However, an approximate solution can be obtained which will be valid for a more or less extended range of W, depending on the zone division. Consider the equation

$$\text{A4-8a}\quad \delta = C\int_{x_n}^{x_n'} T(x)\, J_o(Wx)\, d(x^2) - \int_{r_n}^{r_n'} J_o(Wx)\, d(x^2)$$

To satisfy A4-7, we wish to have $\delta = 0$. Now, we can express $J_o(Wx)$ by a Taylor expansion in $(Wx)^2$ about a point $(WR_n)^2$, where R_n is a point in interval (r_n, r_n') (Note: $J_o(z)$ is an even function.):

$$J_o(Wx) = J_o(WR_n) + (WR_n/2)J_1(WR_n)[1-(x/R_n)^2] + \ldots + \frac{(WR_n)^k J_k(WR_n)}{2^k\, k!}[1-(x/R_n)^2]^k$$

where we have used the property that $\frac{1}{x}\frac{d^k}{dx^k} J_o(x) = (-1)^k J_k(x)/x^k$ .Hence,

$$\int_{r_n}^{r_n'} J_o(Wx)d(x^2) = R_n^2 \sum_0^\infty \frac{(WR_n)^k J_k(WR_n)}{(k+1)!\,2^k}\left[\{1-(r_n/R_n)^2\}^{k+1} - \{1-(r_n'/R_n)^2\}^{k+1}\right]$$

Similarly,

$$\int_{x_n}^{x_n'} T(x)\, J_o(Wx)d(x^2) = \sum_0^\infty \frac{(WR_n)^k J_k(WR_n)}{k!\ 2^k}\int_{x_n}^{x_n'} T(x)\, [1-(x/R_n)^2]^k\, d(x^2)$$

So that A4-8a becomes:

$$\text{A4-8b}\quad \delta = \sum_0^\infty \frac{(WR_n)^k J_k(WR_n)}{k!\ 2^k}\left[\int_{x_n}^{x_n'} T(x)\, \{1-(x/R_n)^2\}^k\, d(x^2) - \frac{CR_n^2}{k+1}\{(1-r_n^2/R_n^2)^{k+1} - (1-r_n'^2/R_n^2)^{k+1}\}\right]$$

Note that the expression between square brackets is independent of W. Although the condition $\delta=0$ for all W cannot be satisfied exactly, δ can be made small for a certain range of W by requiring that one or more low order terms in A4-8b be zero. For ex., requiring that the first term (k=0) be zero gives:

$$\text{A4-9}\quad r_n'^2 - r_n^2 = 1/C\int_{x_n}^{x_n'} T(x)\, d(x^2)$$

Given a zone division, this relation is not sufficient to determine r_n and r_n'; a further equation is required, which is obtained by putting the second term (k=1) equal to zero. This gives:

$$\int_{x_n}^{x_n'} T(x)\, d(x^2) - [1/R_n^2] \int_{x_n}^{x_n} T(x)\, x^2 d(x^2) = C(r_n'^2 - r_n^2) + \frac{C}{2R_n^2}(r_n^4 - r_n'^4)$$

But using A4-9, this becomes $r_n'^4 - r_n^4 = 2/C \int_{x_n}^{x_n'} T(x)\, x^2 d(x^2)$ and dividing this expression by A4-9, it becomes:

$$\text{A4-10a} \quad r_n'^2 + r_n^2 = 2 \int_{x_n}^{x_n'} T(x)\, x^2 d(x^2) \Big/ \int_{x_n}^{x_n'} T(x)\, d(x^2)$$

Combining A4-10a with A4-9 gives:

$$\text{A4-10b or A4-10} \quad r_n'^2 = \frac{\int_{x_n}^{x_n'} T(x)\, x^2 d(x^2)}{\int_{x_n}^{x_n'} T(x)\, d(x^2)} + \frac{1}{2C} \int_{x_n}^{x_n'} T(x)\, d(x^2)$$

$$r_n^2 = \frac{\int_{x_n}^{x_n'} T(x)\, x^2 d(x^2)}{\int_{x_n}^{x_n'} T(x)\, d(x^2)} - \frac{1}{2C} \int_{x_n}^{x_n'} T(x)\, d(x^2)$$

Whence r_n and r_n' are completely determined once x_n and x_n' and C are given. The expression A4-10 , however, can be somewhat difficult to handle, and to simplify the calculation, we rewrite A4-10a approx. by putting

$$\int_{x_n}^{x_n'} T(x) x^2 d(x^2) \simeq T(\beta_n) \int_{x_n}^{x_n'} x^2\, d(x^2) \text{ and } \int_{x_n}^{x_n'} T(x) d(x^2) \simeq T(\beta_n') \int_{x_n}^{x_n'} d(x^2).$$

where β_n and β_n' are points inside (x_n, x_n'); if this interval is small, and if T(x) is relatively slow-varying, then we have approx. $T(\beta_n) = T(\beta_n')$, and hence A4-10a becomes

$$\text{A4-11} \qquad r_n'^2 + r_n^2 = x_n^2 + x_n'^2$$

If the interval (x_n, x_n') is small, then A4-11 will be almost equivalent to

$$\text{A4-12} \qquad r_n' + r_n = x_n + x_n'$$

since $r_n r_n' \simeq x_n x_n'$ in that case. Hence, to determine r_n and r_n', either A4-11 or A4-12 can be used in conjunction with A4-9, or the more accurate relations A4-10 can be used alone. (Note: the reason for wanting to use equation A4-12 instead of A4-11 in some cases is that calculations involving the former can be done much faster for a given accuracy than those involving the latter; this consideration can be very important when calculating F.S. having large numbers of rings or/and using iterative procedures to determine the zone division.) Having calculated all the (r_n, r_n'), the F.S. can be improved in the following manner: if all the r_n, r_n' are multiplied by the same constant H, say, then the diffraction pattern does not change in aspect, but is contracted or expanded[8] with a corresponding increase or decrease in E(W) for any given W depending on whether H is greater than or less than unity resp. Now, the pupil considered here has radius 1; however, r_N', as calculated from A4-9 through A4-12, is in most cases less than 1. If so, the pupil space from r_N' to 1 is, in effect, lost; it is desirable, then, to make $r_N'=1$ (without of course altering the aspect of the diffraction pattern). This can be done quite simply by multiplying all of the r_n, r_n' by the factor $H=1/r_N'$ i.e.,

$$\text{A4-13} \qquad \underline{r}_n = r_n / r_N' \qquad \underline{r}_n' = r_n' / r_N'$$

This process is called an homothetic transformation. To illustrate the effect of such transformation, the diffraction patterns of F.S. 2-A2 and

2-A2-H (differing from the preceding by homothetic transformation only) are both shown in Fig A4-1.

Note: In the above treatment, we have assumed no aberrations or defect of focus. However, it can be seen from equation A4-7 that the effect of aberrations or defect of focus would be to multiply the integral on both sides of the equation by the same function $e^{i\phi(x)}$. To a first order approximation, this factor can be taken out of the integrals and cancelled: the work of the next chapter will show that very little error is introduced in flux selector calculations by making first order approximations. Hence, we expect that the flux selectors calculated as above will be valid when aberrations are present, provided these are not too severe.

Equations A4-9 through A4-13 constitute the basic formulae that were used in all the flux selector work considered in this thesis. Lansraux has calculated several flux selectors using a 5 term expansion for T(x,5). Choosing the simplest type of zone division, i.e., N zones of equal width ($x_n' = n/N$), he has calculated 10 and 20 ring flux selectors choosing C such that $r_1=0$. He has made the calculation using A4-9 and A4-12, and then, using A4-9 and A4-11, and has found little difference between the two cases, thus justifying, for that case at least, the validity of the approximation of A4-11 by A4-12. Choosing a slightly different zone division, i.e., putting the first zone equal to a/2, then the following N-1 zones equal to a, and the last zone equal to a/2, i.e., a total of N + 1 zones, he has calculated 11 and 21 ring flux selectors, again choosing C such that $r_1=0$, and putting $r_{N+1}=1$. These calculations were performed using A4-9 and A4-12. In this type of flux selector, condition A4-12 is not applied to the marginal zone. (This method of zonal division was chosen in analogy to certain methods in numerical integration, where it is found that dividing the integration interval in N-1 full zones bordered by two half zones gives better results that dividing the interval into N equal zones). Note: the flux selectors and diffraction patterns calculated by Lansraux were re-calculated (to a higher degree of precision) in our work, and will be considered in the next section.

The results of the above work were very encouraging; however, to check their validity, the work should be carried further by using the more exact expression A4-10, and by using a more accurate expansion for T(x,5). Furthermore, before seeking to annul a third term in A4-8b (which would remove all freedom of choice of the (x_n, x_n'), it was necessary to make a thorough investigation of the different types of flux selectors which could be obtained by changing the zone division. This extension of the work done by Lansraux was one of the purpose of the theoretical part of our work.

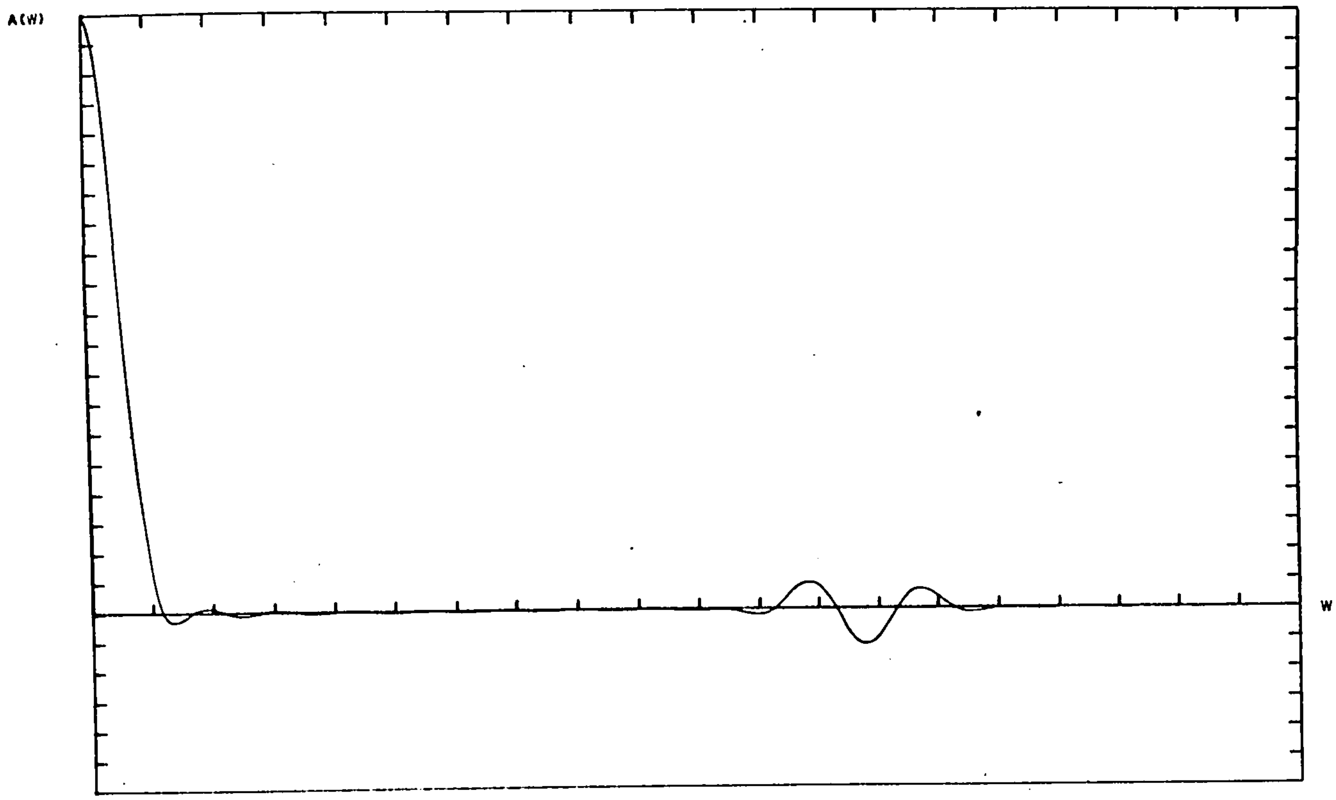

Fig. A4-1(a) Diffraction pattern formed by the F.S. 10(2-A2)

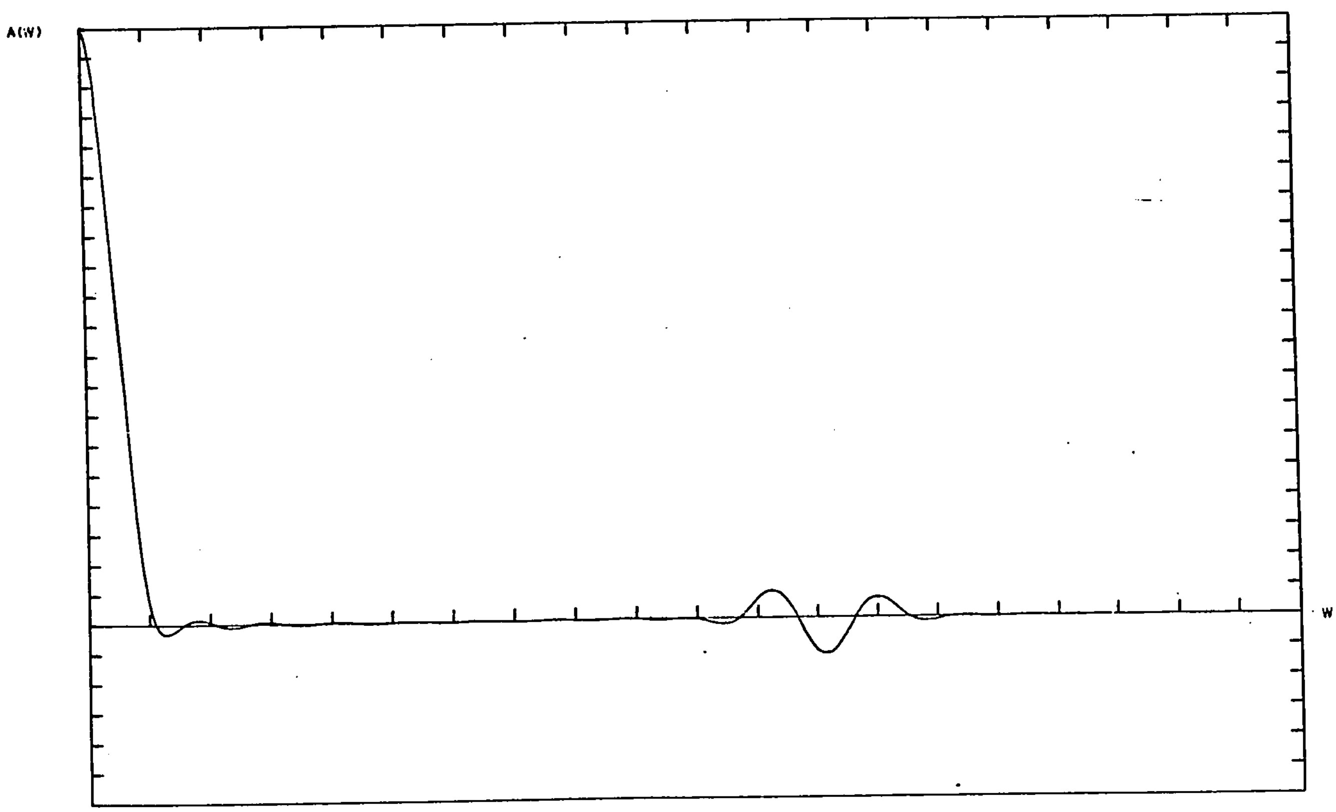

Fig. A4-1(b) Diffraction pattern formed by the F.S. 10(2-A2-H)

CHAPTER V

INVESTIGATION AND COMPARISON OF VARIOUS TYPES OF FLUX SELECTORS.

The amplitude filter $T(x,5)$ was used in all the flux selector calculations described in this chapter. In order to simplify the writing, we shall denote $T(x,5)$ by $T(x)$.

Furthermore, it is assumed that the optical system is aberration-free and correctly focussed, i.e., $\phi(x) \equiv 0$.

A - PRELIMINARY REMARKS:

1- Calculation of flux selectors:

Most of the calculations described in this chapter were carried out with an IBM 1620 computer. Since all the flux selector calculations require the evaluation of the integrals given in either equa. A4-9 or in equa. A4-10, it is worthwhile describing briefly how this was done. Consider equa. A1-6. Putting $a_p = pk_p$, $T(x) = \sum_1^n ap(1-x^2)^{p-1}$, and then the integral $\int T(x)d(x^2)$ can be re-written $I = \sum_1^n a_p \int (1-x^2)^{p-1} d(x^2)$; hence,

$$\text{A5-1} \quad \int T(x)\, d(x^2) = -\sum_1^n \frac{ap}{p} (1-x^2)^p$$

A subroutine was developped to calculate A5-1, for a given x. Hence, this subroutine could be used in any program to evaluate A4-9. Consider now equations A4-10. Part of these can be evaluated using the above subroutine. The integral $\int T(x)\, x^2 d(x^2)$ can be evaluated as follows:

$$\int T(x)\, x^2 d(x^2) = \int \sum_1^n a_p (1-x^2)^{p-1} x^2 d(x^2) = \sum_1^n a_p \int x^2 (1-x^2)^{p-1} d(x^2)$$

$$= \sum_1^n a_p \left[(1-x^2)^{p+1} / p+1 - (1-x^2)^p / p \right] \quad \text{A5-2}$$

A subroutine was developped to calculate the above expression, given x. With these two subroutines, equations A4-9 and A4-10 could readily be evaluated given the zone division.

2- Calculation of diffraction pattern formed by flux selectors:

The diffraction pattern formed by a flux selector was calculated in the following manner: from equation A1-3, the diffraction pattern formed by a light transmitting annulus having inner and outer radii r_n and r_n' resp. is $\gamma_n(W) = M\int_{r_n}^{r_n'} J_o(Wx)d(x^2)$, or, putting $Wx=U$,

$$\gamma_n(W) = (2M/W^2)\int_{Wr_n}^{Wr_n'} J_o(U)UdU;\text{but, } d[UJ_1(U)] = UJ_o(U)\ dU,\text{whence,}$$

$\gamma_n(W)=(2M / W^2)\ [Wr_n'\ J_1(Wr_n') - Wr_nJ_1(Wr_n)]$. The diffraction pattern formed by the N annuli of the flux selector is then

$$A(W) = 2M\sum_1^N[r_n'J_1(Wr_n') - r_nJ_1(Wr_n)] / W \quad \text{A5-3}$$

Now, we wish to have a normalized diffraction pattern, i.e., $A(0) = 1$. To determine M, we put W=0 in the first equation above:

$A(0) = M\sum_1^N (r_n'^2 - r_n^2) = MT$ so that $M=1/T$, where T is the transmission factor of the flux selector; therefore,

$$A(W) = 2\sum_1^N [r_n'\ J_1(Wr_n') - r_nJ_1(Wr_n)] / WT$$

Obviously, the evaluation of this expression for many values of W requires the use of a computer, and for the latter, the main task will consist in calculating $J_1(Wr_n')$ and $J_1(Wr_n)$. Due to the importance of this calculation for the above work and for work to be described later, the methods used in the computation of Bessel functions will now be described.

3- Calculation of Bessel functions with the computer:

The easiest method of calculating Bessel functions with a computer is to use the MacLaurin expansion

$$J_n(z) = \sum_{0}^{\infty} (-1)^m \, (z/2)^{n+2m} \; / \; m!(n+m)!$$

One can set up an iterative procedure which calculates and sums the successive terms until the absolute value of the latter becomes smaller than or equal to the test value representing the maximum permissible error: since the series is convergent, then the error made in truncating the series at a given term is less in absolute value than the first neglected term; hence, every term gives the accuracy of the series up to that point. A subroutine was developped to calculate $J_n(z)$ (given n,z) using the above procedure. However, the following difficulties arise: for large arguments, the number of terms required is very large, and accumulative errors in the computer calculations cause the accuracy to deteriorate very fast; consequently, the calculations have to be carried out with a much larger number of significent figures than is required in the value of $J_n(z)$. Even then, this procedure is only good up to arguments $z \simeq 40$. Furthermore, the speed of computation is quite slow, especially for large arguments. To calculate $J_n(z)$ for large z ($z > 20$, say), an asymptotic expansion can be used[13]. The difficulty in using these series lies in the fact that they are not convergent; hence the truncation point has to be chosen more or less arbitrarily. A subroutine was developped to calculate $J_1(z)$ from an asymptotic expansion, truncating the series at their minimum point, or when the terms reached a certain pre-determined value, whichever came first. This subroutine and the one described above for arguments z less than 20, could be used to calculate $J_1(z)$ to 10 significant places (max. error = 10^{-10}) and for any argument: the only drawback was the slow speed of the calculations. For ex., calculating the diffraction pattern of a 10 ring flux selector for 200 values of W takes about 8 hours on the IBM 1620. This was unacceptable, so that a faster method had to be found, even at the sacrifice of some accuracy. E.E. Allen, in M.T.A.C.[14] review, gives the results of such a method, based on Chebyshev polynomials, and used to calculate $J_0(z)$ and $J_1(z)$. With this method, $J_0(z)$ and $J_1(z)$ could be calculated for any z with a max. error of $3x10^{-8}$, and an average speed about 8 times faster than that of the previous method. For diffraction pattern calculations, the reduced precision of this last method was not critical. However, for the calculation of certain types of flux selectors, or of special diffraction patterns, the first method was used because higher precision was required or because higher order Bessel functions were to be calculated. Hence, in all the work that follows, Bessel functions were calculated by one of the two methods described above, the choice of method depending on the speed vs. accuracy requirement.

4- Special Diffraction Patterns:

a) Circular Grating:

This "grating" consists of alternate opaque and light transmitting rings all having the same width. It is the analogue, in rotationally symmetric pupils, of the ordinary plane diffraction grating. This grating, as well as the diffraction pattern it forms, are included in our work for comparison purposes (See Fig. A5-3). Note that the diffraction pattern formed by this type of grating is even worse than the Airy pattern, so that it could not be used to improve the quality of optical images; (for an infinite number of rings, the circular grating would give a diffraction pattern identical to the Airy pattern).

b) Amplitude filter T(x):-

In this chapter, the diffraction pattern formed by T(x) for values of W from 0 to 325 is needed for comparison purposes. Gauss' method of numerical integration (chapter III) is not suitable for such an extended range of W; hence, we have used instead the following method. From A1-3, and using expression A1-6 for T(x), we have that

$$A(W) = M \sum_{1}^{n} pk_p \int_0^1 (1-x^2)^{p-1} \, Jo(Wx) \, dx^2$$

The integrals inside the summation sign are the well-known Hankel transforms. Hence, with $M = \Sigma k_p$ so that $A(o) = 1$, the diffraction pattern formed by T(x) is given by

$$A(W) = \frac{\sum_{1}^{n} p \, k_p \, 2^p \, (p-1)! \, J_p \, (W)}{W^p \sum_{1}^{n} k_p}$$

The diffraction pattern calculated from this expression for values of W from 0 to 100 is shown in Fig A5-2. The expression above can also be used for the calculation of the diffraction pattern formed by T(x,M).

B - CLASSIFICATION OF FLUX SELECTORS:-

Because of the many different types of flux selectors possible, it soon became necessary to assign a code number to each flux selector for reference purposes. The code number consists of 2 or 3 sections, separated from each other by hyphens.

The first section indicates which of equations A4-9 to A4-13 were used for the calculations: A4-9 + A4-11 are denoted by 1b - (or 1B-), A4-9 + A4-12 by 1a - (or 1A), and A4-10 by 2- . Note that in each case, the 1 or 2 also give the number of terms that are annulled in A4-8.

The second section is composed of one (or more) letters, followed by a number. The letter(s) designates the type of zone division used in calculating the flux selector; if more than one letter is used, the additional ones indicate subdivisions in the class designated by the first letter. For example, PA, PB, PC, denote three types of zone division, all included in a certain class P. The number following the letter(s) designates the choice of C in A4-9 or A4-10. Grouping zone types (such as PA, PB, PC) or some constants C in a class can result either from an arbitrary choice (e.g. for reference purposes) or from some analytical relation between them.

The last section consists of the single letter H and is included if the flux selector is Homothetically transformed and is omitted if it is not.

Finally, if it is desired to state the number of rings in a flux selector, this can be done by enclosing the code number in brackets and putting the number of rings in front; thus, 10(2-A2-H) means a 10 ring flux selector of the type 2-A2-H.

<u>Examples</u>:

(1) 1a-A2-H: flux selector calculated using A4-9 and A4-12, having a zone division given by $x_n' = n/N$, and C being chosen such that $r_1=0$; the flux selector is homothetically transformed.

(2) 1a-A4-H: same as above, except that C is chosen such that $r_1' = r_2$, and $r_1=0$. (Because of these two simultaneous conditions, relation A4-12 is not applied to first zone).

(3) 2-A2-H: same as (1), except that equations A4-10 are used to perform the calculations.

(4) 2-A51-H, 2-A52-H, 2-A53-H: same as (3) except for the choice of C: the numbers 51, 52, 53 represent C=50, 10 and 5 respectively.

C - DISCUSSION OF VARIOUS FLUX SELECTORS CALCULATED:

P.N.

The flux selectors described below are grouped according to their type of zone division. The results of the calculations for these flux selectors are given in Fig. and Tables A5-4 to A5-22 in the same order. The data sheets give the following information:

(1) the transmission factor $T = \sum_{1}^{n} (r_n'^2 - r_n^2)$ = ratio of the amount of light transmitted by the flux selector to the total amount of incident light.

(2) the zone boundaries x_n' , denoted by XP(I); note that X(I) = XP(I-1) and that X(1)=0.0 in all cases.

(3) the inner and outer radii (r_n and r_n') of the light transmitting rings in the flux selector [r_n or $\underline{r}_n \equiv R(I)$, r_n' or $\underline{r}_n' \equiv RP(I)$].

(4) the diffraction pattern formed by the flux selector for W = 0 to 100.

The W axis is divided at intervals of 5, whereas the A axis is divided at intervals of .05. All the diffraction patterns are normalized so that A(0)=1 in all cases. The curves are accurate to about ±.004 (approx. the thickness of the line).

-1- ZONE DIVISION TYPE A:

The zone division in type A flux selectors is given by the equation $x'_n=n/N$. This is a-priori the simplest type of zone division. The various flux selectors using type A zone division will now be described.

1a-A2-H : Fig and Table A5-4

This is one of the flux selectors which was already calculated by Lansraux. It has been re-calculated here with greater precision. The calculations were done for 10 zones and can be represented schematically as follows:

$$\text{A5-4} \quad [\,(\text{A4-9}/\text{A4-12}) \div \text{A4-12}] \times 1/2 \rightarrow r'_n = 1/2\,[x_n+x'_n+1/C\int_{x_n}^{x'_n} T(x)\,d(x^2) \Big/ x_n+x'_n]$$

$$\text{A5-5} \quad [(\text{A4-9}/\text{A4-12})-\text{A4-12}]\text{x } 1/2 \rightarrow r_n=1/2[x_n+x'_n - 1/C\int_{x_n}^{x'_n} T(x)\,d(x^2) \Big/ x_n+x'_n]$$

$$\text{and } r_1 = 0 \rightarrow C = \int_0^{x'_1} T(x)\ d(x^2) \Big/ x'^2_1$$

Homothetic transformation: $\underline{r}'_n = r'_n/r'_N$, $\underline{r}_n = r_n/r_N$

1b-A2-H: Fig and Table A5-5

This flux selector was calculated previously by Lansraux. The calculations were done here for N=10. We have:

$$\text{A5-6} \quad (\text{A4-9} + \text{A4-11})\text{x } 1/2 \rightarrow r'^2_n = 1/2[x'^2_n + x^2_n + 1/C\int_{x_n}^{x'_n} T(x)\ d(x^2)]$$

$$\text{A5-7} \quad (\{\text{A4-11}\}- \{\text{A4-9}\})\text{x } 1/2 \rightarrow r^2_n = 1/2[x'^2_n + x^2_n - 1/C\int_{x_n}^{x'_n} T(x)\ d(x^2)]$$

The condition $r_1 = 0$ gives the same value of C as in 1a-A2-H, and the F.S. was homothetically transformed, as before.

The requirement $r_1=0$, which determines C in both of the above flux selectors, results from practical considerations, viz., the difficulty of producing an opaque spot at the center of a lens, and the desire of maximizing the transmission factor of the F.S.

Fig and Table A5-4 and Fig and Table A5-5 give the results of the calculations for F.S. 1a-A2-H and 1b-A2-H resp. Note that these two F.S. are almost identically the same. It appears, then, that for type A zone division, at least, it makes very little difference whether we use A4-11 or A4-12 in calculating the F.S.

It will be noticed that the diffraction pattern formed by the above flux selectors is already very similar to the one formed by the amplitude filter T(x), except for the region around W=60, where very luminous rings appear; these rings (or principal maxima) are analogous to the principal maxima occurring with the ordinary plane diffraction grating, and hence can be thrown back to a sufficiently large value of W by increasing the number N of rings in the F.S.

<u>1a-A4-H</u>: Fig and Table A5-6.

A brief inspection of the ring radii for F.S. 1a-A2-H (or 1b-A2-H) shows how narrow the first opaque ring (r_2-r_1') is; in practice, such narrow rings are difficult to make. We could eliminate this ring by putting $r_1'=r_2$. This condition, coupled with added condition $r_1=0$, would not only determine the constant C, but would also mean that equation A4-12 would not be applied to innermost zone. Flux selector 1a-A4-H was calculated according to the above requirements. The constant C was determined in the following manner:

From A4-9, we have $r_1'^2 = 1/C \int_0^{.1} T(x)\, d(x^2)$. From A5-5, we have $r_2 = .15 - .33 \times \dfrac{\int_{.1}^{.2} T(x) d(x^2)}{2C}$. Equating r_1' and r_2 , we obtain a quadratic equation in C (after squaring), which has two roots; one of these roots was rejected because it causes overlapping of some rings. With the other root, the flux selector was calculated, then homothetically transformed; comparing this 9 ring F.S. with the previous ones, we find that it gives a diffraction pattern that is almost identical to the latter's with the added advantages that its transmission factor is slightly higher and, more important, the first opaque ring is 3 times as wide as in 1a-A2-H(.002), and 2 times as wide as in 1b-A2-H(.003).

<u>1b-A4-H</u>: Fig and Table A5-7.

Noting that in type 1b-A2-H, the first opaque ring is wider that that in 1a-A2-H, we have calculated the flux selector 1b-A4-H (similar to 1a-A4-H but using A4-11 instead of A4-12) to see if we can get any further gain in the width of the first opaque ring. C is calculated as follows: for the first zone, we have, from A4-9, $r_1'^2 = 1/C \int_0^{.1} T(x)\, d(x^2)$, and for the second zone, from A5-7, $r_2^2 = .025 - [1/2C] \int_{.1}^{.2} T(x) d(x^2)$.

Equating these two expressions, we get $C = 40 \left[\int_0^{.1} T(x) d(x^2) + .5 \int_{.1}^{.2} T(x) d(x^2) \right]$.

With this value of C, the flux selector was calculated from equations A5-6 and A5-7, then homothetically transformed. The results are slightly better than those for 1a-A4-H: the diffraction pattern formed by 1b-A4-H would be undistinguishable from that formed by 1a-A4-H but the former has an innermost opaque ring of .0065 compared to .0060 for the latter.

2-A2-H: Figures and Tables A5-8 to A5-11

This flux selector was calculated from equations A4-10, and, as the code indicates, C was chosen such that $r_1 = 0$, i.e.,

$$\frac{1}{2C} = \frac{\int_0^{x_1'} T(x)x^2 d(x^2)}{\left[\int_0^{x_1'} T(x)\ d(x^2)\right]^2}$$

The flux selector was homothetically transformed as usual. This F.S. was calculated for 9, 10, and 11 rings, (the 9 and 11 for comparison with other 9 or 11 ring F.S., such as 1a-A4-H or 1b-B2-H resp.). If we compare the data for 10(2-A2-H) with the corresponding data for 1a-A2-H and 1b-A2-H, we note that the transmission factor is slightly better for 2-A2-H and there is very little difference in the flux selector radii and in the diffraction patterns.

These comparisons show that for type A zone division, it makes very little difference in the diffraction patterns what mode of calculation we use (1a, 1b, or 2). This will be the more so the larger the number of rings. Since type 1a takes the least time to calculate, then it would be the most convenient to use for large numbers of rings (N= 100 to 1000). At this point, we could envisage simplifying the F.S. calculations even further, for large N, by writing A4-9 approximately as

$$\text{A5-8} \qquad r_n'^2 - r_n^2 \simeq (1/C)T(\beta_n)\ (x_n'^2 - x_n^2)$$

where β_n is the abscissa of a point inside (x_n, x_n'), and we could choose it to be either $\beta_n = \dfrac{x_n + x_n'}{2}$ or $\beta_n = \sqrt{\dfrac{x_n'^2 + x_n^2}{2}}$

One of these, as well as A5-8 and A4-11 or A4-12, could be used to calculate flux selectors for large N. This type of F.S. would be denoted by Oxy-..., where O indicates that no terms are annulled (exactly) in A4-8, x is a or b depending on whether A4-12 or A4-11 resp. is used, and y is a or b depending on what choice of β_n is made.

2-A5...-H Series: (Figs and Tables A5-12 to A5-14)

In F.S. 2-A2-H, C was chosen to make $r_1=0$. This is in fact the minimum possible value of C, since making it any smaller would make $r_1'^2$ negative in A4-10; this value of C is also the one which makes the transmission factor max., and the width of the rings max. We could have chosen C differently. The larger we make it, the smaller the transmission factor, and the narrower the rings; but what is the effect on the diffraction pattern? Could a larger value of C improve or otherwise modify the aspect of the diffraction pattern? To answer this question, flux selectors were calculated with 1/2C equal to .01, .05, .1, .3, and .5 . The flux selectors corresponding to these values of 1/2C are denoted 2-A51-H, 2-A52-H, 2-A53-H, 2-A54-H, and 2-A55-H resp. (Note: for 2-A2-H, 1/2C≃.53). The data for three of these is given. It will be seen that the diffraction patterns are not improved, quite the contrary. Hence, this group of flux selectors has no practical interest.

-2- ZONE DIVISION TYPE B:

This type of zone division was considered by Lansraux in some of the flux selectors he calculated (see introduction): there are N+1 zones, whose widths vary as a/2, a, a, ... a, a/2 . The zone boundaries are given by $x_n' = (2n-1) / 2N$, n= 1 to N, with $x_{N+1}' = 1$ as usual.

<u>1a-B2-H</u>: Fig and Table A5-15

This flux selector was calculated by Lansraux. It is re-calculated here to a higher precision. The case N=10 was considered. Again, the constant C is determined by requiring $r_1=0$; hence, $C = 400\int_0^{.05} T(x)\, d(x^2)$. The inner and outer radii of the N first rings are determined from equations A5-4 and A5-5. The last zone is treated slightly differently than in previous cases. Only equations A4-9 is applied to it, and r'_{N+1} is set equal to 1. This determines r_{N+1}. (This F.S. need not be homothetically transformed since $r'_{N+1}=1$ already). From the data sheets, the following observations can be made about F.S. 1a-B2-H.

(1) The inner opaque ring and the outer transparent ring are very narrow (cf. F.S. 1a-A2-H).

(2) The amplitudes of the secondary maxima are lower than those in F.S. 11(2-A2-H).

(3) Its transmission factor is 4% lower than that of 11(2-A2-H).

As in type A zone division, we can increase the width of the innermost opaque ring by choosing C such that $r'_1=r_2$ (i.e., eliminate first opaque ring). The procedure is exactly the same as for F.S. 1a-A4-H and 1b-A4-H. The resulting F.S. 1a-B4-H and 1b-B4-H are given in Fig & Table A5-16 and A5-17. Again, we note that 1a-B2-H and 1a-B4-H (hence, 1b-B4-H) give the same diffraction pattern, but that 1a-B4-H and 1b-B4-H have much wider innermost opaque rings. Type 1b-B4-H is the best of the group in that respect.

-3- <u>ZONE DIVISION TYPE C</u>:

<u>2-C2-H</u>: Fig and Table A5-18.

From a practical point of view, it would be convenient if we could have a flux selector whose transparent rings all had the same width; i.e.,

$r_n' - r_n$ = a constant. If we further require that $r_1=0$, then these two conditions determine completely the (x_n, x_n')(type C zone division). Equations A4-10 were used to determine the solution. The latter cannot be obtained explicitly; however, with a computer, it can be obtained by using an iterative procedure. For a given N, we have found only one solution. The procedure used can be summarized as follows:

The calculation is divided into two parts (programs); the first part (the "scan") determines if the solution exists and gives approx. values for the parameters involved; the second part (called the "convergence") uses the results of the scan to determine the solution accurately. In the scanning program, an initial value of $x_1' = (1/N)^{\alpha}$ is chosen by giving to α a certain arbitrary value. From equations A4-10, the width W of the first ring is calculated. Then, by means of an iterative procedure, a value of x_2' is determined such that the width of the second ring equal W. This procedure is repeated for the successive zones until X_{N-1}' is determined. x_N' is always 1, of course, so that we have no control over the last ring. However, the width W_N of the last ring is calculated, and the difference $DEL=W-W_N$ formed. Now, by repeating all of the above calculations for various values of α, DEL is observed to vary from positive to negative values, meaning that there exists a value of α_0 for which DEL=0 (which is what we want). Determining exactly this value of α_0 (and hence, the x_n, x_n', r_n, r_n' i.e., the F.S. itself) by means of an iterative procedure applied to the parameter α is the purpose of the convergence program. The latter uses as input data some approx. values of α_0 determined by graphical interpolation from a DEL vs α plot obtained from the results of the scanning program. The whole calculation is quite lengthy (approx. 2 hours on IBM1620) and the resulting F.S. gives a diffraction pattern which is poor compared to the ones produced by types A and B F.S. (see data sheet). However, for large numbers of rings, the results might prove to be more interesting. Note that this type of flux selector would be one of the easiest to make for large N, not only because of the constant width of the rings, but also because this width is quite large compared to that of the outer rings of flux selectors of type A or B having the same number of rings. Note also that transmission factor is about 10% greater than for type A.

-4- ZONE DIVISION TYPE P: Fig & Table A5-20 to A5-22

This type of zone division results from the following discussion: Consider equation A5-3 giving the (un-normalized) diffraction pattern produced by a flux selector. This equation can be re-written $A(W)=\Sigma^{N}\gamma_n(W)$ with $\gamma_n(W)=(2M/W^2)[z'_n\ J_1(z'_n) - z_n\ J_1(z_n)]$ where $z'_n=Wr'_n$ and $z_n=Wr_n$. Suppose we could find a value of $W = W_o$ and a set of values r_n, r'_n (with their associated x_n, x'_n) which, while satisfying equations A4-10, would be such that the z'_n and z_n would be distributed along the curve $uJ_1(u)$ in the manner illustrated below (Fig. A5-19).

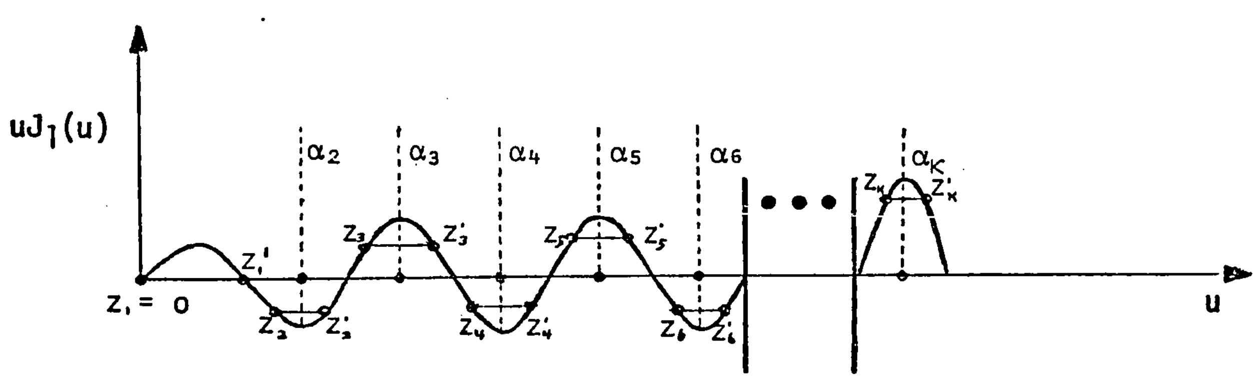

Fig. A5-19

$z_1'=\beta_1$ is the first root of $J_1(x)=0$; the k^{th} extremum of the curve $uJ_1(u)$ occurs at a value u given by $u_k = \alpha_k$, where α_k is the k^{th} root of $J_o(x)=0$.

What can be said about a flux selector satisfying the above conditions?

(1) r_1 would be zero

(2) for $W = W_o$, every $\gamma_n(W_o) = 0$, hence $A(W_o) = 0$

(3) if we vary W about W_o, every contribution $\gamma_k(W)$ to $A(W)$ will have opposite parity to that of $\gamma_{k-1}(W)$ [or to $\gamma_{k+1}(W)$], so that the resultant $A(W)$ will be small; hence, we can expect a relatively dark region around W_o.

(4) from Fig A5-19, we can see that $(z_n' + z_n) / 2 \simeq \alpha_k$; hence, $W_oR_N \simeq \alpha_N$; but $\alpha_k \simeq k\pi$, and $R_N \simeq 1$, whence $W_o \simeq N\pi$. For N= 10, then, $W_o \simeq 31$ (which would be situated about halfway between the center and the first principal maxima in diffraction patterns of type A F.S.

We can summarize as follows the conditions imposed on the F.S. defined above (if it exists):

A5-10 (a) $r_1=0$ (b) W_o, r_n, r_n' such that $z_n' J_1(z_n') - z_n J_1(z_n) = 0$ for all n

(c) $W_o(r_n' + r_n) / 2 \simeq \alpha_n$ (d) equations A4-10 satisfied.

Finding a flux selector which will satisfy all of the above requirements is not an easy task. Also, such a flux selector will not exist for any value of W. The solution(s) to this problem should give us W_o as well as the zone division, and the values of the ring radii r_n, r_n'. The solution (again, if it exists,) cannot be obtained explicitly, but only by means of a lengthy iterative procedure. As in the case of type C zones, the calculation is divided into two parts: a scanning program and a converging program. The iteration parameter will be W. The iterative procedures can be summarized as follows:

(1) Scan: With initial value of W (chosen a-priori), put $r_1' = \beta_1/W$. Using equations A4-10, and an iterative procedure, determine x_1' corresponding to the above r_1'; then, use iteration to determine x_2' (hence r_2' and r_2) such that A5-10 (b), (c) and (d) are satisfied; repeat this last step to determine x_3', etc., until x_{N-1}' is determined. Of course, $x_N'=1$, so that $\theta = r_N' J_1(Wr_N') - r_N J_1(Wr_N)$ is already determined and is not zero in general. All of the above procedure is repeated for various values of W, and a plot of θ vs W indicates if any solution ($\theta = 0$) exists. (Such a plot indicates, in fact, that for a given N, more than one solution exists.)

(2) Converging program: from the graph obtained above, the approximate value(s) of W for which the solution(s) exists is deduced, and introduced into a converging program, which is almost the same as the scanning program, except that it introduces an iterative procedure re W and θ to determine exactly the value W_0 for which $\theta = 0$. (Note: the condition A5-10(c) cannot be guaranteed for the last ring since the latter is determined completely from the calculations of the previous rings. However, inspection of the scanning results indicates which solutions would or would not satisfy A5-10(c), and only the former could be selected if it was so desired.)

RESULTS

The calculations were made for N=10. The scan indicated that no solutions existed below $W \simeq 20$. In the range W = 20 to 40, 3 solutions existed, and these are given in Fig & Tables A5-20 to A5-22. The values of W for which a solution can be obtained are 29.27(2-PA2-H),32.38 (2-PB2-H),40.23(2-PC2-H). Beyond W = 40, other solutions would exist, but these would not be interesting, as can be deduced by inspection of the data for 2-PC2-H. F.S. 2-PA2-H and 2-PB2-H are of the same type, 2-PA2-H being the N=9 solution. (Because of the way the calculation is carried out, the solutions for both N and N-1 can be obtained for a given N.) We may note that condition A5-10(c) is satisfied for the last ring in both PA and PB, whereas it is not for PC. (where we have that $W_0(r'_N + r_N) / 2 \simeq \alpha_{N+1}$). It then appears as if, for a given N, there is only one solution satisfying all the conditions A5-10. For N=10, this solution is the F.S. 2-PB2-H. The most remarkable thing about this F.S. is its striking similarity to F.S. 10(2-A2-H). There is little difference between the zone boundaries of these two flux selectors, especially for the outer zones. The same can be said about the values of the ring radii. The diffraction patterns, finally, are almost identical, apart from a phase difference π in the structure of the principal maxima. Exactly the same comments can be made about flux selectors 9(2-A2-H) and 2-PA2-H. Hence, we are led to induce that whatever the number N of ring, type P will always be very similar to type A. The above results explain why type A (or type B by extension) flux selectors gave good diffraction patterns.

-5- ZONE DIVISION TYPE Q:

2-Q2-H: Fig. and Table A5-23

Type Q zone division is such that all the opaque rings have the same width. Such a F.S. would be easier to make than types A, B, or P, and presents an alternative to type C flux selectors (which were calculated for the same purpose). The method of calculation is similar to that for type C, and, consequently, will not be exposed here. See Fig A5-23 for the results of the calculations, and the diffraction pattern. The latter is not too interesting for N = 10, but perhaps might be for large N.

-6- MISCELLANEOUS TYPES OF ZONE DIVISION:

Several more types of zone division were considered, but these will be discussed only briefly, since we have found a-posteriori that these flux selectors are not useful.

2-M2-H:

Zone division such that rings all have the same area. This flux selector was calculated by means of an iterative procedure.

2-DE2-H:

Similar to type P, except that successive even roots of J_0 are used in calculations; this F.S. was an attempt to minimize the amplitude of the first principal maxima in the diffraction pattern.

2-DO2-H:

Same as above, except odd roots of J_0 were used.

2-E2-H,2-F2-H,2-G2-H:

Zone division given by $x'_n = (n/N)^{\alpha}$, α = .5 , .75 , 1.25 resp.

2-K2-H

This type represents an attempt to throw back to larger W the first principal maxima; zone division of the type a, 2a, 3a, ...

2-L2-H

Same purpose as above, except zone division is of the type a, 3a, 5a, ...

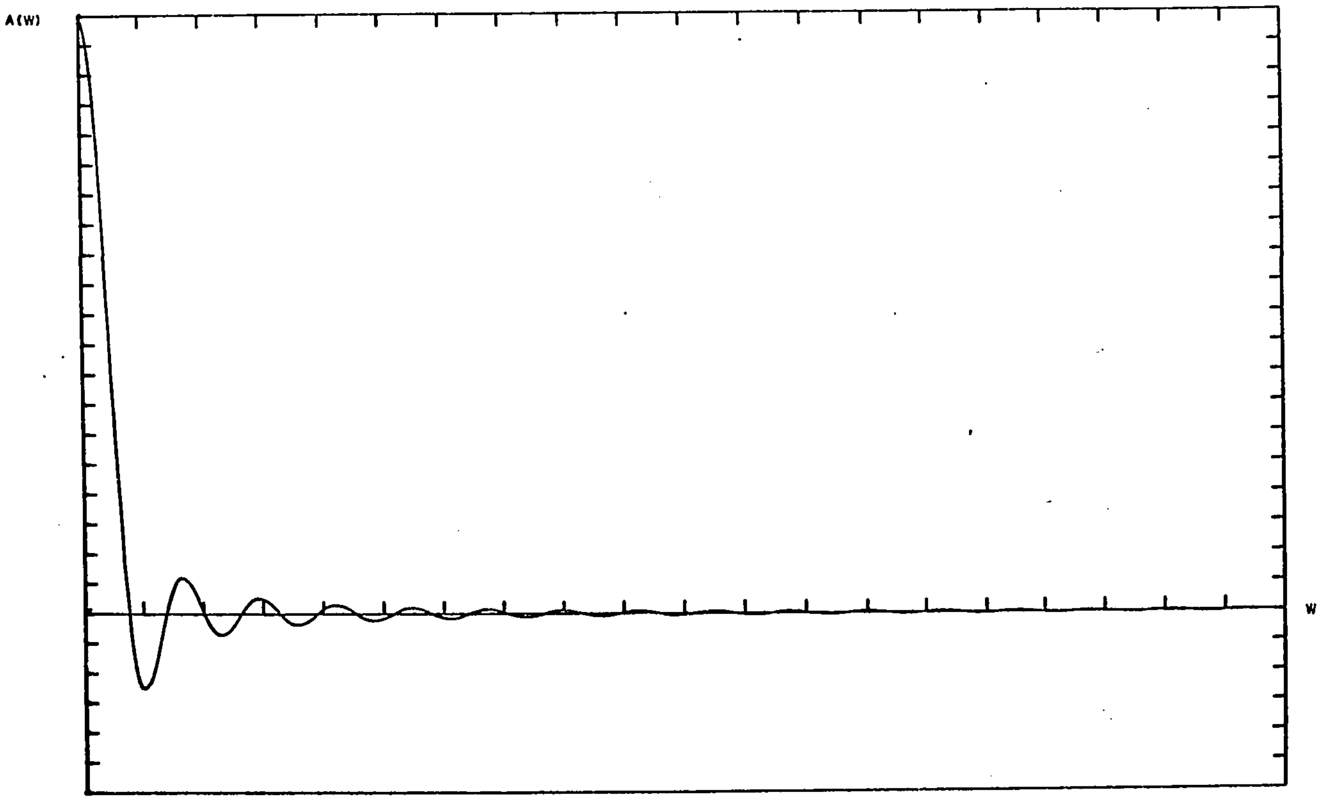

Fig. A5-1 Airy pattern (= diffraction pattern formed by the pupil T(x)≡1)

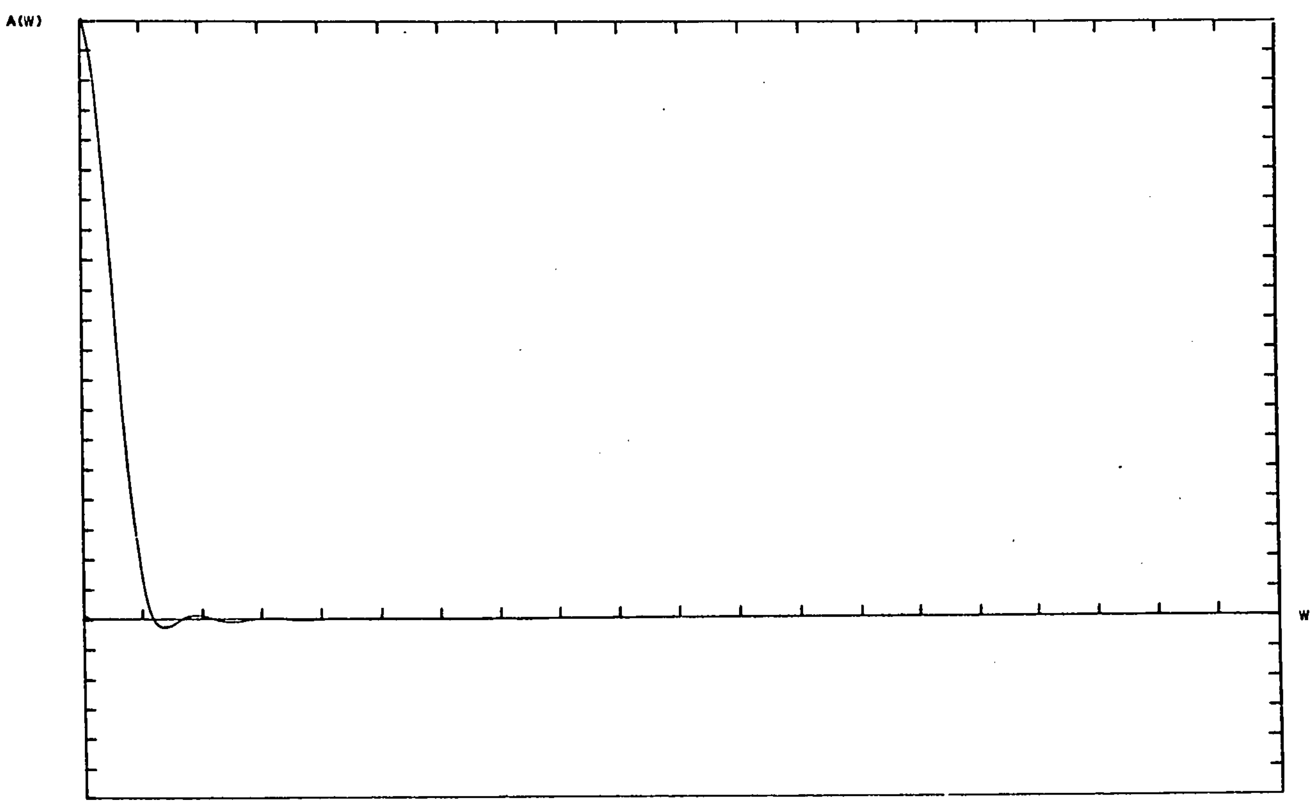

Fig. A5-2 Diffraction pattern formed by the amplitude filter T(x,5)

TABLE A5-3

10 RINGS CIRCULAR GRATING

TRANSMISSION FACTOR T OF FLUX SELECTOR

T= 0.52632

VALUES OF XP(I)

0.10000	0.20000	0.30000	0.40000	0.50000
0.60000	0.70000	0.80000	0.90000	1.00000

VALUES OF INNER AND OUTER RADII OF RINGS

I= 1	R(I)= 0.0	RP(I)= 0.05263
I= 2	R(I)= 0.10526	RP(I)= 0.15789
I= 3	R(I)= 0.21053	RP(I)= 0.26316
I= 4	R(I)= 0.31579	RP(I)= 0.36842
I= 5	R(I)= 0.42105	RP(I)= 0.47368
I= 6	R(I)= 0.52632	RP(I)= 0.57895
I= 7	R(I)= 0.63158	RP(I)= 0.68421
I= 8	R(I)= 0.73684	RP(I)= 0.78947
I= 9	R(I)= 0.84211	RP(I)= 0.89474
I= 10	R(I)= 0.94737	RP(I)= 1.00000

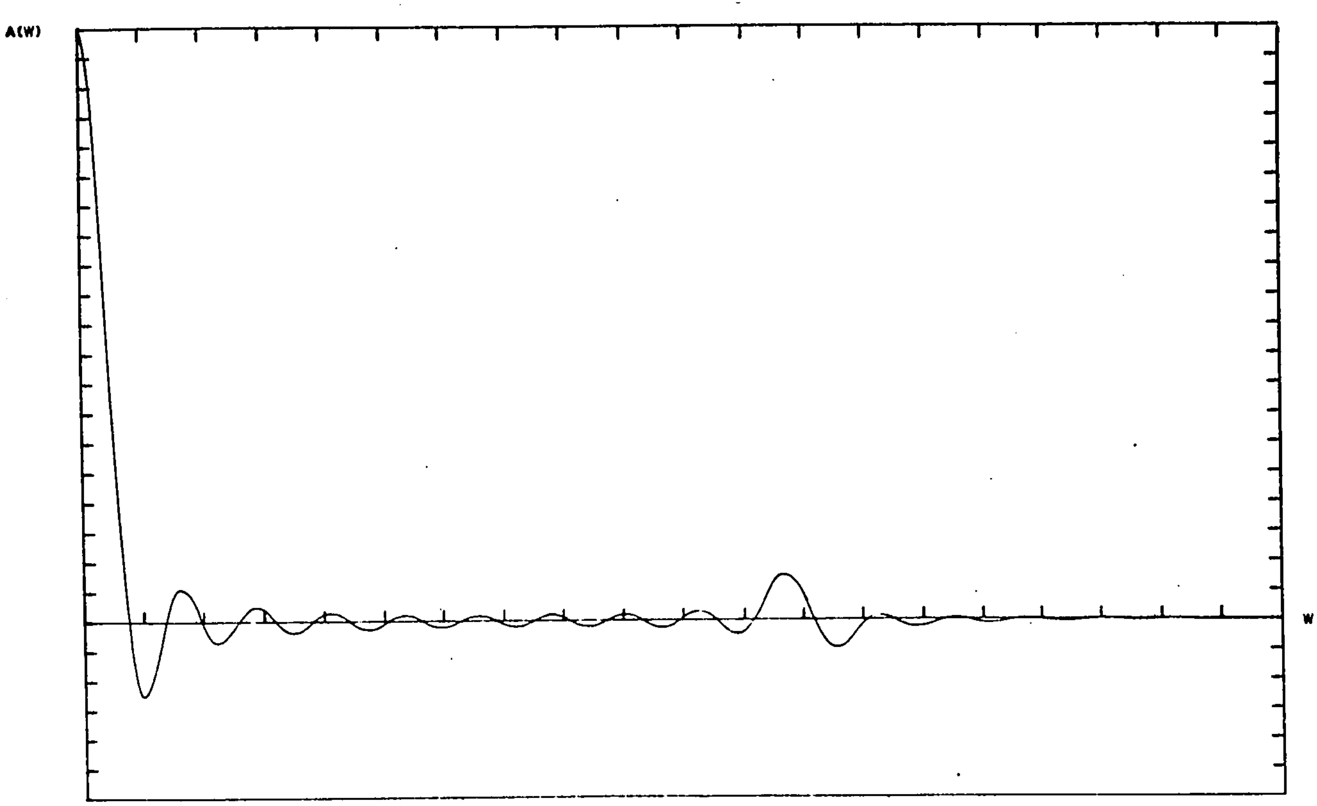

Fig. A5-3 Diffraction pattern formed by the 10 rings circular grating

TABLE A5-4

10 RINGS FLUX SELECTOR 1A-A2-H

TRANSMISSION FACTOR T OF FLUX SELECTOR

T= 0.44179

VALUES OF XP(I)

0.10000	0.20000	0.30000	0.40000	0.50000
0.60000	0.70000	0.80000	0.90000	1.00000

VALUES OF INNER AND OUTER RADII OF RINGS

I= 1	R(I)= 0.0	RP(I)= 0.10470
I= 2	R(I)= 0.10672	RP(I)= 0.20739
I= 3	R(I)= 0.21527	RP(I)= 0.30824
I= 4	R(I)= 0.32530	RP(I)= 0.40762
I= 5	R(I)= 0.43635	RP(I)= 0.50598
I= 6	R(I)= 0.54787	RP(I)= 0.60386
I= 7	R(I)= 0.65935	RP(I)= 0.70179
I= 8	R(I)= 0.77030	RP(I)= 0.80024
I= 9	R(I)= 0.88038	RP(I)= 0.89957
I= 10	R(I)= 0.98935	RP(I)= 1.00000

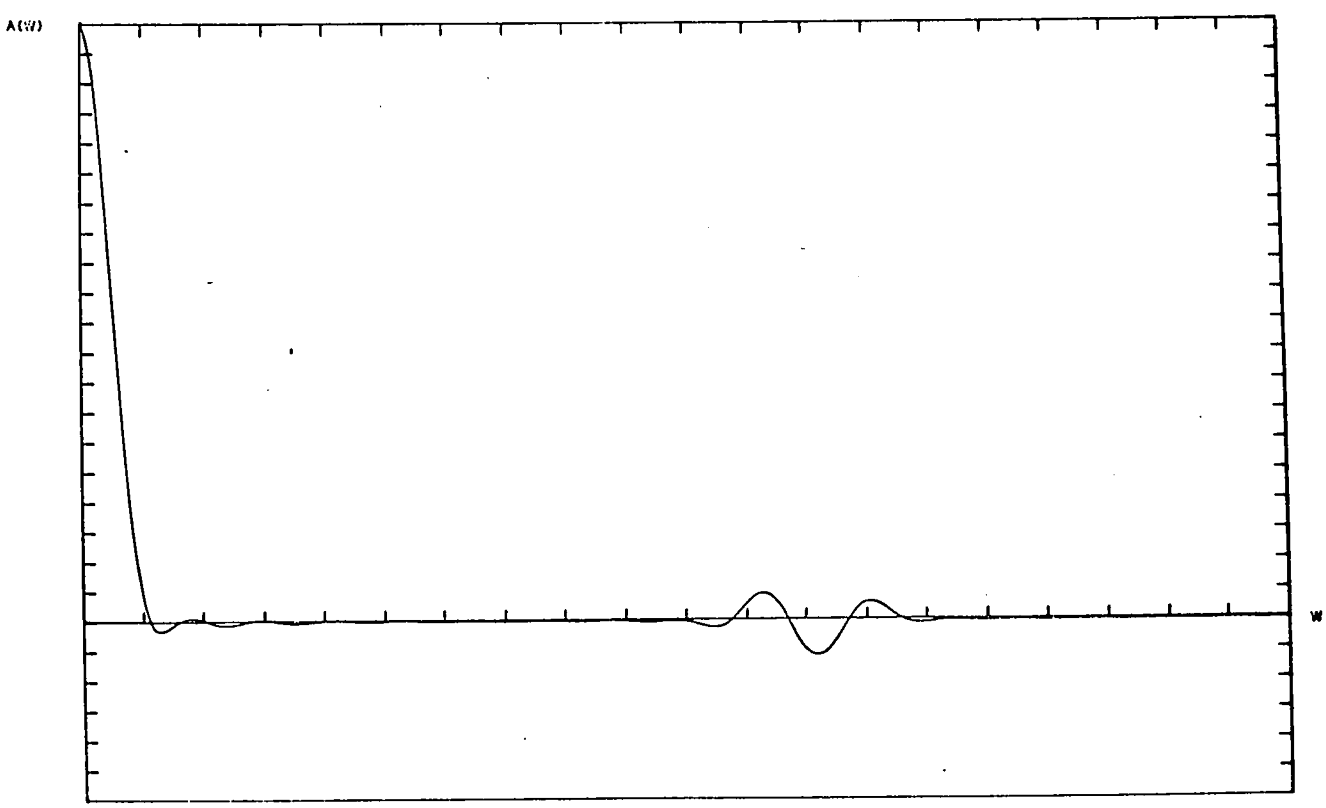

Fig. A5-4 Diffraction pattern formed by the F.S. 10(1a-A2-H)

TABLE A5-5

10 RINGS FLUX SELECTOR 1B-A2-H

TRANSMISSION FACTOR T OF FLUX SELECTOR

T= 0.44179

VALUES OF XP(I)

0.10000	0.20000	0.30000	0.40000	0.50000
0.60000	0.70000	0.80000	0.90000	1.00000

VALUES OF INNER AND OUTER RADII OF RINGS

I= 1	R(I)= 0.0	RP(I)= 0.10456
I= 2	R(I)= 0.10754	RP(I)= 0.20761
I= 3	R(I)= 0.21632	RP(I)= 0.30876
I= 4	R(I)= 0.32647	RP(I)= 0.40834
I= 5	R(I)= 0.43750	RP(I)= 0.50680
I= 6	R(I)= 0.54891	RP(I)= 0.60466
I= 7	R(I)= 0.66019	RP(I)= 0.70247
I= 8	R(I)= 0.77089	RP(I)= 0.80072
I= 9	R(I)= 0.88069	RP(I)= 0.89982
I= 10	R(I)= 0.98938	RP(I)= 1.00000

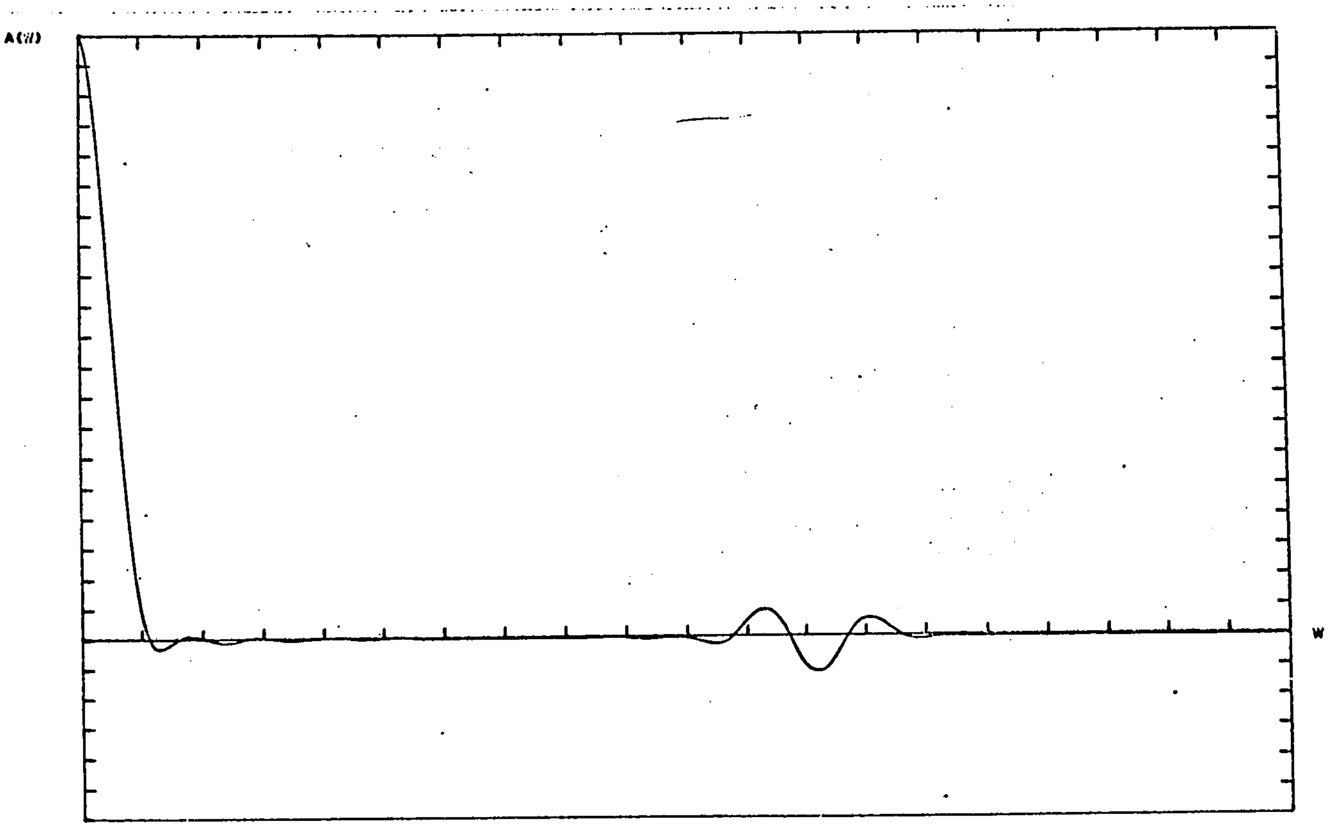

Fig. A5-5 Diffraction pattern formed by the F.S. 10(1b-A2-H)

TABLE A5-6

9 RINGS FLUX SELECTOR 1A-A4-H

TRANSMISSION FACTOR T OF FLUX SELECTOR

T= 0.45040

VALUES OF XP(I)

0.10000	0.20000	0.30000	0.40000	0.50000
0.60000	0.70000	0.80000	0.90000	1.00000

VALUES OF INNER AND OUTER RADII OF RINGS

I=	1	R(I)=	0.0	RP(I)=	0.20836
I=	2	R(I)=	0.21433	RP(I)=	0.30913
I=	3	R(I)=	0.32446	RP(I)=	0.40838
I=	4	R(I)=	0.43562	RP(I)=	0.50661
I=	5	R(I)=	0.54726	RP(I)=	0.60435
I=	6	R(I)=	0.65886	RP(I)=	0.70213
I=	7	R(I)=	0.76993	RP(I)=	0.80045
I=	8	R(I)=	0.88010	RP(I)=	0.89966
I=	9	R(I)=	0.98915	RP(I)=	1.00000

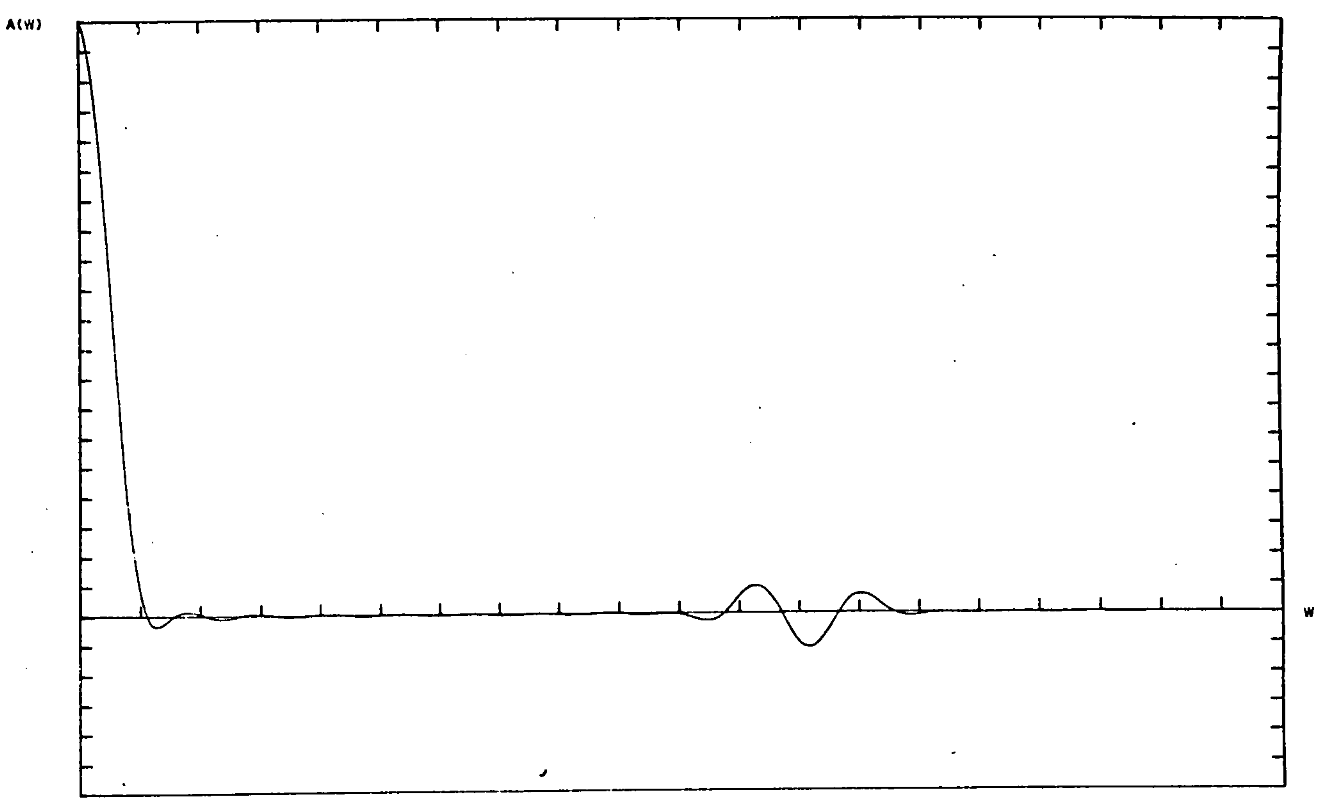

Fig. A5-6 Diffraction pattern formed by the F.S. 9(1a-A4-H)

TABLE A5-7

9 RINGS FLUX SELECTOR 1B-A4-H

TRANSMISSION FACTOR T OF FLUX SELECTOR

T= 0.45091

VALUES OF XP(I)

0.10000	0.20000	0.30000	0.40000	0.50000
0.60000	0.70000	0.80000	0.90000	1.00000

VALUES OF INNER AND OUTER RADII OF RINGS

I= 1	R(I)= 0.0	RP(I)= 0.20848
I= 2	R(I)= 0.21496	RP(I)= 0.30965
I= 3	R(I)= 0.32533	RP(I)= 0.40916
I= 4	R(I)= 0.43656	RP(I)= 0.50750
I= 5	R(I)= 0.54815	RP(I)= 0.60521
I= 6	R(I)= 0.65959	RP(I)= 0.70287
I= 7	R(I)= 0.77043	RP(I)= 0.80097
I= 8	R(I)= 0.88035	RP(I)= 0.89993
I= 9	R(I)= 0.98913	RP(I)= 1.00000

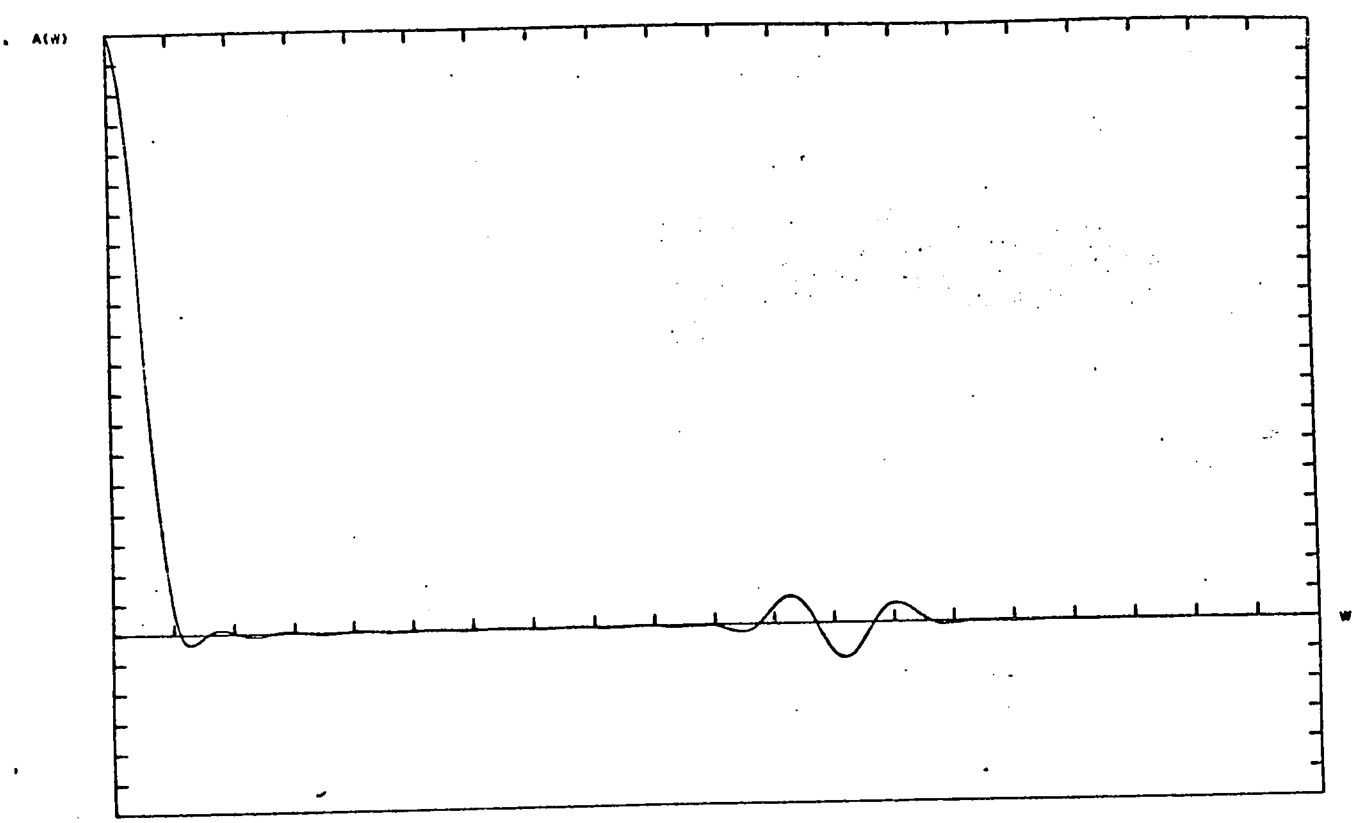

Fig. A5-7 Diffraction pattern formed by the F.S. 9(1b-A4-H)

TABLE A5-8

9 RINGS FLUX SELECTOR 2-A2-H

TRANSMISSION FACTOR T OF FLUX SELECTOR

T= 0.45051

VALUES OF XP(I)

0.11111	0.22222	0.33333	0.44444	0.55556
0.66667	0.77778	0.88889	1.00000	

VALUES OF INNER AND OUTER RADII OF RINGS

I= 1	R(I)= 0.0	RP(I)= 0.11734
I= 2	R(I)= 0.12097	RP(I)= 0.23235
I= 3	R(I)= 0.24379	RP(I)= 0.34476
I= 4	R(I)= 0.36826	RP(I)= 0.45510
I= 5	R(I)= 0.49362	RP(I)= 0.56406
I= 6	R(I)= 0.61901	RP(I)= 0.67245
I= 7	R(I)= 0.74363	RP(I)= 0.78099
I= 8	R(I)= 0.86675	RP(I)= 0.89020
I= 9	R(I)= 0.98752	RP(I)= 1.00000

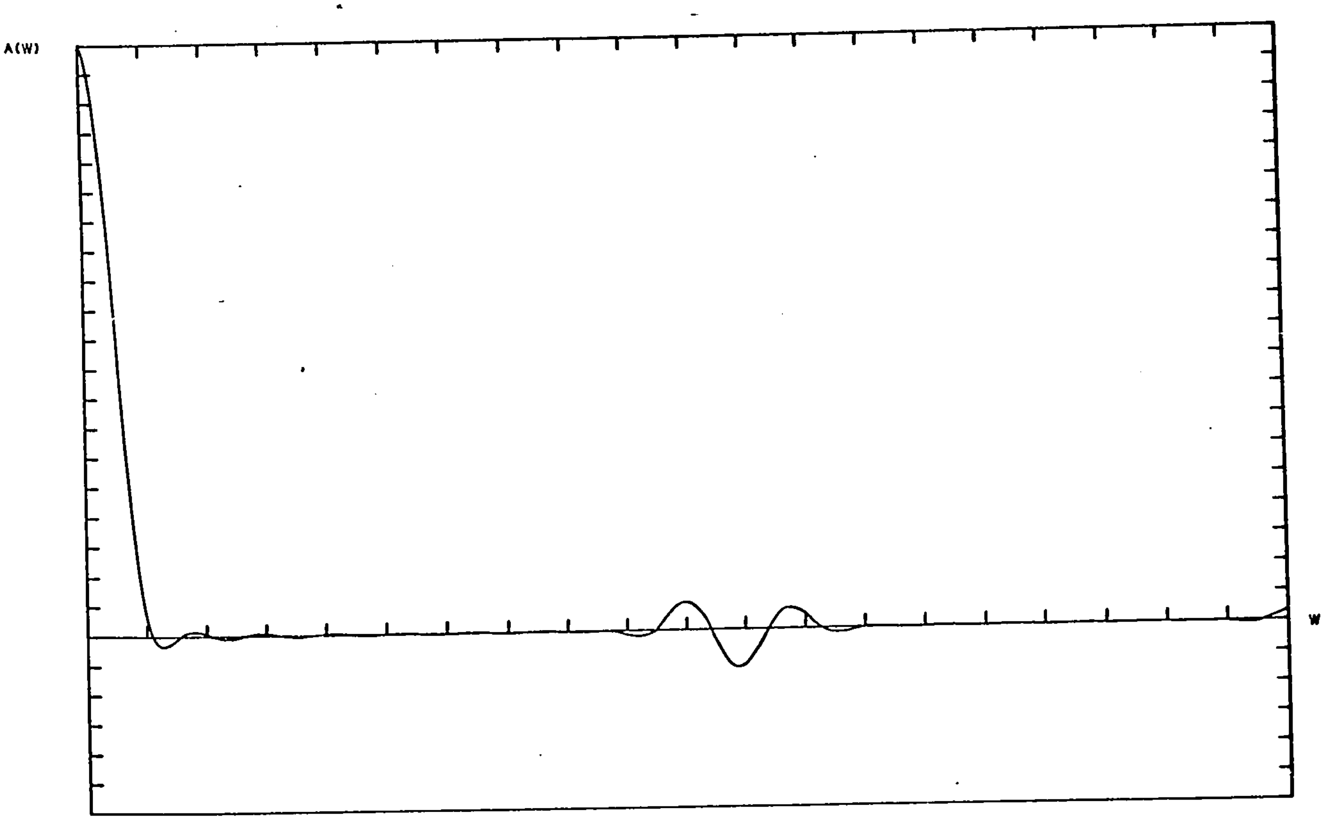

Fig. A5-8 Diffraction pattern formed by the F.S. 9(2-A2-H)

TABLE A5-9

10 RINGS FLUX SELECTOR 2-A2-H

TRANSMISSION FACTOR T OF FLUX SELECTOR

T= 0.44450

VALUES OF XP(I)

0.10000	0.20000	0.30000	0.40000	0.50000
0.60000	0.70000	0.80000	0.90000	1.00000

VALUES OF INNER AND OUTER RADII OF RINGS

I= 1	R(I)= 0.0	RP(I)= 0.10502
I= 2	R(I)= 0.10768	RP(I)= 0.20835
I= 3	R(I)= 0.21675	RP(I)= 0.30976
I= 4	R(I)= 0.32718	RP(I)= 0.40956
I= 5	R(I)= 0.43847	RP(I)= 0.50820
I= 6	R(I)= 0.55007	RP(I)= 0.60618
I= 7	R(I)= 0.66145	RP(I)= 0.70402
I= 8	R(I)= 0.77211	RP(I)= 0.80216
I= 9	R(I)= 0.88157	RP(I)= 0.90085
I= 10	R(I)= 0.98929	RP(I)= 1.00000

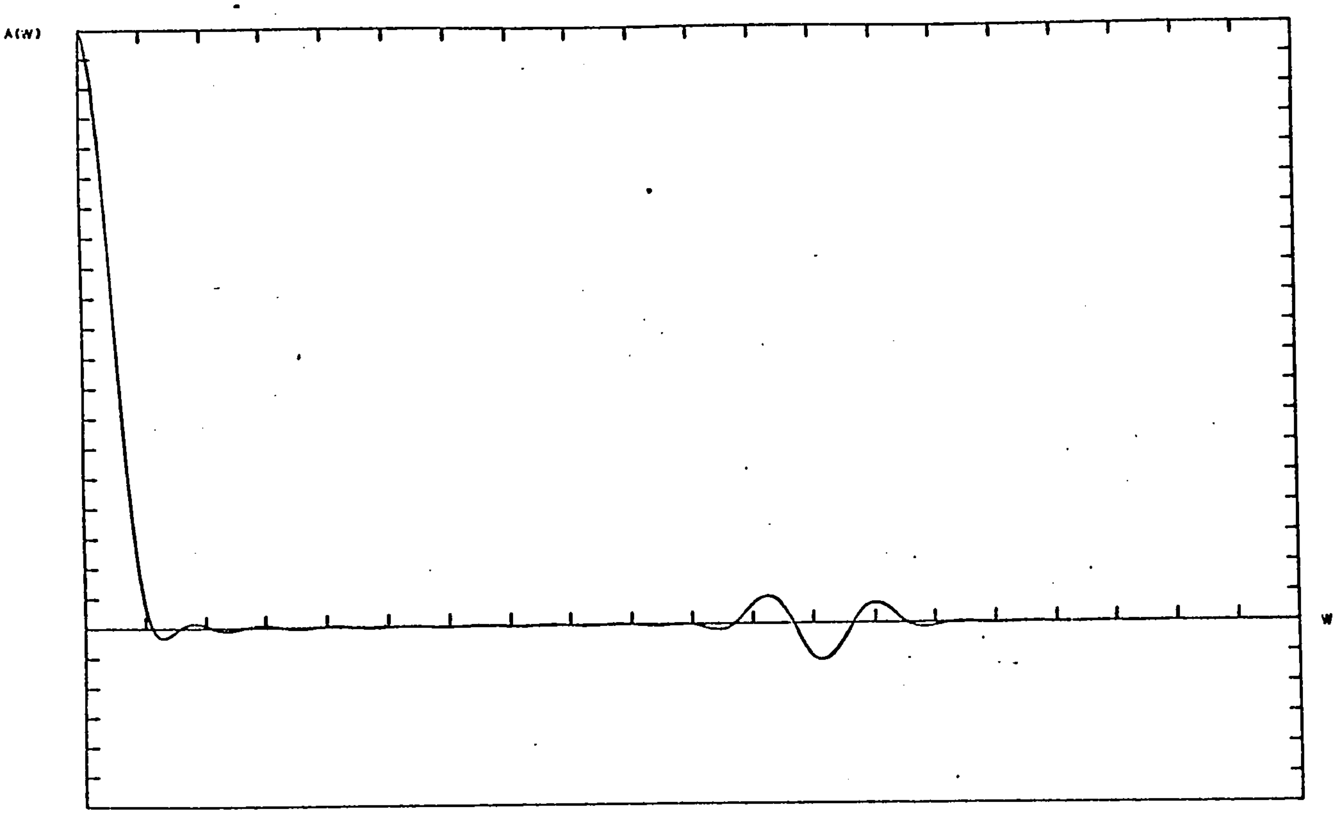

Fig. A5-9 Diffraction pattern formed by the F.S. 10(2-A2-H)

TABLE A5-11

11 RINGS FLUX SELECTOR 2-A2-H

TRANSMISSION FACTOR T OF FLUX SELECTOR

T= 0.43972

VALUES OF XP(I)

0.09091	0.18182	0.27273	0.36364	0.45455
0.54545	0.63636	0.72727	0.81818	0.90909
1.00000				

VALUES OF INNER AND OUTER RADII OF RINGS

I=	1	R(I)=	0.0	RP(I)=	0.09504
I=	2	R(I)=	0.09704	RP(I)=	0.18881
I=	3	R(I)=	0.19516	RP(I)=	0.28113
I=	4	R(I)=	0.29438	RP(I)=	0.37219
I=	5	R(I)=	0.39437	RP(I)=	0.46228
I=	6	R(I)=	0.49478	RP(I)=	0.55172
I=	7	R(I)=	0.59523	RP(I)=	0.64089
I=	8	R(I)=	0.69537	RP(I)=	0.73011
I=	9	R(I)=	0.79437	RP(I)=	0.81965
I=	10	R(I)=	0.89342	RP(I)=	0.90965
I=	11	R(I)=	0.99063	RP(I)=	1.00000

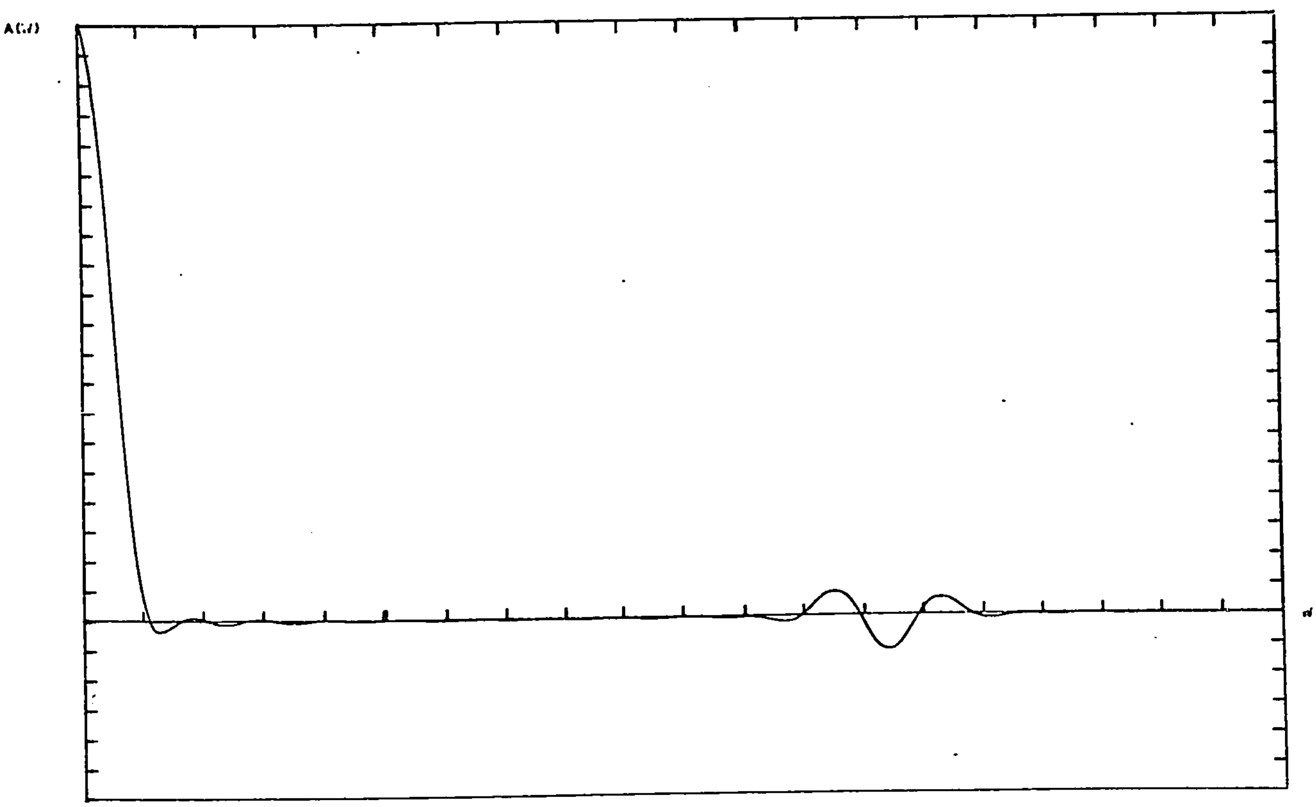

Fig. A5-11 Diffraction pattern formed by the F.S. 11(2-A2-H)

TABLE A5-12

10 RINGS FLUX SELECTOR 2-A51-H

TRANSMISSION FACTOR T OF FLUX SELECTOR

T= 0.00893

VALUES OF XP(I)

0.10000	0.20000	0.30000	0.40000	0.50000
0.60000	0.70000	0.80000	0.90000	1.00000

VALUES OF INNER AND OUTER RADII OF RINGS

I= 1	R(I)= 0.07391	RP(I)= 0.07539
I= 2	R(I)= 0.16575	RP(I)= 0.16766
I= 3	R(I)= 0.26782	RP(I)= 0.26965
I= 4	R(I)= 0.37180	RP(I)= 0.37344
I= 5	R(I)= 0.47642	RP(I)= 0.47781
I= 6	R(I)= 0.58129	RP(I)= 0.58241
I= 7	R(I)= 0.68624	RP(I)= 0.68709
I= 8	R(I)= 0.79112	RP(I)= 0.79172
I= 9	R(I)= 0.89576	RP(I)= 0.89615
I= 10	R(I)= 0.99979	RP(I)= 1.00000

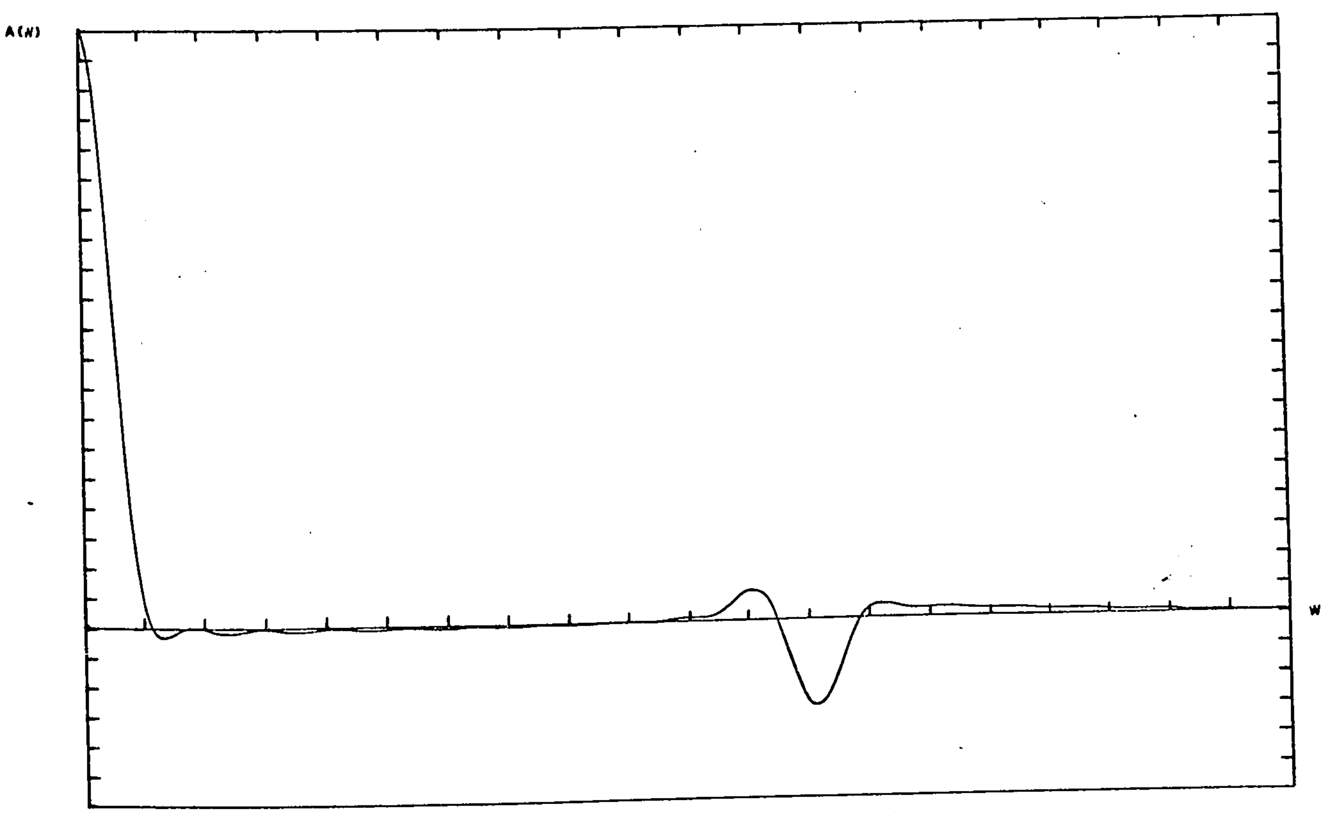

Fig. A5-12 Diffraction pattern formed by the F.S. 10(2-A51-H)

TABLE. A5-13

10 RINGS FLUX SELECTOR 2-A53-H

TRANSMISSION FACTOR T OF FLUX SELECTOR

T= 0.08908

VALUES OF XP(I)

0.10000	0.20000	0.30000	0.40000	0.50000
0.60000	0.70000	0.80000	0.90000	1.00000

VALUES OF INNER AND OUTER RADII OF RINGS

I= 1	R(I)= 0.06676	RP(I)= 0.08166
I= 2	R(I)= 0.15668	RP(I)= 0.17586
I= 3	R(I)= 0.25913	RP(I)= 0.27747
I= 4	R(I)= 0.36400	RP(I)= 0.38034
I= 5	R(I)= 0.46966	RP(I)= 0.48354
I= 6	R(I)= 0.57567	RP(I)= 0.58686
I= 7	R(I)= 0.68174	RP(I)= 0.69023
I= 8	R(I)= 0.78765	RP(I)= 0.79365
I= 9	R(I)= 0.89317	RP(I)= 0.89702
I= 10	R(I)= 0.99786	RP(I)= 1.00000

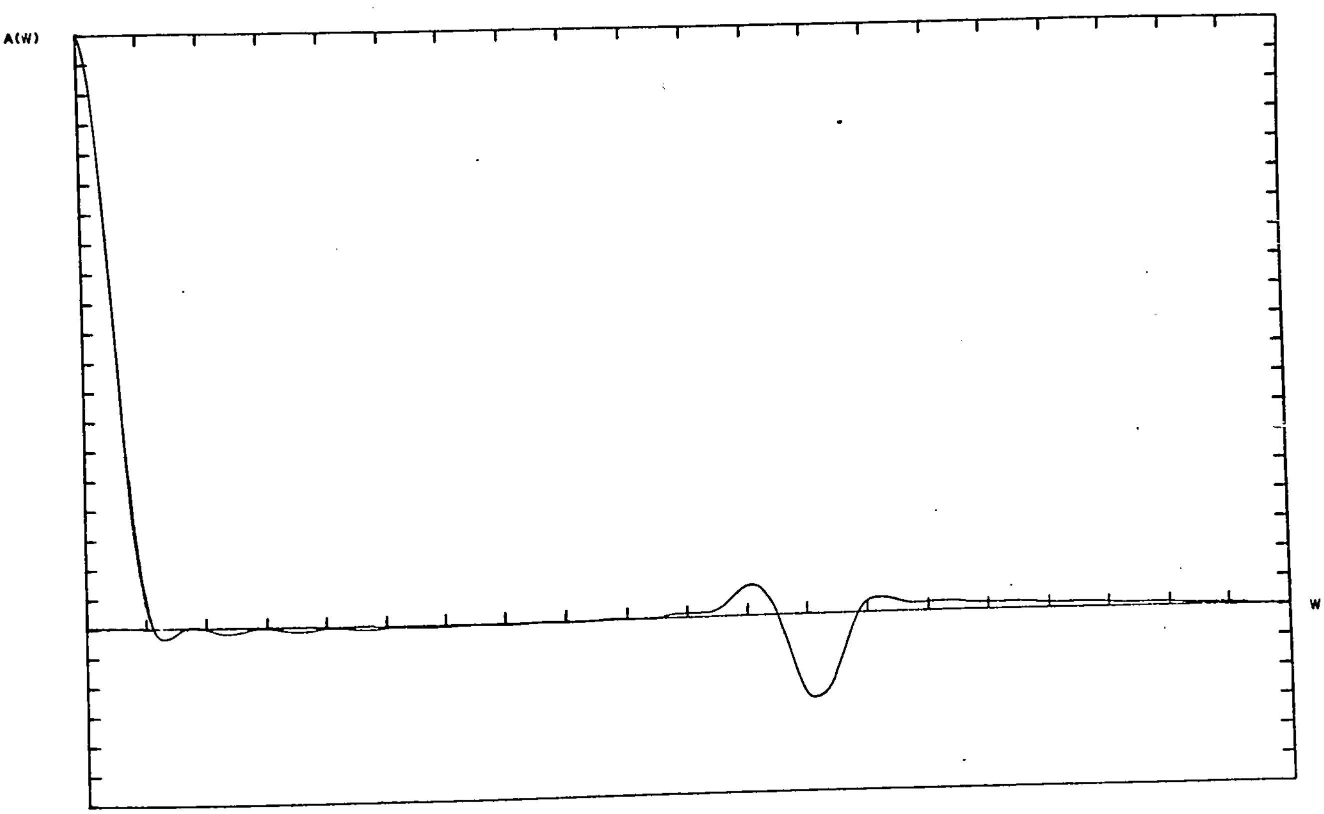

Fig. A5-13 Diffraction pattern formed by the F.S. 10(2-A53-H)

TABLE A5-14

10 RINGS FLUX SELECTOR 2-A54-H

TRANSMISSION FACTOR T OF FLUX SELECTOR

T= 0.26611

VALUES OF XP(I)

0.10000	0.20000	0.30000	0.40000	0.50000
0.60000	0.70000	0.80000	0.90000	1.00000

VALUES OF INNER AND OUTER RADII OF RINGS

I= 1	R(I)= 0.04730	RP(I)= 0.09402
I= 2	R(I)= 0.13452	RP(I)= 0.19273
I= 3	R(I)= 0.23899	RP(I)= 0.29400
I= 4	R(I)= 0.34615	RP(I)= 0.39517
I= 5	R(I)= 0.45439	RP(I)= 0.49598
I= 6	R(I)= 0.56307	RP(I)= 0.59656
I= 7	R(I)= 0.67171	RP(I)= 0.69713
I= 8	R(I)= 0.77995	RP(I)= 0.79790
I= 9	R(I)= 0.88741	RP(I)= 0.89893
I= 10	R(I)= 0.99360	RP(I)= 1.00000

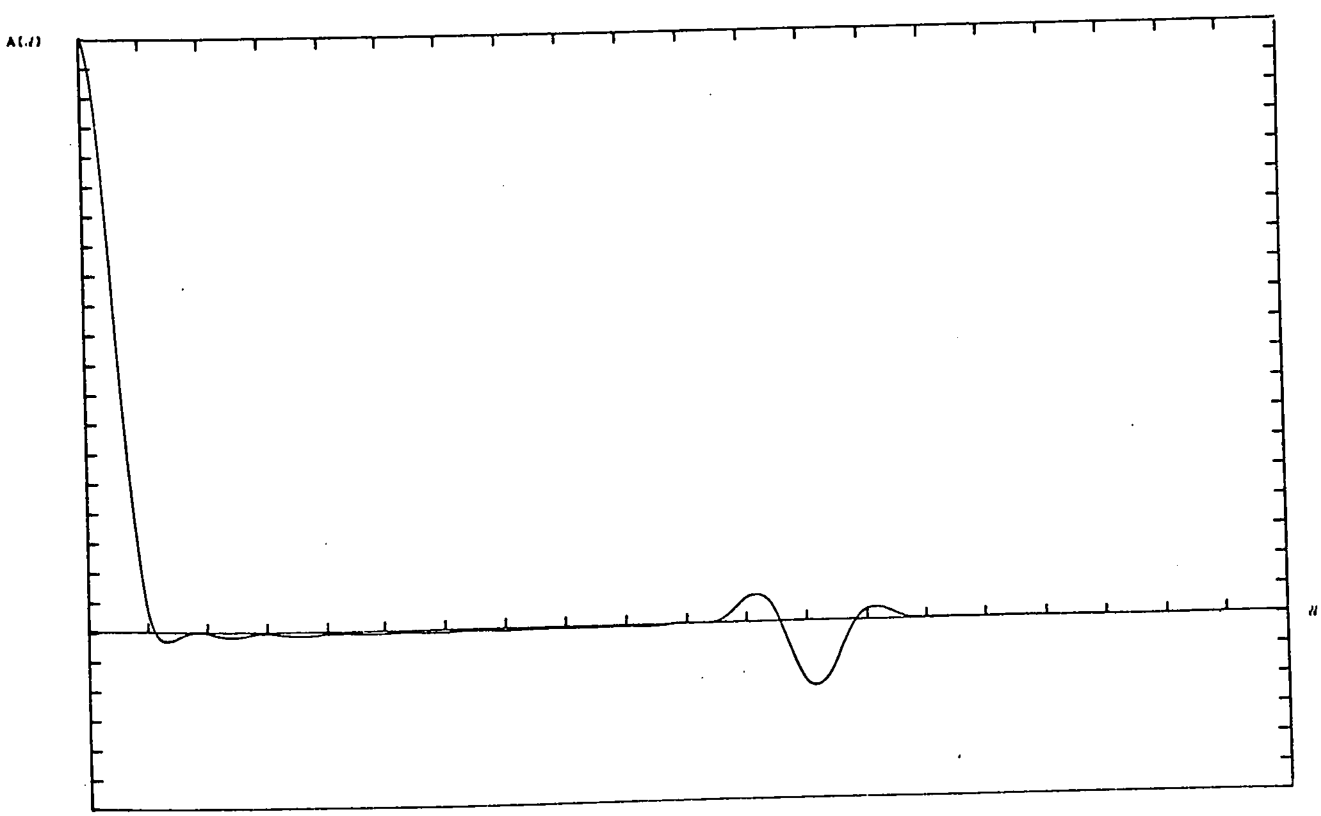

Fig. A5-14 Diffraction pattern formed by the F.S. 10(2-A54-H)

TABLE. A5-15

11 RINGS FLUX SELECTOR 1A-B2-H

TRANSMISSION FACTOR T OF FLUX SELECTOR

T= 0.40005

VALUES OF XP(I)

0.05000	0.15000	0.25000	0.35000	0.45000
0.55000	0.65000	0.75000	0.85000	0.95000
1.00000				

VALUES OF INNER AND OUTER RADII OF RINGS

I= 1	R(I)= 0.0	RP(I)= 0.05000
I= 2	R(I)= 0.05109	RP(I)= 0.14891
I= 3	R(I)= 0.15390	RP(I)= 0.24610
I= 4	R(I)= 0.25830	RP(I)= 0.34170
I= 5	R(I)= 0.36390	RP(I)= 0.43610
I= 6	R(I)= 0.47020	RP(I)= 0.52980
I= 7	R(I)= 0.57671	RP(I)= 0.62329
I= 8	R(I)= 0.68293	RP(I)= 0.71707
I= 9	R(I)= 0.78848	RP(I)= 0.81152
I= 10	R(I)= 0.89307	RP(I)= 0.90693
I= 11	R(I)= 0.99590	RP(I)= 1.00000

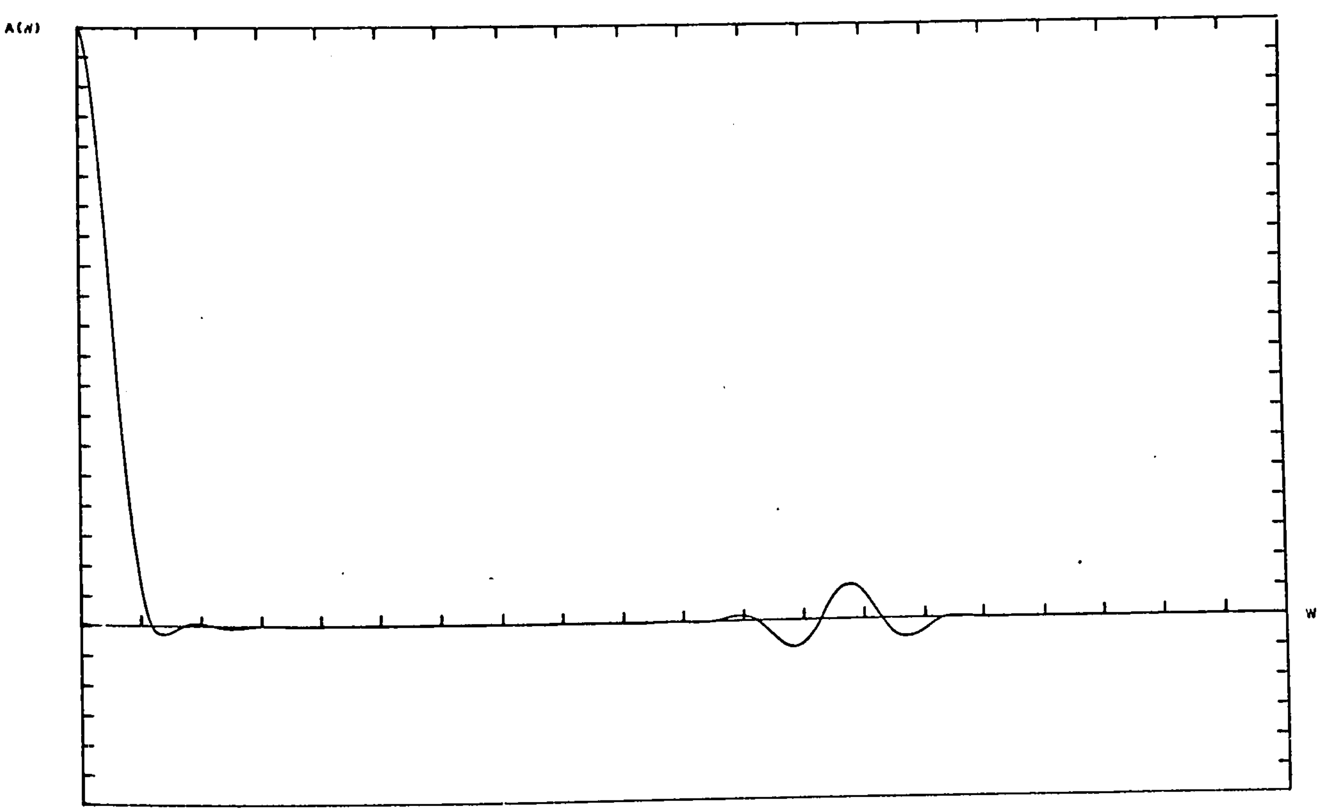

Fig. A5-15 Diffraction pattern formed by the F.S. 11(1a-B2-H)

TABLE A5-16

10 RINGS FLUX SELECTOR 1A-B4-H

TRANSMISSION FACTOR T OF FLUX SELECTOR

T= 0.40595

VALUES OF XP(I)

0.05000	0.15000	0.25000	0.35000	0.45000
0.55000	0.65000	0.75000	0.85000	0.95000
1.00000				

VALUES OF INNER AND OUTER RADII OF RINGS

I= 1	R(I)= 0.0	RP(I)= 0.14963
I= 2	R(I)= 0.15322	RP(I)= 0.24678
I= 3	R(I)= 0.25769	RP(I)= 0.34231
I= 4	R(I)= 0.36336	RP(I)= 0.43664
I= 5	R(I)= 0.46976	RP(I)= 0.53024
I= 6	R(I)= 0.57636	RP(I)= 0.62364
I= 7	R(I)= 0.68268	RP(I)= 0.71732
I= 8	R(I)= 0.78831	RP(I)= 0.81169
I= 9	R(I)= 0.89297	RP(I)= 0.90703
I= 10	R(I)= 0.99584	RP(I)= 1.00000

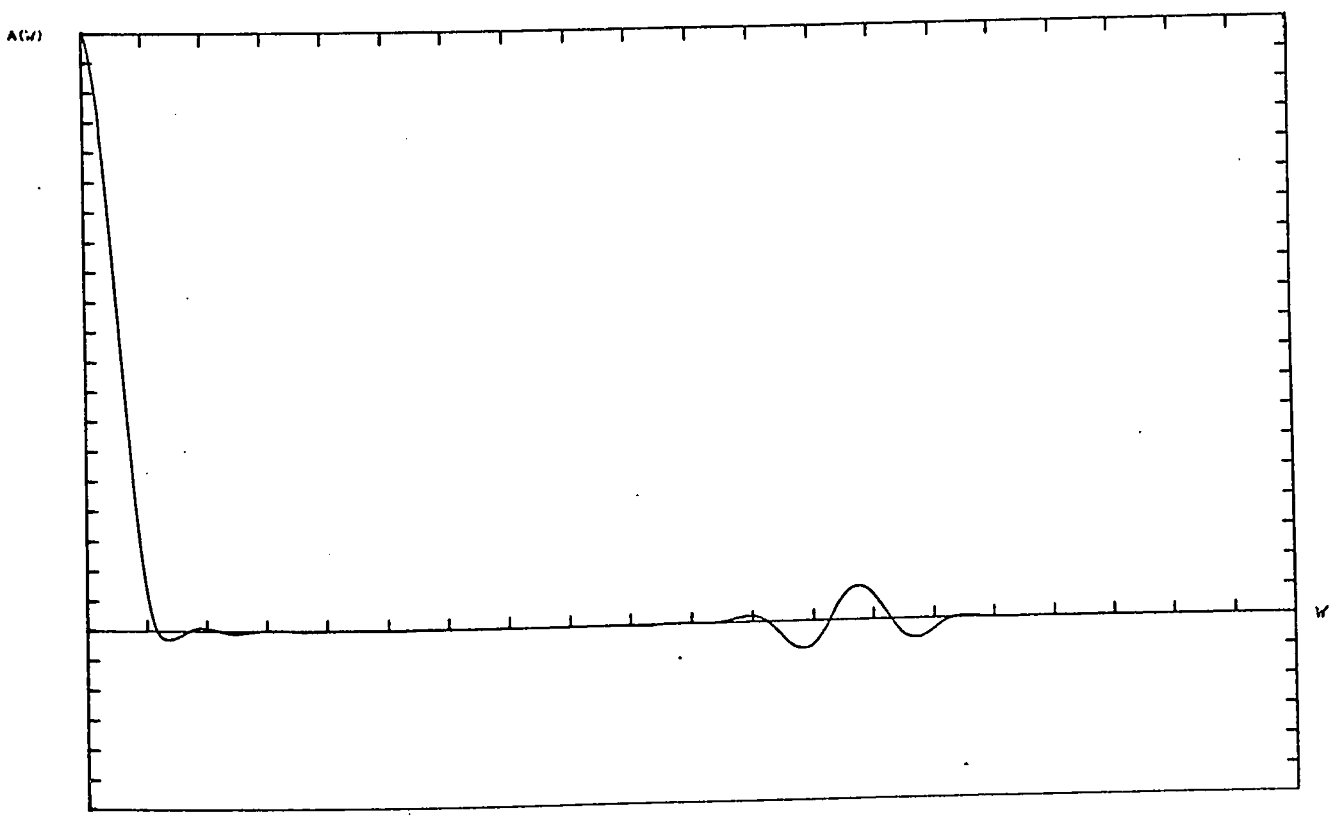

Fig. A5-16 Diffraction pattern formed by the F.S. 10(1a-B4-H)

TABLE A5-17

10 RINGS FLUX SELECTOR 1B-B4-H

TRANSMISSION FACTOR T OF FLUX SELECTOR

T= 0.40715

VALUES OF XP(I)

0.05000	0.15000	0.25000	0.35000	0.45000
0.55000	0.65000	0.75000	0.85000	0.95000
1.00000				

VALUES OF INNER AND OUTER RADII OF RINGS

I= 1	R(I)= 0.0	RP(I)= 0.14985
I= 2	R(I)= 0.15406	RP(I)= 0.24752
I= 3	R(I)= 0.25892	RP(I)= 0.34345
I= 4	R(I)= 0.35484	RP(I)= 0.43806
I= 5	R(I)= 0.47135	RP(I)= 0.53182
I= 6	R(I)= 0.57797	RP(I)= 0.62526
I= 7	R(I)= 0.68424	RP(I)= 0.71890
I= 8	R(I)= 0.78977	RP(I)= 0.81318
I= 9	R(I)= 0.89432	RP(I)= 0.90641
I= 10	R(I)= 0.99583	RP(I)= 1.00000

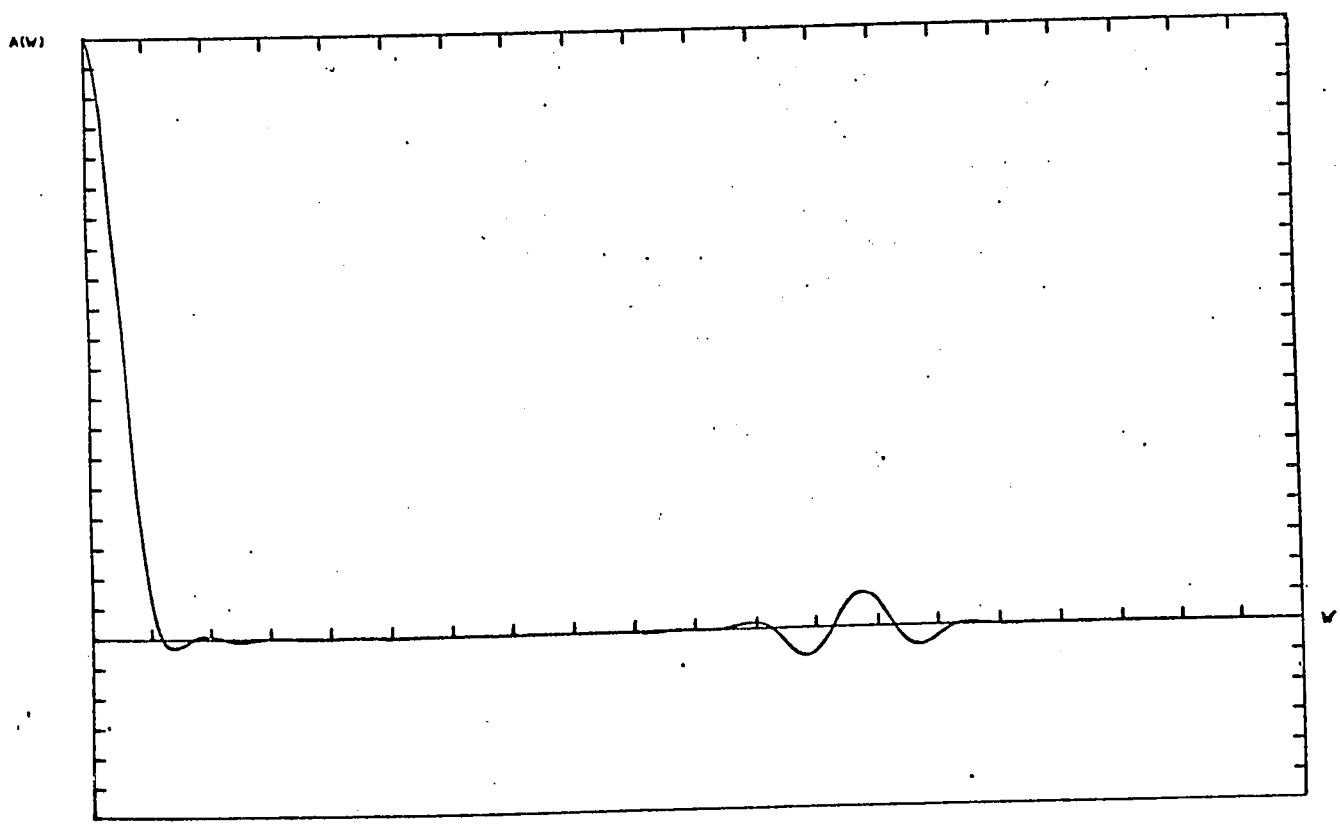

Fig. A5-17 Diffraction pattern formed by the F.S. 10(1b-B4-H)

TABLE A5-18

10 RINGS FLUX SELECTOR 2-C2-H

TRANSMISSION FACTOR T OF FLUX SELECTOR

T= 0.55187

VALUES OF XP(I)

0.05771	0.11626	0.17643	0.23926	0.30615
0.37919	0.46186	0.56111	0.69537	1.00000

VALUES OF INNER AND OUTER RADII OF RINGS

I= 1	R(I)= 0.0	RP(I)= 0.06776
I= 2	R(I)= 0.06836	RP(I)= 0.13611
I= 3	R(I)= 0.13812	RP(I)= 0.20588
I= 4	R(I)= 0.21039	RP(I)= 0.27815
I= 5	R(I)= 0.28660	RP(I)= 0.35436
I= 6	R(I)= 0.36378	RP(I)= 0.43654
I= 7	R(I)= 0.46015	RP(I)= 0.52791
I= 8	R(I)= 0.56667	RP(I)= 0.63443
I= 9	R(I)= 0.70232	RP(I)= 0.77008
I= 10	R(I)= 0.93224	RP(I)= 1.00000

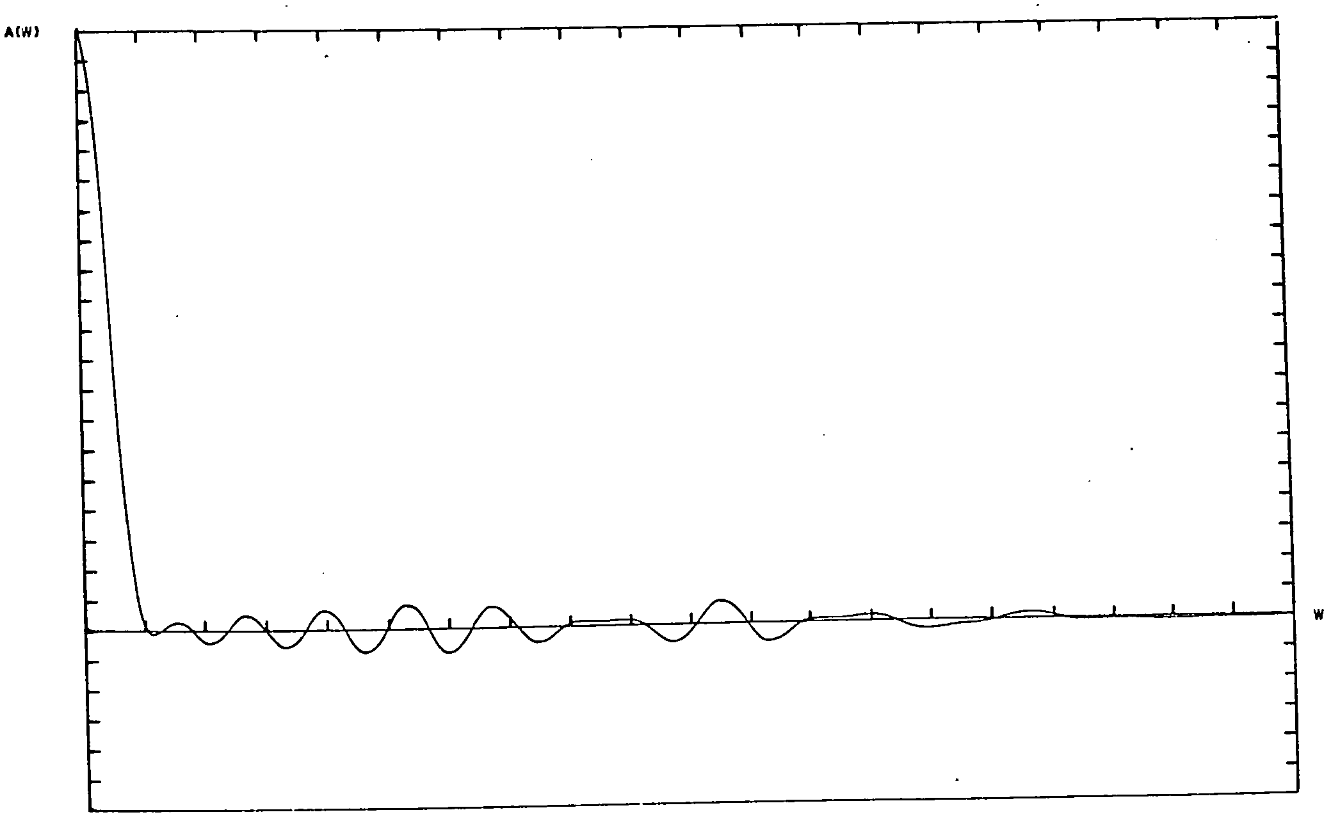

Fig. A5-18 Diffraction pattern formed by the F.S. 10(2-C2-H)

TABLE A5-20

9 RINGS FLUX SELECTOR 2-PA2-H

TRANSMISSION FACTOR T OF FLUX SELECTOR

T= 0.45166

VALUES OF XP(I)

0.13129	0.23983	0.34824	0.45599	0.56423
0.67218	0.78084	0.88943	1.00000	

VALUES OF INNER AND OUTER RADII OF RINGS

I=	1	R(I)=	0.0	RP(I)=	0.13850
I=	2	R(I)=	0.14267	RP(I)=	0.25047
I=	3	R(I)=	0.26287	RP(I)=	0.35984
I=	4	R(I)=	0.38415	RP(I)=	0.46682
I=	5	R(I)=	0.50567	RP(I)=	0.57299
I=	6	R(I)=	0.62752	RP(I)=	0.67855
I=	7	R(I)=	0.74862	RP(I)=	0.78469
I=	8	R(I)=	0.86884	RP(I)=	0.89162
I=	9	R(I)=	0.98757	RP(I)=	1.00000

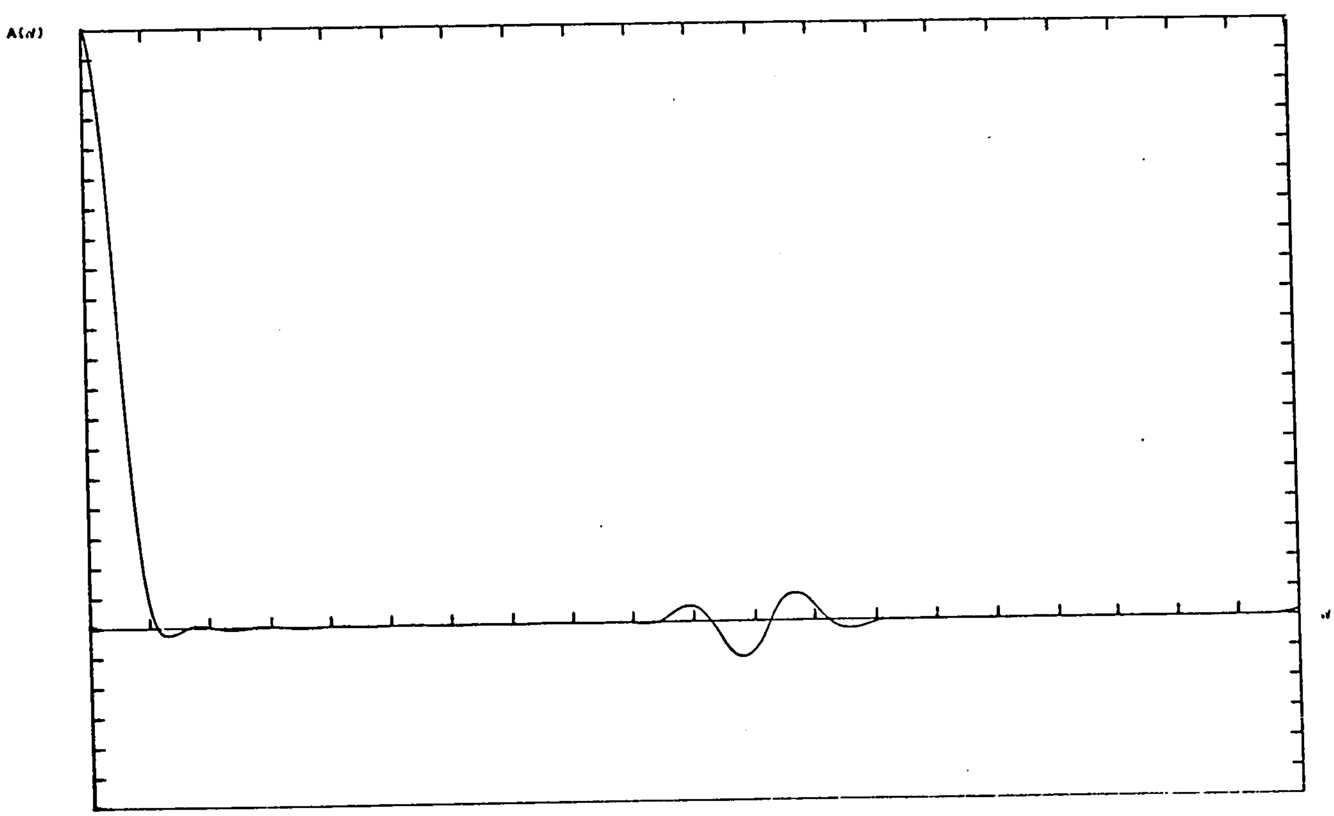

Fig. A5-20 Diffraction pattern formed by the F.S. 9(2-PA2-H)

TABLE A5-21

10 RINGS FLUX SELECTOR 2-PB2-H

TRANSMISSION FACTOR T OF FLUX SELECTOR

T= 0.44514

VALUES OF XP(I)

0.11862	0.21680	0.31465	0.41200	0.50966
0.60708	0.70493	0.80264	0.90110	1.00000

VALUES OF INNER AND OUTER RADII OF RINGS

I= 1	R(I)= 0.0	RP(I)= 0.12442
I= 2	R(I)= 0.12750	RP(I)= 0.22550
I= 3	R(I)= 0.23472	RP(I)= 0.32447
I= 4	R(I)= 0.34270	RP(I)= 0.42154
I= 5	R(I)= 0.45098	RP(I)= 0.51782
I= 6	R(I)= 0.55973	RP(I)= 0.61339
I= 7	R(I)= 0.66816	RP(I)= 0.70913
I= 8	R(I)= 0.77620	RP(I)= 0.80518
I= 9	R(I)= 0.88329	RP(I)= 0.90213
I= 10	R(I)= 0.98943	RP(I)= 1.00000

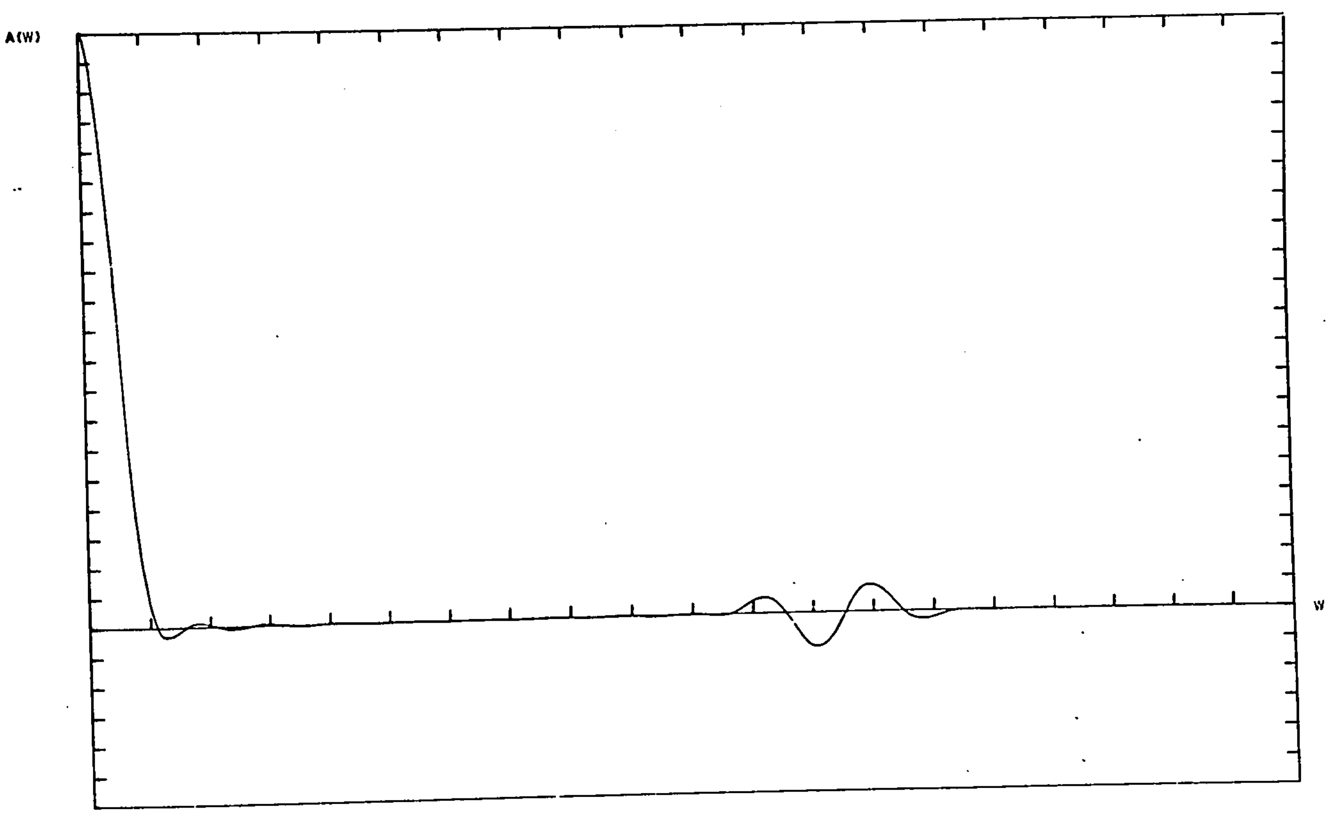

Fig. A5-21 Diffraction pattern formed by the F.S. 10(2-PB2-H)

TABLE A5-22

10 RINGS FLUX SELECTOR 2-PC2-H

TRANSMISSION FACTOR T OF FLUX SELECTOR

T= 0.53791

VALUES OF XP(I)

0.09539	0.17445	0.25310	0.33141	0.40982
0.48809	0.56652	0.64486	0.72339	1.00000

VALUES OF INNER AND OUTER RADII OF RINGS

I=	1	R(I)=	0.0	RP(I)=	0.11025
I=	2	R(I)=	0.11205	RP(I)=	0.20054
I=	3	R(I)=	0.20594	RP(I)=	0.28931
I=	4	R(I)=	0.30013	RP(I)=	0.37679
I=	5	R(I)=	0.39459	RP(I)=	0.46363
I=	6	R(I)=	0.48954	RP(I)=	0.54978
I=	7	R(I)=	0.58458	RP(I)=	0.63573
I=	8	R(I)=	0.67971	RP(I)=	0.72152
I=	9	R(I)=	0.77457	RP(I)=	0.80752
I=	10	R(I)=	0.94344	RP(I)=	1.00000

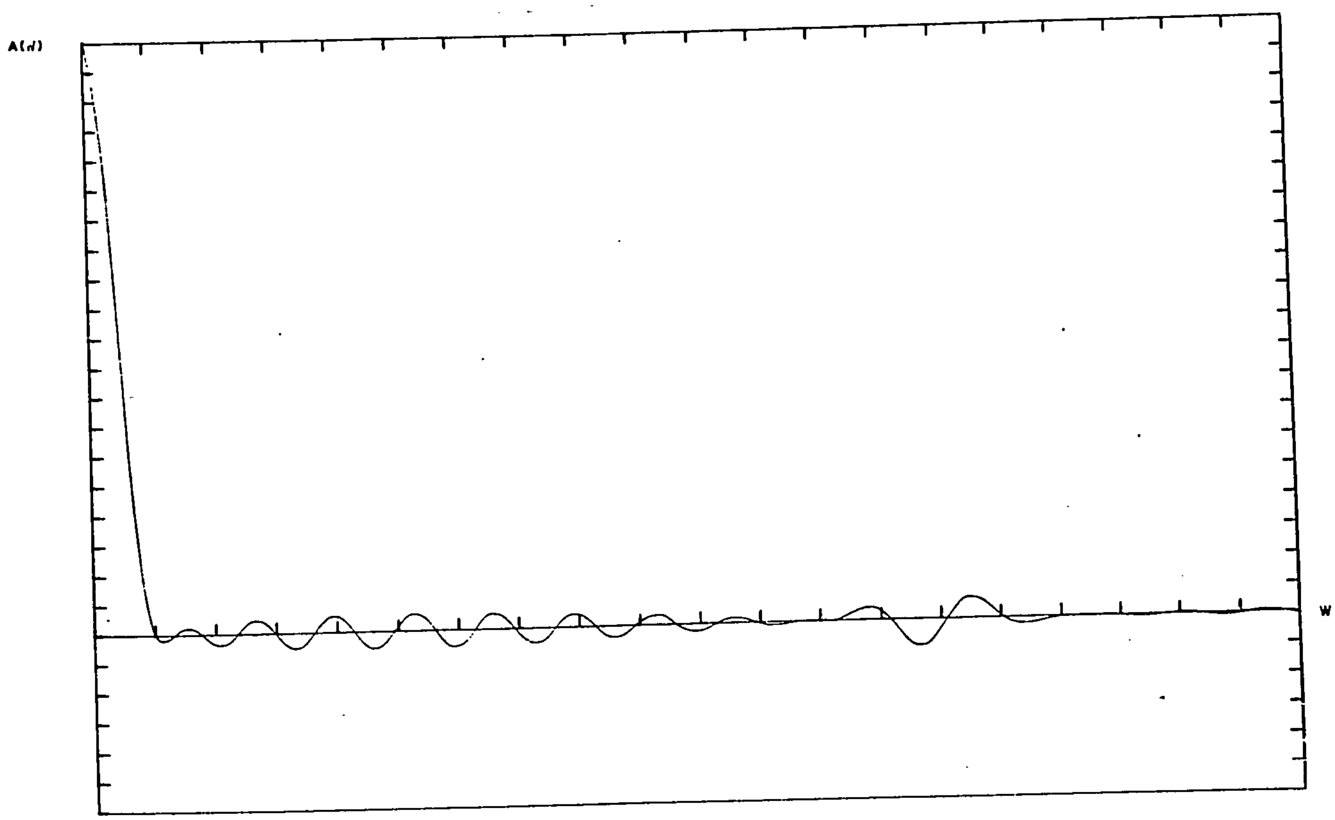

Fig. A5-22 Diffraction pattern formed by the F.S. 10(2-PC2-H)

TABLE A5-23

10 RINGS FLUX SELECTOR 2-Q2-H

TRANSMISSION FACTOR T OF FLUX SELECTOR

T= 0.48053

VALUES OF XP(I)

0.45524	0.57692	0.63972	0.71527	0.75879
0.82176	0.85580	0.91431	0.94115	1.00000

VALUES OF INNER AND OUTER RADII OF RINGS

I= 1	R(I)= 0.0	RP(I)= 0.45171
I= 2	R(I)= 0.48950	RP(I)= 0.57115
I= 3	R(I)= 0.60894	RP(I)= 0.64239
I= 4	R(I)= 0.68018	RP(I)= 0.71275
I= 5	R(I)= 0.75054	RP(I)= 0.76573
I= 6	R(I)= 0.80352	RP(I)= 0.82123
I= 7	R(I)= 0.85902	RP(I)= 0.86667
I= 8	R(I)= 0.90446	RP(I)= 0.91478
I= 9	R(I)= 0.95257	RP(I)= 0.95623
I= 10	R(I)= 0.99403	RP(I)= 1.00000

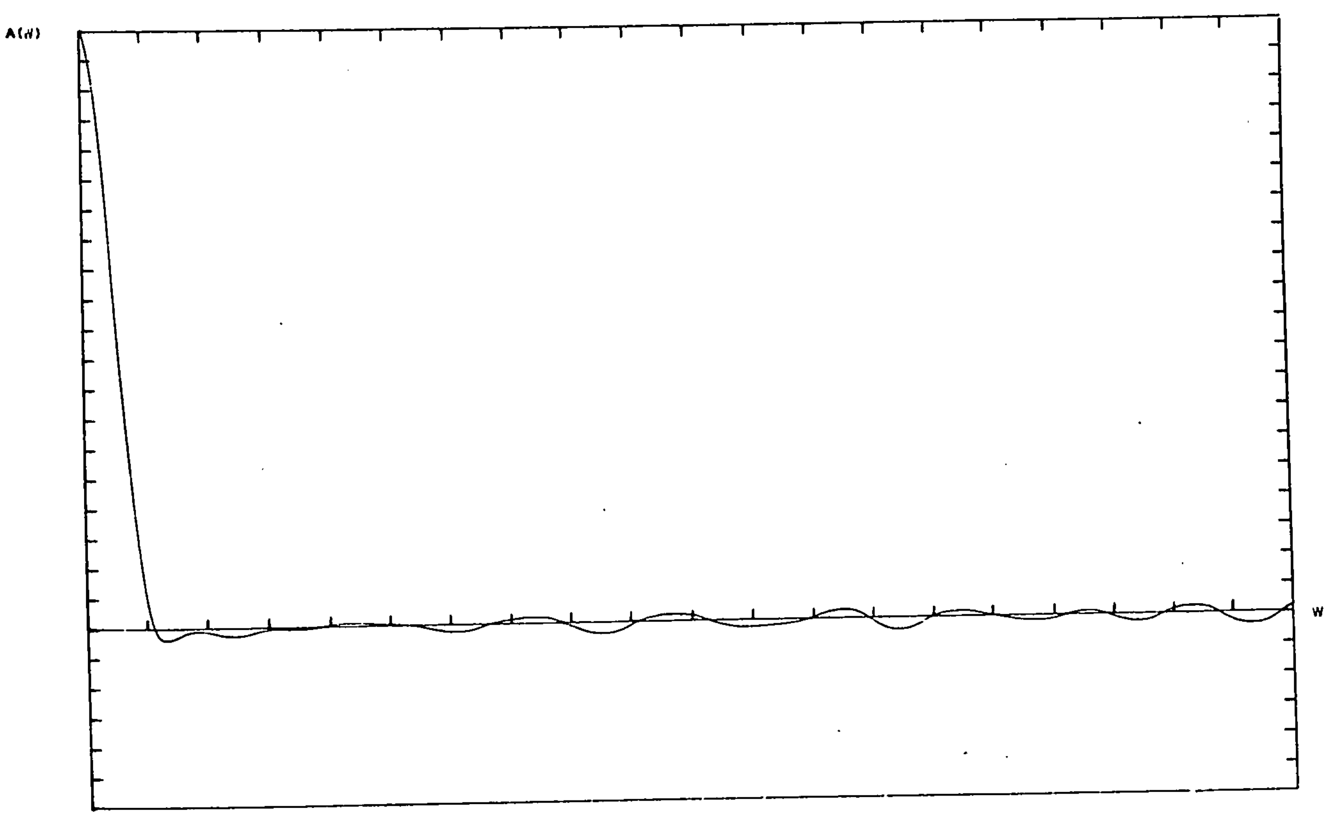

Fig. A5-23 Diffraction pattern formed by the F.S. 10(2-Q2-H)

CONCLUSIONS:

Most of the calculations described above were performed for N = 10. It is supposed that as N is increased, the diffraction pattern formed by any given flux selector will improve, but that the relative merits of the various flux selectors will not change. To corroborate this supposition, consider an example: F.S. 21(1a-B2-H) and 20(1b-A2-H) were calculated by Lansraux, and their diffraction patterns differ from that of their 10(11) ring counterparts only by the fact that (1) the first principal maxima occur at $W \simeq 130$ (instead of approx. 65) and are of lower amplitude (2) the secondary maxima have slightly smaller amplitudes. The differences between 20(1b-A2-H) and 21(1a-B2-H) are exactly of the same nature as those in their 10(11) rings counterparts. [Note:(1) the diffraction patterns for types A, B, and P show only one set of principal maxima (which we have referred to as "the first principal maxima"). Just as in plane diffraction gratings, there are more princiapl maxima for greater W, and these (including the first one) appear to occur at values of W obtained by treating the flux selector as a plane diffraction grating. As N is increased, then, it appears as if all the principal maxima are pushed back to larger W (as they would be in a plane diffraction grating).

(2) We see from equation A4-7 that the amplitude at the center of the diffraction pattern formed by a flux selector is

$$\text{A4-14} \quad \Sigma \left(r_n'^2 - r_n^2\right) = C\,\Sigma \int_{x_n}^{x_n'} T(x)\,dx^2 = C \int_0^1 T(x)\,dx^2$$

Since in practice C is very close to 1, as we have seen, this means that the amplitude at the center of the diffraction pattern associated with a flux selector is almost the same as that associated with the corresponding amplitude filter (see equa. A1-3). The left hand side of A4-14 also represents the transmission factor of the flux selector; however, in the case of the amplitude filter, the transmission factor is given by $\int_0^1 T^2(x)\, dx^2$, which is smaller than that associated with the flux selector: the difference between these two transmission factors represents the amount of energy which is distributed in the principal maxima of the diffraction pattern formed by a flux selector. Note that this amount of energy is practically independent of the number N of rings in the flux selector, but depends only on the type of amplitude filter T(x) considered: for T(x,5) it is about 43% of the energy transmitted by the flux selector, whereas for T(x,M) it represents 33%. Consequently, as N is increased, we expect the principal maxima to decrease in intensity as they are pushed further out from the center.]

Of the various types of flux selectors calculated, the best diffraction patterns, for small N at least, are produced by types A, B, and P; the diffraction patterns produced by types A and P are almost identical for reasons given earlier; because of this, and because type P is much longer to calculate, it was not considered in further calculations. Type B flux selectors were also rejected for further work because (1) they have a very narrow inner opaque ring and outer transparent ring compared to type A flux selectors of the same number of zones, which would make them more difficult to make; and (2) they do not produce diffraction patterns which are significantly better than those produced by type A.

A comparison of the different flux selectors of the type A shows that very little improvement is achieved by using a 2 term (2-...) rather than a 1 term (1..-A...) approximation. Furthermore, type 1b-A4-H is the best from the practical point of view since it has the widest inner opaque ring. It was this type of flux selector, then, that we have selected for the practical realization of a 50 zone flux selector. We have calculated the 49 rings flux selectors of the type 1b-A4-H corresponding to the amplitude filters T(x,5) and T(x,M). See tables A5-24 and A5-25 for the data associated with these flux selectors. The diffraction patterns corresponding to these two flux selectors were calculated. In table A5-26 are given the amplitudes in the diffraction patterns for the amplitude filter, for the corresponding flux selector 49(1b-A4-H) and the differences in amplitude between the two for both T(x,5) and T(x,M), and for W up to 25. We have also calculated the positions and values of the maxima and minima (the extrema) in the diffraction patterns associated with the amplitude filters and with their corresponding flux selectors 49(1b-A4-H). These calculations were done for the range W = 0 to 325: see table A5-27 for T(x,5) and table A5-28 for T(x,M).

We note that:

(1) In both flux selectors, the first principal maxima occur at about W = 314, as we would have expected. This further verifies the hypothesis made earlier that as the number of rings in the flux selector is increased, the principal maxima occur at proportionally greater values of W. For the flux selector corresponding to T(x,5), we note (by comparing with the corresponding 10 ring flux selector) that the amplitudes of the first principal maxima have decreased by about half, and hence the amount of energy in the first principal maxima is about the same, which we would also expect from comments made earlier. (The same would probably hold for the T(x,M) case)

(2) When comparing the diffraction patterns formed by either amplitude filter and by its corresponding flux selector, we can divide the interval

W = 0 to 325 into three regions:

(a) In the first region [W≃0 to 200 for T(x,5), W≃0 to 150 for T(x,M)], the flux selectors are very good approximations to the amplitude filters: i.e., the extrema in the diffraction patterns that they form differ very little in position and value (less than 1 or 2 $\times 10^{-4}$) from those formed by the corresponding amplitude filters.

(b) In the second region [W ≃ 200 to 240 for T(x,5), W ≃ 150 to 200 for T(x,M)], the flux selector diffraction pattern extrema increase with increasing W (while the corresponding extrema in the amplitude filter diffraction pattern are decreasing with W), but are still smaller than the corresponding extrema in the Airy pattern.

(c) In the third region [W ≃ 240 to 325 for T(x,5), and W ≃ 200 to 325 for T(x,M)], the flux selector extrema are greater than the corresponding ones in the Airy pattern. This region, where the flux selector "breaks down", corresponds roughly to the first principal maxima, and can be rejected to greater W if the number of rings in the flux selector is increased.

From the above, we conclude that flux selectors can replace amplitude filters in optical systems providing they have a sufficiently large number of rings so that the principal maxima are rejected outside the useful image field.

In the second part of this work, we shall describe how the flux selectors discussed above were made, and give some of the experimental results obtained with them.

Table A5-24 F.S. 49(1b-A4-H) corresponding to amplitude filter T(x,5)

49 RINGS FLUX SELECTOR 1B-A4-H

TRANSMISSION FACTOR T OF FLUX SELECTOR

T= 0.40706

VALUES OF XP(I)

0.02000	0.04000	0.06000	0.08000	0.10000
0.12000	0.14000	0.16000	0.18000	0.20000
0.22000	0.24000	0.26000	0.28000	0.30000
0.32000	0.34000	0.36000	0.38000	0.40000
0.42000	0.44000	0.46000	0.48000	0.50000
0.52000	0.54000	0.56000	0.58000	0.60000
0.62000	0.64000	0.66000	0.68000	0.70000
0.72000	0.74000	0.76000	0.78000	0.80000
0.82000	0.84000	0.86000	0.88000	0.90000
0.92000	0.94000	0.96000	0.98000	1.00000

VALUES OF INNER AND OUTER RADII OF RINGS

I= 1	R(I)= 0.0	RP(I)= 0.04037
I= 2	R(I)= 0.04042	RP(I)= 0.06053
I= 3	R(I)= 0.06066	RP(I)= 0.08067
I= 4	R(I)= 0.08091	RP(I)= 0.10080
I= 5	R(I)= 0.10118	RP(I)= 0.12091
I= 6	R(I)= 0.12146	RP(I)= 0.14100
I= 7	R(I)= 0.14176	RP(I)= 0.16109
I= 8	R(I)= 0.16207	RP(I)= 0.18115
I= 9	R(I)= 0.18239	RP(I)= 0.20121
I= 10	R(I)= 0.20273	RP(I)= 0.22125
I= 11	R(I)= 0.22308	RP(I)= 0.24128
I= 12	R(I)= 0.24344	RP(I)= 0.26129
I= 13	R(I)= 0.26382	RP(I)= 0.28130
I= 14	R(I)= 0.28420	RP(I)= 0.30129
I= 15	R(I)= 0.30459	RP(I)= 0.32127
I= 16	R(I)= 0.32500	RP(I)= 0.34124
I= 17	R(I)= 0.34541	RP(I)= 0.36171
I= 18	R(I)= 0.36583	RP(I)= 0.38116
I= 19	R(I)= 0.38625	RP(I)= 0.40111
I= 20	R(I)= 0.40668	RP(I)= 0.42106
I= 21	R(I)= 0.42712	RP(I)= 0.44099
I= 22	R(I)= 0.44756	RP(I)= 0.46093
I= 23	R(I)= 0.46801	RP(I)= 0.48085
I= 24	R(I)= 0.48846	RP(I)= 0.50078
I= 25	R(I)= 0.50891	RP(I)= 0.52070
I= 26	R(I)= 0.52936	RP(I)= 0.54062
I= 27	R(I)= 0.54981	RP(I)= 0.56055
I= 28	R(I)= 0.57026	RP(I)= 0.58047
I= 29	R(I)= 0.59071	RP(I)= 0.60029
I= 30	R(I)= 0.61115	RP(I)= 0.62032

Table A5-24 Continued

I=	31	R(I)=	0.63160	RP(I)=	0.64024
I=	32	R(I)=	0.65204	RP(I)=	0.66017
I=	33	R(I)=	0.67247	RP(I)=	0.68011
I=	34	R(I)=	0.69290	RP(I)=	0.70005
I=	35	R(I)=	0.71333	RP(I)=	0.71999
I=	36	R(I)=	0.73375	RP(I)=	0.73994
I=	37	R(I)=	0.75416	RP(I)=	0.75990
I=	38	R(I)=	0.77457	RP(I)=	0.77986
I=	39	R(I)=	0.79497	RP(I)=	0.79983
I=	40	R(I)=	0.81536	RP(I)=	0.81981
I=	41	R(I)=	0.83575	RP(I)=	0.83980
I=	42	R(I)=	0.85612	RP(I)=	0.85979
I=	43	R(I)=	0.87649	RP(I)=	0.87979
I=	44	R(I)=	0.89685	RP(I)=	0.89980
I=	45	R(I)=	0.91720	RP(I)=	0.91983
I=	46	R(I)=	0.93754	RP(I)=	0.93986
I=	47	R(I)=	0.95787	RP(I)=	0.95989
I=	48	R(I)=	0.97819	RP(I)=	0.97994
I=	49	R(I)=	0.99850	RP(I)=	1.00000

Table A5-25 F.S. 49(1b-A4-H) corresponding to amplitude filter T(x,M)

49 RINGS FLUX SELECTOR 1b-A4-H

TRANSMISSION FACTOR T OF FLUX SELECTOR

T= 0.60223

VALUES OF XP(I)

0.02000	0.04000	0.06000	0.08000	0.10000
0.12000	0.14000	0.16000	0.18000	0.20000
0.22000	0.24000	0.26000	0.28000	0.30000
0.32000	0.34000	0.36000	0.38000	0.40000
0.42000	0.44000	0.46000	0.48000	0.50000
0.52000	0.54000	0.56000	0.58000	0.60000
0.62000	0.64000	0.66000	0.68000	0.70000
0.72000	0.74000	0.76000	0.78000	0.80000
0.82000	0.84000	0.86000	0.88000	0.90000
0.92000	0.94000	0.96000	0.98000	1.00000

VALUES OF INNER AND OUTER RADII OF RINGS

I=	1	R(I)=	0.0	RP(I)=	0.04030
I=	2	R(I)=	0.04032	RP(I)=	0.06043
I=	3	R(I)=	0.06049	RP(I)=	0.08057
I=	4	R(I)=	0.08067	RP(I)=	0.10069
I=	5	R(I)=	0.10085	RP(I)=	0.12081
I=	6	R(I)=	0.12104	RP(I)=	0.14092
I=	7	R(I)=	0.14124	RP(I)=	0.16102
I=	8	R(I)=	0.16144	RP(I)=	0.18112
I=	9	R(I)=	0.18165	RP(I)=	0.20121
I=	10	R(I)=	0.20187	RP(I)=	0.22130
I=	11	R(I)=	0.22209	RP(I)=	0.24137
I=	12	R(I)=	0.24232	RP(I)=	0.26144
I=	13	R(I)=	0.26256	RP(I)=	0.28151
I=	14	R(I)=	0.28281	RP(I)=	0.30156
I=	15	R(I)=	0.30306	RP(I)=	0.32161
I=	16	R(I)=	0.32332	RP(I)=	0.34165
I=	17	R(I)=	0.34359	RP(I)=	0.36169
I=	18	R(I)=	0.36386	RP(I)=	0.38172
I=	19	R(I)=	0.38414	RP(I)=	0.40174
I=	20	R(I)=	0.40443	RP(I)=	0.42175
I=	21	R(I)=	0.42472	RP(I)=	0.44175
I=	22	R(I)=	0.44503	RP(I)=	0.46175
I=	23	R(I)=	0.46534	RP(I)=	0.48174
I=	24	R(I)=	0.48565	RP(I)=	0.50173
I=	25	R(I)=	0.50598	RP(I)=	0.52171
I=	26	R(I)=	0.52631	RP(I)=	0.54168
I=	27	R(I)=	0.54664	RP(I)=	0.56164
I=	28	R(I)=	0.56699	RP(I)=	0.58160
I=	29	R(I)=	0.58734	RP(I)=	0.60155
I=	30	R(I)=	0.60769	RP(I)=	0.62149

Table A5-25 Continued

I=	31	R(I)=	0.62806	RP(I)=	0.64143
I=	32	R(I)=	0.64842	RP(I)=	0.66136
I=	33	R(I)=	0.66879	RP(I)=	0.68129
I=	34	R(I)=	0.68917	RP(I)=	0.70121
I=	35	R(I)=	0.70955	RP(I)=	0.72113
I=	36	R(I)=	0.72993	RP(I)=	0.74105
I=	37	R(I)=	0.75032	RP(I)=	0.76096
I=	38	R(I)=	0.77071	RP(I)=	0.78087
I=	39	R(I)=	0.79110	RP(I)=	0.80078
I=	40	R(I)=	0.81149	RP(I)=	0.82069
I=	41	R(I)=	0.83188	RP(I)=	0.84060
I=	42	R(I)=	0.85227	RP(I)=	0.86051
I=	43	R(I)=	0.87266	RP(I)=	0.88042
I=	44	R(I)=	0.89304	RP(I)=	0.90033
I=	45	R(I)=	0.91342	RP(I)=	0.92025
I=	46	R(I)=	0.93379	RP(I)=	0.94018
I=	47	R(I)=	0.95416	RP(I)=	0.96011
I=	48	R(I)=	0.97451	RP(I)=	0.98005
I=	49	R(I)=	0.99486	RP(I)=	1.00000

Table A5-26

DIFFRACTION PATTERNS FORMED BY AMPLITUDE FILTERS T(X,5) AND T(X,M) AND THEIR ASSOCIATED FLUX SELECTORS 49(1B-A4-H)

	T(X,5)			T(X,M)		
W	A.F.	F.S.	DIF.	A.F.	F.S.	DIF.
0.5	0.98056	0.98019	0.0004	0.97580	0.97544	0.0004
1.0	0.92405	0.92266	0.0014	0.90579	0.90441	0.0014
1.5	0.83568	0.83278	0.0029	0.79735	0.79453	0.0028
2.0	0.72339	0.71879	0.0046	0.66166	0.65726	0.0044
2.5	0.59684	0.59066	0.0062	0.51211	0.50637	0.0057
3.0	0.46630	0.45895	0.0073	0.36261	0.35602	0.0066
3.5	0.34139	0.33349	0.0079	0.22572	0.21900	0.0067
4.0	0.23013	0.22240	0.0077	0.11125	0.10516	0.0061
4.5	0.13813	0.13124	0.0069	0.02523	0.02043	0.0048
5.0	0.06824	0.06273	0.0055	-0.03046	-0.03352	0.0031
5.5	0.02061	0.01679	0.0038	-0.05780	-0.05899	0.0012
6.0	-0.00695	-0.00906	0.0021	-0.06190	-0.06139	-0.0005
6.5	-0.01836	-0.01895	0.0006	-0.04977	-0.04801	-0.0018
7.0	-0.01840	-0.01788	-0.0005	-0.02905	-0.02666	-0.0024
7.5	-0.01194	-0.01081	-0.0011	-0.00676	-0.00438	-0.0024
8.0	-0.00328	-0.00203	-0.0012	0.01166	0.01348	-0.0018
8.5	0.00437	0.00534	-0.0010	0.02294	0.02383	-0.0009
9.0	0.00911	0.00956	-0.0004	0.02606	0.02592	0.0001
9.5	0.01033	0.01018	0.0002	0.02200	0.02097	0.0010
10.0	0.00843	0.00780	0.0006	0.01311	0.01154	0.0016
10.5	0.00454	0.00364	0.0009	0.00238	0.00070	0.0017
11.0	0.00002	-0.00088	0.0009	-0.00730	-0.00867	0.0014
11.5	-0.00382	-0.00449	0.0007	-0.01378	-0.01452	0.0007
12.0	-0.00613	-0.00641	0.0003	-0.01597	-0.01593	-0.0000
12.5	-0.00653	-0.00637	-0.0002	-0.01394	-0.01318	-0.0008
13.0	-0.00520	-0.00467	-0.0005	-0.00873	-0.00747	-0.0013
13.5	-0.00269	-0.00195	-0.0007	-0.00198	-0.00056	-0.0014
14.0	0.00021	0.00097	-0.0008	0.00451	0.00572	-0.0012
14.5	0.00274	0.00331	-0.0006	0.00920	0.00993	-0.0007
15.0	0.00431	0.00455	-0.0002	0.01117	0.01125	-0.0001
15.5	0.00463	0.00450	0.0001	0.01023	0.00967	0.0006
16.0	0.00376	0.00331	0.0005	0.00689	0.00585	0.0010
16.5	0.00203	0.00139	0.0006	0.00219	0.00094	0.0012
17.0	-0.00004	-0.00071	0.0007	-0.00263	-0.00376	0.0011
17.5	-0.00192	-0.00244	0.0005	-0.00639	-0.00714	0.0008
18.0	-0.00316	-0.00341	0.0003	-0.00830	-0.00849	0.0002
18.5	-0.00351	-0.00343	-0.0001	-0.00804	-0.00764	-0.0004
19.0	-0.00296	-0.00259	-0.0004	-0.00586	-0.00499	-0.0009
19.5	-0.00173	-0.00117	-0.0006	-0.00244	-0.00132	-0.0011
20.0	-0.00016	0.00044	-0.0006	0.00132	0.00241	-0.0011
20.5	0.00132	0.00182	-0.0005	0.00449	0.00527	-0.0008
21.0	0.00238	0.00264	-0.0003	0.00635	0.00664	-0.0003
21.5	0.00277	0.00275	0.0000	0.00655	0.00630	0.0003
22.0	0.00246	0.00216	0.0003	0.00515	0.00443	0.0007
22.5	0.00156	0.00107	0.0005	0.00261	0.00161	0.0010
23.0	0.00024	-0.00021	0.0005	-0.00040	-0.00143	0.0010
23.5	-0.00037	-0.00136	0.0005	-0.00312	-0.00393	0.0008
24.0	-0.00181	-0.00210	0.0003	-0.00492	-0.00531	0.0004
24.5	-0.00224	-0.00227	0.0000	-0.00543	-0.00532	-0.0001
25.0	-0.00210	-0.00186	-0.0002	-0.00460	-0.00402	-0.0006

Table A5-27

EXTREMA OF AMPLITUDE IN THE DIFFRACTION PATTERN FORMED BY AN AMPLITUDE FILTER T(X,5) COMPARED WITH THOSE OF THE DIFFRACTION PATTERN FORMED BY THE ASSOCIATED FLUX SELECTOR 49(1B-A4-H)

N	AMPLITUDE FILTER W	AMPLITUDE FILTER A	FLUX SELECTOR W	FLUX SELECTOR A	DIF. OF AMP. DIF.
1	6.753	-0.01919	6.701	-0.01984	0.00065
2	9.446	0.01035	9.353	0.01031	0.00004
3	12.366	-0.00659	12.240	-0.00664	0.00005
4	15.384	0.00466	15.231	0.00469	-0.00003
5	18.444	-0.00352	18.262	-0.00353	0.00001
6	21.529	0.00277	21.329	0.00279	-0.00002
7	24.627	-0.00226	24.397	-0.00228	0.00002
8	27.729	0.00183	27.474	0.00191	-0.00003
9	30.853	-0.00160	30.560	-0.00163	0.00003
10	33.971	0.00138	33.642	0.00141	-0.00003
11	37.100	-0.00121	36.750	-0.00124	0.00003
12	40.231	0.00107	39.843	0.00110	-0.00003
13	43.359	-0.00095	42.950	-0.00099	0.00004
14	46.488	0.00086	46.045	0.00089	-0.00003
15	49.618	-0.00078	49.131	-0.00082	0.00004
16	52.750	0.00071	52.250	0.00074	-0.00003
17	55.897	-0.00065	55.344	-0.00069	0.00004
18	59.017	0.00060	58.469	0.00064	-0.00004
19	62.143	-0.00056	61.571	-0.00059	0.00003
20	65.292	0.00051	64.679	0.00056	-0.00005
21	68.442	-0.00048	67.788	-0.00052	0.00004
22	71.542	0.00045	70.904	0.00049	-0.00004
23	74.700	-0.00042	74.000	-0.00046	0.00004
24	77.850	0.00039	77.114	0.00044	-0.00005
25	80.972	-0.00037	80.205	-0.00042	0.00005
26	84.100	0.00035	83.306	0.00040	-0.00005
27	87.250	-0.00033	86.417	-0.00038	0.00005
28	90.393	0.00031	89.562	0.00036	-0.00005
29	93.528	-0.00030	92.639	-0.00035	0.00005
30	96.679	0.00028	95.750	0.00034	-0.00006
31	99.750	-0.00027	98.875	-0.00032	0.00005
32	102.964	0.00026	101.964	0.00031	-0.00005
33	106.083	-0.00025	105.107	-0.00030	0.00005
34	109.250	0.00024	108.187	0.00030	-0.00006
35	112.417	-0.00023	111.321	-0.00028	0.00005
36	115.500	0.00022	114.437	0.00028	-0.00006
37	118.650	-0.00021	117.536	-0.00027	0.00006
38	121.833	0.00020	120.667	0.00026	-0.00006
39	124.917	-0.00020	123.750	-0.00026	0.00006
40	128.050	0.00019	126.833	0.00025	-0.00006

Table A5-27 Continued

EXTREMA OF AMPLITUDE IN THE DIFFRACTION PATTERN FORMED BY AN AMPLITUDE FILTER T(X,5) COMPARED WITH THOSE OF THE DIFFRACTION PATTERN FORMED BY THE ASSOCIATED FLUX SELECTOR 49(1B-A4-H)

N	AMPLITUDE FILTER W	AMPLITUDE FILTER A	FLUX SELECTOR W	FLUX SELECTOR A	DIF. OF AMP. DIF.
60	190.750	0.00010	189.050	0.00021	-0.00011
61	194.000	-0.00010	192.167	-0.00021	0.00011
62	197.083	0.00010	195.250	0.00021	-0.00011
63	200.250	-0.00009	198.350	-0.00021	0.00012
64	203.500	0.00009	201.500	0.00021	-0.00012
65	206.500	-0.00009	204.625	-0.00021	0.00012
66	209.750	0.00009	207.750	0.00022	-0.00013
67	212.917	-0.00009	210.833	-0.00022	0.00013
68	216.083	0.00009	213.950	0.00022	-0.00013
69	219.250	-0.00008	217.036	-0.00023	0.00015
70	222.250	0.00008	220.107	0.00023	-0.00015
71	225.500	-0.00008	223.250	-0.00024	0.00016
72	228.500	0.00008	226.393	0.00024	-0.00016
73	231.583	-0.00008	229.450	-0.00024	0.00016
74	234.917	0.00008	232.583	0.00025	-0.00017
75	237.750	-0.00007	235.667	-0.00025	0.00018
76	241.250	0.00007	238.821	0.00026	-0.00019
77	244.250	-0.00007	241.893	-0.00027	0.00020
78	247.500	0.00007	245.036	0.00028	-0.00021
79	250.500	-0.00007	248.125	-0.00029	0.00022
80	253.583	0.00007	251.250	0.00030	-0.00023
81	256.917	-0.00007	254.321	-0.00031	0.00024
82	260.000	0.00007	257.437	0.00032	-0.00025
83	263.250	-0.00006	260.562	-0.00034	0.00028
84	266.250	0.00006	263.687	0.00036	-0.00030
85	269.250	-0.00006	266.750	-0.00038	0.00032
86	272.500	0.00006	269.850	0.00040	-0.00034
87	275.750	-0.00006	272.932	-0.00044	0.00038
88	278.750	0.00006	276.042	0.00046	-0.00040
89	282.000	-0.00006	279.159	-0.00052	0.00046
90	285.000	0.00006	282.250	0.00055	-0.00049
91	288.250	-0.00005	285.312	-0.00064	0.00059
92	291.250	0.00005	288.363	0.00068	-0.00063
93	294.250	-0.00005	291.455	-0.00086	0.00081
94	297.750	0.00005	294.479	0.00089	-0.00084
95	300.750	-0.00005	297.524	-0.00126	0.00121
96	303.750	0.00005	300.072	0.00071	-0.00066
97	307.250	-0.00005	303.430	-0.00651	0.00646
98	310.250	0.00005	307.773	0.02304	-0.02299
99	313.250	-0.00005	312.369	-0.02912	0.02907
100	316.500	0.00005	316.898	0.01470	-0.01465
101	319.750	-0.00005	320.922	-0.00233	0.00228
102	323.000	0.00005	323.711	0.00090	-0.00085

Table A5-28

EXTREMA OF AMPLITUDE IN THE DIFFRACTION PATTERN FORMED BY AN AMPLITUDE FILTER T(X,M) COMPARED WITH THOSE OF THE DIFFRACTION PATTERN FORMED BY THE ASSOCIATED FLUX SELECTOR 49(1B-A4-H)

N	AMPLITUDE FILTER W	AMPLITUDE FILTER A	FLUX SELECTOR W	FLUX SELECTOR A	DIF. OF AMP. DIF.
1	5.876	-0.06240	5.826	-0.06235	-0.00005
2	8.967	0.02608	8.893	0.02607	0.00001
3	12.009	-0.01597	11.919	-0.01598	0.00001
4	15.088	0.01122	14.978	0.01125	-0.00003
5	18.190	-0.00846	18.057	-0.00850	0.00004
6	21.312	0.00666	21.151	0.00672	-0.00006
7	24.440	-0.00544	24.254	-0.00548	0.00004
8	27.567	0.00454	27.361	0.00459	-0.00005
9	30.697	-0.00386	30.469	-0.00392	0.00006
10	33.836	0.00334	33.576	0.00341	-0.00007
11	36.972	-0.00293	36.689	-0.00299	0.00006
12	40.107	0.00259	39.805	0.00266	-0.00007
13	43.241	-0.00232	42.919	-0.00239	0.00007
14	46.380	0.00208	46.032	0.00216	-0.00008
15	49.522	-0.00189	49.140	-0.00197	0.00008
16	52.665	0.00172	52.262	0.00180	-0.00008
17	55.803	-0.00158	55.384	-0.00166	0.00008
18	58.944	0.00146	58.500	0.00154	-0.00008
19	62.074	-0.00135	61.611	-0.00144	0.00009
20	65.217	0.00125	64.721	0.00134	-0.00009
21	68.371	-0.00117	67.847	-0.00125	0.00008
22	71.500	0.00109	70.957	0.00118	-0.00009
23	74.646	-0.00102	74.078	-0.00112	0.00010
24	77.772	0.00096	77.192	0.00106	-0.00010
25	80.917	-0.00090	80.312	-0.00101	0.00011
26	84.060	0.00086	83.437	0.00096	-0.00010
27	87.222	-0.00081	86.542	-0.00092	0.00011
28	90.355	0.00077	89.659	0.00088	-0.00011
29	93.485	-0.00073	92.775	-0.00084	0.00011
30	96.632	0.00070	95.882	0.00081	-0.00011
31	99.750	-0.00066	99.013	-0.00078	0.00012
32	102.906	0.00063	102.125	0.00076	-0.00013
33	106.036	-0.00060	105.250	-0.00072	0.00012
34	109.179	0.00058	108.368	0.00071	-0.00013
35	112.327	-0.00056	111.485	-0.00068	0.00012
36	115.481	0.00053	114.594	0.00066	-0.00013
37	118.596	-0.00051	117.719	-0.00065	0.00014
38	121.750	0.00049	120.844	0.00063	-0.00014
39	124.886	-0.00047	123.950	-0.00061	0.00014
40	128.042	0.00046	127.062	0.00060	-0.00014

Table A5-28 Continued

EXTREMA OF AMPLITUDE IN THE DIFFRACTION PATTERN FORMED BY AN AMPLITUDE FILTER T(X,M) COMPARED WITH THOSE OF THE DIFFRACTION PATTERN FORMED BY THE ASSOCIATED FLUX SELECTOR 49(1B-A4-H)

N	AMPLITUDE FILTER W	A	FLUX SELECTOR W	A	DIF. OF AMP. DIF.
60	190.893	0.00025	189.417	0.00049	-0.00024
61	194.050	-0.00024	192.542	-0.00049	0.00025
62	197.107	0.00024	195.635	0.00049	-0.00025
63	200.333	-0.00023	198.750	-0.00050	0.00027
64	203.417	0.00023	201.886	0.00049	-0.00026
65	206.550	-0.00022	205.000	-0.00050	0.00028
66	209.750	0.00022	208.125	0.00050	-0.00028
67	212.850	-0.00021	211.250	-0.00051	0.00030
68	216.000	0.00021	214.365	0.00051	-0.00030
69	219.150	-0.00020	217.481	-0.00052	0.00032
70	222.250	0.00020	220.596	0.00053	-0.00033
71	225.375	-0.00019	223.712	-0.00054	0.00035
72	228.550	0.00019	226.827	0.00055	-0.00036
73	231.750	-0.00018	229.964	-0.00056	0.00038
74	234.875	0.00018	233.071	0.00057	-0.00039
75	238.000	-0.00018	236.183	-0.00059	0.00041
76	241.083	0.00018	239.317	0.00060	-0.00042
77	244.250	-0.00018	242.406	-0.00062	0.00044
78	247.375	0.00017	245.531	0.00064	-0.00047
79	250.550	-0.00017	248.656	-0.00066	0.00049
80	253.750	0.00016	251.750	0.00068	-0.00052
81	256.875	-0.00016	254.889	-0.00071	0.00055
82	260.000	0.00016	258.000	0.00074	-0.00058
83	263.083	-0.00015	261.118	-0.00078	0.00063
84	266.250	0.00015	264.250	0.00081	-0.00066
85	269.375	-0.00015	267.345	-0.00086	0.00071
86	272.500	0.00015	270.458	0.00092	-0.00077
87	275.750	-0.00014	273.570	-0.00098	0.00084
88	278.875	0.00014	276.676	0.00106	-0.00092
89	282.000	-0.00014	279.802	-0.00115	0.00101
90	285.125	0.00014	282.911	0.00125	-0.00111
91	288.250	-0.00013	286.021	-0.00140	0.00127
92	291.417	0.00013	289.122	0.00157	-0.00144
93	294.583	-0.00013	292.227	-0.00184	0.00171
94	297.625	0.00013	295.312	0.00215	-0.00202
95	300.750	-0.00012	298.394	-0.00283	0.00271
96	304.000	0.00012	301.433	0.00406	-0.00394
97	307.083	-0.00012	304.885	-0.00878	0.00866
98	310.250	0.00012	308.736	0.01787	-0.01775
99	313.417	-0.00012	312.816	-0.02088	0.02076
100	316.500	0.00012	316.823	0.01322	-0.01310
101	319.750	-0.00011	320.471	-0.00569	0.00558
102	322.750	0.00011	323.630	0.00324	-0.00313

PART B - EXPERIMENTAL WORK

Introduction:

We now consider the problem of making the flux selectors discussed in the previous chapters. What are some of the difficulties involved?

(1) Since the flux selector and associated optics is an image forming system, it must be made with a high degree of perfection: in the case of ordinary plane diffraction gratings, which are used mainly for spectroscopic purposes, slight imperfections in the grating (apart from periodic ones) are not critical; this is not the case for flux selectors, whose purpose is to improve image quality; imperfections here would seriously deteriorate image quality.

(2) In general, the widths of both opaque and transparent rings vary continuously from the center to the edge of the flux selector. At the center, the opaque rings are very narrow and the light transmitting rings are relatively very wide, whereas the reverse is true at the edge. This variation in line width from one extreme to the other complicates the production of flux selectors, especially for a large number of rings. For example, a 10 ring, 2 cm radius F.S. of the type 2-A2-H has an outermost light transmitting ring which is already only .2mm wide, whereas the innermost opaque ring is only .054 mm wide.

What methods can one consider in order to make such flux selectors? Before describing the method which we have used, we shall review briefly other methods, and state why they have not been used for our work.

(a) Evaporation of aluminum through a suitable mask onto the plane surface of the lens being used: Lansraux has used this method successfully in order to produce a flux selector of the type 11(1a-B2-H). However, this method is not suitable to produce flux selectors having a larger number of rings because of the difficulty in producing the mask: the latter is produced mechanically and this allows a precision of the order of $\pm 25\mu$ only; furthermore, as the number of rings increases, the mask would become intolerably fragile.

(b) Ruling the desired rings directly on the glass: impractical because each ring would require a needle of a different size, and these needles would be difficult and expensive to make.

(c) Coating the lens with a thin layer of photographic emulsion, and then contact printing a negative of the required F.S. directly onto the lens. This would first require the production of a good negative of the F.S. This is feasible but not easy (see below). The flux selector produced by such a method would probably give poor results because:

(1) The graininess in the photographic image, especially at the edges of the rings, would scatter and diffuse light.

(2) The gelatin layer of the photographic emulsion would distort the wavefront of the light emerging from the lens.

The method which we have adopted for our work makes use of the photoetching process. The lenses used have a diameter of 7.5 cm, a focal length of 160 cms, and are plano-convex. The flux selectors were produced on the plane surface of the lenses and have a diameter of 4 cm.

The procedure for making the flux selectors can be summarized as follows:

First, a photographic reduction method is used to make a mask which consists of a 1 : 1 negative image of the flux selector desired. The plane surface of the lens is coated with a very thin ($\approx$400 Å) but opaque layer of copper. Then, on top of this layer is coated a thin layer ($\simeq 1\ \mu$) of photoetching emulsion. Then the mask is contact printed onto this emulsion by means of a suitable light source. The lens is then immersed in photoetching developper, which removes all the unexposed emulsion, so that there remains on top of the copper layer a positive image of the flux selector. The portions of copper which are not covered by the image are then removed by means of a suitable etchant, and there remains on the lens only the required flux selector rings, covered by the resist image, which is then removed with a solvent.

In the following chapters, we shall describe in detail the main steps of the above procedure. We shall then show the effect of these flux selectors in optical systems under various conditions.

copper. Then, on top of this layer is coated a thin layer ($\approx 1\ \mu$) of photoetching emulsion. Then the mask is contact printed onto this emulsion by means of a suitable light source. The lens is then immersed in photoetching developper, which removes all the unexposed emulsion, so that there remains on top of the copper layer a positive image of the flux selector. The portions of copper which are not covered by the image are then removed by means of a suitable etchant, and there remains on the lens only the required flux selector rings, covered by the resist image, which is then removed with a solvent.

In the following chapters, we shall describe in detail the main steps of the above procedure. We shall then show the effect of these flux selectors in optical systems under various conditions.

CHAPTER I

PRODUCTION OF THE NEGATIVE

We need a 1 : 1 negative of the required flux selector; what precision should we aim for in the negative? We have adopted the following criterion: if an error in a F.S. causes the amplitudes of the secondary maxima in the diffraction pattern that it forms to differ from those produced by the true F.S. by no more than about 10^{-4}, then this error is acceptable. This value 10^{-4} was chosen because:

(1) It is impossible to make lenses which produce a background intensity of less than 10^{-8}; this is due to the residual defects in the optical glass (such as bubbles, striae), and on its surface (even after polishing).

(2) The flux selectors considered form diffraction patterns whose extrema differ from those of the corresponding amplitude filters by about this value in the central and intermediate regions (which are the ones of interest to us).

An IBM computer program was written to introduce a random error of 1 micron max. in the ring radii of a flux selector (i.e., a max error of 2 microns in the widths of the rings). A 49(1B-A4-H) flux selector was thus modified, and its corresponding diffraction pattern calculated. It was found that this diffraction pattern agreed with that corresponding to the original flux selector well within the "tolerance" stated above. We have thus chosen ±1 micron on ring radii, and ±2 microns on ring widths as our goal as far as the precision of both the negative and the final flux selector. (The above values also represent about the limit of precision with which measurements can be made on a F.S. having the dimensions used).

In order to make the F.S. negative, various methods can be considered. Only two of these have been studied in detail and will be described here: although only the photographic reduction method was finally used, the glass cone (axicon) method will also be described because of the amount of work devoted to its study and the interest this method can have in other applications.

(a) Glass cone or Axicon method.

This method for making the mask negative results from the following observation: if a point source, a glass cone (so-called "axicon"), and a lens are set up, in that order, so that the cone axis coincides with the optical axis, then a well-defined ring image is formed by the lens in the image space. (Fig. B1-1) Furthermore, it is found that the radius of the ring varies approx. linearly with the distance between the point source and the axicon. Similarly, but independently, as the size of the source is increased or decreased, the width of the ring varies proportionally. The above behaviour results from the fact that the beam emerging from the axicon appears to come from a virtual ring source situated near the plane of the source. For very small angles α, the radius of this ring is $R=(n-1)\alpha Z/\cos^2(\theta)$ (see Fig. B1-2 for symbols). Also, for small source sizes, the width of the virtual ring $\approx$ the width of the source. The above observations suggest the use of such a set-up to produce the flux selector mask negative on a photographic plate. (Again, see fig. B1-1 for a possible experimental arrangement.) The iris diaphragm controls the width of the ring, whereas the distance Z controls its radius. A shutter is situated in the image plane of L_1 to cut off the light beam while changing the position of the axicon and varying the opening of the iris. A method based on the above would have the advantages of requiring more compact apparatus, of not requiring the construction of a lucite enlargment, and hence, could be used for many different types of flux selectors.

However, before developping this method, it was necessary to investigate in detail the properties of the axicon. Consider an ideal point source on the axis of an axicon oriented as shown in Fig. B1-2. The light beam emerging from the axicon appears to come from a virtual ring: how well defined

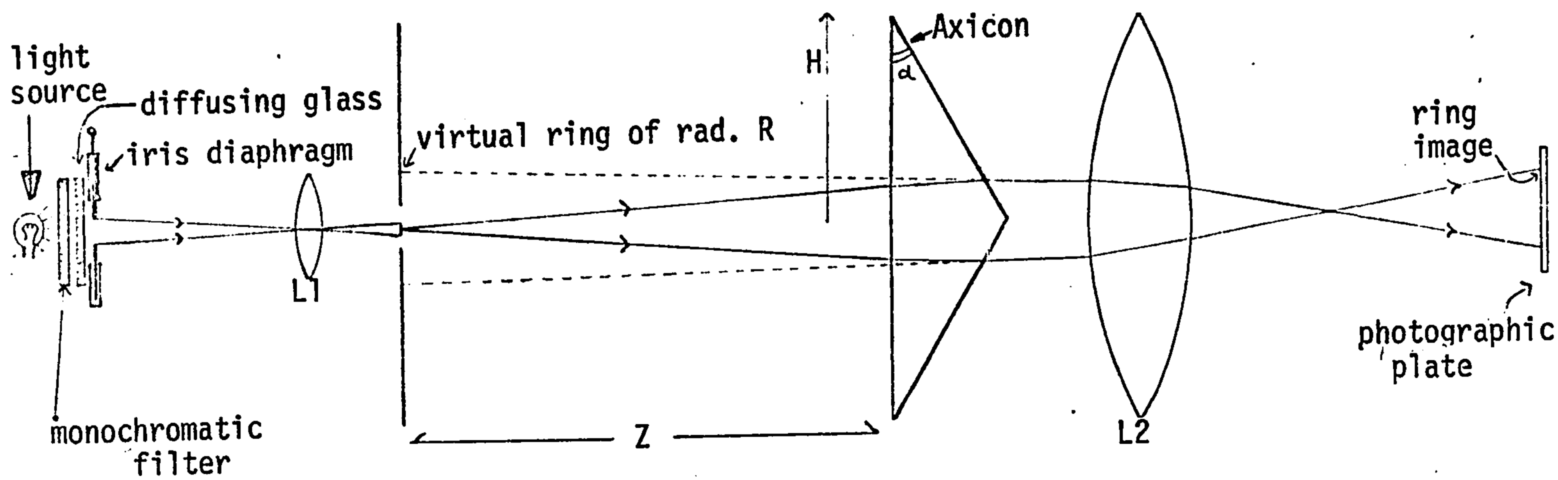

Fig. B1-1 Diagram showing how an axicon could be used to make a flux selector negative.

is this ring and where is it located? To answer these questions, an accurate ray-tracing was done of rays incident on the axicon at various angles: the parameters considered are shown below (Fig. B1-2).

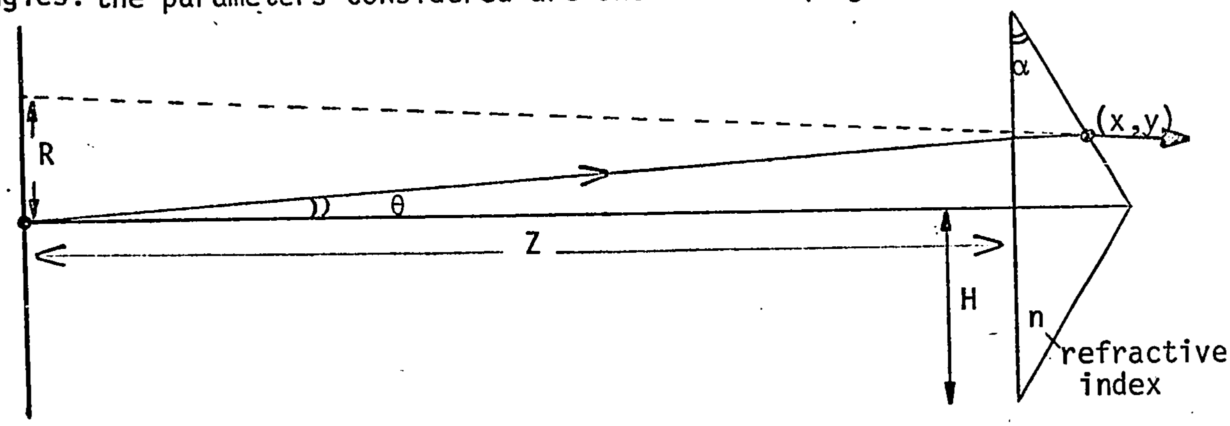

Fig. B1-2

The ray tracing was carried out for the following values of these parameters:

α = 5,10,15,20,25 Deg. $\Big\{$ H = 4,8,12 cm. $\Big\{$ Z = 2,25,75,100 cm. $\Big\{$ θ= 0,.1Θ,.2Θ, ...,Θ where $\Theta=\tan^{-1}(H/Z)$

α = 4,3,2,1,.5,.4,.3,.2,.1 Deg. $\Big\{$ H = 4 cm. $\Big\{$ " " " " " " $\Big\{$ " " "

where a bracket indicates that everything that follows was executed for each one of the parameters immediately preceding the bracket.

In Fig. B1-3 to B1-18, we give the ray tracings corresponding to H = 4 cm, and to α = 5,10,15 and 25 degrees. These ray tracings were done by an IBM Plotter, and are accurate to about the line width. The ray tracings corresponding to other values of H are very similar; Z_{max} was chosen to be 1 m. because this represents about the largest value that would be practical for the optical bench available.The ray tracings show only the virtual rays, i.e.,the dotted line in Fig B1-2.The source is located at the point O.As can be seen from the ray tracings, as α increases, for a given Z, the virtual ring plane moves closer to the axicon, the astigmatism in the virtual ring increases, and the radius of the ring increases. Note, in particular, that for any α, for small Z, the astigmatism is very large. This results from large angles of incidence encountered at low Z. This would not occur in practice (in an arrangement of the type shown in Fig. B1-1) because of the type of point source that would be used. We can say that, in a typical case, the pencil of rays diverging from the point source would have an angle of about 5^o max. (to completely cover the axicon at max. Z). Ray tracings were done for this case (i.e., pencil of rays such that axicon is completely covered with light at max. Z). For a given α, the astigmatism increases with Z, and is then max. for max. Z. (This astigmatism, as well as the exact position of the virtual ring, was determined accurately by a separate program.) Hence, with the type of arrangement above, with an infinitesimal point source, the (geometrical) width of the ring produced in the image plane of the lens would increase with the radius R, and the (geometrical) limit of the axicon method can be represented as the width of a 2 cm. radius ring produced with this arrangement; this would correspond roughly to the narrowest outermost transparent ring that could be produced . This width can be written $W_c = 2\ W(Z_{max},\alpha)\ /R(Z_{max},\alpha)$ where $R(Z_{max},\alpha)$ is the mean radius of the virtual ring produced by an axicon of angle α located at a distance Z_{max} (here 1 meter) from the point source, and $W(Z_{max},\alpha)$ is the width of this ring in its focal plane. (Note: since $W(Z,\alpha)$ (= focal dispersion, or astigmatism in virtual ring) increases with Z, it is not obvious that W_c, for a given α, would decrease with Z,i.e., would be optimum for max. Z, as we have tacitly assumed above; however, this point was verified carefully, and it is found to be so.) Calculating W_c for various values of α, it was found that W_c decreased with α down to a value of about 20μ at $\alpha=5^o$, and then remained constant with decreasing α. This behaviour can be predicted, using the small angle approximation to R stated earlier, if one assumes that the virtual ring is in the plane of the point source. This then appears to be the geometrical limit of this type of system; (in practice, it would be worse than this due to the fact that as soon as one departs from a true point source, other aberrations will be introduced by the axicon); this limit could be decreased by increasing Z_{max}, or by using a smaller pencil of rays (not completely covering the axicon at Z_{max}) but both of these modifications are impractical, and both would deteriorate the diffraction limit of this method: a 5^{o} pencil already produces a minimum point source size of about 12μ (central spot size of Airy pattern). Decreasing the angle of the pencil of rays would make this worse (increasing diameter of axicon would increase the geometrical aberration); furthermore, the diffraction at the axicon and in L_2 (Fig. B1-1) (difficult to analyze theoretically) would impose a higher limit to the width of ring which can be produced in the image plane of L_2 even with an infinitesimally small point source and an aberration-free axicon. It appears, then, as if the axicon method would be fairly limited in precision. As a result of the above facts, as well as other considerations, such as vignetting of rays emerging from the axicon, displacement of the focal plane of virtual ring with Z, etc.... which complicate the practical aspect of the problem, the axicon method was temporarily set aside.

Note: In Fig. B1-2, the axicon could have been oriented the other way, i.e., with the vertex facing the source; the ray tracing analysis was repeated with this orientation; the results, for small angles specially, are almost the same as before, and lead to the same conclusions as above.

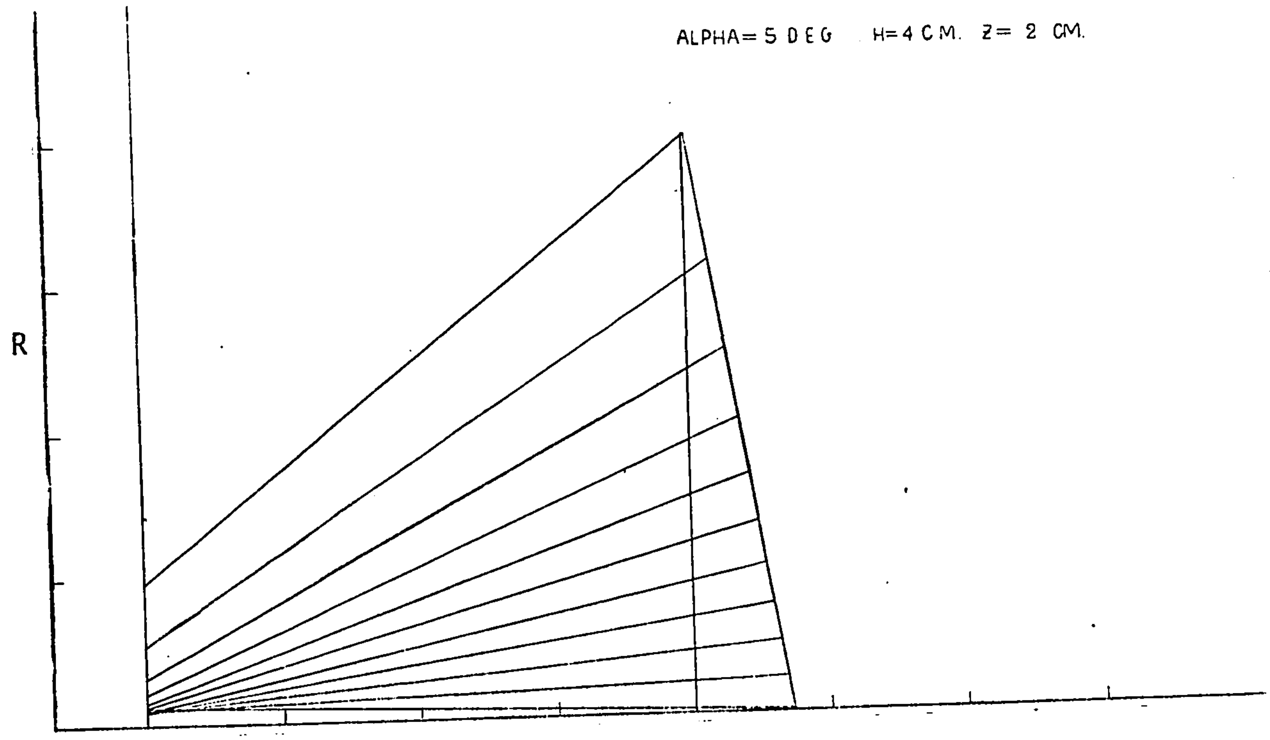

Fig. B1-3

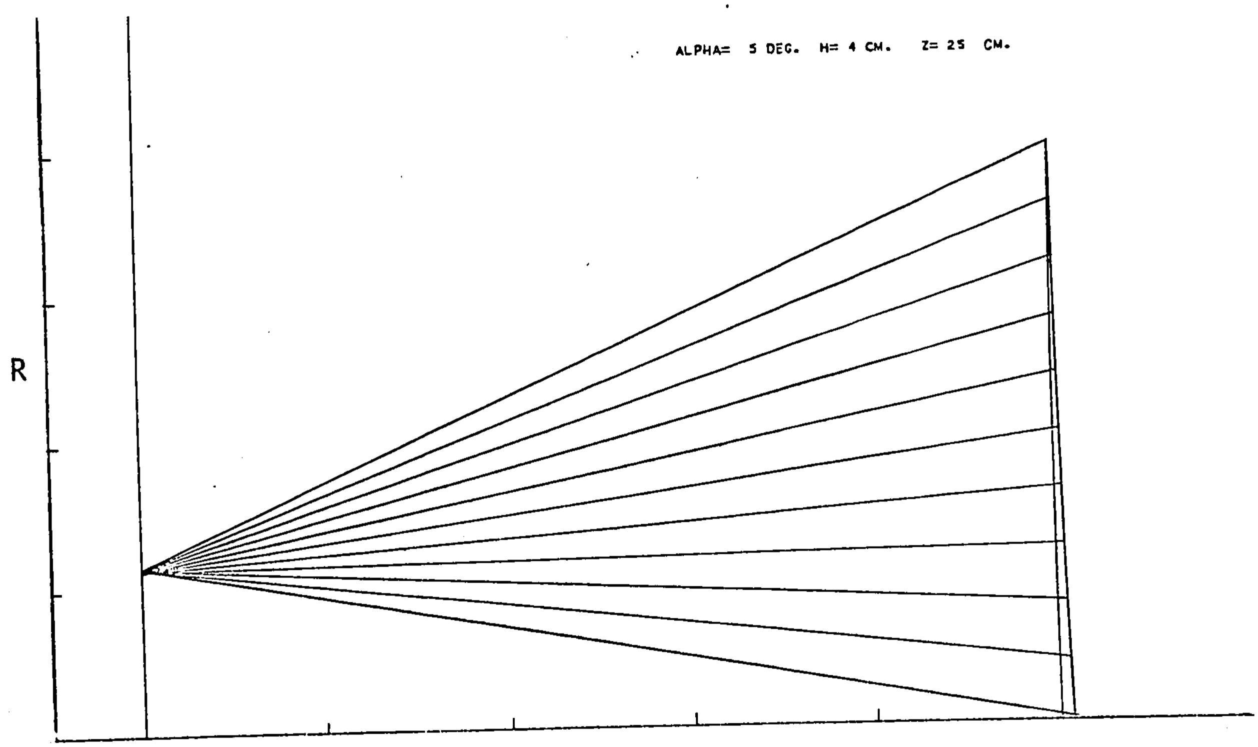

Fig. B1-4

Ray tracings for a 5 deg. axicon situated at distances of 2 cm.(B1-3) and 25 cm.(B1-4) from a point source O.R axis divisions = 1 cm.

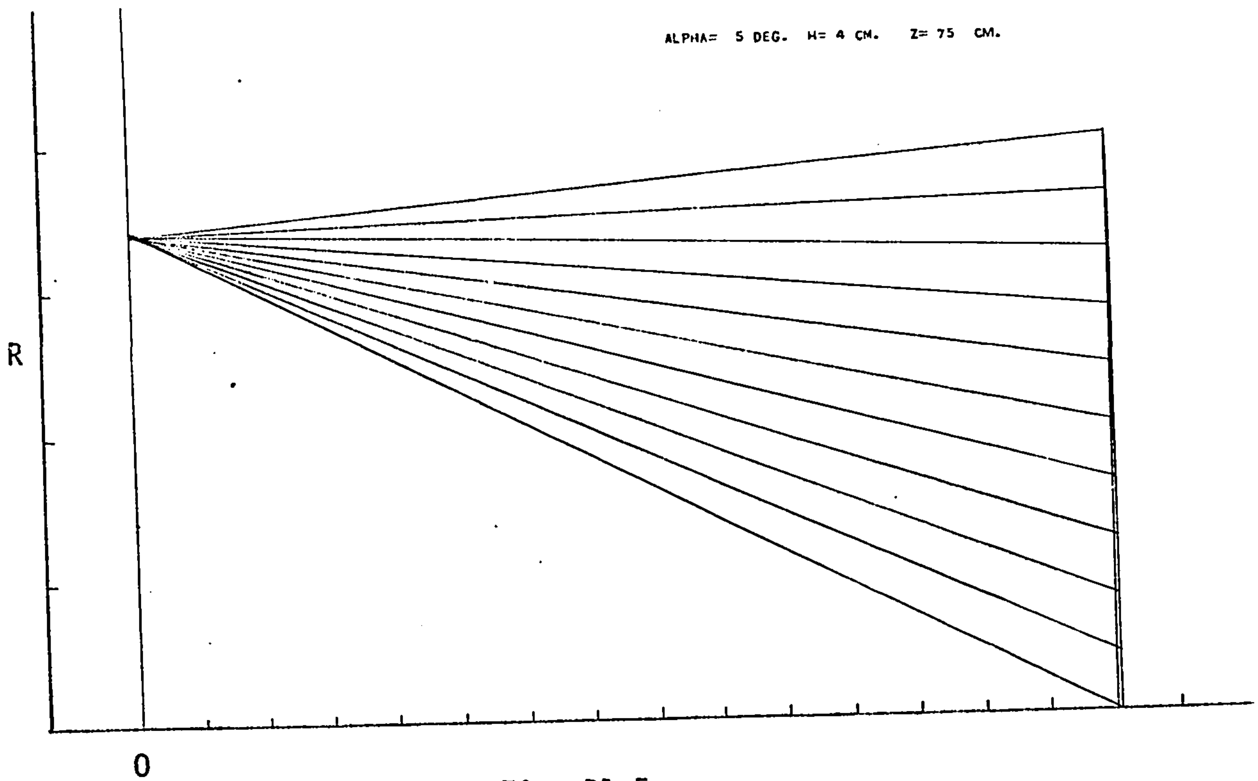

Fig. B1-5

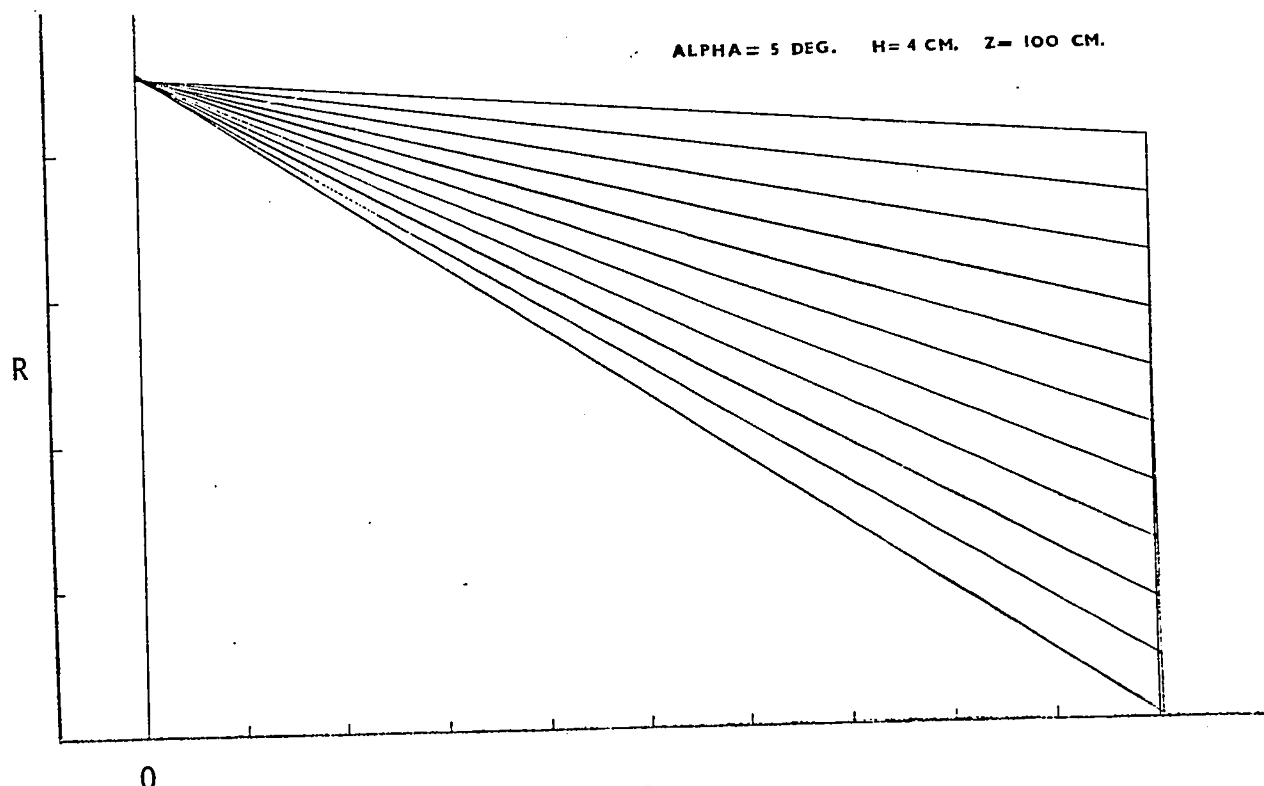

Fig. B1-6

Ray tracings for a 5 deg. axicon situated at distances of 75 cm.(B1-5) and 100 cm.(B1-6) from a point source O. R axis divisions = 1 cm.

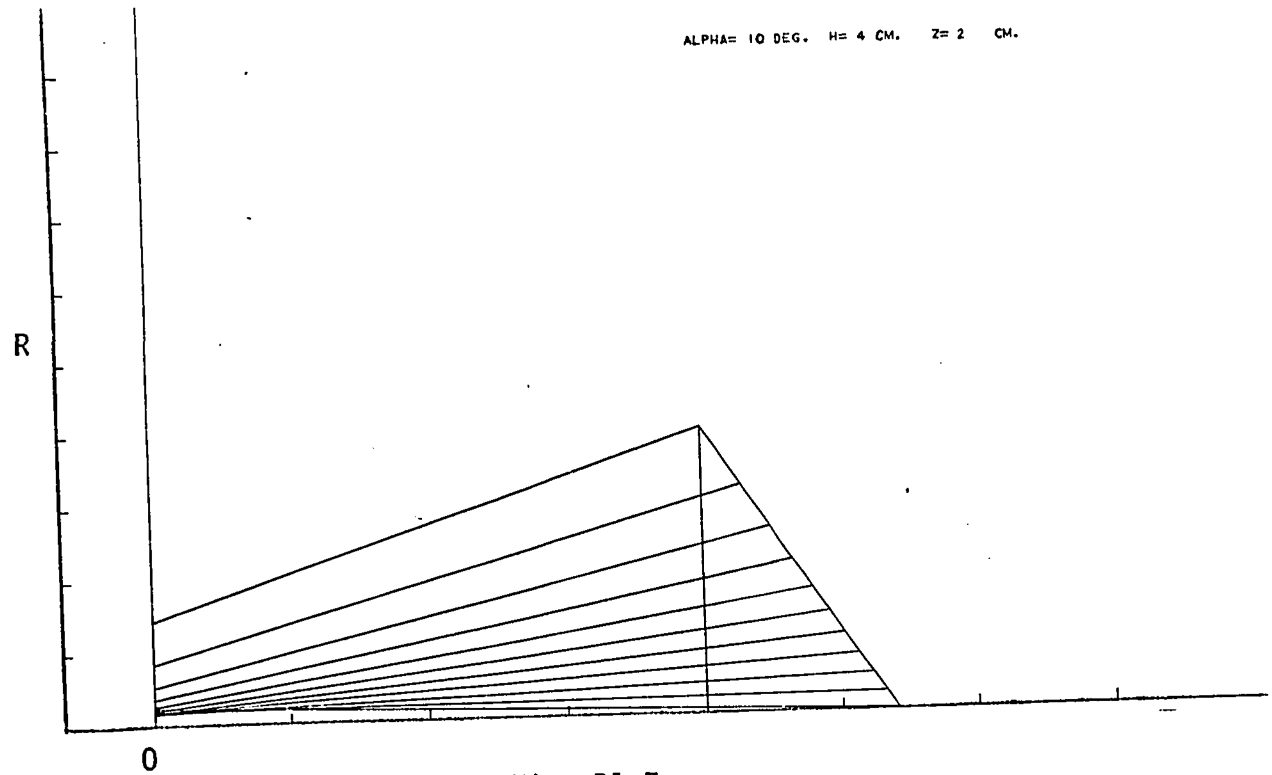

Fig. B1-7

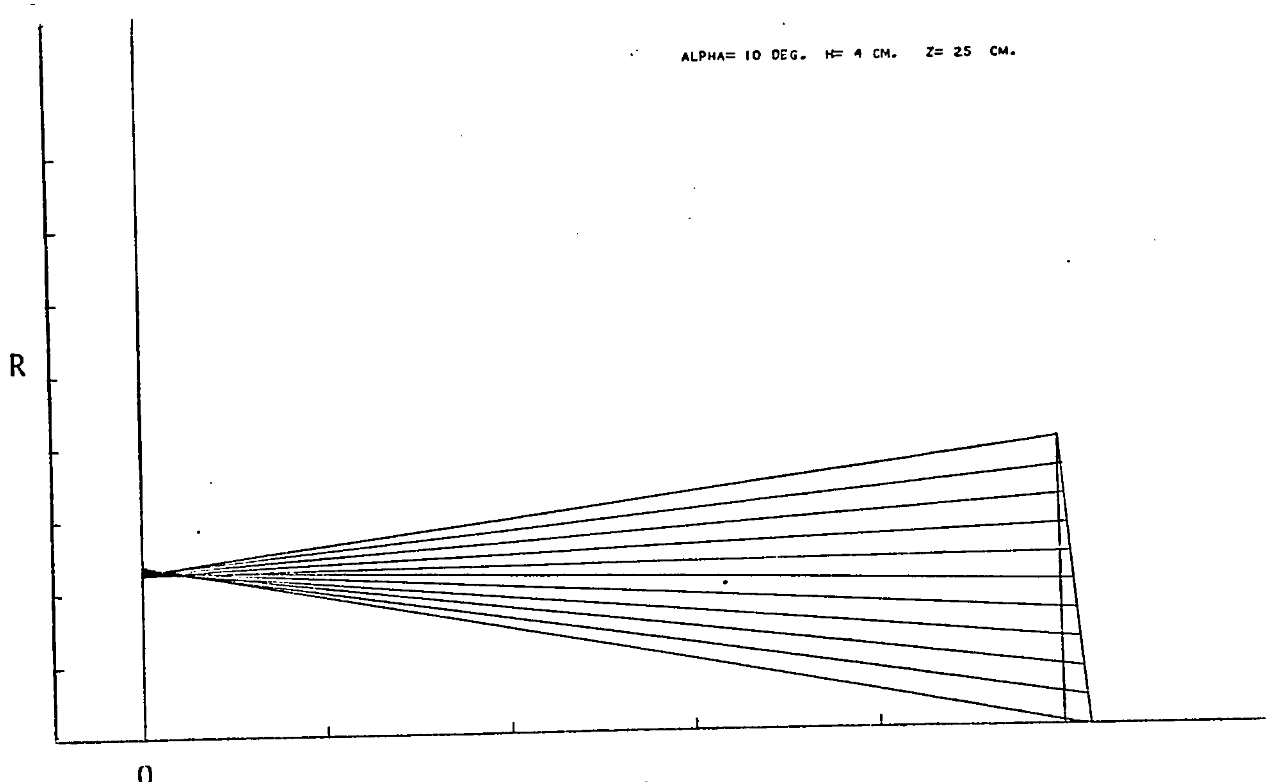

Fig. B1-8

Ray tracings for a 10 deg. axicon situated at distances of 2 cm.(B1-7) and 25 cm.(B1-8) from a point source O. R axis divisions = 1 cm.

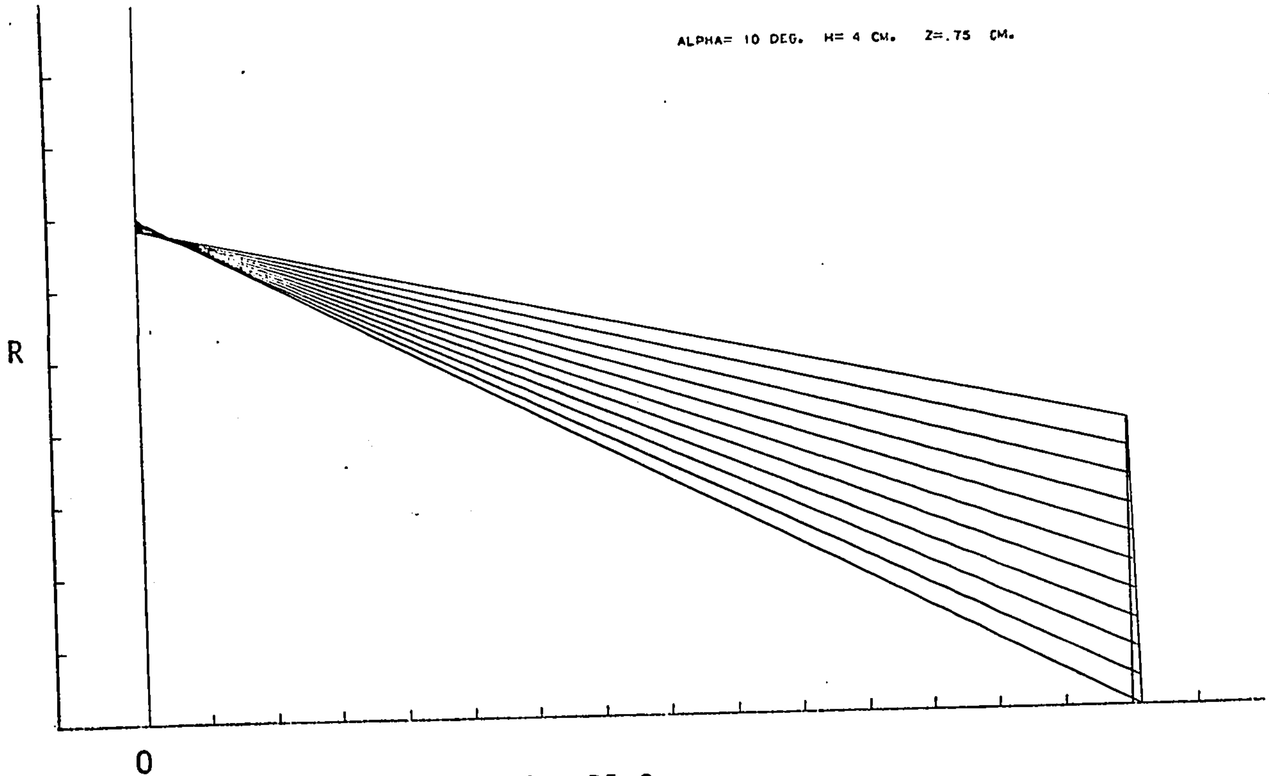

Fig. B1-9

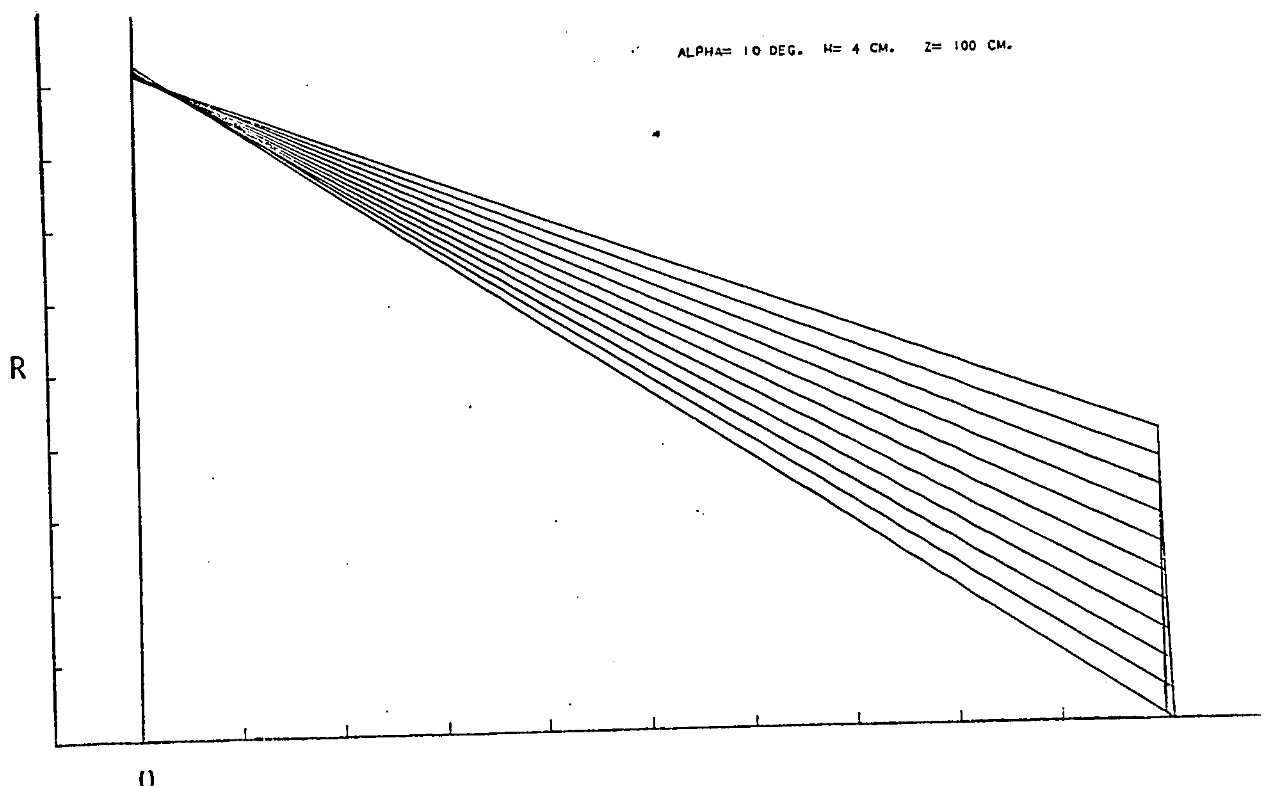

Fig. B1-10

Ray tracings for a 10 deg. axicon situated at distances of 75 cm.(B1-9) and 100 cm.(B1-10) from a point source 0. R axis divisions = 1 cm.

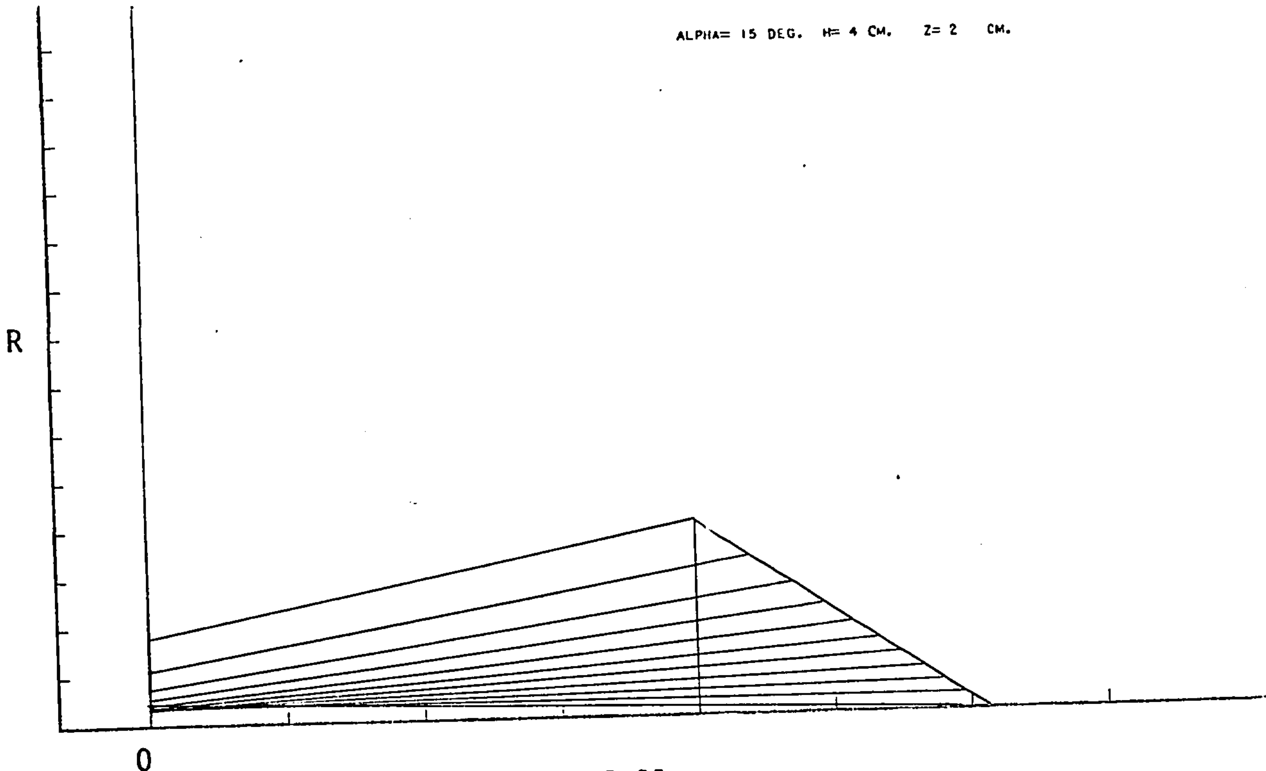

Fig. B1-11

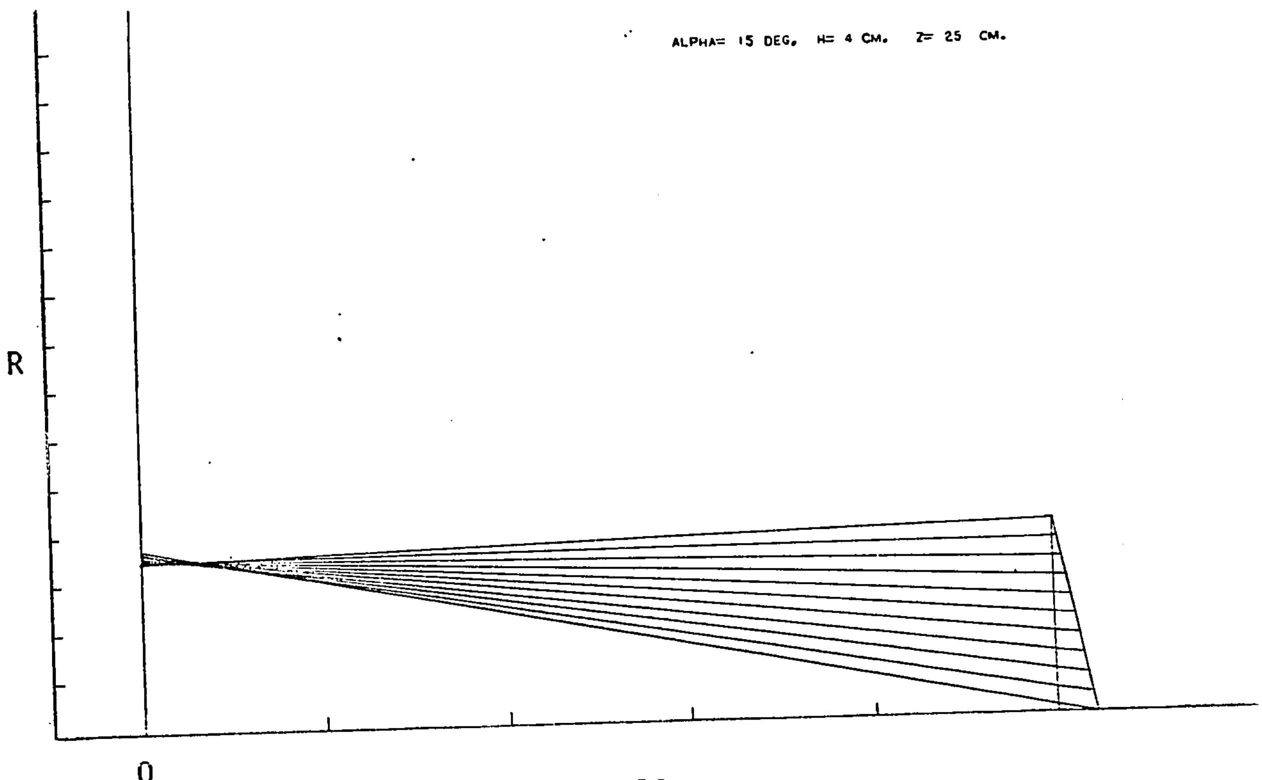

Fig. B1-12

Ray tracings for a 15 deg. axicon situated at distances of 2 cm.(B1-11) and 25 cm.(B1-12) from a point source 0. R axis divisions = 1 cm.

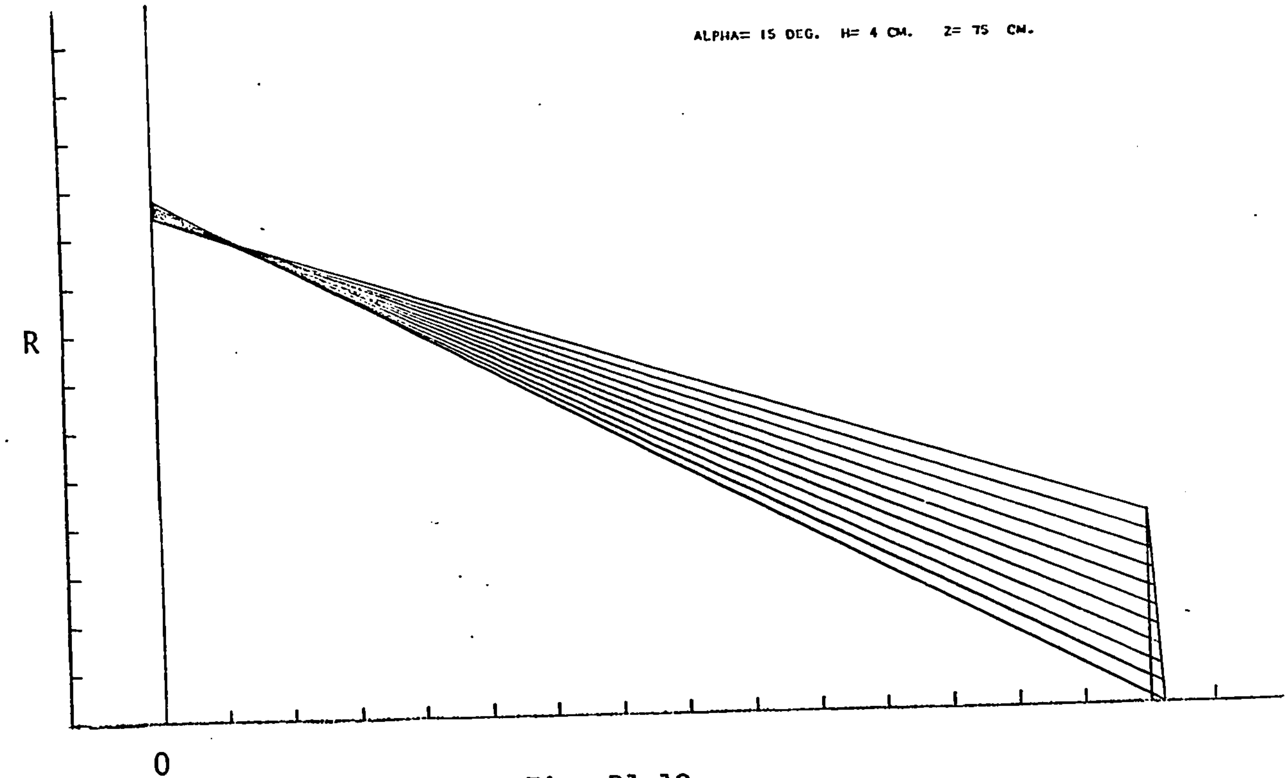

Fig. B1-13

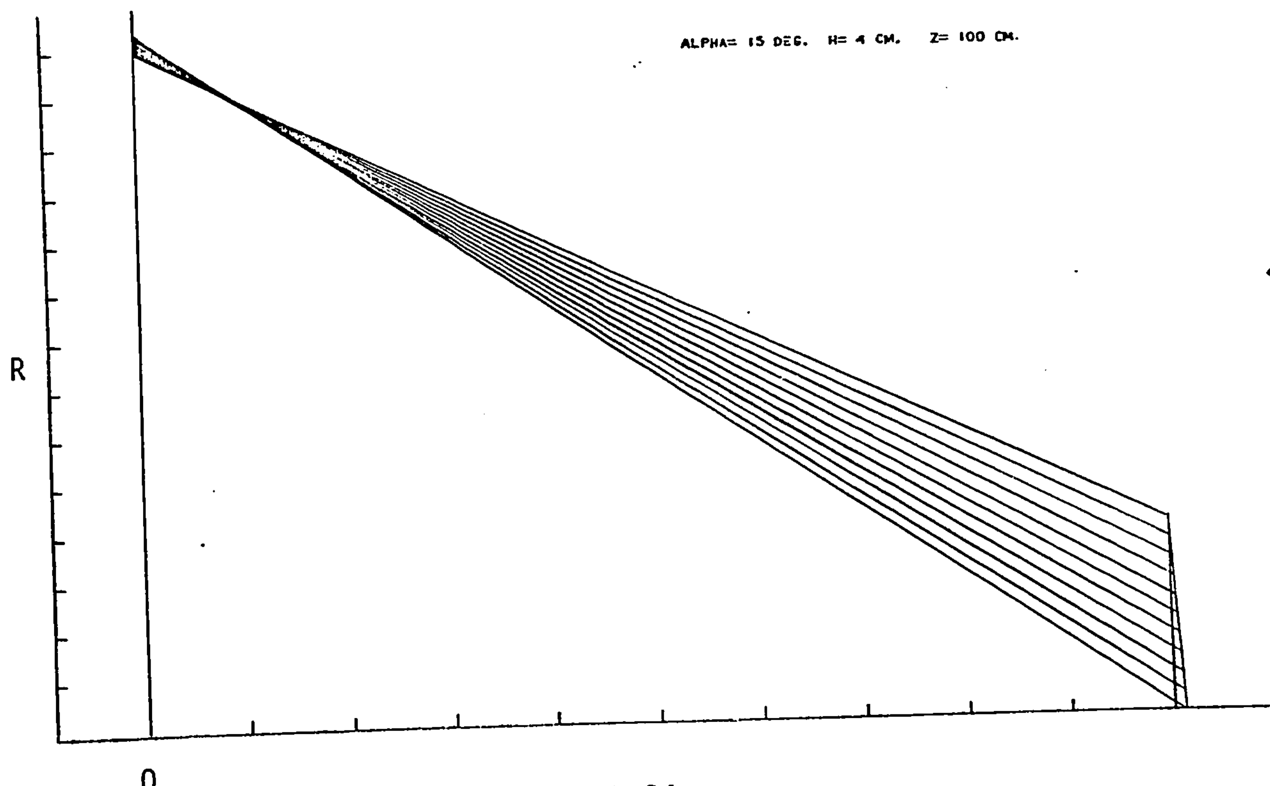

Fig. B1-14

Ray tracings for a 15 deg. axicon situated at distances of 75 cm.(B1-13) and 100 cm.(B1-14) from a point source O. R axis divisions = 1 cm.

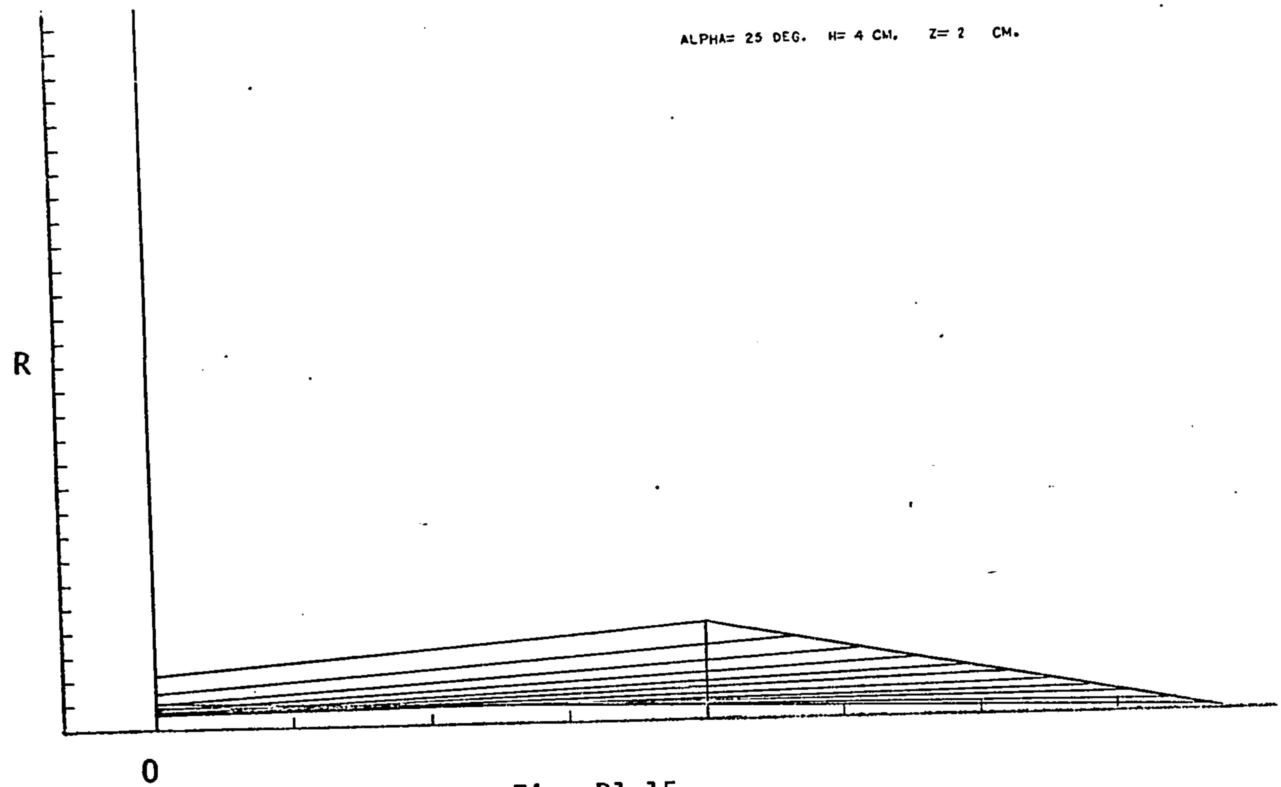

Fig. B1-15

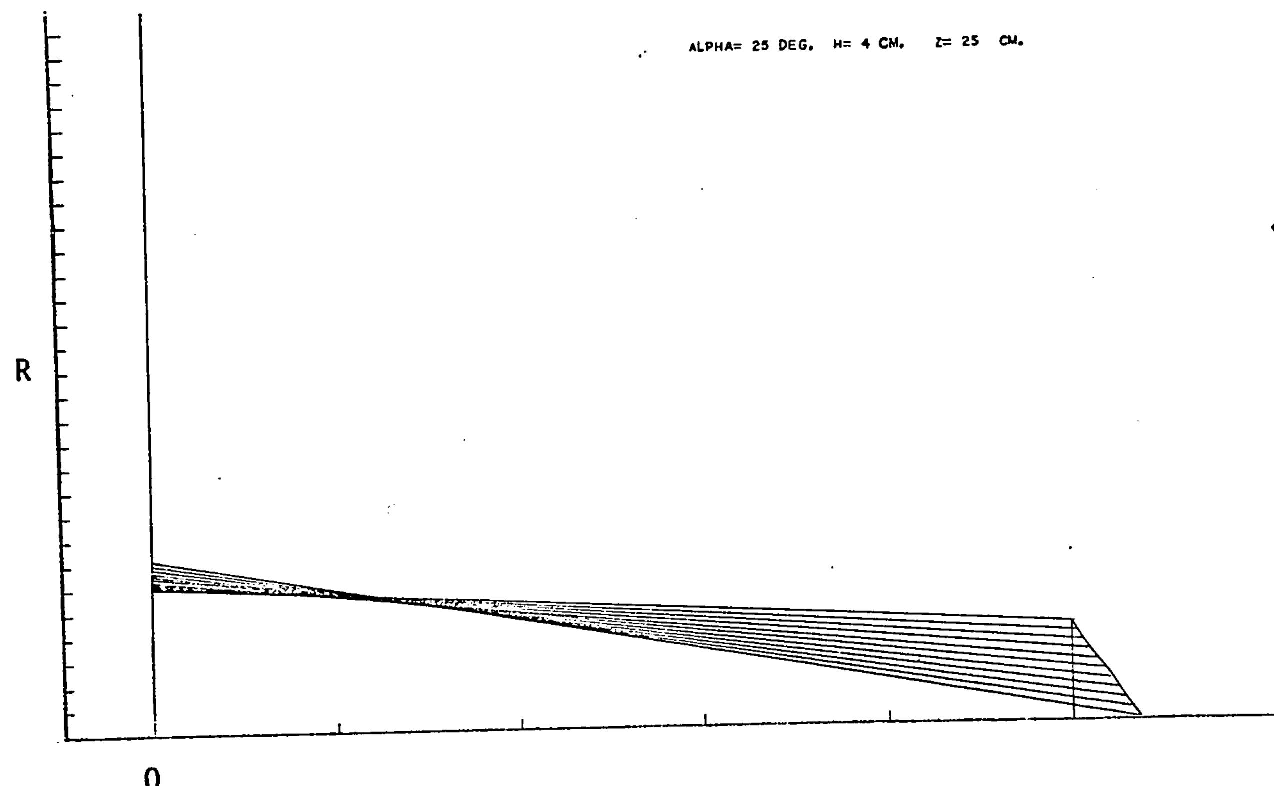

Fig. B1-16

Ray tracings for a 25 deg. axicon situated at distances of 2 cm.(B1-15) and 25 cm.(B1-16) from a point source 0. R axis divisions = 1 cm.

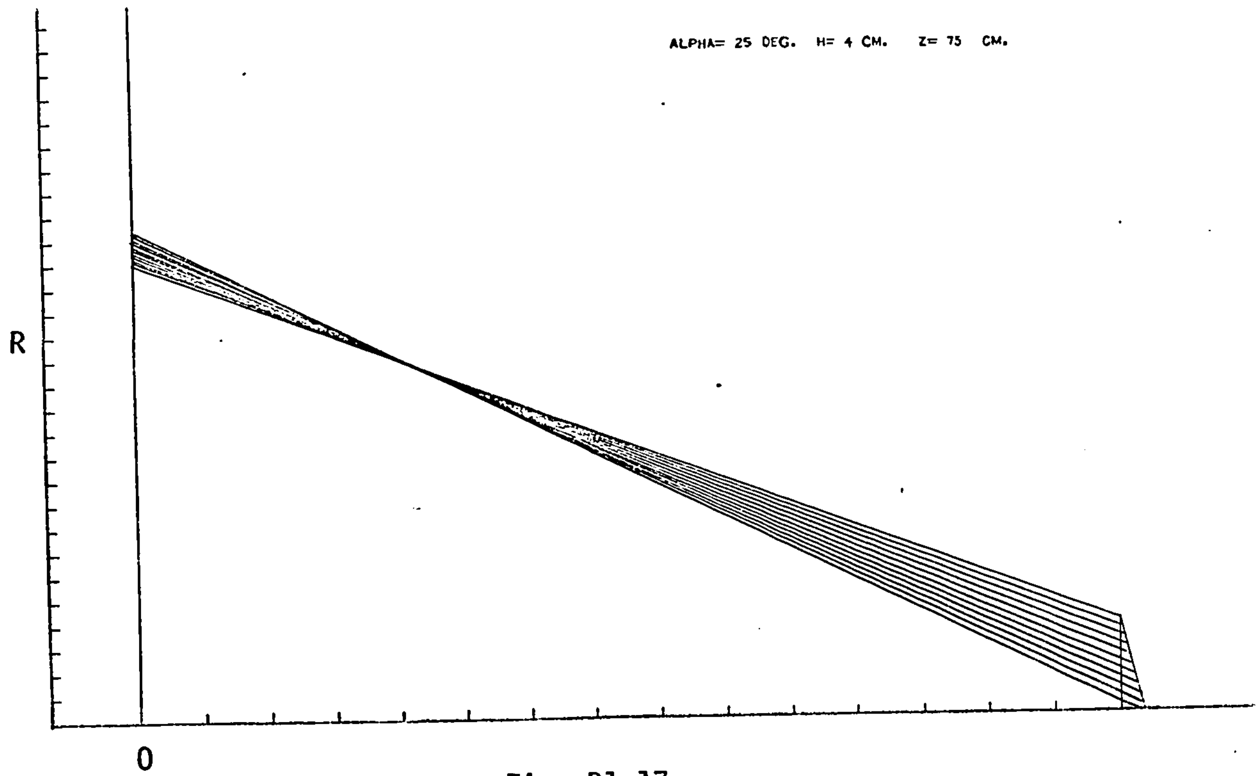

Fig. B1-17

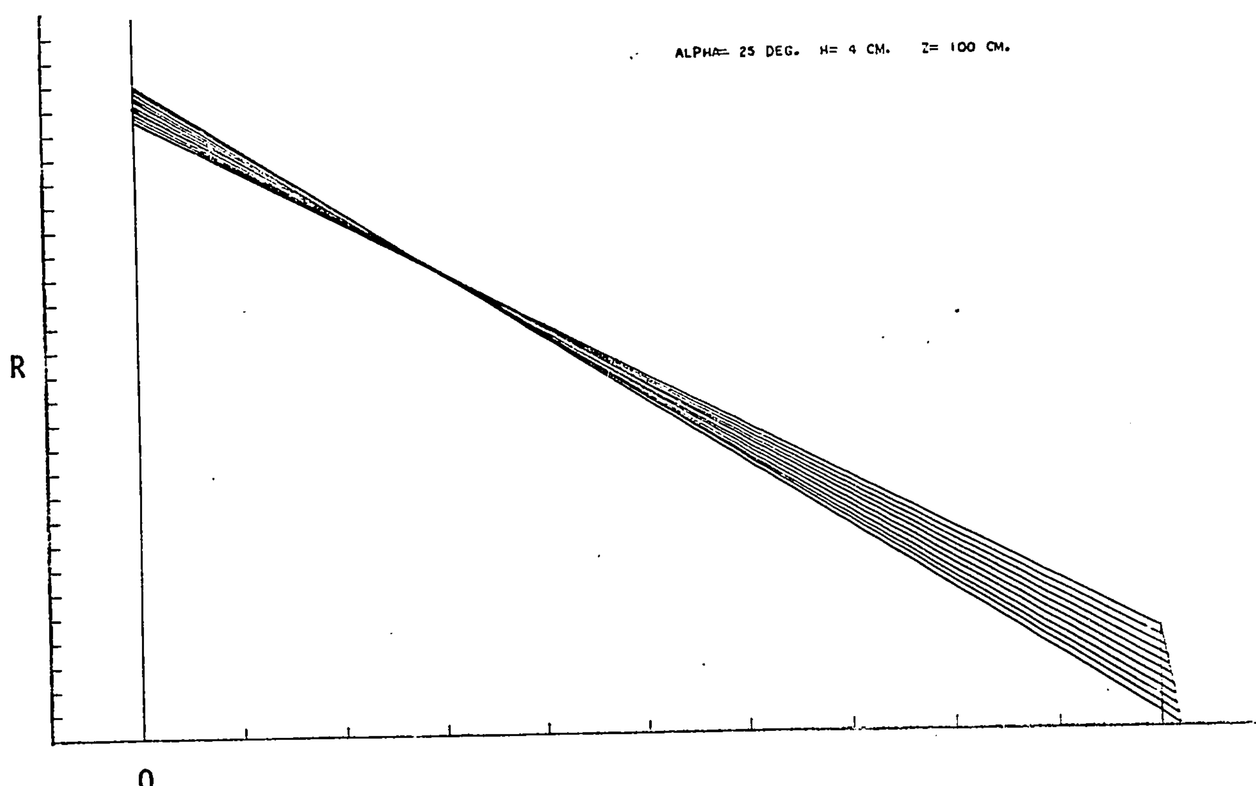

Fig. B1-18

Ray tracings for a 25 deg. axicon situated at distances of 75cm.(B1-17) and 100 cm.(B1-18) from a point source 0. R axis divisions = 1 cm.

(b) Photographic Reduction:-

This method can be summarized as follows: a large scale model (positive) of the desired flux selector is cut into a lucite plate which is photographed (with the proper reduction) onto a high resolution plate to produce the required mask negative. (See fig. B1-19 for a schematic diagram.) At first glance, this method seems quite simple, but a closer inspection reveals many difficulties.

(1) Construction of the lucite (plexiglass) model:-

The high precision desired in the flux selector requires a reduction ratio of about 10:1 since with the lathes available, the tolerance on the widths of the rings cut into the lucite plate would be on the average 25 microns (i.e. .001"). Hence, the lucite flux selector has to be about 40 cm in diameter. For preliminary work, a lucite model (10:1) of flux selector 11(1a-B2-H) was made. The grooves (opaque rings) were about .030" deep and filled with black paint: painting the grooves was necessary because the de-polishing effect produced by the tool does not make the grooves sufficiently opaque for the photographic process, even when using high contrast plates. The results obtained with this lucite model were unsatisfactory: the fact that the grooves were relatively deep caused a sort of shadow effect on the rings which, when photographing the work, introduced a systematic error in the radii of the rings on the negative: the resulting error in the ring widths increased from about 0 at the center to about -7 to-10 microns at the edge. In order to avoid this error, the following lucite flux selectors were cut with the minimum groove depth possible (about

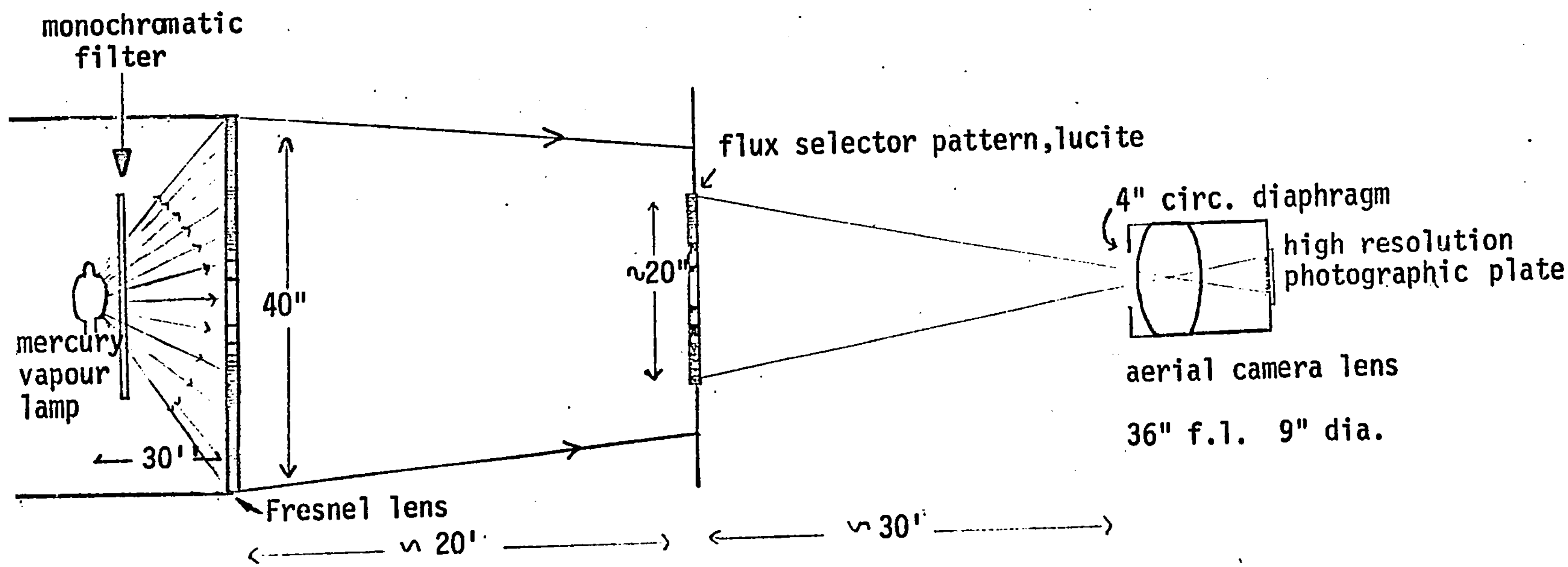

Fig. B1-19 Schematic diagram of the photographic reduction method for making the flux selector negative.

.005"). This measure was effective, but it complicated the construction because it imposed severe tolerances on the flatness of the pieces of lucite used, and it also rendered the filling of the grooves with black paint much more difficult.

For our experimental work, we have decided to make flux selectors of the type 49(1B-A4-H) corresponding to the amplitude filters T(x,5) and T(x,M). A brief inspection of the ring radii of these two F.S.'s (tables A5-24 and A5-25) shows that the opaque rings at the center are very narrow. Since narrow grooves are very difficult to cut, and since the opaque rings at the center do not affect the diffraction patterns very much, we have decided to delete opaque rings at the center so as to simplify the construction. The number of rings to be deleted was determined as follows: the difference between the extrema of amplitude in the diffraction pattern formed by the flux selector and those of the diffraction pattern formed by the same flux selector in which successively 1, 2, 3, etc... opaque rings are deleted was calculated: the maximum number K of rings which can be thus deleted without introducing a difference greater than 10^{-3} (central region) or 10^{-4} (intermediate and far regions) in the diffraction patterns was thus determined and the flux selector was constructed with K opaque rings deleted at the center. For the flux selector corresponding to T(x,5), K was found to be 5, whereas it was found to be 9 for that corresponding to T(x,M).

(2) <u>Optical system used for photographic reduction</u>:

We require a lens which will:

(a) form an image free of distortion within 1 or 2 microns over a surface

4 cm in diameter.

(b) have a depth of focus of at least 50 microns: it is essential that the image be correctly focussed throughout the thickness of the photographic emulsion; although the latter has a thickness of only 4 microns, the glass plates themselves are flat to about 10 microns per cm; hence, for an image 4 cm in diameter, the depth of focus should be at least 50 microns. The focal tolerance for an aberration-free lens is about $2\lambda F^2$ (F= F number). Hence, we should have a nominal focal ratio of at least F7. Note that, in addition, the lens should form an image flat to at least 25 microns (in a 2 cm radius) in order to ensure proper focussing everywhere on the photographic plate.

(c) On the other hand, the larger the F number, the more diffraction limited the system becomes. Therefore, we must keep the F number as low as possible compatible with the considerations in (b).

(d) Assuming an uniformly illuminated object, the illuminance in the image plane will vary roughly as $\cos^4\theta$, where θ is the angle which a point in the image subtends at the center of the lens with respect to the optical axis. To minimize this variation, one requires a relatively long focal length lens.

The above considerations have led us to choose a 36" focal length, 9" diameter, 7 component aerial camera lens, with a 4" diameter diaphragm in the entrance pupil. (See fig B1-20 for a photograph of the lens). Observations have shown that the image formed by such a lens is distortion free and flat over a suitably extended range in the image plane, and has a depth of focus of at least 100 microns; however, the large size of the lens has introduced other difficulties, which we shall now briefly discuss.

First, because of the 10:1 reduction, the object-image distance is almost 33 feet, and over such a distance, air turbulence can introduce distortions in the image. To avoid this, the optical system was set-up in a temperature controlled tunnel. Then comes the problem of optical alignment: the F.S. lucite model must be mounted exactly perpendicular to the optical axis of the lens and centered with respect to it: failure to satisfy this requirement introduces distortions in the image, as shown in appendix A. An accurate method of alignment was found to be the following: a small laser is mounted on a tripod about 40 feet away from the lens (on the object side), and the beam allowed to fall on the entrance lens. There are many beams of light reflected by the lens, corresponding to the different components of the lens. The laser beam was adjusted so as to coincide with the optical axis of the first component lens: the latter reflects two beams of light, and when the laser beam coincides with the optical axis, these two beams overlap and produce a set of Newton-like interference fringes whose center is on the axis. The fringes are viewed in the exit window plane of the laser. After this adjustment is made, the lucite F.S. is mounted in front of the lens, at the proper distance from it (33 feet). Its position is adjusted so that the laser beam passes through its center, and is reflected back upon itself. The F.S. was thus adjusted so as to be centered on the optical axis to within about 1 mm and normal to it to within about 1/10 of a degree.

Fig. B1-21 Optical system used for making the flux selector negative by photographic reduction of a large scale model.

Fig. B1-20 Aerial camera lens,front view: the 4" diaphragm shown is placed in front of the lens to reduce aberrations and increase the depth of focus.

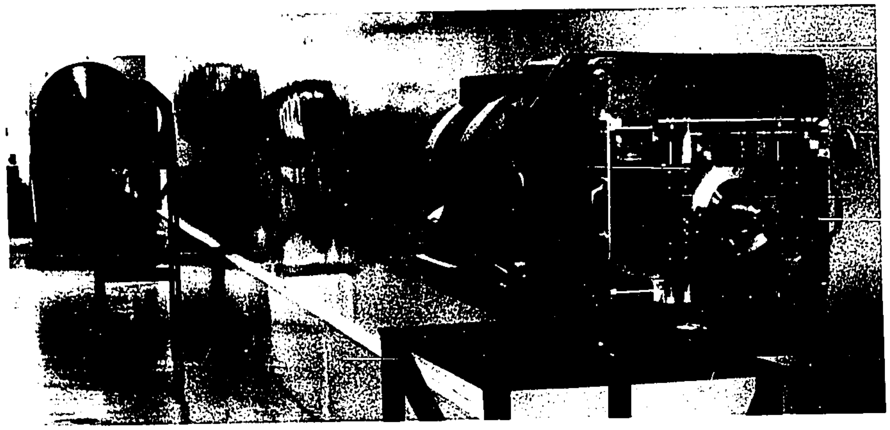

Fig. B1-21 Optical system used for making the flux selector negative by photographic reduction of a large scale model.

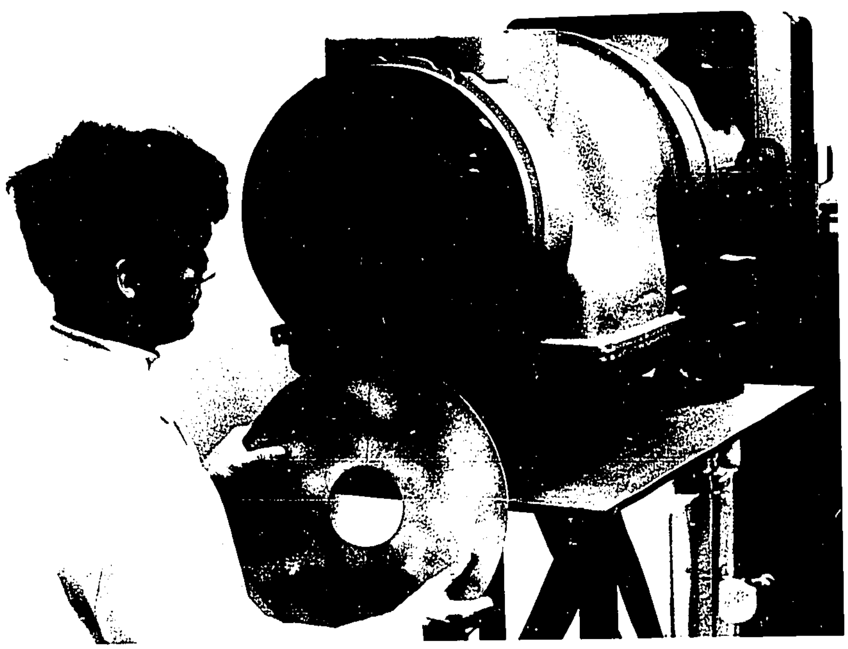

Fig. B1-20 Aerial camera lens, front view: the 4" diaphragm shown is placed in front of the lens to reduce aberrations and increase the depth of focus.

It would seem at first glance that the optical system used would give poor edge definition in the image due to diffraction: the Airy pattern formed by the lens has a central disc of 13 microns in diameter. However, because of the type of photographic plates used, the actual precision achievable is about 1 or 2 microns.

(3) Photographic plates used:

The plates chosen were 2" x 2" Kodak High Resolution plates (.060" thick, standard grade flatness). The principal reasons for this choice were:

(a) They have extremely high contrast (gamma = 10 typically): this eliminates troublesome secondary reflections in the lens; also, it allows the photographic image to have sharper edges than those in the aerial image (where diffraction causes an intensity gradient at the edges).

(b) They have extremely fine grain: this is necessary in order to have edges as sharp and smooth as possible in the negative.

(c) They have extremely high resolution (about 2,000 lines per mm): this is necessary in order to obtain good image quality with images having line widths as small as 15 microns (and ultimately as small as 4 microns).

On the other hand, these plates have one serious disadvantage: they have a very low sensitivity. Their A.S.A. speed is .025 (compared to 125 for Plus-x Pan, for example). Hence, an intense light source is required to illuminate the object (see next section). Focussing of the aerial image on the emulsion of the plates is done as follows: a special plate holder was built which incorporates a removable x and y travelling microscope and which is mounted on the lens back.Fig. B1-22 (a) and (b) shows the lens back without and with the travelling microscope attachment

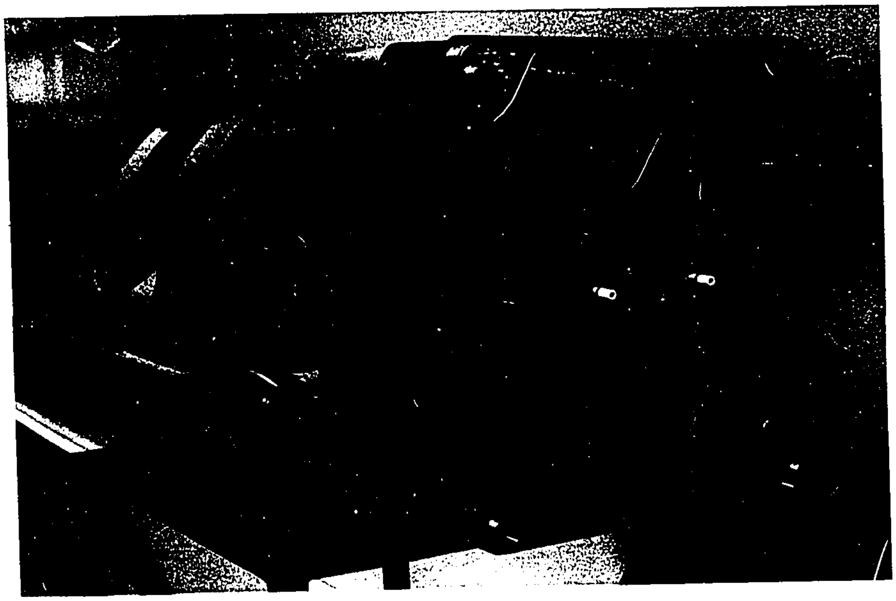

(a)

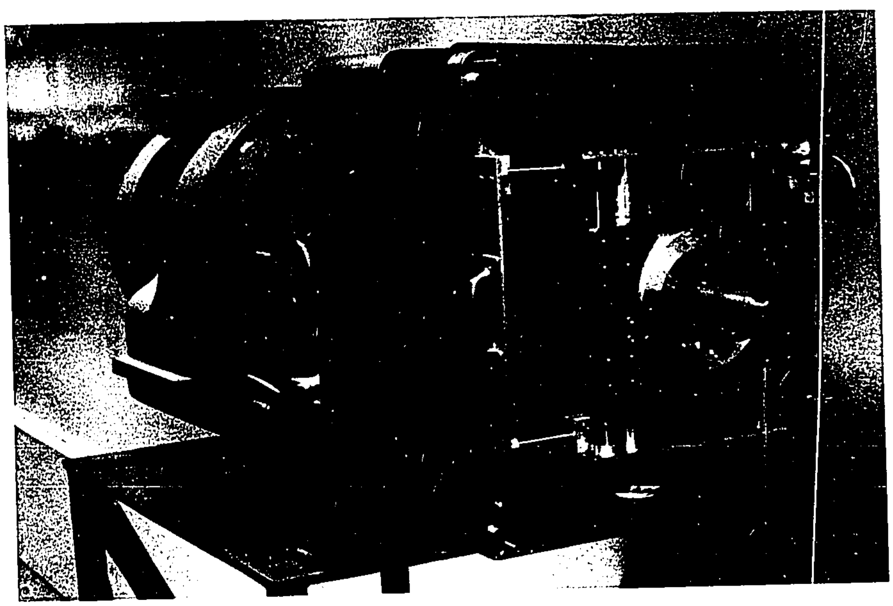

(b)

Fig B1-22 Aerial camera lens:back view,showing (a) the photographic plate holder and (b) the removable x-and-y travelling microscope.

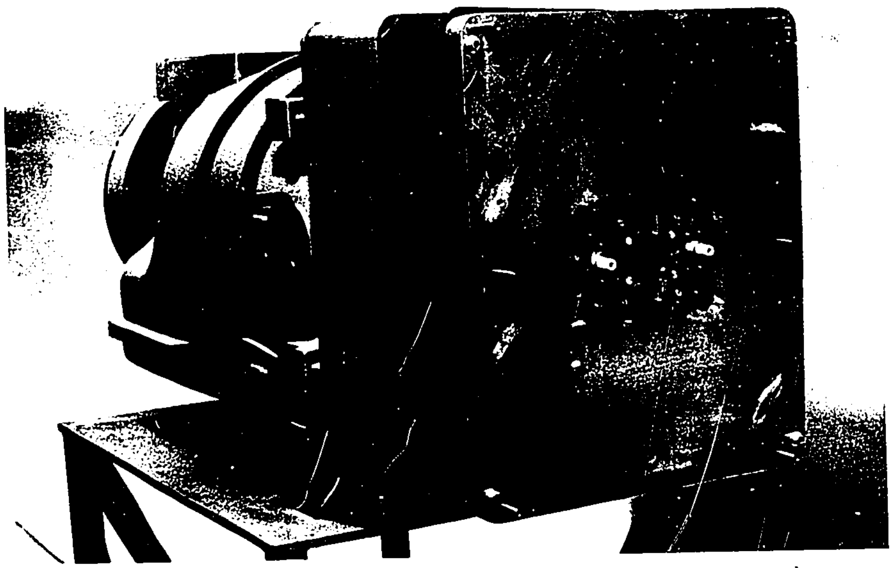

(a)

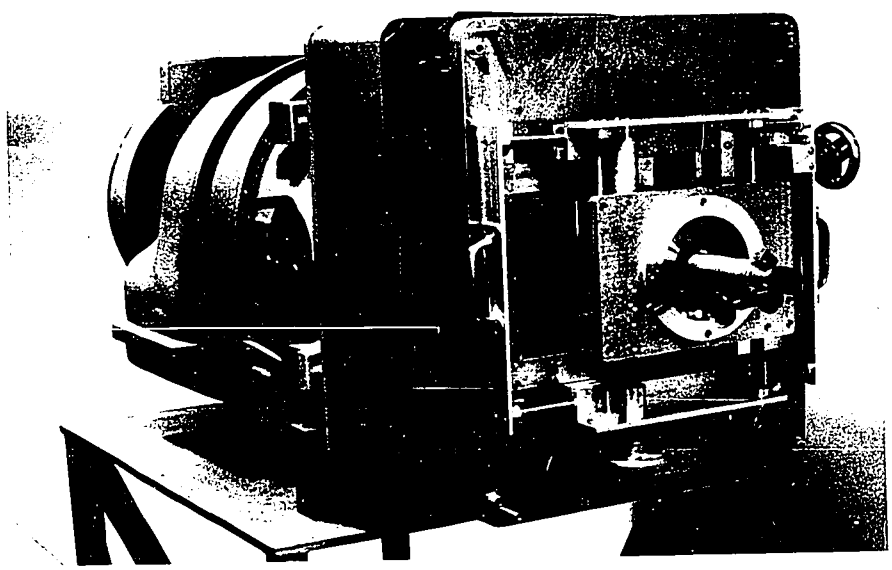

(b)

Fig B1-22 Aerial camera lens:back view,showing (a) the photographic plate holder and (b) the removable x-and-y travelling microscope.

respectively. A grid network has been ruled in the emulsion of a high resolution plate, which is mounted in the plateholder, emulsion side towards the lens. By means of the travelling microscope, the image is viewed at 100x and the lens moved forward or backwards to bring the image in coincidence with the grid network. The travelling microscope is then displaced along the x axis to see if the image remains in the same plane as the grid everywhere. If not, the plate holder is tilted in the proper direction, and the procedure repeated until the focussing is good all along the x axis. The procedure is then repeated along the y axis. To take a photograph, the focussing grid is replaced by a photographic plate.

(4) Light source:

From the foregoing discussion, it is evident that an intense light source is required; it also has to be monochromatic in order to eliminate chromatic aberrations in the lens. Such a light source was built and can be described as follows: a 700 watt mercury lamp is located on the optical axis of a 30" focal length, 40" diameter Fresnel lens, whose purpose is to condense the light onto the lucite pattern. The lamp is mounted on a series of movable platforms which allow the lamp to be moved horizontally, vertically, and along the axis in order to center the beam on the aerial camera lens. A monochromatic filter consisting of Wratten No. 77 and No. 58 10" x 10" filters is used to isolate the green line at 5461 Å: this line was chosen because it is the most intense one emitted by the lamp, and the sensitivity of both the human eye and the high resolution plates are almost maximum at this wavelength. A 20" diameter shutter, which can be operated by remote control, is interposed between the Fresnel lens and the lamp. The lamp and filter are cooled by means of three fans, two of which have the specific task of cooling the heat sensitive filter assembly; the latter is further protected by a thermoregulator which automatically turns off the lamp if the filter overheats. The lamp house is completely enclosed, i.e., no air is exhausted from the housing by means of fans or chimneys: such streams of air could cause unwanted turbulence in the air, whereas natural convection from the whole surface of the lamp house would not have a tendency to do this. Fig. B1-23 (a) and (b) shows photographs of the lamp house.

The lamp house is located about 15 feet behind the lucite pattern: it is not placed closer than that in order to produce a more uniform illumination in the image plane of the aerial camera lens. Fig B1-21 shows a photograph of the optical system used for photographic reduction. The beam of light emerging from the lamp house is centered on the optical axis of the system as follows: a small cross-like diaphragm is mounted in front of the lamp, and centered on the optical axis of the Fresnel lens. The position of the lamp is adjusted so that the latter is also centered on the optical axis of the Fresnel lens. The lamp house is displaced horizontally and vertically so that the image of the Fresnel lens be centered on the optical axis of the aerial camera lens in the image plane of the latter. The lamp plus cross-diaphragm are then displaced along the axis of the Fresnel lens so that the primary image of the cross be formed in the entrance pupil of the aerial camera lens. The lamp house is then tilted horizontally and vertically so that the cross image be centered on the entrance pupil of the lens. This completes the adjustment of the lamp house.

In the image plane of the aerial camera lens, the illumination produced by the above system is not uniform: it is maximum at the center and falls off to about 60% at the edge of the image. In order to correct this, a rotating sector was mounted between the shutter and the Fresnel lens to compensate for the intensity variation. (This rotating sector is not shown in Fig. B1-23.See Fig.B1-24 for a schematic diagram). Since the exposure time is of the order of 3 to 4 minutes, a speed of rotation of about 100 rpm was sufficient. The shape of the sector was determined empirically as follows: starting with a tear shaped sector, and with the lucite flux selector removed from its holder, a photograph was taken of the illumination field in the image plane of the aerial camera lens. The processed plate was not uniformly darkened, but showed a variation in density which parallelled the variation in intensity in the image plane. The plate was scanned with a densitometer to determine quantitatively the variation in intensity. The sector was then trimmed accordingly, and the process repeated until the uniformity of the illumination was deemed satisfactory (i.e., a variation of 10 to 15% max., with the high intensity point in the intermediate region). The photographic plates used for this work were 2" x 2" Kodak projector slide plates (medium contrast type). These plates are blue sensitive and, thus, although they are much faster than high resolution plates when exposed to tungsten light, they are of comparable speed when exposed to 5461 Å radiation. Thus, they had a suitably long (about 2 min.) exposure time for the rotating sector to be effective. The characteristic curve for these plates was determined by exposing a plate through a 5461 Å interference filter and a photographic step tablet to a uniform

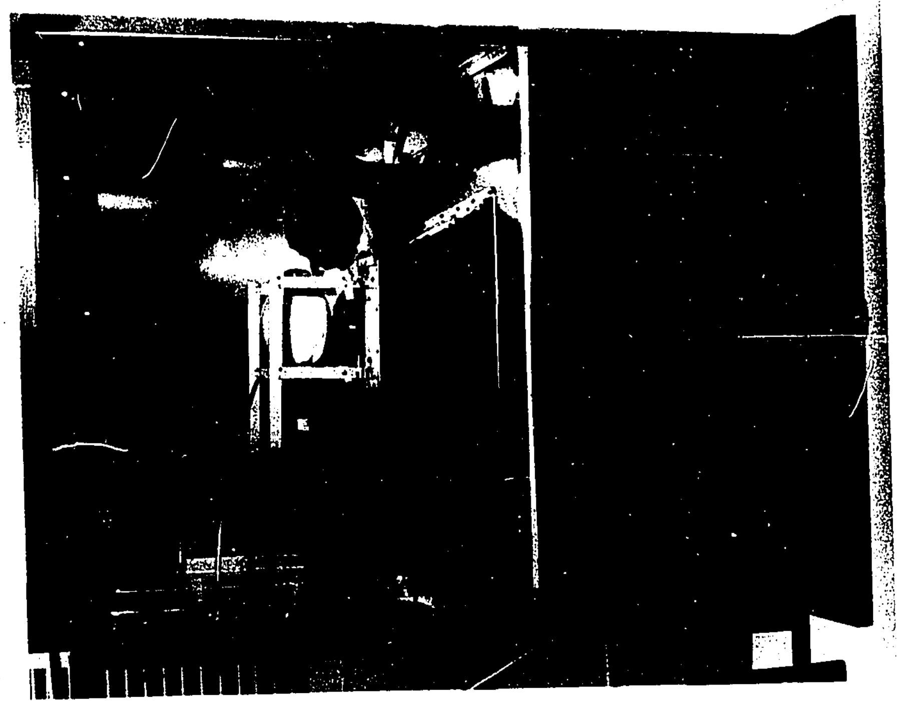

(a)

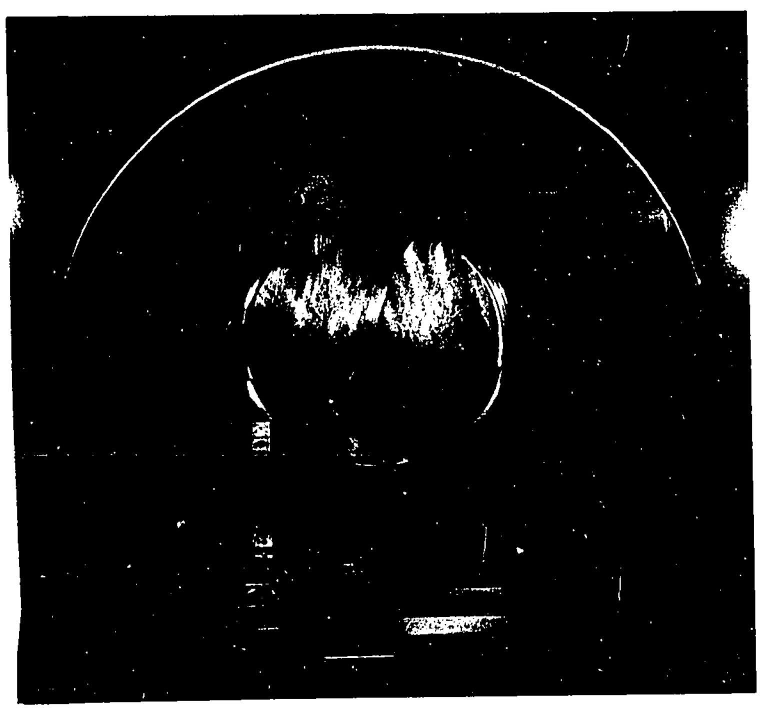

(b)

Fig. B1-23 Light source used in the photographic reduction method for making the flux selector negative: (a) Side view (b) Front view (Fresnel lens removed)

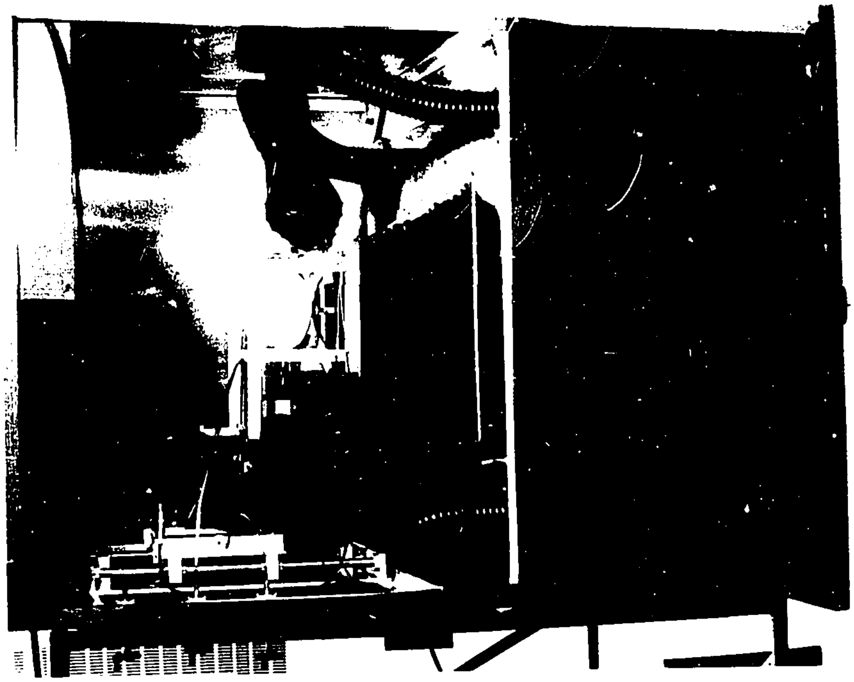

(a)

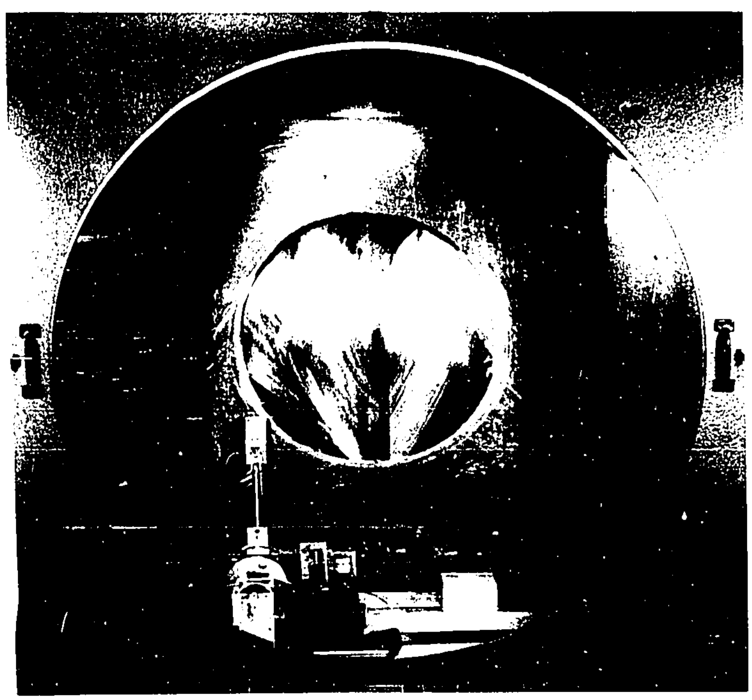

(b)

Fig. B1-23 Light source used in the photographic reduction method for making the flux selector negative: (a) Side view (b) Front view (Fresnel lens removed)

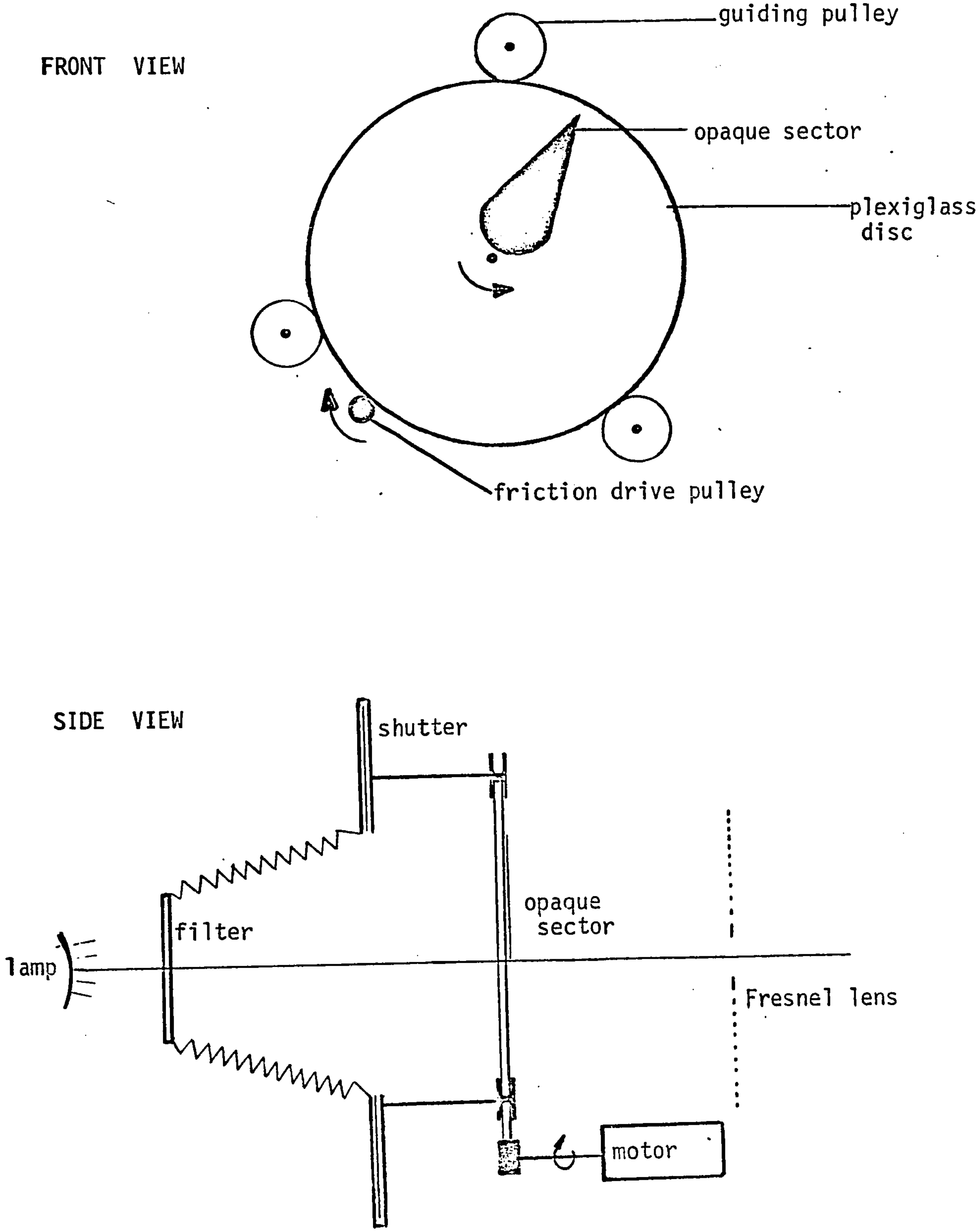

Fig. B1-24 Schematic diagram of the rotating sector used in the lamp house.

collimated beam; the plate was then processed, and scanned with a densitometer. From the density vs exposure data thus obtained, the characteristic curve, hence the gamma (= 2.3) was determined.

(5) Measurements on the negatives:

The flux selector negatives produced by the above method required exposure times of about 4 minutes (with rotating sector) and were processed as recommended by Kodak. Measurements were made on these negatives (using a Jena comparator) in order to compare the actual ring radii and widths with the theoretical values. The measurements were done as follows: The position of the negative on the comparator table was adjusted so that the scan axis coincided with a diameter. The negative was then firmly clamped, and the positions of all the edges of the rings carefully measured as the negative was scanned from one side to the other. The measurements were reproducible to 1 micron or better. This data was then processed by an IBM program, which computed the inner and outer radii and the width of each ring. The program also calculated the center corresponding to the inner and outer edge of each ring: this is necessary in order to check that the rings are truly concentric. Before being compared to the theoretical values, the ring radii were normalized with respect to the outer radius of the last ring, because the reduction ratio of the aerial camera lens was not exactly 10, but was about 9.95. The above measurements were made along two mutually perpendicular axes. These measurements have shown that the negatives produced had the following precision:

a) Ring radii (inner and outer): ±1 micron in general, ±2 microns maximum.

b) Ring widths: ±1 micron in general, ±2 microns max.

c) Concentricity: ± 1 micron maximum from the mean center.

d) Ellipticity: 1 to 2 microns difference between the major and minor axes.

The worst imperfection in the negatives consists of the small defects due to occasional dust particles or small scrapes or scuffs on the lucite flux selector, which are reproduced on the negative. However, it is felt that these defects have a negligible effect on the diffraction patterns formed by the flux selectors. In Fig. B1-25 (a) and (b) are shown prints made from the flux selector negatives.

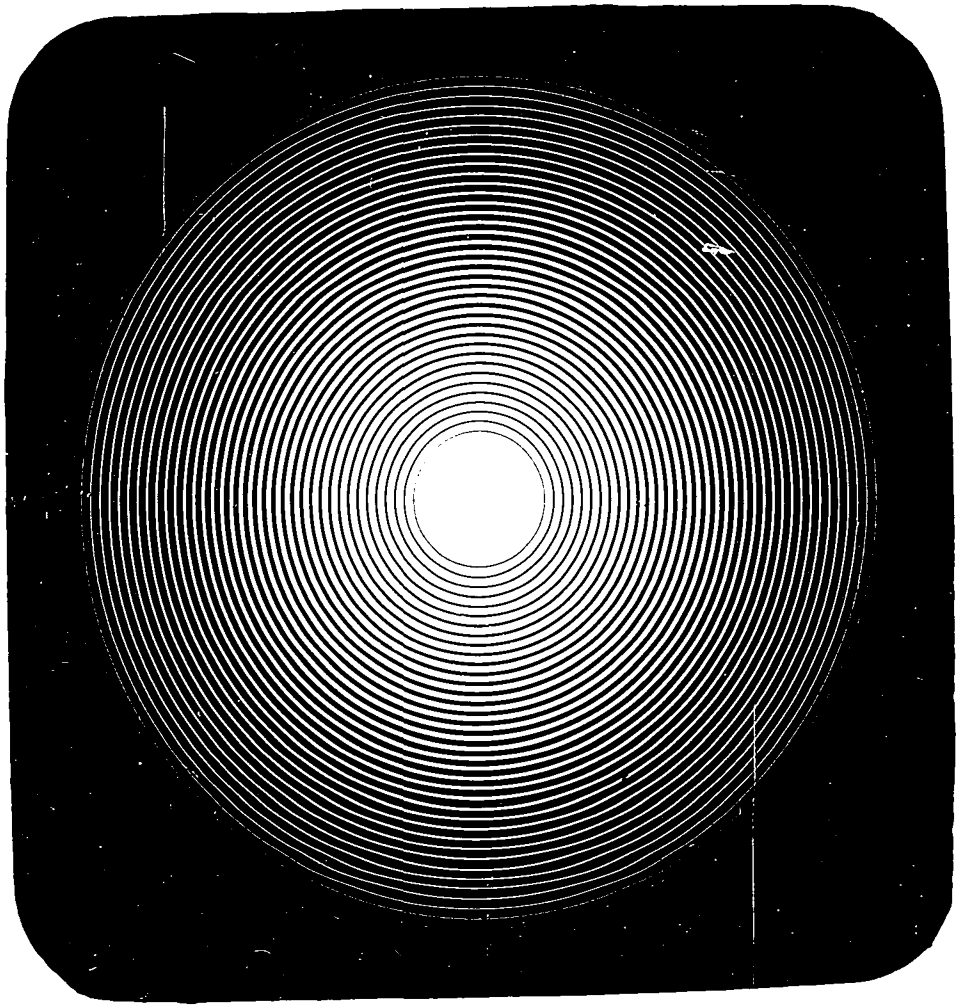

(a) Flux selector 49(1b-A4-H) corresponding to the amplitude filter T(x,5),and having 5 opaque rings deleted at the center.The F.S. is shown at 3 times the actual size.

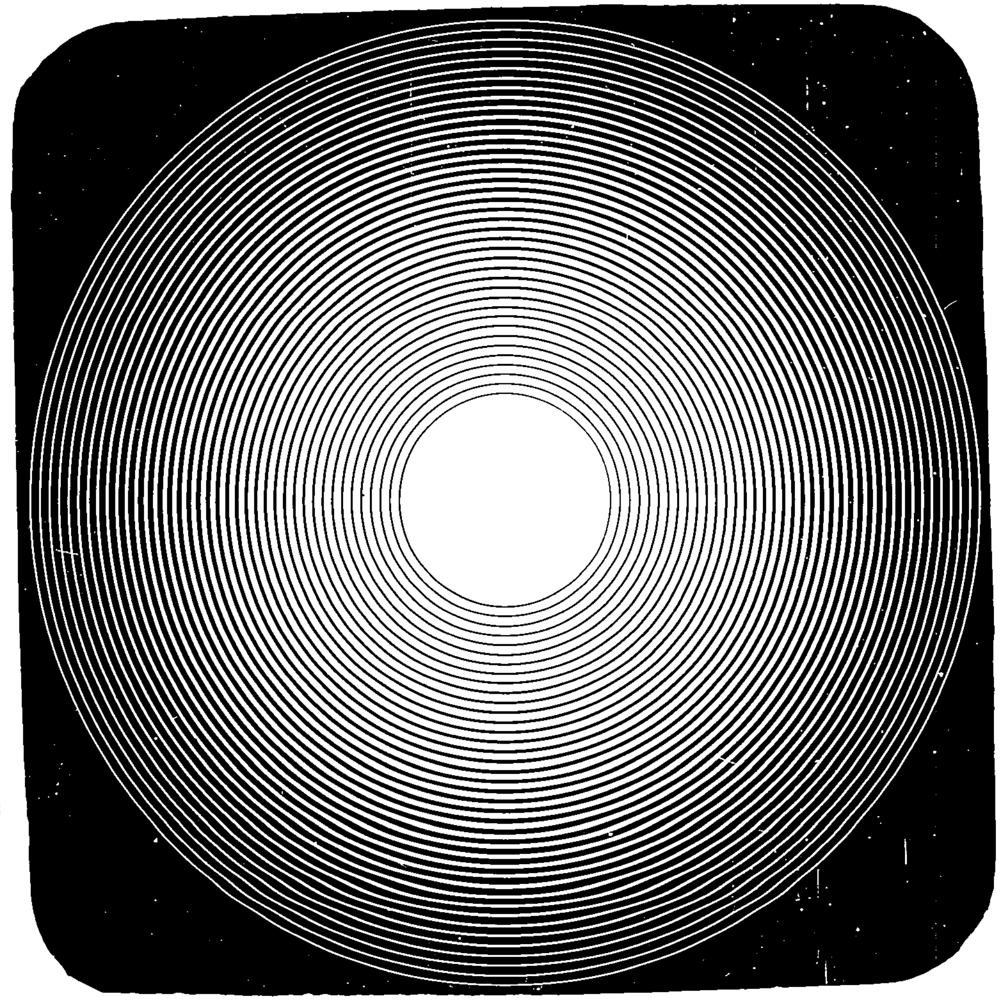

(b) Flux selector 49(1b-A4-H) corresponding to the amplitude filter T(x,M),and having 9 opaque rings deleted at the center.The F.S. is shown at 3 times the actual size.

Fig. B1- 25

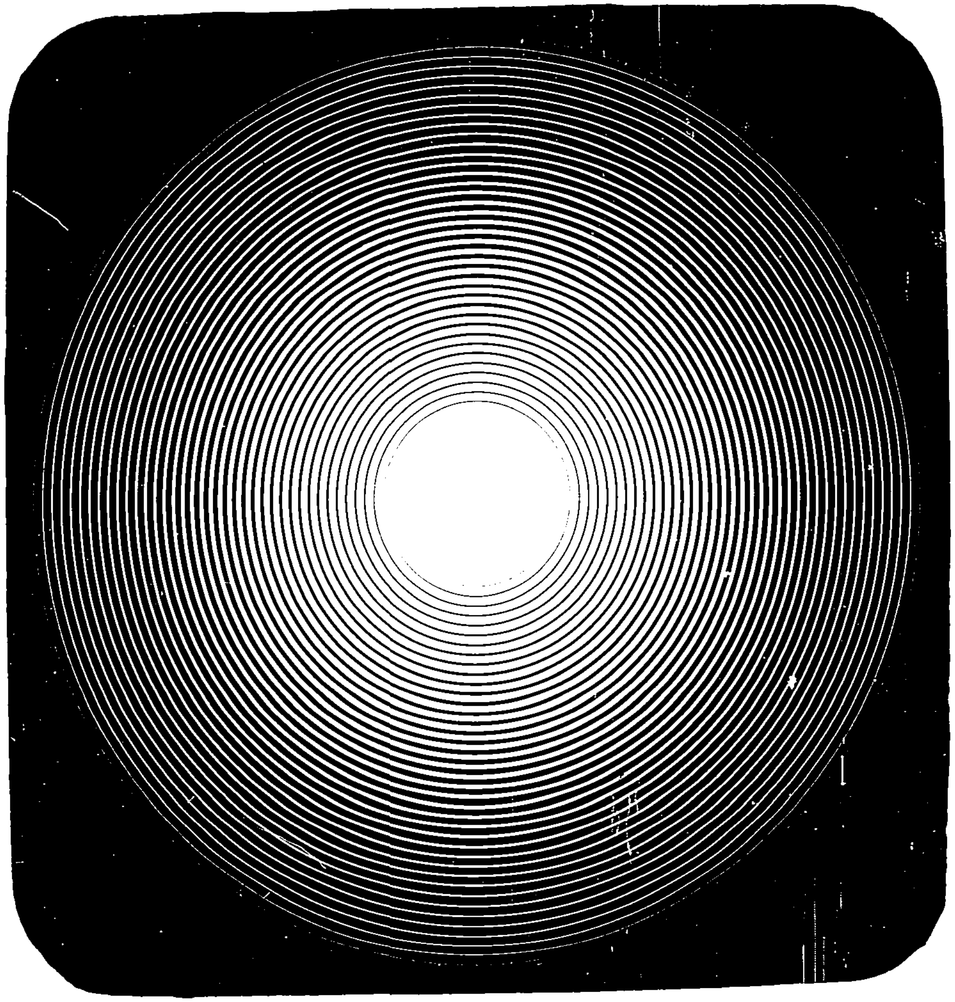

(a) Flux selector 49(1b-A4-H) corresponding to the amplitude filter T(x,5),and having 5 opaque rings deleted at the center.The F.S. is shown at 3 times the actual size.

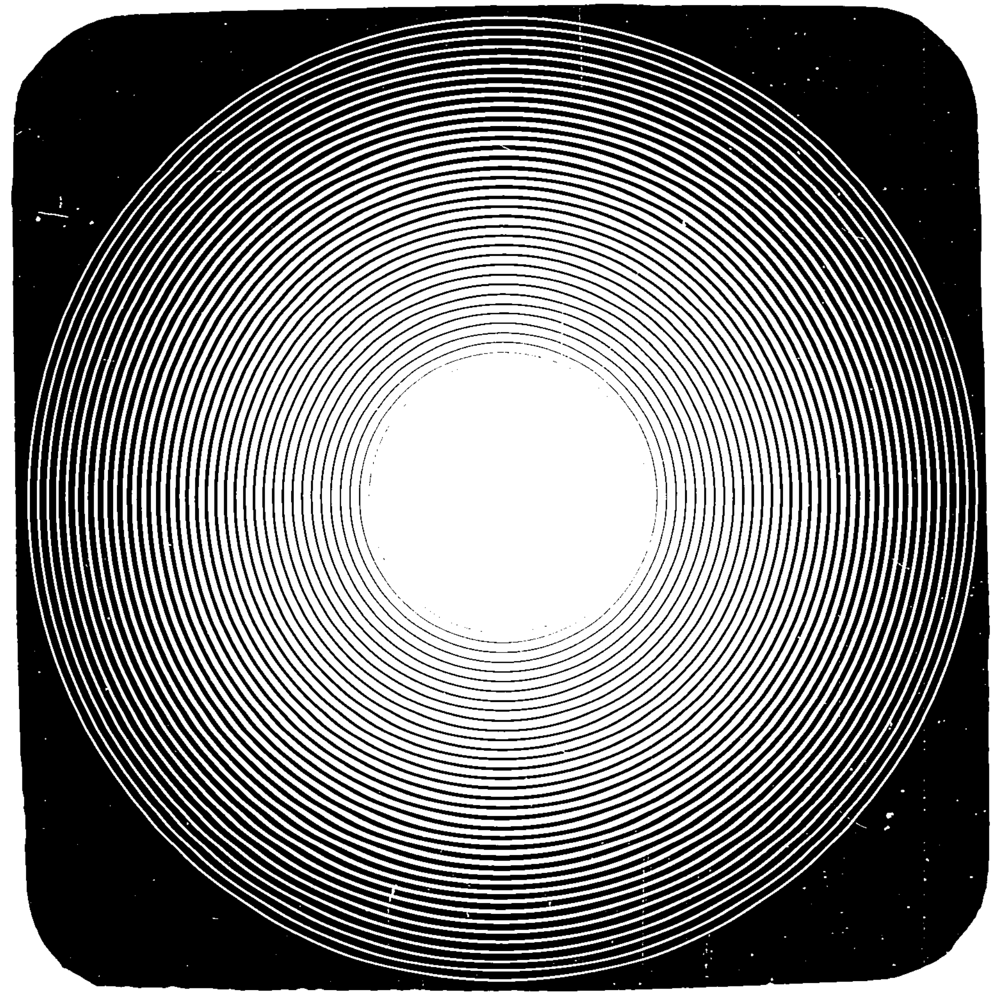

(b) Flux selector 49(1b-A4-H) corresponding to the amplitude filter T(x,M),and having 9 opaque rings deleted at the center.The F.S. is shown at 3 times the actual size.

Fig. B1- 25

CHAPTER 2

PHOTO-ETCHING PROCESS

The photo-etching process, as we have outlined earlier, consists (for our work) essentially of 5 steps: coating the plane side of a plano-convex lens with a thin metallic layer; coating this metallic layer with a thin layer of photo-etching emulsion; contact printing the flux selector negative onto this emulsion layer; developping the latent image of the flux selector thus formed in the emulsion and then etching the work. This procedure will now be described in detail.

(1) Coating the work with a metallic layer:

The metallic layer is to be deposited on the lens by evaporation in a vacuum. What metal should be used? In order to answer this question, we must first list the desirable properties of the metallic layer.

a) It must be tough, optically thin, uniform, opaque, and free of pinholes.
b) Ideally it should be black in order to minimize the reflections inside the lens.
c) It must be easily etched, and the etching solution should not damage the surface of the lens.

The metals most commonly used for this type of work are chromium, aluminum, and copper. Of these, chromium yields the toughest layer, but because of its relatively high melting point, it is much more difficult to obtain a suitably uniform and opaque layer, free of pinholes. Because of this, we have rejected it for our work.

Aluminum and copper both give layers which are thin (circa 500 Å), uniform and opaque, and which can be made virtually free of pinholes if special precautions are taken. The layers are also suitably resistant to abrasion for the type of treatment they are subjected to. Apparently, evaporated films of these two metals cannot be chemically blackened without damaging, or altogether destroying the metallic coatings. for aluminum, we have tried the familiar anodizing process, but the latter completely destroyed the metallic layer; other processes exist, but since most of them require hot solutions and/or the presence of acids, it is very doubtful that these would be more successful. For copper, we have tried a simple reaction, in which the work is dipped in a solution of potassium sulfide at room temperature; the copper is transformed into copper sulfide, but the latter is too porous, and fails to adhere to the glass surface. Again, it is doubtful whether other processes would be any more successful. Hence, both copper and aluminum films would have to be used as such, without blackening. From the point of view of minimizing reflections, then, the copper would be preferable to aluminum, since it has a much lower reflectivity than aluminum, except in the red part of the spectrum. There are more important reasons for choosing copper, however. Consider a collimated beam of light impinging at normal incidence on an emulsion coated aluminised surface during the contact printing step. The incident and reflected beams will interfere to form standing waves inside the emulsion layer, and the nodes corresponding to a given wavelength will have almost zero amplitude due to the high reflectivity of the aluminum. It can be shown[15] that the positions of the nodes, measured from the aluminum surface, are given by $x = (k + \frac{1}{2} - \frac{\phi}{2\pi}) \frac{\lambda}{2}$ where $k = 0, 1, 2, \ldots$, and ϕ is the phase change upon reflection, and is close to π (e.g. about $.82\pi$ at 4,500 Å).

Thus, there will be a node (k=0) very close to the aluminum-emulsion interface for all wavelengths. At that point, the emulsion will be under-exposed relative to the rest of the emulsion layer, and this can cause the resist image to light off in the etching bath. In order to correct this, one has to use very diffuse illumination, which impairs resolution in the contact printing, or use excessively long exposure times. This problem does not present itself, or at least, not nearly to the same extent, with a copper coating, because the reflectivity of copper is relatively low (about .45 at .5 microns) in the spectral range to which the emulsion is sensitive. As far as etching is concerned, copper is again preferable to aluminum for the following reasons: the usual etchants for aluminum are hydrochloric acid, potassium hydroxide, or sodium hydroxide. These etchants react violently with aluminum, and hydrogen is evolved in the form of small bubbles; the formation of the latter at the edges of the resist image can cause the emulsion to be uplifted, and even detached from the metallic layer. On the other hand, copper is etched easily with a ferric chloride solution, and no gas is evolved to detach the emulsion. (In theory, it should be possible to etch aluminum with ferric chloride, but in practice, the etch is very irregular, and the metal is detached in flakes more than it is dissolved.)

For the reasons outlined above, then, we have chosen copper for our work.

(2) Coating the metallized surface with photoetching emulsion:

After the plane side of the lens has been coated with a thin copper film, it must next be coated with a layer of photoetching emulsion.

We shall discuss briefly the desirable properties of this coating:

(a) It must adhere well to the copper film, and be unaffected by the copper etchant.

(b) It must be very thin, and free of pinholes, globules, dust particles, etc.

(c) It must be uniform in thickness so as to have uniform exposure of the emulsion layer.

Conditions (a) dictate the kind of photoetching emulsion to use. For a copper substrate, Kodak recommends KPR or KOR. We have tried both emulsions, and have found that although KPR requires longer exposure times than KOR, it produces a cleaner image than KOR, and undercutting in the etching solution is less severe; because of this, we have used only KPR for our work.

The layer of emulsion must be very thin in order to achieve maximum resolution. A thin layer also decreases exposure times, is easier to dry, and can be made more uniform than a thick layer. The ideal layer, then, is the thinnest one which is free of pinholes, and resists the action of the etchant. The actual thickness to use is determined by trial and error. Dust particles and globules in the layer must be eliminated because these prevent a good contact between the negative and the emulsion coated surface.

The metallised surface of the lens is covered with emulsion as follows: a special cabinet was constructed which incorporates a two-speed fan and an air filter assembly; the latter produces a laminar flow of dust-free air over a spindle which is activated by a variable speed motor under the desk top. The lens is mounted in a special holder

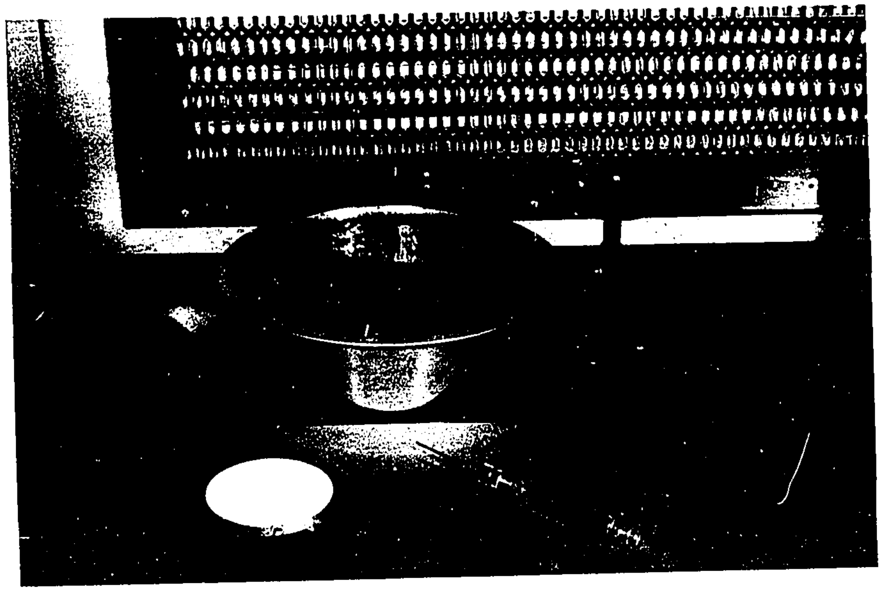

(a)

(b)

Fig. B2-1 Apparatus used for coating the lens with a thin layer of photo-etching emulsion.

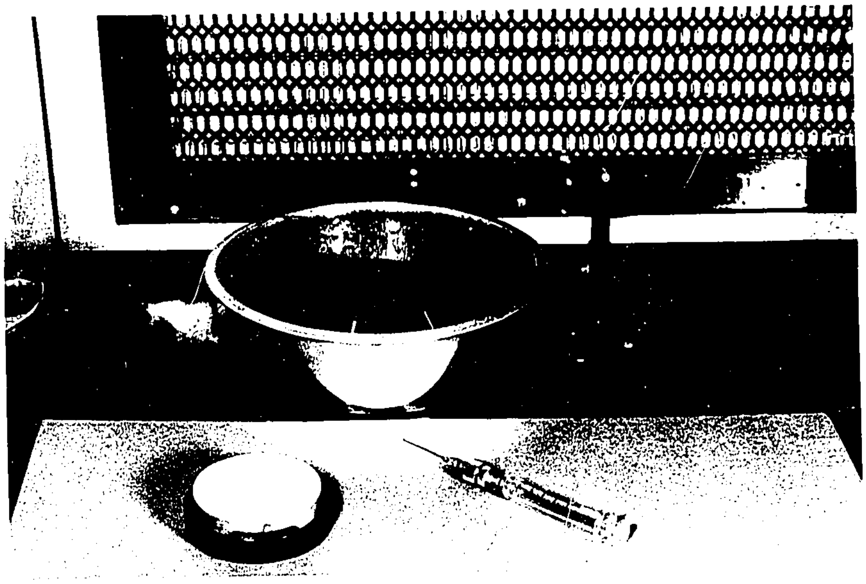

(a)

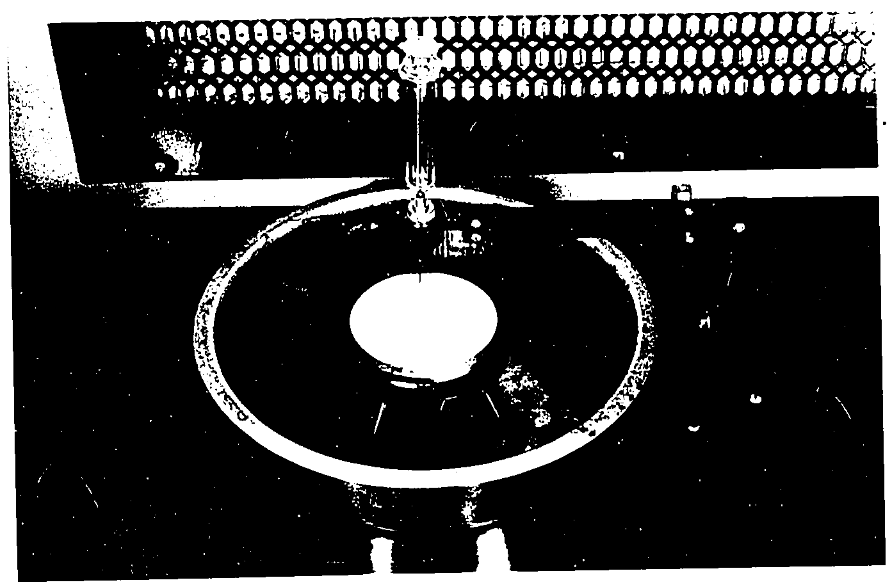

(b)

Fig. B2-1 Apparatus used for coating the lens with a thin layer of photo-etching emulsion.

which screws onto the spindle head. See Fig. B2-1 (a) and (b). While the spindle is rotating, the emulsion is injected by means of a syringe onto the rotating lens: the syringe incorporates a Millipore filter attachment which retains all particles 1 micron or larger in size. The cabinet is illuminated by means of a 35 watt tungsten lamp equipped with a Kodak type OC safelight filter. This prevents the emulsion from being exposed during coating.

The thickness of the emulsion layer thus produced depends on the viscosity of the emulsion and the speed of rotation of the spindle. We have found that using un-diluted KPR, a speed of rotation of about 900 to 950 rpm produces a clean, uniform emulsion layer having a thickness of about .6 to .7 microns. The uniformity of the layer is easy to check by viewing the layer briefly under a low-power mercury vapour lamp. Because the layer is very thin, it appears coloured due to interference of the light inside the layer, and a variation in thickness produces a variation in colour. For example, in our case, the layer appears uniformly greenish when viewed at normal incidence, and when the coating has been properly done.

The interferential colours give no information about the thickness of the layer, on which depend the proper drying time, exposure time, and development time of the photoetching emulsion. Therefore, it became necessary for us to develop a method which would enable us to determine approximately the thickness of the emulsion, and to detect accurately a change in this thickness, without destroying or exposing the emulsion. The method we have developped is based on the observation of the channelled spectrum formed by a collimated beam of white light (tungsten) reflected from the layer at grazing incidence. Although the interference fringes formed under these circumstances are of the multiple reflection type, the facts that the emulsion layer is bounded by only one metallic interface, and that the angle of incidence is near grazing have given a few interesting properties to the fringes thus formed. Because of this, we have given a theoretical derivation in Appendix B. This derivation shows that in order to have fringes of good contrast (or visibility), it is necessary that the angle of incidence be near-grazing; this condition will also optimize the finesse of the fringes. Furthermore, since the positions of the fringes depends on the state of polarization of the light beam, it is necessary to polarize the latter either parallel or perpendicular to the plane of incidence in order to have good fringe visibility, and to be able to estimate the thickness of the layer from measurements on the fringes.

The experimental set up used for observing the channelled spectra is shown schematically in Fig. B2-2. The positions of the dark fringes are given by

$$2\,nd\cos\theta' = (m - \phi')\lambda \qquad m = 0, 1, 2, \ldots.$$

where n is the refractive index, θ' is the angle of refraction inside the emulsion, d the thickness of the emulsion, λ the wavelength, and ϕ' the phase change produced by the copper layer. If we denote by subscripts 1 and 2 the positions of two successive fringes, we have

$$\frac{2\,nd\cos\theta'\,(\lambda_2 - \lambda_1)}{\lambda_1\,\lambda_2} = \phi_2' - \phi_1' \pm 1$$

(where we have assumed that the variation of n and θ' with λ is negligible) Now, according to theory and experimental measurements, the phase change at normal incidence for an opaque copper layer (covered with a dielectric having a refractive index $n = 1.5$) varies by about .35 radians maximum from about $\lambda = .4$ microns to $\lambda = .65$ microns; if we suppose this variation to be no greater for angles $\theta' \leqslant 40°$ (corresponding to grazing incidence on the emulsion), then $\phi_2' - \phi_1'$ represents a correction term of only 5 to 10% compared to 1 . Thus, we can write approx.

$$d \simeq \lambda_1 \lambda_2 \; / \; 2n \cos \theta' \, (\lambda_2 - \lambda_1)$$

The angle of incidence was adjusted to give max. visibility around $\lambda = .5$ microns. Using the above method, we have determined the thickness of the emulsion coatings to be .66± .1 microns.

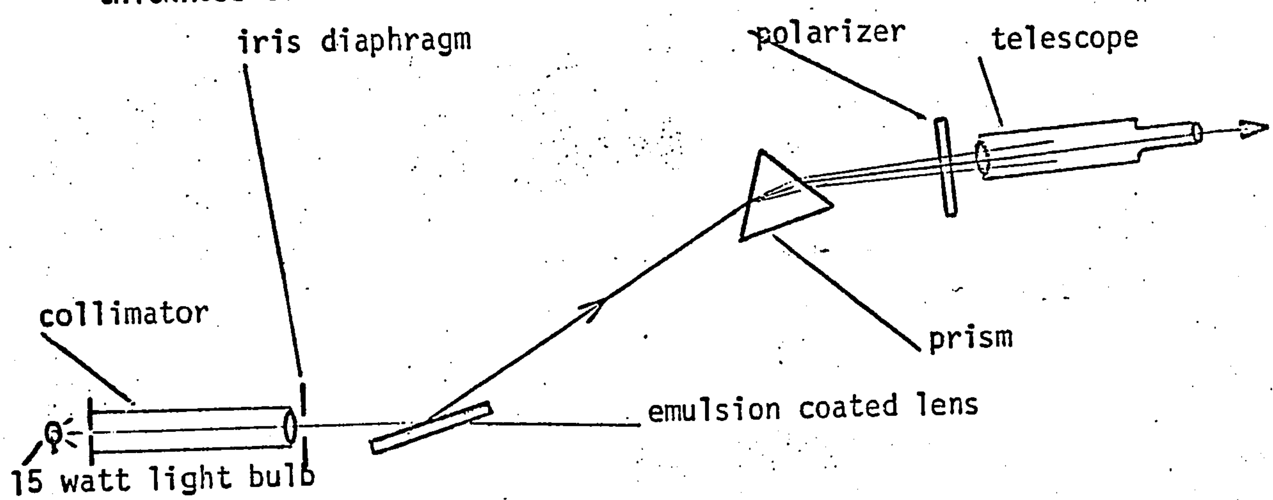

Fig. B2-2

(3) Contact Printing:

The apparatus used for contact printing the flux selector negative onto the emulsion coated lens is shown in Fig. B2-3 (a), (b), and (c). The negative is clamped onto a supporting plate having a $1\frac{7}{8}$ " clearance hole bored into it. The emulsion coated lens is held by means of an O-ring in a metallic ring which screws onto a set of gimbals attached to a tube which slides up and down above the negative mount: the lens is allowed to rest on top of the negative, and the contact assured by the weight of the lens and support; the gimbals give the lens freedom of rotation about two mutually perpendicular axes in a horizontal plane, thus permitting a good contact between the lens and the negative. The 1/2" thick glass plate separating the lamp source compartment (not shown) from the top compartment serves as a dust shield, and a heat shield: the 650 watt lamp used for the exposures evolves much heat; consequently, the air surrounding the lamp becomes hot, and it is necessary to prevent that air from getting into the top compartment and increasing the ambient temperature, which could cause the gelatin of the negative and the emulsion on the lens to stick together. The lamp also emits a large amount of infra-red radiation, which could also cause over-heating of the negative or the lens: the glass plate absorbs most of the infra-red radiation emitted by the lamp and thus protects the negative and lens.

The light source used is a 650 watt tungsten halogen lamp having a filament temperature of 3400° K, and mounted in a reflector which produces a relatively diffuse illumination on the negative. Although in theory it is preferable to use a collimated beam of light in order to achieve maximum resolution, this is not so desirable in practice because the least scratch or particle of dust on the negative would project a shadow on the emulsion. Furthermore, the standing wave effect discussed earlier would be much more important with a collimated beam. With the set-up used, we have obtained satisfactory results: line width broadening due to diffusion of illumination does not exceed 1 or 2 microns, which is deemed acceptable at the present stage; exposure times are relatively short (1 1/2 minutes). The

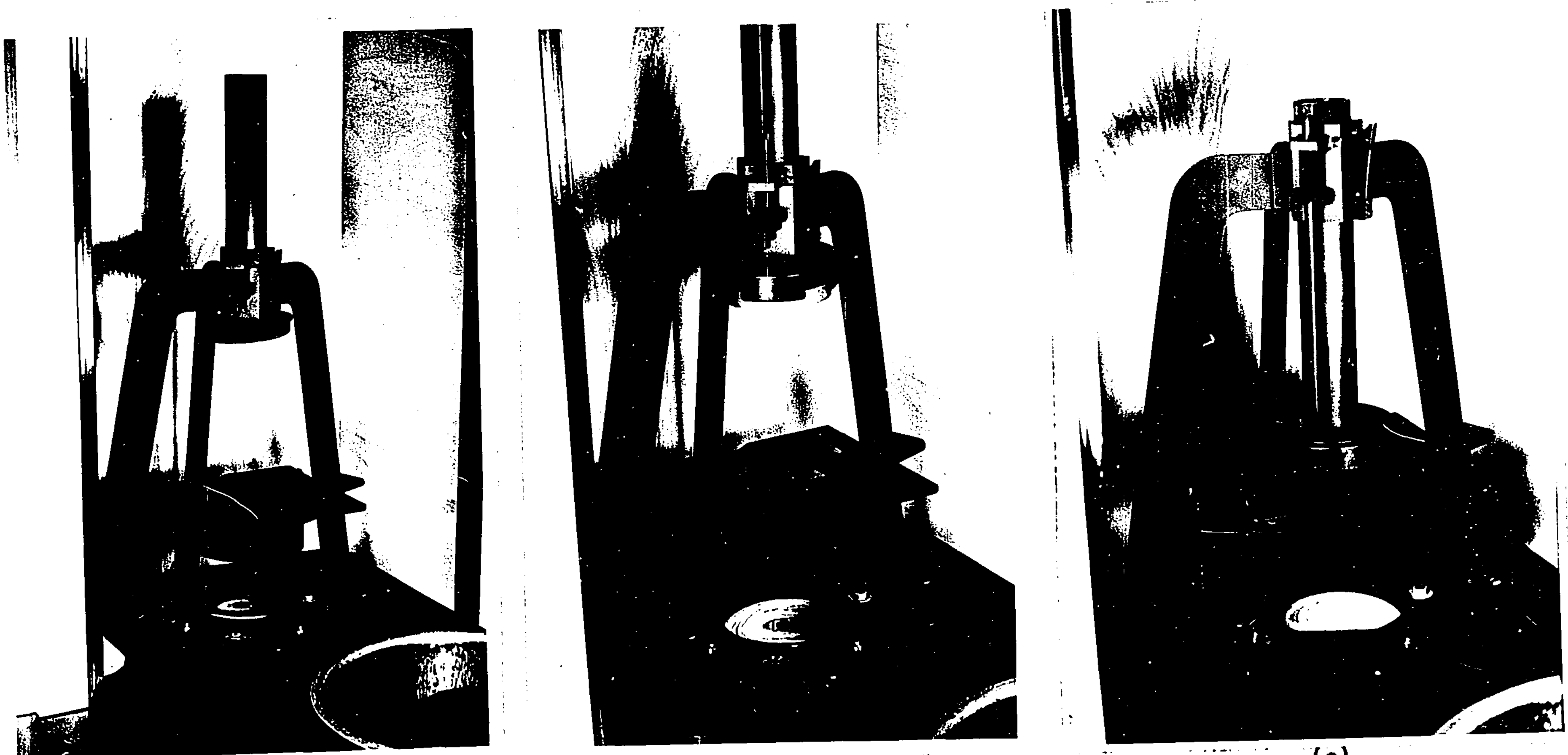

(a) (b) (c)

Fig. B2-3 Apparatus used for contact printing the flux selector negative onto the emulsion coated lens

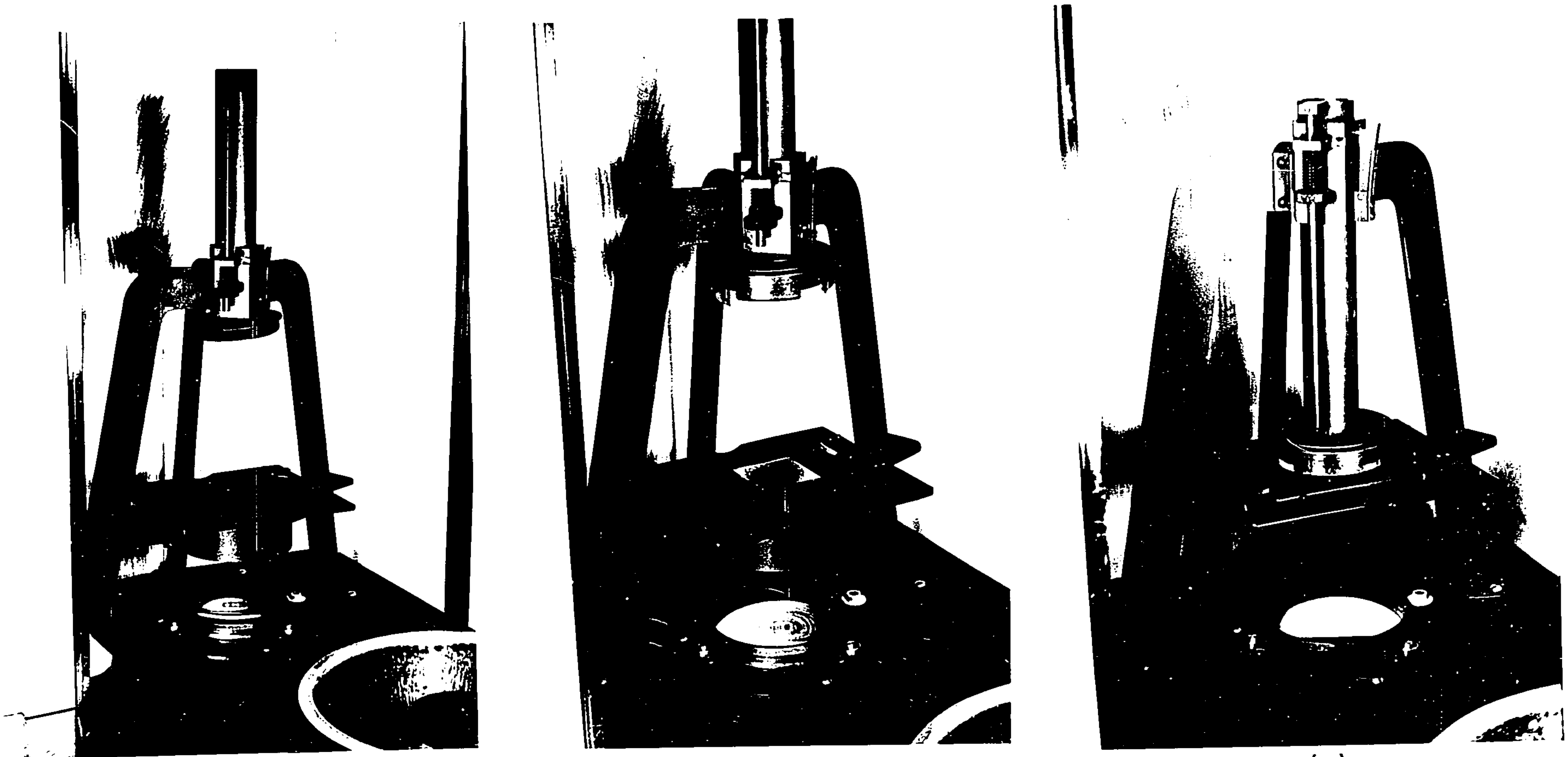

(a) (b) (c)

Fig. B2-3 Apparatus used for contact printing the flux selector negative onto the emulsion coated lens intensity in the plane of the negative decreases from the center of the opening to the edge by about 15%, but the photo-etching emulsion has sufficient exposure latitude to make this variation un-important. The intensity of the illumination is controlled as follows: a photo-sensitive probe, consisting essentially of a photo-conductive cell and its associated electric circuit, was assembled as shown schematically below:

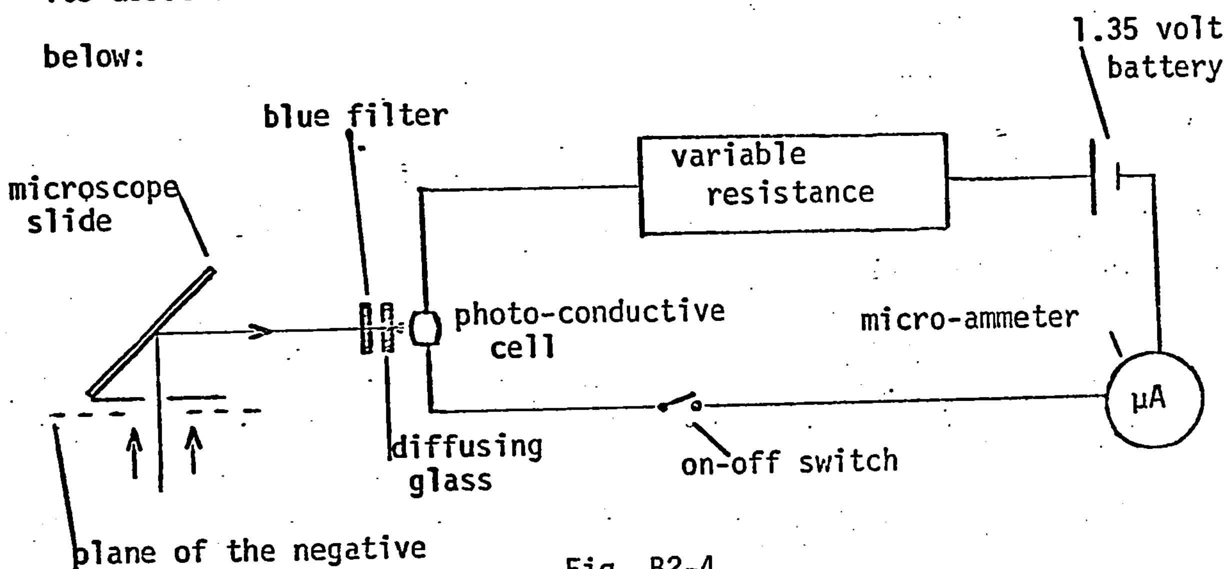

Fig. B2-4

(Only the blue portion of the spectrum is used because this matches roughly the spectral sensitivity of the photoetching emulsion). The probe measures the light intensity in the plane of the negative. The variable resistance is adjusted so as to get almost full scale deflection on the ammeter at the operating intensity of the lamp. The probe was calibrated (at a fixed resistance) by introducing successively various neutral density filters in front of the cell and noting the current corresponding to each. From the calibration curve, we have determined that a change in intensity of 2% is easily detectable. This simple device provides an easy and sensitive way of monitoring the intensity of the lamp.

(4) Development and etching of the photoresist image.

After the exposure, the lens is removed from its mount, and immersed into a large beaker containing the developper. It is allowed to stand vertically without agitation for about two minutes, after which it is removed, rinced with a 2 to 1 mixture of developper and acetone, then rinced with a 1 to 2 mixture of the same solvents. It is allowed to dry for about 3 hours. Because the clearance hole in the negative support is only 1 7/8", the emulsion layer outside of this diameter has not been exposed, hence has been removed in the developper. Since this portion of the copper surface must not be etched, it is now covered with a layer of unexposed photoetching emulsion, which is then allowed to dry. The work is then etched in a ferric chloride solution at room temperature. The concentration of the etchant is about 100 grams per liter, which is dilute enough to allow the etching action to proceed slowly, i.e., controlably. To remove the residual photoresist image after etching, the surface of the work is swabbed with a soft cloth saturated with trichloroethylene.

In order to check the quality of the etch, the work is examined under a microscope at 600x. The microscope is equipped with a micrometer ocular (Tesa) which allows measurements to be made on the flux selector with an accuracy of ±1 micron. The precision in the flux selectors produced was determined to be $\pm 1\ \mu$ on the ring widths for most of the rings; at the edge, the precision is slightly less, i.e., about $\pm 2\ \mu$. There are small defects in these etched flux selectors (due to small defects in the negatives, occasional pinholes in the metallic coating, etc...) but these do not seriously affect the diffraction patterns formed by the flux selectors. In Fig. B2-5 is shown a photograph of a flux selector produced by the method described in this thesis, and mounted in a lens holder.

Fig. B2-5 Flux selector produced by the photo-etching of a copper film deposited in vacuum on the plane surface of a lens; the latter is mounted in a special holder for use in the rotary lens mount.

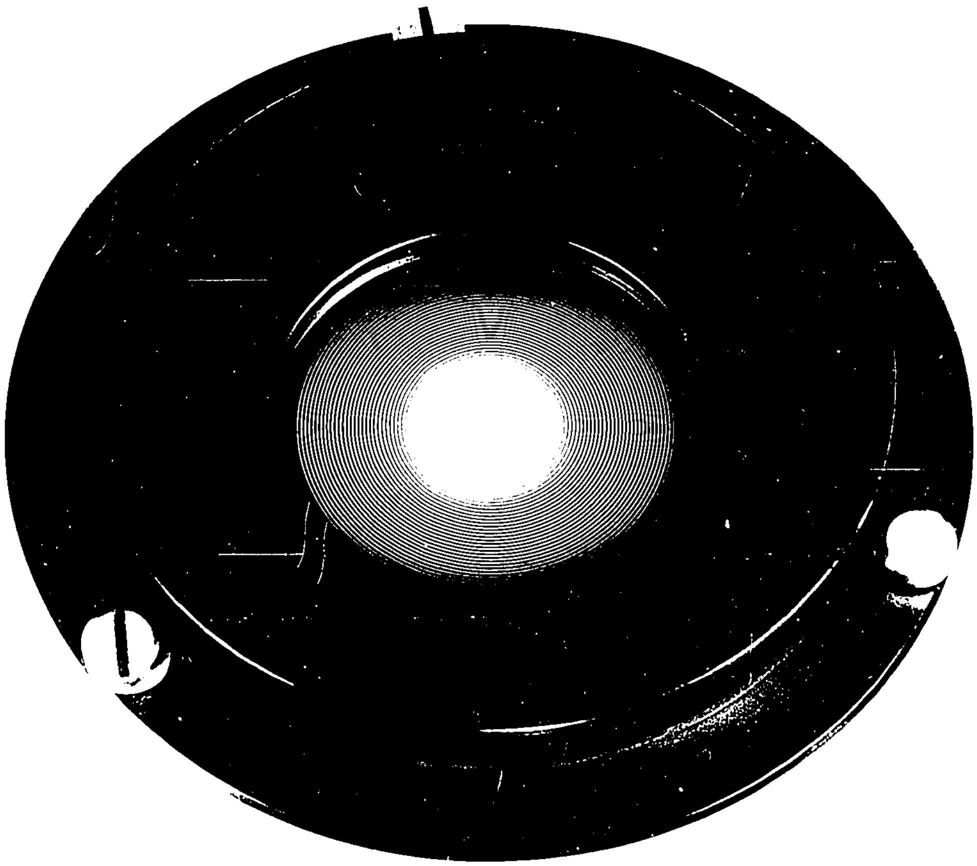

Fig. B2-5 Flux selector produced by the photo-etching of a copper film deposited in vacuum on the plane surface of a lens: the latter is mounted in a special holder for use in the rotary lens mount.

CHAPTER 3

EXPERIMENTAL WORK DONE WITH THE FLUX SELECTORS

In this chapter, we shall describe the experimental work done in order to compare the diffraction patterns formed by the flux selectors with those formed by the uniformly transmitting pupil. The diffraction patterns were recorded photographically; a study of the photographs obtained allowed us to compare the various cases studied with the theoretical calculations, and, in particular, to show the remarkable improvement that flux selectors bring to the images formed by lenses.

The optical system used is shown schematically in Fig. B3-1. A helium-neon laser is used as a monochromatic light source (λ= 6328Å). The light beam is focussed by a microscope objective onto a 32 microns pinhole, which acts as a point source for the optical system. Three lenses, one with the 44 rings F.S. [T(x,5)], another with the 40 rings F.S.[T(x,M)], and the third one with a 4 cm. diameter circular diaphragm, are mounted in a rotary lens mount located 20 meters from the pinhole. The lens mount can rotate about an axis parallel to the optical axis of the system, so that each lens, in turn, can be brought into position on the optical axis; this allows quick interchangeability of the lenses, without necessitating re-adjustment of the latter. The individual lenses, and the rotary lens mount as a whole, can be displaced in a direction parallel to the axis of rotation in order to focus the images. The image formed by each lens is much too small to be photographed directly; for example, the Airy pattern formed by the lens with the 4 cm. diaphragm has a central spot only 63 μ in diameter. A Barlow lens having a focal length of 10 cm. is used to magnify the image about 17 times. The magnified image is projected in the film plane of an Hasselblad camera. The

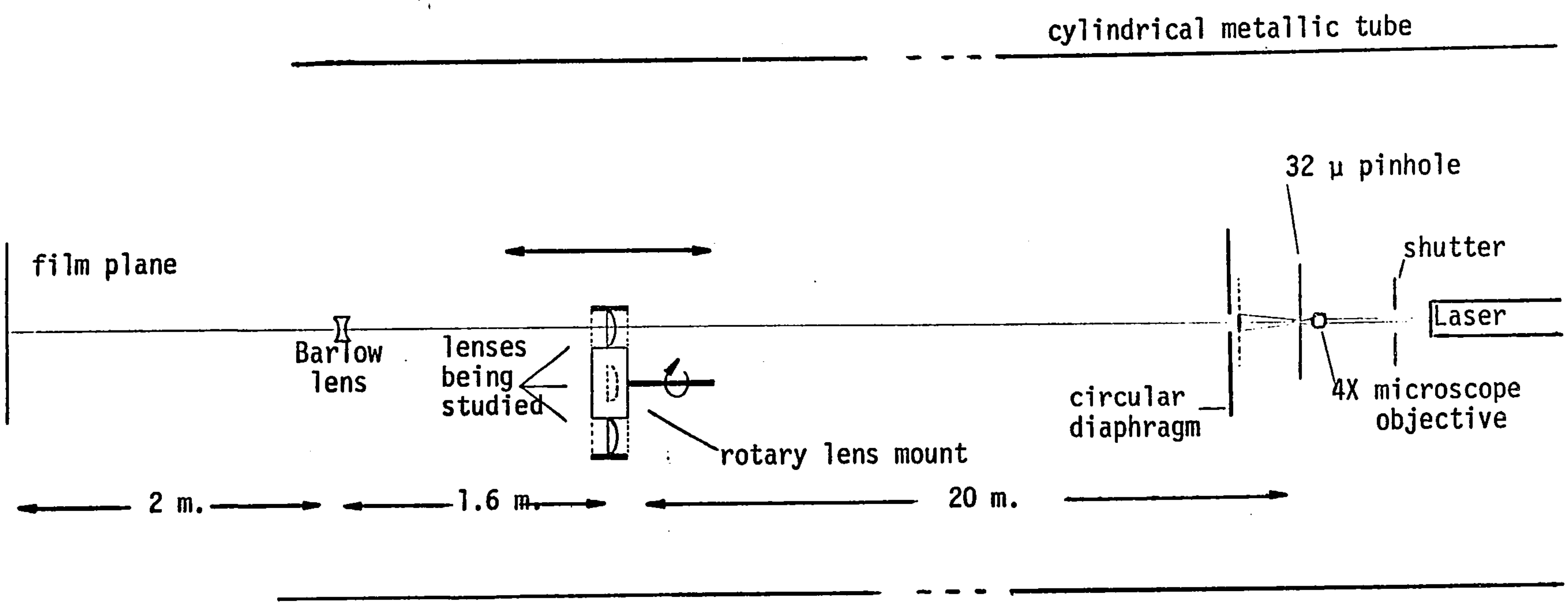

Fig. B3-1 Schematic diagram of the optical system used for the study of the diffraction patterns formed by flux selectors.

part of the optical system between the laser and the Barlow lens is contained inside a cylindrical metallic tube having a diameter of about 60 cm.; this greatly reduces image degradation due to air turbulence and vibration. The optical system is aligned as follows: The rotary lens mount was built so that the lens being studied is centered on the axis of the cylindrical tube; with the pinhole and microscope objective removed, the laser is adjusted so that the beam is centered on this lens. The rotary lens mount as a whole is then adjusted so that the lens is perpendicular to the laser beam (as well as centered on it), and the axis of rotation of the lens mount is parallel to the optical axis (= laser axis). The microscope objective (4X) is then put into place and adjusted so that its optical axis coincides with the laser beam. The pinhole is adjusted so as to be centered on the optical axis, and such that the light beam emerging from it has maximum intensity. The Barlow lens is then set up as shown in Fig. B3-1, and the position of the camera adjusted so that the magnified image is centered and focussed in the film plane. The other lenses in the rotary lens mount are then brought, in turn, into the light beam, and are adjusted individually so that the resulting magnified images are also centered and focussed in the film plane.

With this optical system, we have studied the following cases:

(1) Aberration-free optical system, correctly focussed. ($\phi(x)=0$)

(2) Aberration-free optical system, with defect of focus of $\pi/2$, π, $3\pi/2$, 2π. ($\phi(x) = \pi x^2/2$, πx^2, $3\pi x^2/2$ and $2\pi x^2$ resp.)

Also, we have studied the images formed by the three lenses (correctly focussed) when an object consisting of a group of randomly distributed small points replaces the pinhole; the object is illuminated by means of a mercury vapour lamp equipped with an interference filter which isolates the 5461Å line; thus, an incoherent but monochromatic illumination is provided.

The images were recorded on Agfa Isopan Record film. We have chosen this film because its associated characteristic curve is linear over a wide range of exposures ($\simeq 10^4$:1) and it is quite sensitive to light (ASA speed = 1250 at 5500 Å) yet has adequate resolution for our work.

The characteristics of an emulsion can vary slightly from one roll of film to another; furthermore, it is difficult to process identically two different rolls of film. In order to avoid these small variations, and so, make a completely objective comparison between the images formed by the three lenses, we have always recorded the images corresponding to the three lenses, for a given case, on the same roll of film; furthermore, the rotary lens mount enabled us to take the three corresponding exposures in a short interval of time. Thus, the correctly focussed series was recorded on one roll of film, all the defect of focus series on a second roll of film, and the images of the group of points on a third roll of film.

When the optical system is correctly focussed, the intensity at the center of the diffraction patterns formed by the lenses equipped with flux selectors is T^2 smaller than the intensity at the center of the Airy pattern. (T = transmission factor. See chap. 5) This has been verified experimentally with a photometer. Consequently, in order to have equivalent photographic exposures, the photographs corresponding to the 44 rings and 40 rings flux selectors were given 6 times and 2.8 times resp. the exposure given to the photographs corresponding to the uniformly transmitting pupil.

The negatives were developped with a solution consisting of 10 parts Pota developper, and 1 part Atomal developper. Pota is a very low contrast developper. Diluted with Atomal in the above proportions, it gives a γ of about .3. With such a low gamma, it is possible to record the wide range of intensities ($\simeq 10^7$:1) encountered in the diffraction patterns in a relatively short density interval ($\simeq$ 2) on the negative. This is necessary because the range of exposure of a photographic paper for which it is usable without loss of information is at most 100:1. Furthermore, if we represent by I the variation of intensity in a diffraction pattern, say, then the intensity re-radiated from the corresponding print will vary roughly as $I^{\gamma_p \gamma_f}$, provided the paper and film are used in the linear regions of their associated characteristic curves. (γ_p and γ_f refer to the γ of the paper and film resp.) Hence, in order that a print give approximately the same visual impression as the original diffraction pattern (for the central region at least), we should have $\gamma_p \gamma_f \simeq 1$, i.e., in our case, $\gamma_p \simeq 3.3$. In order to achieve this condition, we have printed the negatives on F4 paper, which has a gamma of about 3 when processed normally.

The prints made from the negatives corresponding to the cases studied are given in the following pages. For a given case, the prints associated with the 3 lenses were made at the same magnification, and were given the same exposure times and processing.

The diffraction patterns formed by the two flux selectors and the uniformly transmitting pupil in the case of a correctly focussed optical system are shown in Fig. B3-2. The magnification relative to the primary image is about 53X. As predicted theoretically, the flux selectors form diffraction patterns in which the intensities of the secondary maxima have been greatly reduced relative to those of the Airy pattern, but in which the central spots are wider than that in the Airy pattern. The

Fig. B3-2

Diffraction patterns formed by (a) the 40 rings flux selector [corresponding to amplitude filter T(x,M)], (b) the uniformly transmitting pupil, and (c) the 44 rings flux selector[corresponding to amplitude filter T(x,5)], for the case:

$$\phi(x) = 0$$

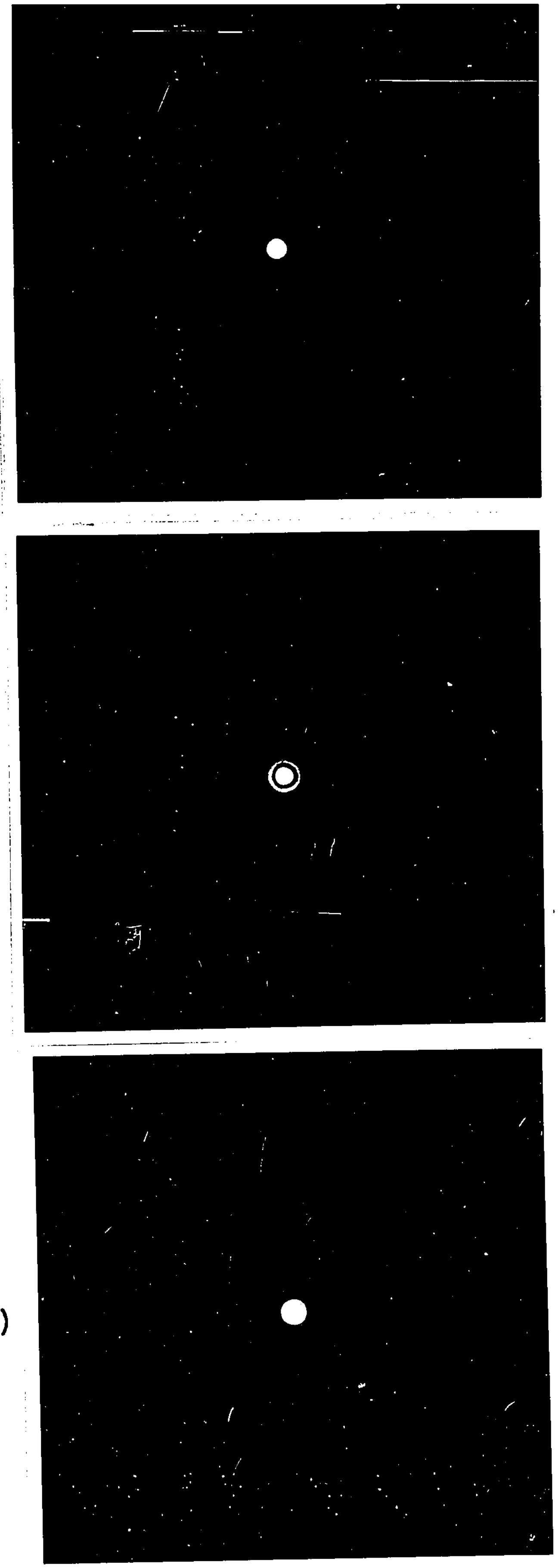

(a)

(b)

(c)

Fig. B3-2

Diffraction patterns formed by (a) the 40 rings flux selector [corresponding to amplitude filter $T(x,M)$], (b) the uniformly transmitting pupil, and (c) the 44 rings flux selector[corresponding to amplitude filter $T(x,5)$], for the case:

$$\phi(x) = 0$$

(a)

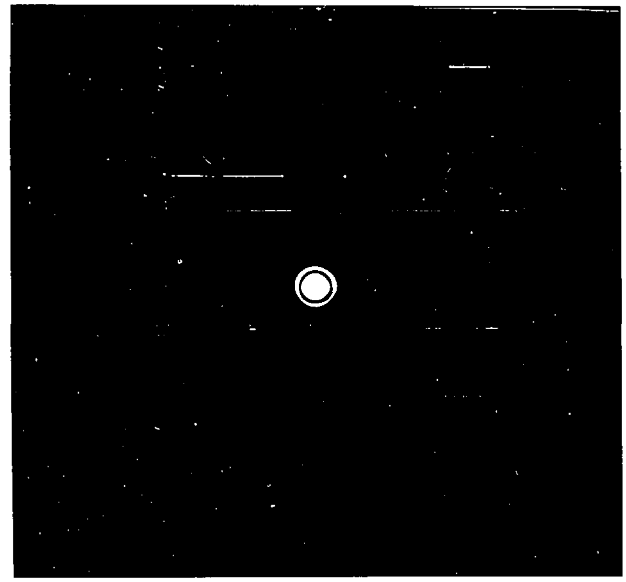

(b)

(c)

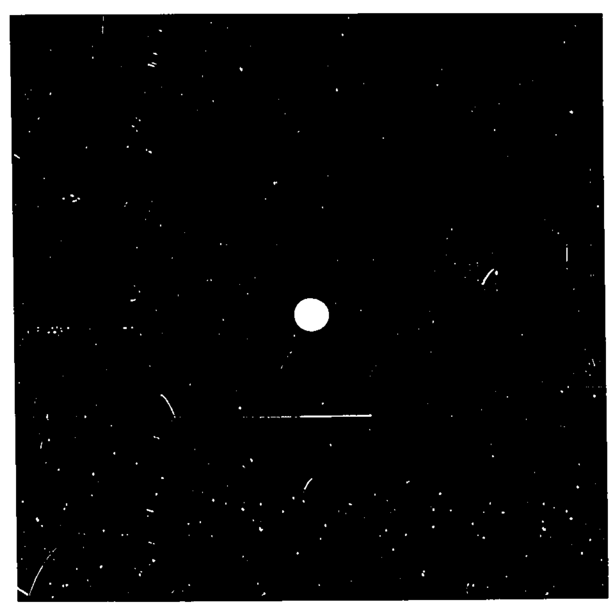

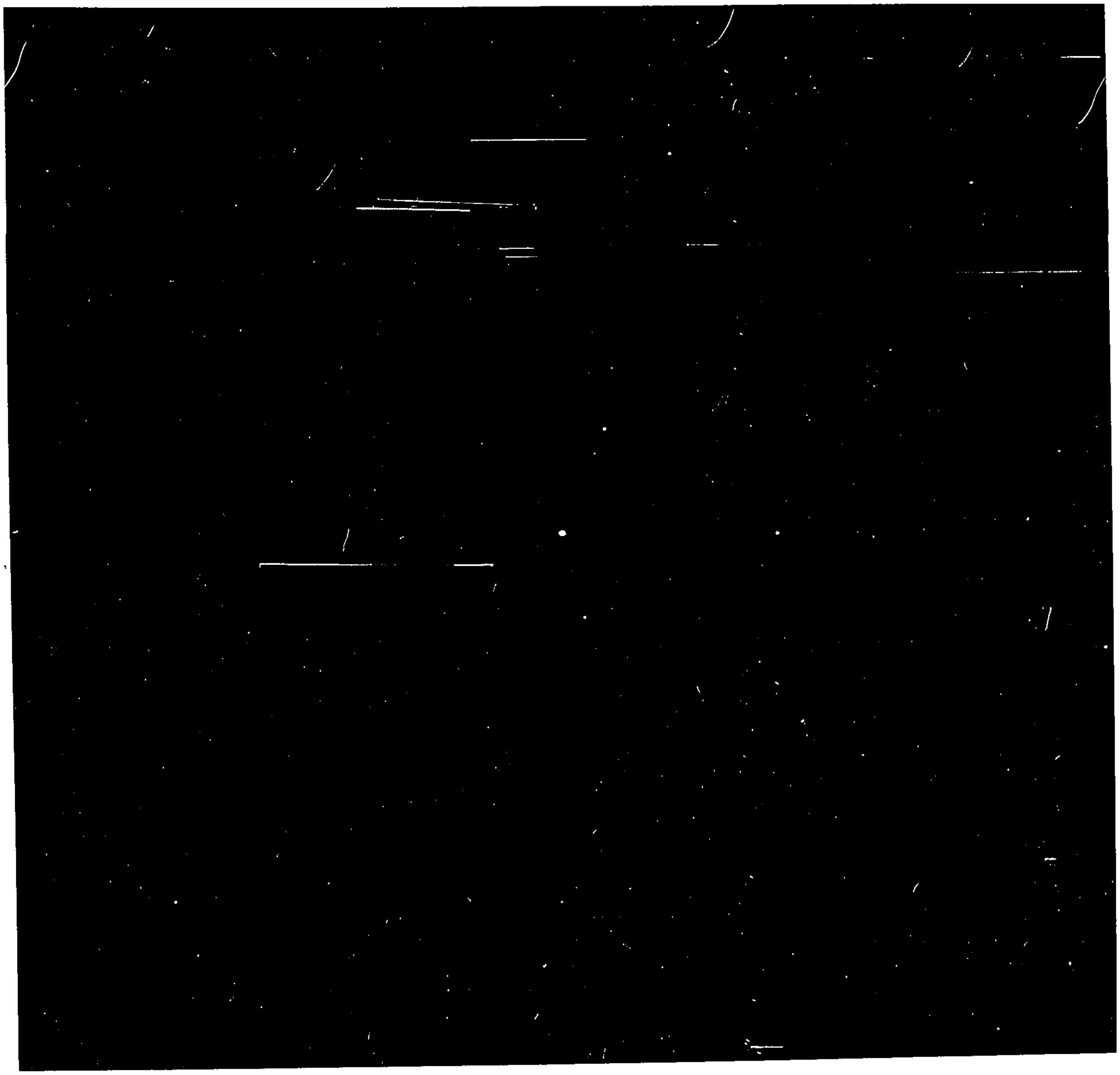

Fig. B3-3 Diffraction pattern formed by the 40 rings flux selector [corresponding to amplitude filter T(x,M)] for the case $\phi(x) = 0$. (Same as Fig. B3-2(a), but the magnification is 3.5 times smaller, in order to show the first two principal maxima.)

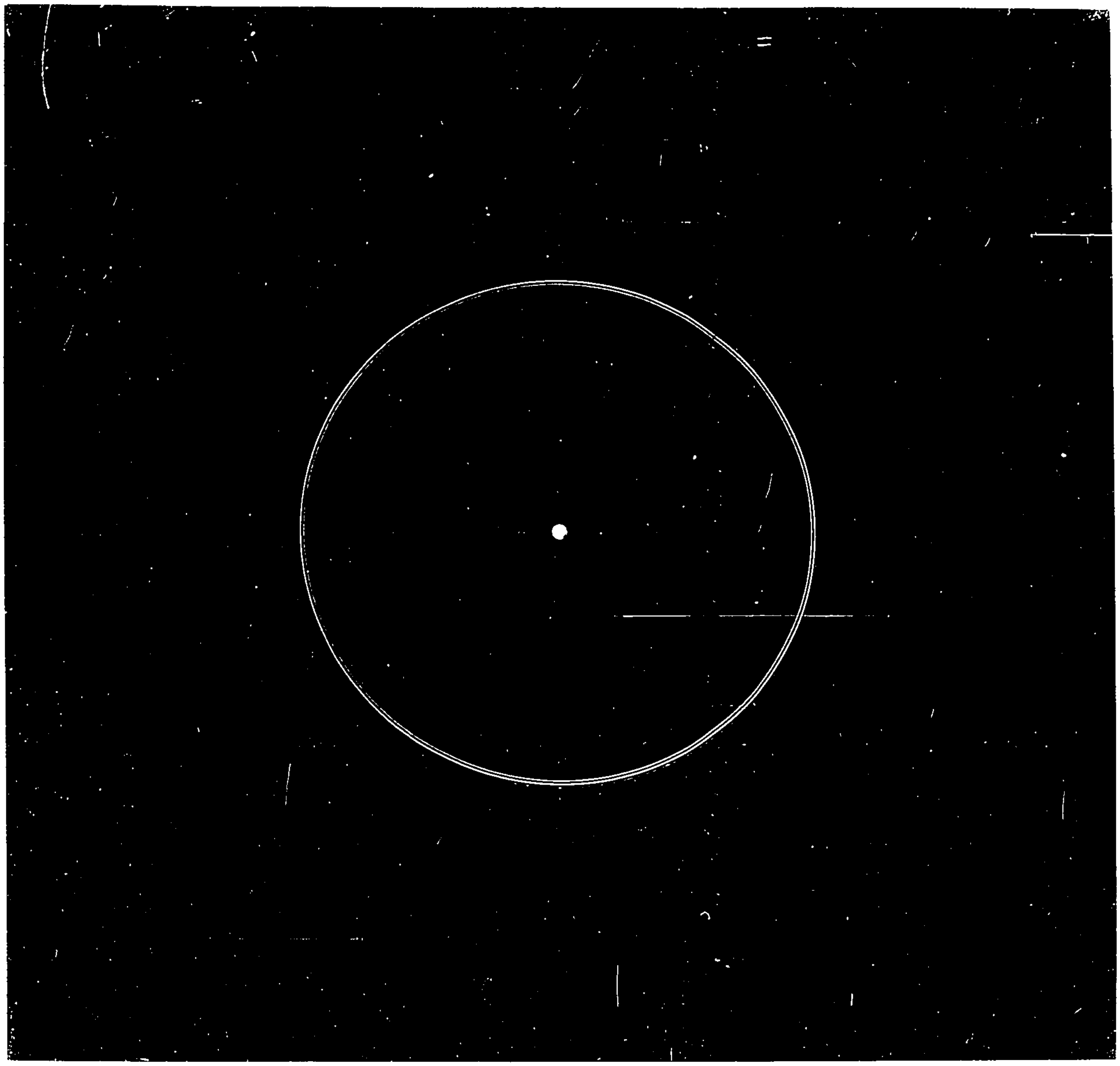

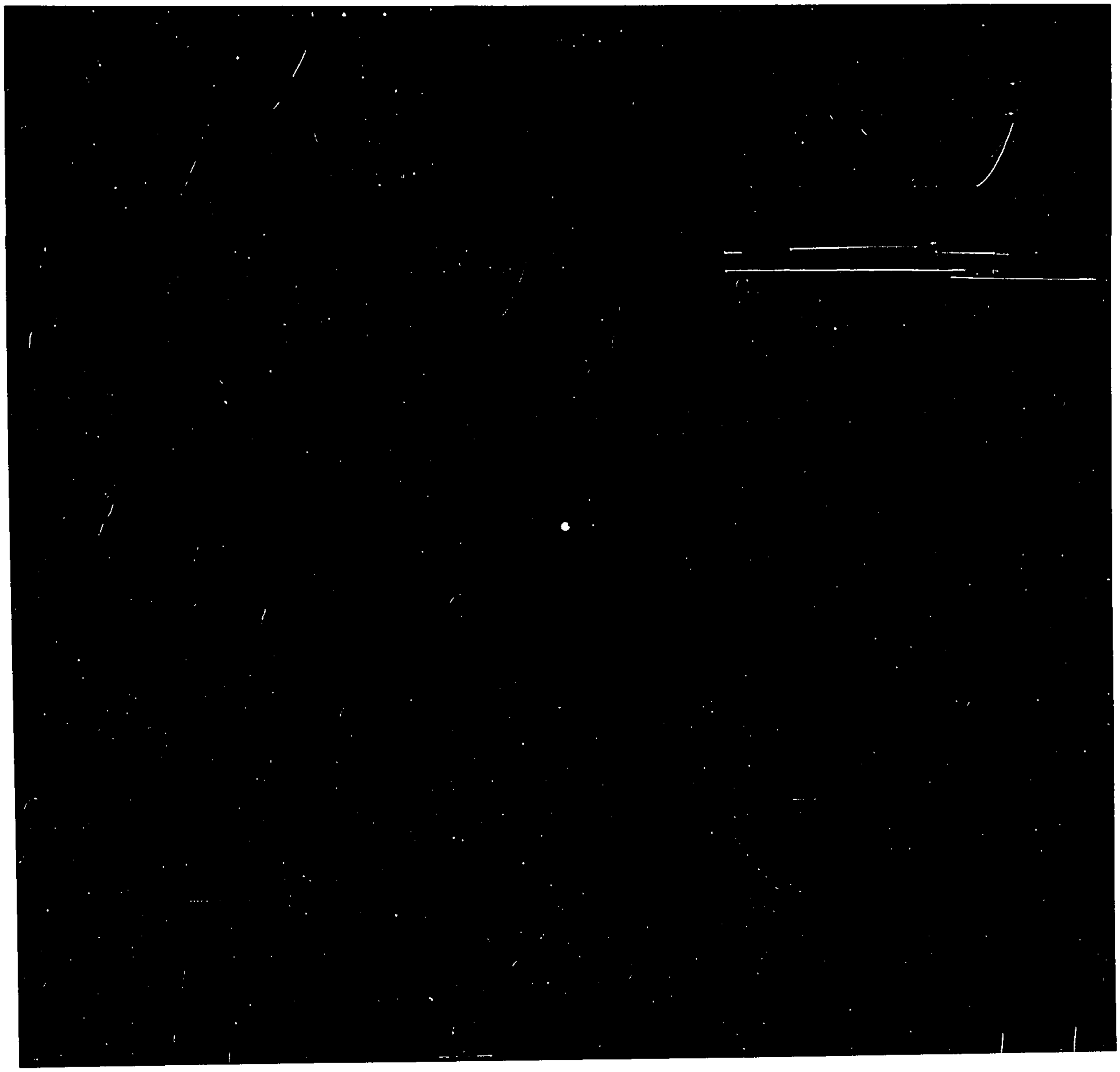

Fig. B3-4 Diffraction pattern formed by the uniformly transmitting pupil for the case $\phi(x) = 0$. (Same as Fig. B3-2(b), but the magnification is 3.5 times smaller.)

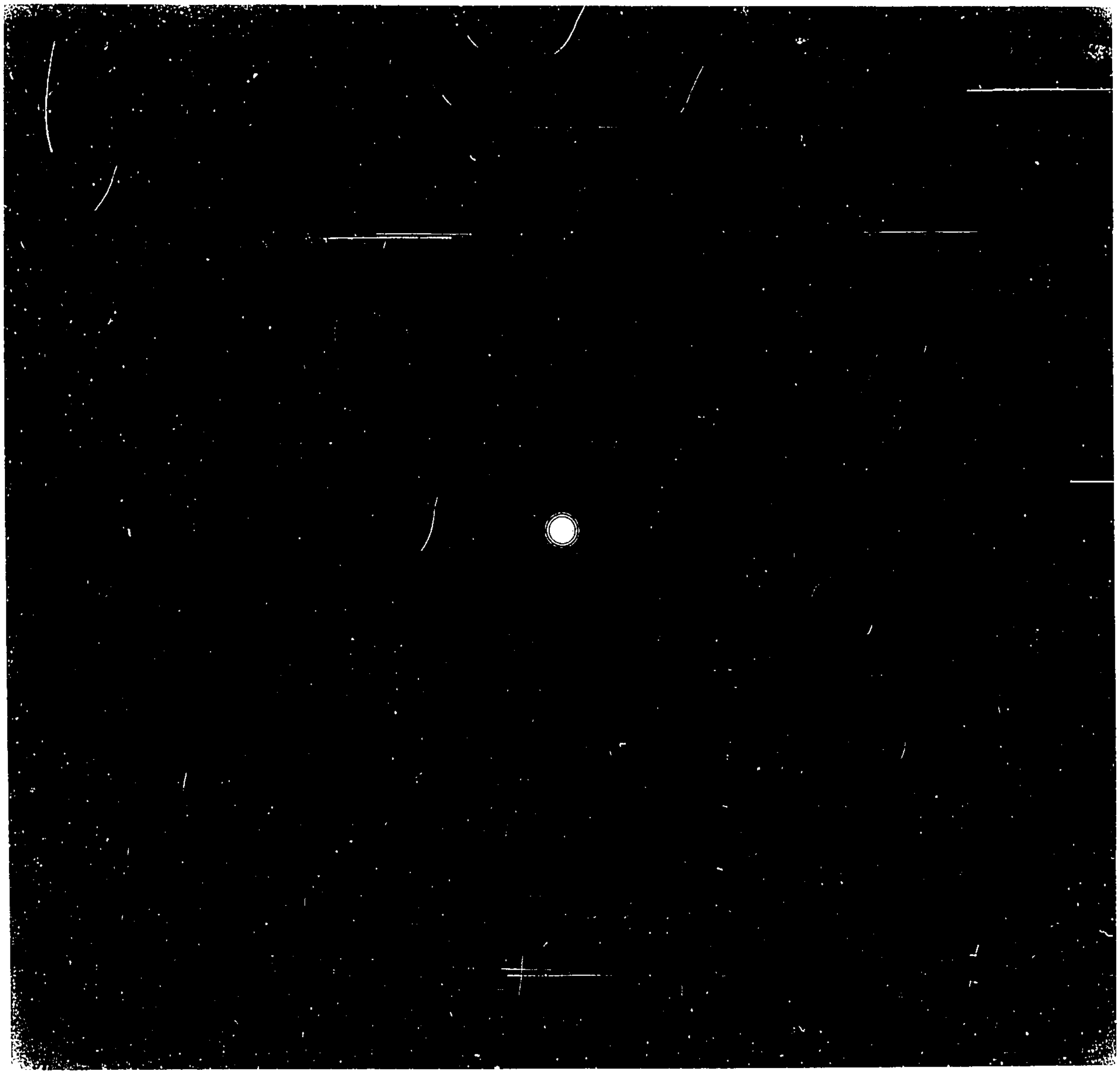

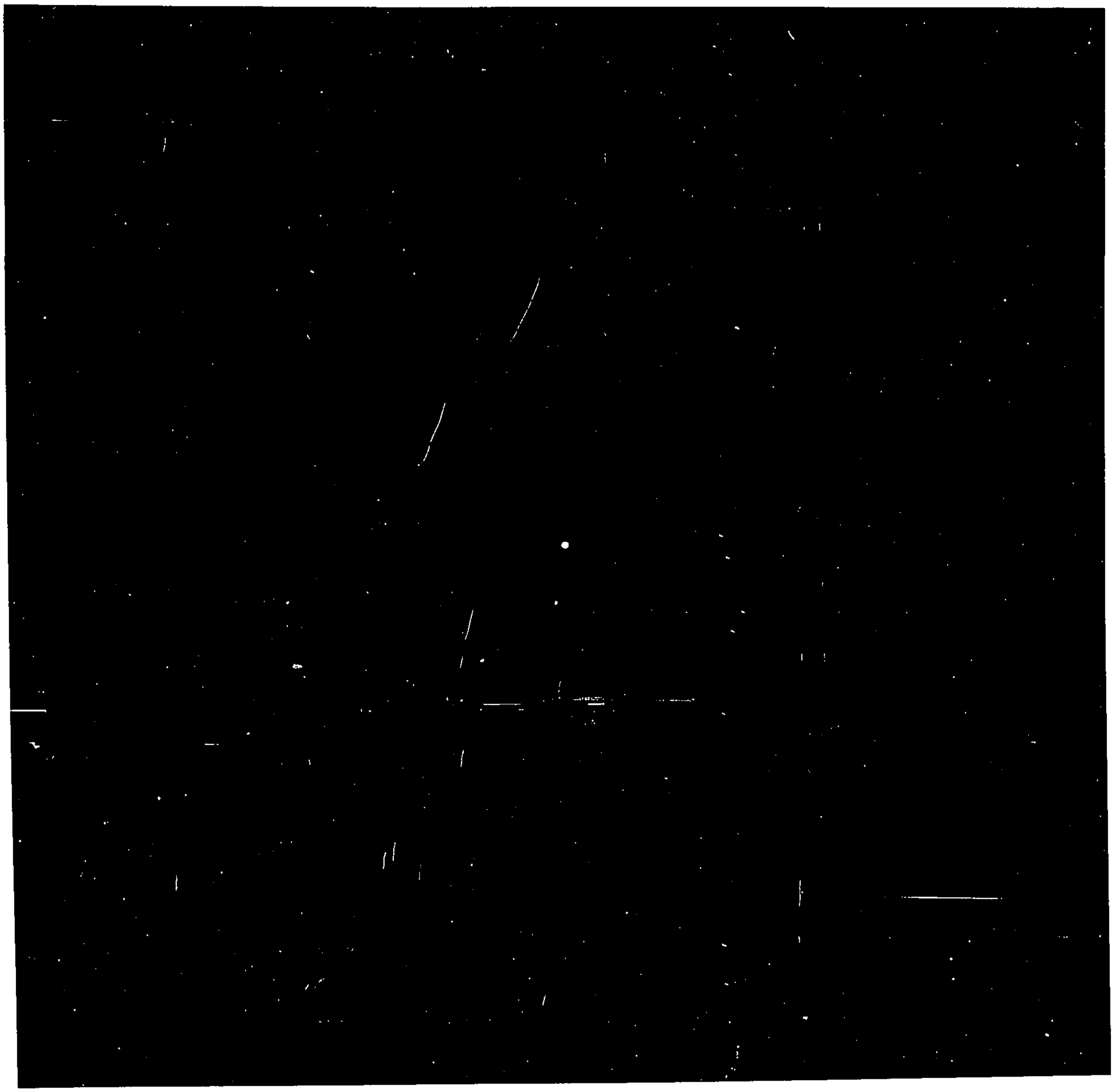

Fig. B3-5 Diffraction pattern formed by the 44 rings flux selector [corresponding to amplitude filter $T(x,5)$] for the case $\phi(x) = 0$. (Same as Fig. B3-2(c),but the magnification is 3.5 times smaller, in order to show the first two principal maxima.)

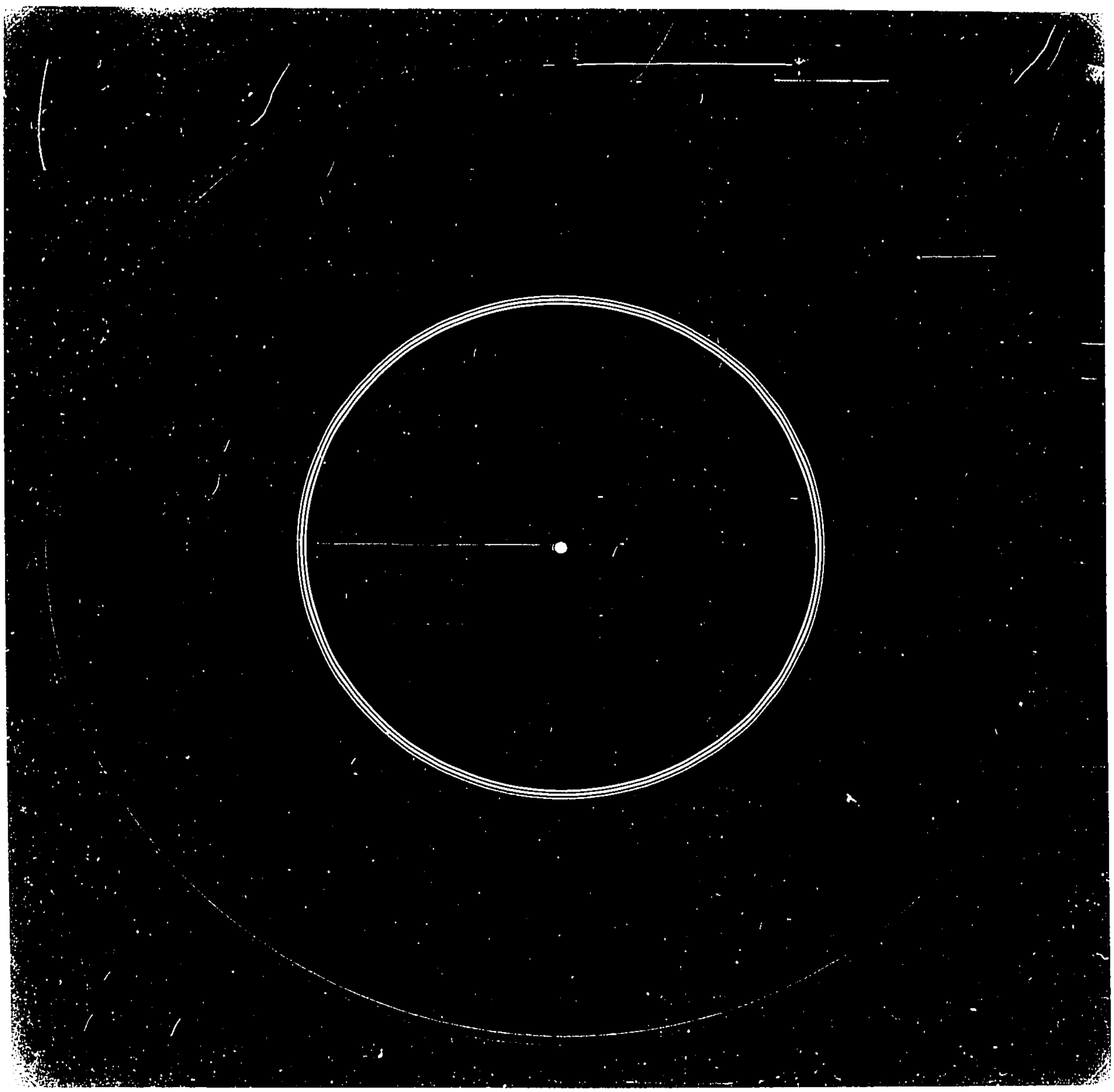

Fig. B3-6

Diffraction patterns formed by (a) the 40 rings flux selector [corresponding to amplitude filter T(x,M)], (b) the uniformly transmitting pupil, and (c) the 44 rings flux selector [corresponding to amplitude filter T(x,5)], for the case:

$$\phi(x) = .5\pi x^2$$

(a)

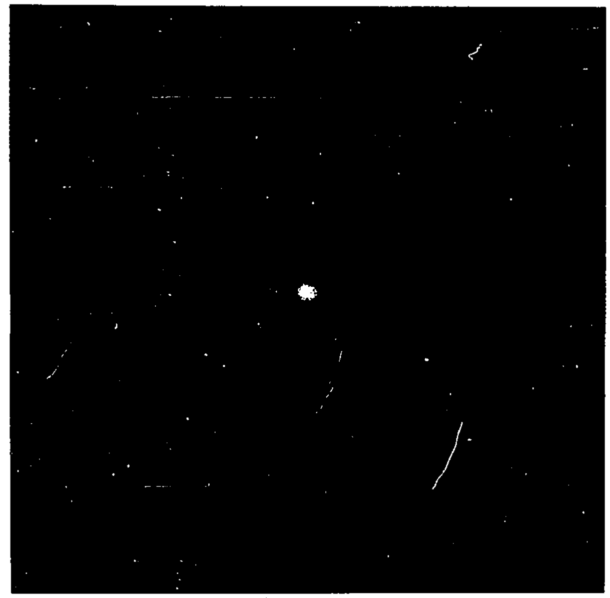

(b)

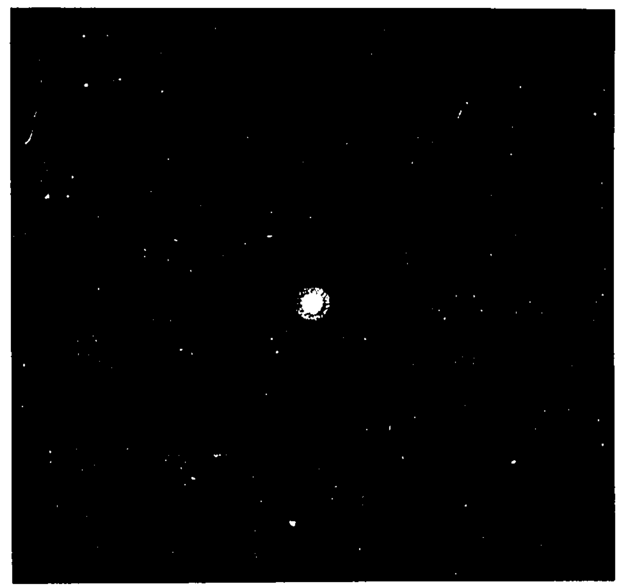

(c)

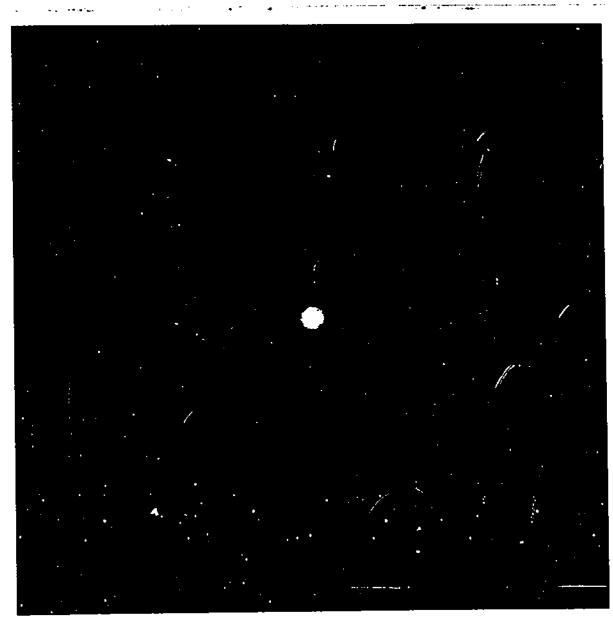

Fig. B3-6

Diffraction patterns formed by (a) the 40 rings flux selector [corresponding to amplitude filter T(x,M)], (b) the uniformly transmitting pupil, and (c) the 44 rings flux selector [corresponding to amplitude filter T(x,5)], for the case:

$$\phi(x) = .5\pi x^2$$

(a)

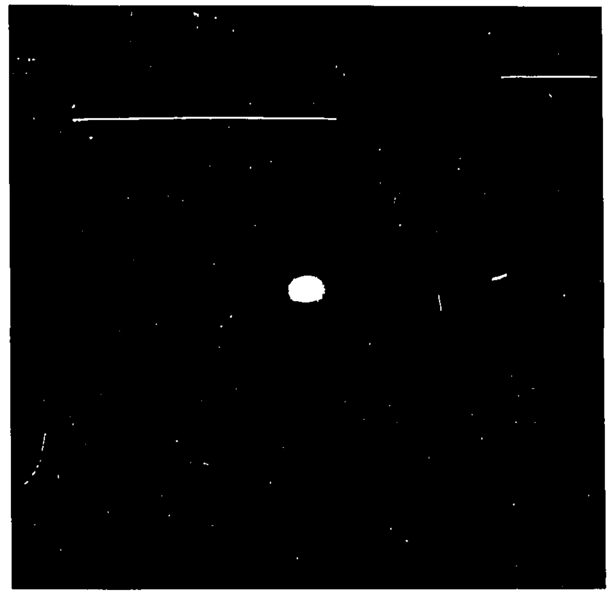

(b)

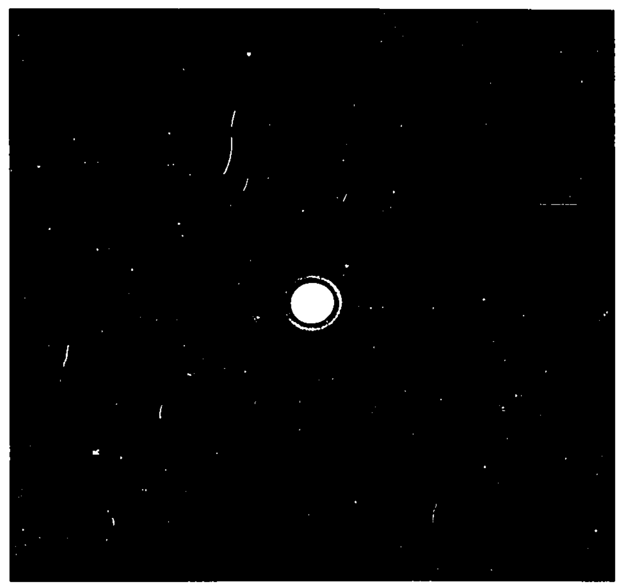

(c)

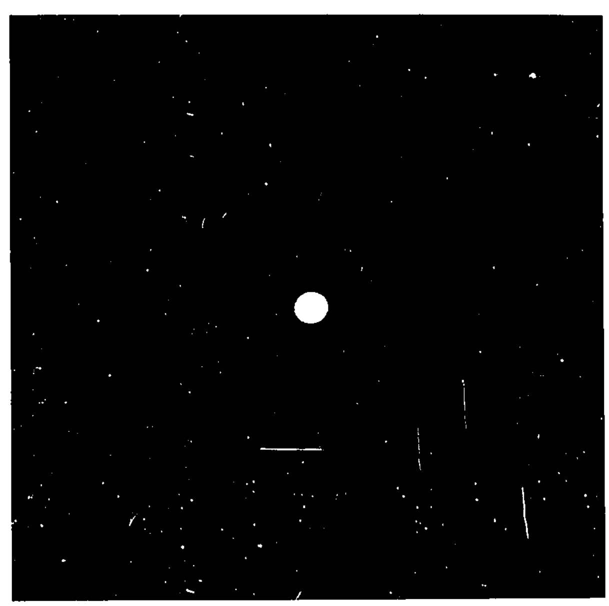

Fig. B3-7

Diffraction patterns formed by (a) the 40 rings flux selector [corresponding to amplitude filter T(x,M)], (b) the uniformly transmitting pupil, and (c) the 44 rings flux selector [corresponding to amplitude filter T(x,5)], for the case:

$$\phi(x) = \pi x^2$$

(a)

(b)

(c)

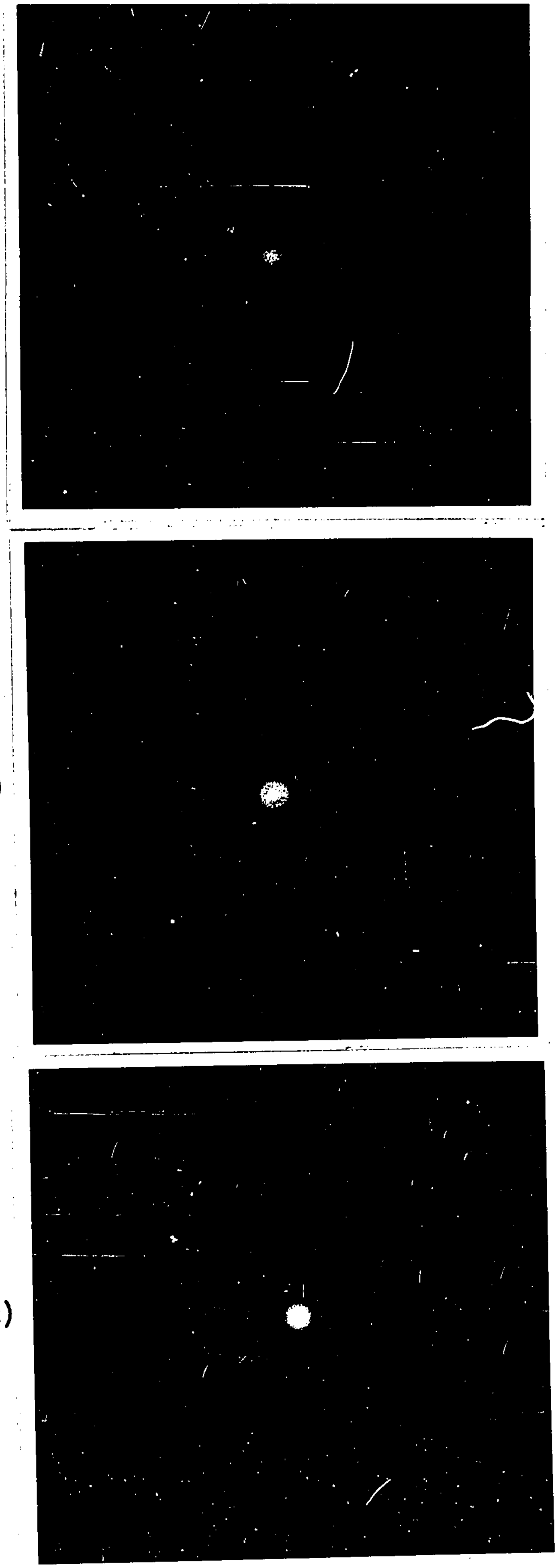

Fig. B3-7

Diffraction patterns formed by (a) the 40 rings flux selector [corresponding to amplitude filter $T(x,M)$], (b) the uniformly transmitting pupil, and (c) the 44 rings flux selector [corresponding to amplitude filter $T(x,5)$], for the case:

$$\phi(x) = \pi x^2$$

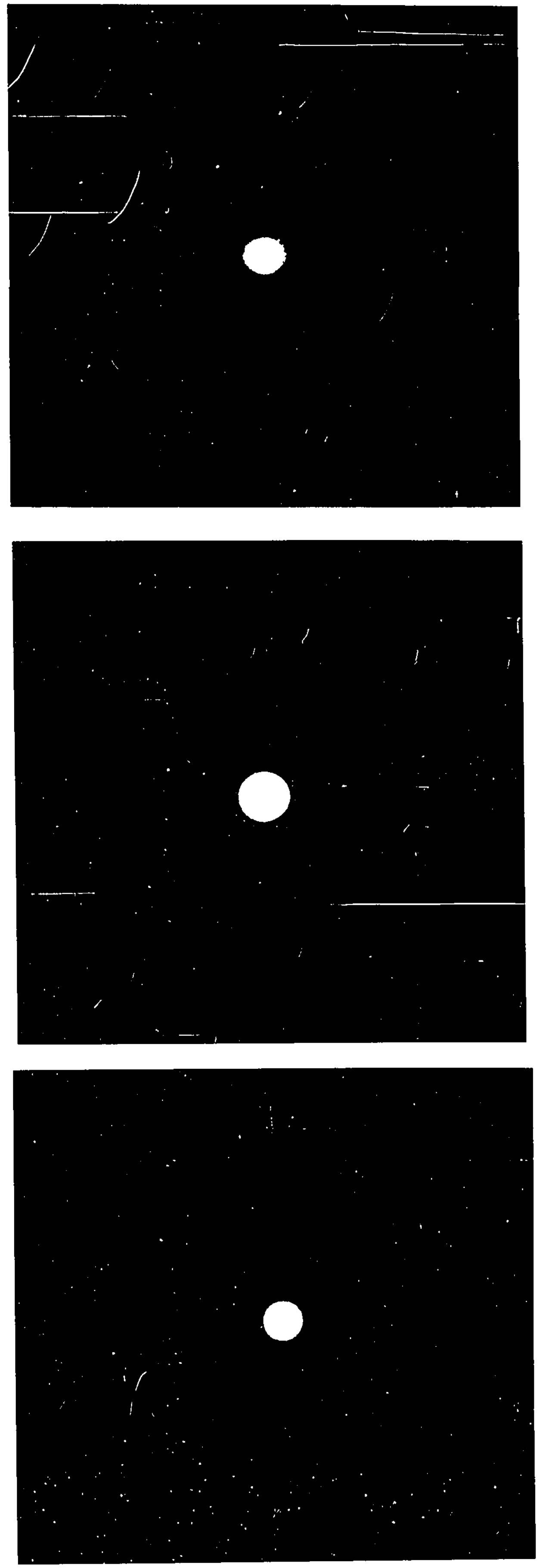

(a)

(b)

(c)

Fig. B3-8

Diffraction patterns formed by (a) the 40 rings flux selector [corresponding to amplitude filter $T(x,M)$], (b) the uniformly transmitting pupil, and (c) the 44 rings flux selector [corresponding to amplitude filter $T(x,5)$], for the case:

$$\phi(x)=1.5\pi x^2$$

(a)

(b)

(c)

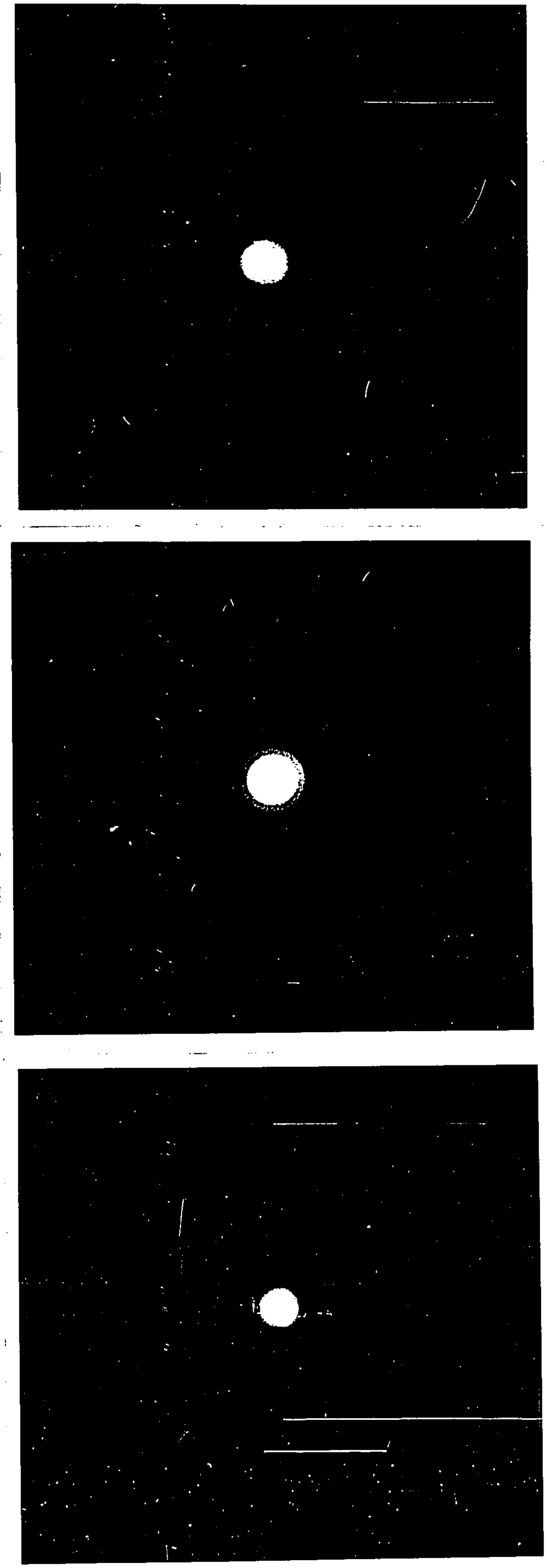

Fig. B3-8

Diffraction patterns formed by (a) the 40 rings flux selector [corresponding to amplitude filter T(x,M)], (b) the uniformly transmitting pupil, and (c) the 44 rings flux selector [corresponding to amplitude filter T(x,5)], for the case: $\phi(x)=1.5\pi x^2$

(a)

(b)

(c)

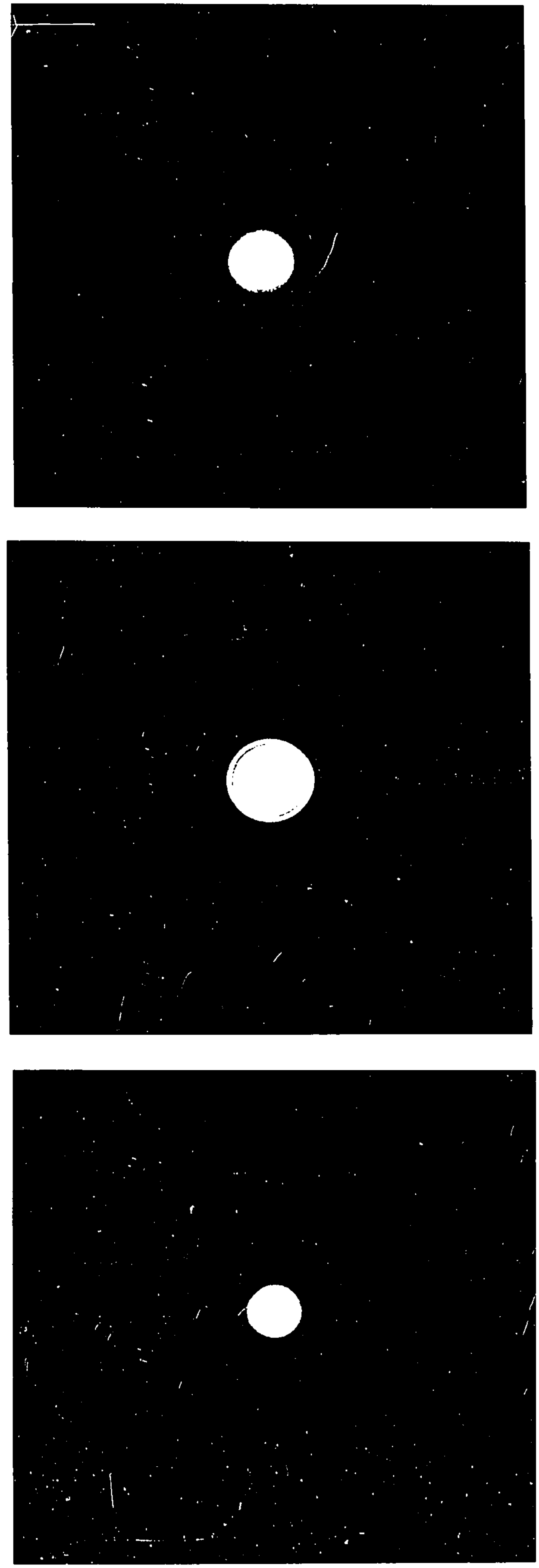

Fig. B3-9

Diffraction patterns formed by (a) the 40 rings flux selector [corresponding to amplitude filter T(x,M)], (b) the uniformly transmitting pupil, and (c) the 44 rings flux selector [corresponding to amplitude filter T(x,5)], for the case:

$$\phi(x) = 2\pi x^2$$

(a)

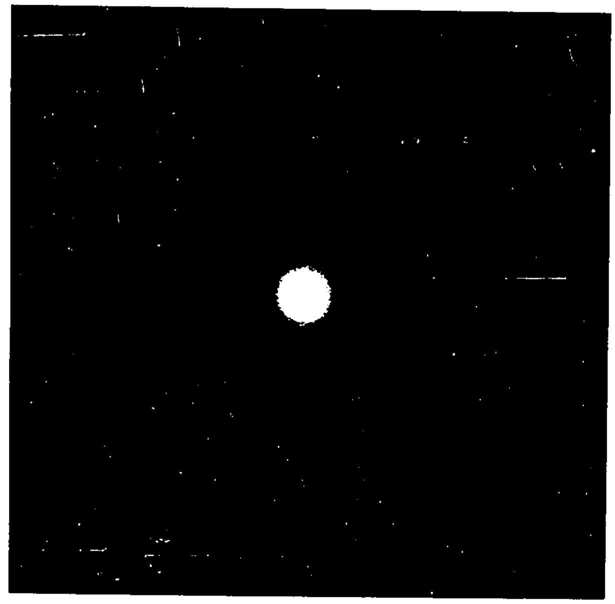

(b)

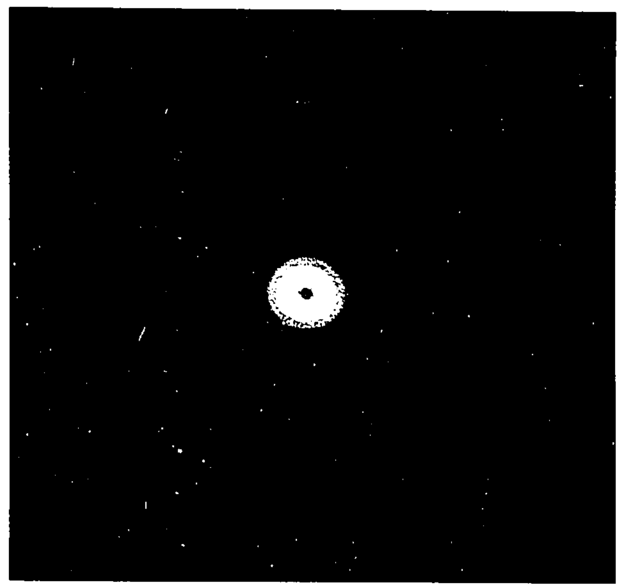

(c)

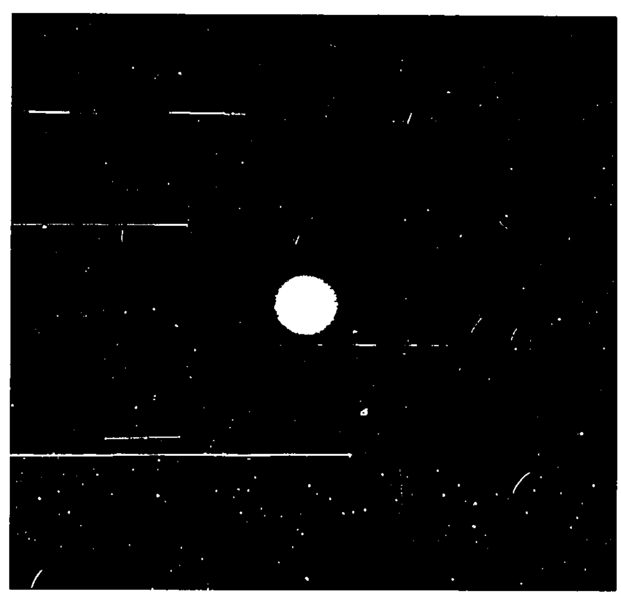

Fig. B3-9

Diffraction patterns formed by (a) the 40 rings flux selector [corresponding to amplitude filter $T(x,M)$], (b) the uniformly transmitting pupil, and (c) the 44 rings flux selector [corresponding to amplitude filter $T(x,5)$], for the case:

$$\phi(x) = 2\pi x^2$$

(a)

(b)

(c)

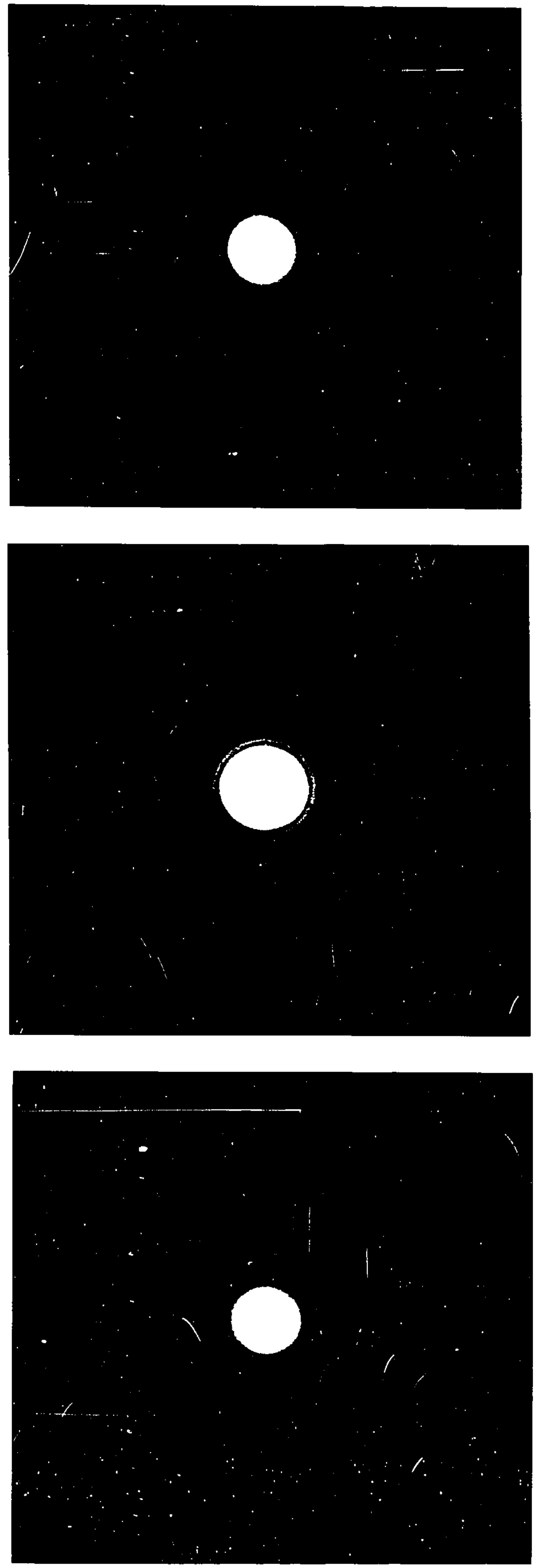

Fig. B3-10

Images(correctly focussed) formed by (a) the 40 rings flux selector [corresponding to amplitude filter T(x,M)], (b) the uniformly transmitting pupil, and (c) the 44 rings flux selector [corresponding to amplitude filter T(x,5)], of an object consisting of a group of points of various intensities.

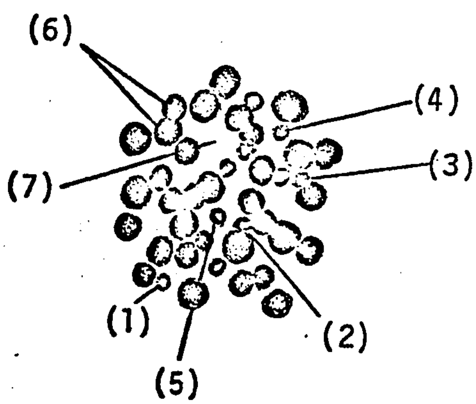

(a)

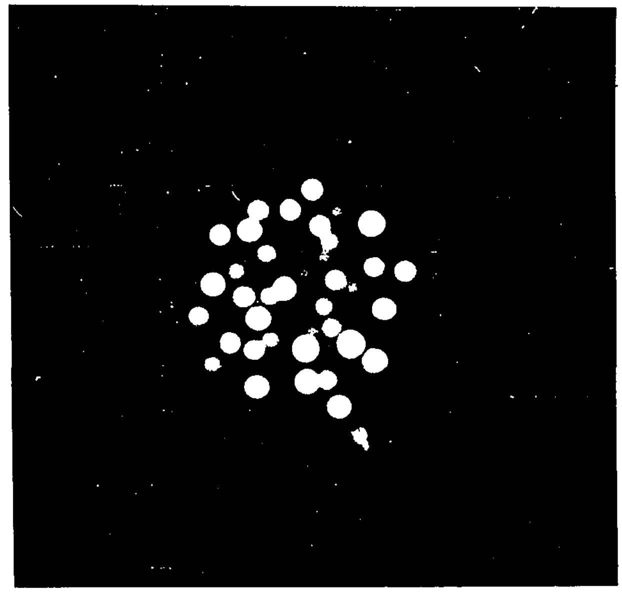

(b)

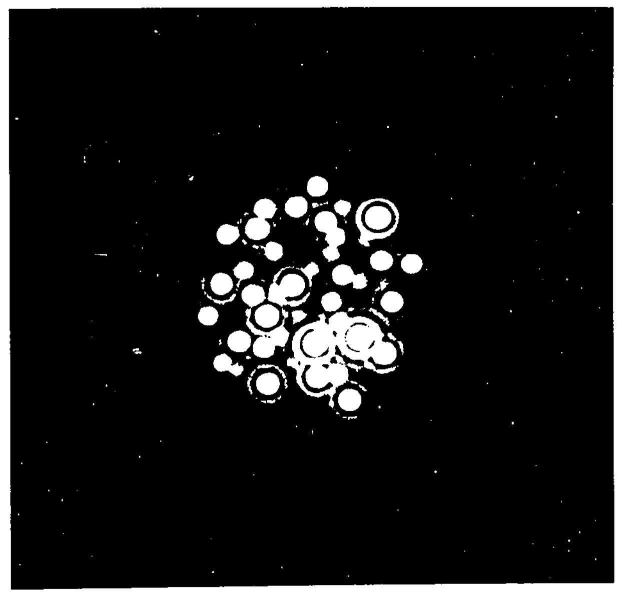

(c)

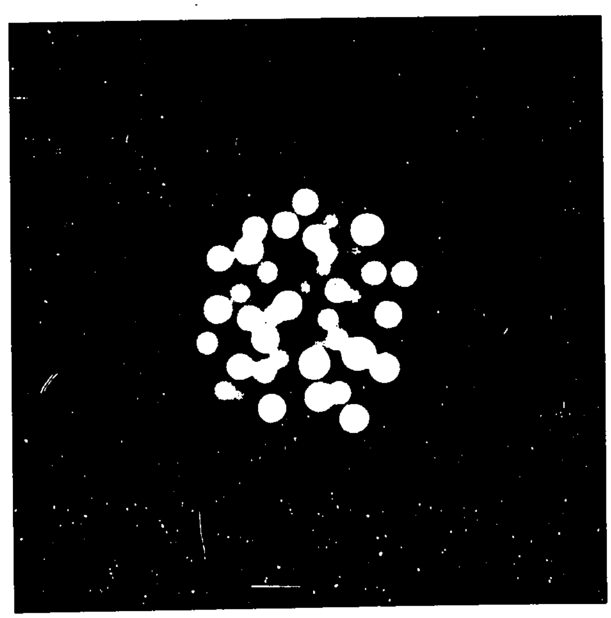

Fig. B3-10

Images(correctly focussed) formed by (a) the 40 rings flux selector [corresponding to amplitude filter T(x,M)], (b) the uniformly transmitting pupil, and (c) the 44 rings flux selector [corresponding to amplitude filter T(x,5)], of an object consisting of a group of points of various intensities.

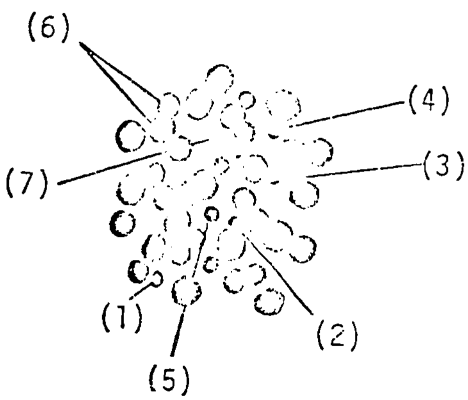

(a)

(b)

(c)

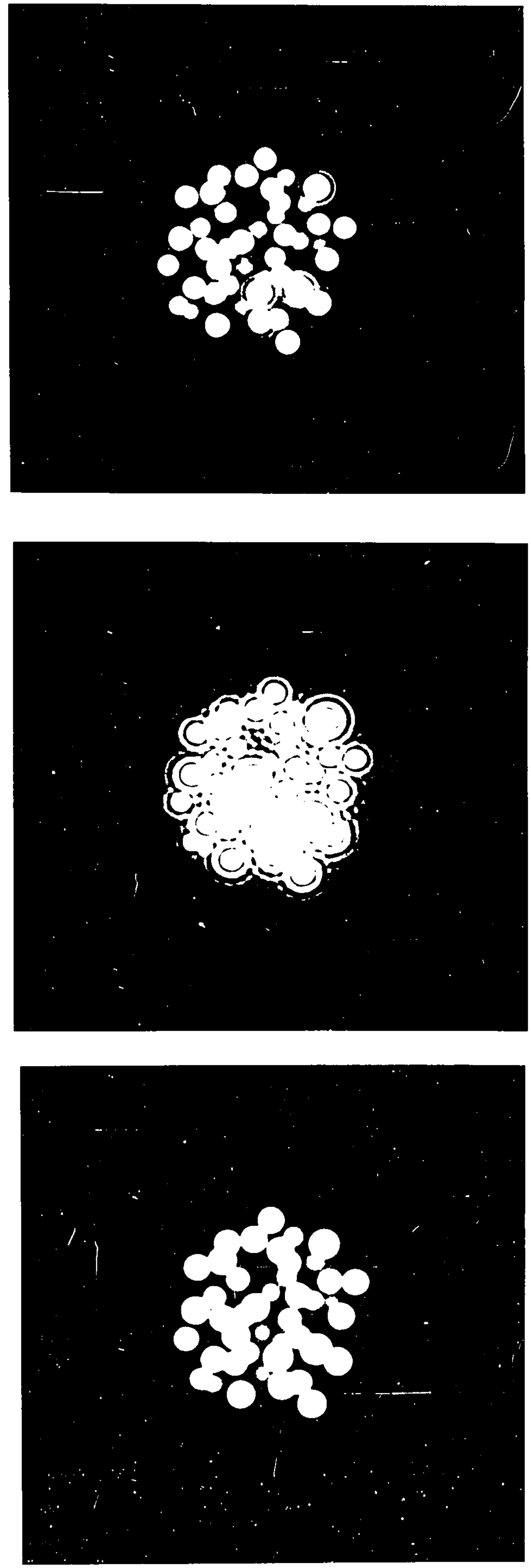

theoretical ratios of central spot width in the F.S. diffraction pattern to that in the Airy pattern are 1.25 and 1.53 for the 40 rings and 44 rings flux selector resp. The corresponding ratios as determined from measurements made on the photographs are 1.19 ±.08 and 1.47 ±.08 resp. The agreement between theoretical and experimental values is good, within the estimated uncertainty in the experimental values.

In Fig. B3-3, B3-4, and B3-5 are shown the diffraction patterns corresponding to the same case as above, but in which the magnification is 3.5 times smaller in order to show the first two principal maxima in the diffraction patterns formed by the flux selectors. From these photographs, the improvement in the concentration of energy towards the center brought by the flux selectors can be readily seen. If we compare the first principal maxima in the diffraction patterns formed by both flux selectors with the corresponding theoretically calculated maxima given in Tables A5-27 and A5-28, we note that:

(1) The general aspect of these maxima agrees very well with the theoretical calculations as far as the number of rings and their relative intensities are concerned.

(2) The diameters of the rings relative to the diameter of the central spot agree to about 1% with the theoretical calculations.

(3) As expected, the principal maxima in the diffraction pattern formed by the 44 rings F.S. are more intense (relative to the intensity at the center of the pattern) than the corresponding maxima for the 40 rings F.S.

In Fig. B3-6 to B3-9 are shown the photographs of the diffraction patterns corresponding to a defect of focus of about $\pi/2$, π, $3\pi/2$, and 2π resp. These photographs were made at the same magnification as those of Fig. B3-2. Generally speaking, the aspect of the diffraction patterns agrees well with the theoretical calculations. In particular, the photographs show the improvement in the depth of focus brought by the flux selectors: as the defect of focus increases, the intensity at the center of the pattern does not drop as fast for the flux selectors as for the uniformly transmitting pupil; also, the concentration of energy towards the center does not deteriorate as fast for the flux selectors and is always much higher than it is for the other pupil. Furthermore, beyond a defect of focus of about $3\pi/2$, the diameter of the central "spot" in the diffraction pattern is actually greater in the case of the uniformly transmitting pupil than in the case of the flux selectors. (This can be best observed by looking at the diffraction patterns from a distance of about 6 feet).

The photographs of the images of a group of points are shown in Fig. B3-10. The magnification is about 50X. The points are very close together; for example, the points (6) are separated from each other by a distance which is almost equal to the Rayleigh resolution limit. The remarkable improvement brought by the flux selectors can be readily appreciated in these photographs. For example, the points (2), (3), (4), and (5) are almost invisible in (b), whereas they can easily be seen in (a), and specially in (c). Furthermore, in (b), the interactions of the diffraction rings associated with the individual points create a confusing background, which sometimes introduces spurious points. (See for example the intersticial region (7) in the photographs). Such a background greatly impairs information retrieval from an image. This background is either greatly reduced [(a)] or eliminated [(c)] with flux selectors. Furthermore, the use of flux selectors does not seem to seriously impair resolution, even for objects which contain fine details, which is the case in Fig. B3-10.

Conclusions

From the photographs shown in Fig. B3-2 to B3-10 resp., we conclude that flux selectors can be used to improve the quality of images formed by optical systems. The improvement brought by flux selectors to optical systems in the presence of spherical aberration has not been verified; however, the work done with aberration-free optical systems with and without defect of focus has shown that the flux selectors form diffraction patterns which are in good agreement with the theoretical calculations. Hence, we expect that the flux selectors will also improve the images formed when spherical aberration is present, as was predicted theoretically in chapter 3.

What type of flux selector is best, i.e., corresponding to filter T(x,M) or T(x,5), would depend on the particular application considered. In our work, we have found the F.S. corresponding to T(x,5) better. However, in other applications, where maximum image intensity would be desired, or where a compromise would be sought between the reduction of the intensity of the diffraction rings and the increase in the central spot diameter, the F.S. corresponding to T(x,M) would be better.

The only practical limitations of the flux selectors are the presence of the principal maxima and the reduction of image illuminance. By constructing flux selectors with a sufficiently large number of rings, the principal maxima can be rejected far enough from the center so that they do not limit the useful image field of the optical system. A flux selector having 500 rings, for example, would give an image field of about 2°, which is sufficiently extended for many applications; making such a flux selector is by no means impossible.

The reduced intensity in the images formed by flux selectors would probably not be a serious limitation in the applications where flux selectors could be used; with modern research tools, such as image intensifiers, high-gain photomultipliers, high-sensitivity photographic emulsions, etc..., the most serious limitation in an image is not so much a low intensity as a low signal-to-noise ratio. As can be seen in Fig. B3-10, flux selectors can be used to improve this ratio.

We conclude this thesis by giving a few examples of possible applications of flux selectors.

(1) Plasma Physics: The study of small angle forward scattering of light by a plasma in which a laser beam is focussed; the amount of light in the diffraction rings seriously impairs the signal-to-noise ratio; flux selectors greatly reduce the amount of light in the diffraction rings, and hence could be used to improve the signal to noise ratio.

(2) Astronomical observations: Flux selectors could be used to detect faint stars in star clusters; to improve the accuracy of brightness measurements of faint stars, when they are surrounded by relatively bright stars; in a coronograph, to improve observations and measurements made on the solar corona.

(3) Storage of information, microfilm and microcircuits industries: Flux selectors could be used to enhance the contrast and reduce the background noise in the micro-images.

(4) Microscopy: Flux selectors would be useful not only to improve the contrast but also to increase the depth of focus of the images.

REFERENCES:

(1) Lord Rayleigh, Phil. Mag. (5), 8(1879), 261

(2) Sparrow, C., 1916, Astrophys. J. 44, 76

(3) Wilkins, J.E., 1950, J. Opt. Soc. Am. 40, 222;

(4) Gal'Pern, D. Yu., 1960, Optics and Spectroscopy 9[4] 291

(5) Wilkins, J.E., 1961, J. Opt. Soc. Am. 51, 911

(6) Jacquinot, P., and Roizen-Dossier, B. "Apodisation" (Progress in Optics, Vol. 111, 1964)

(7) Lansraux, G. and Boivin, G. 1961 Can J. Phys., 39, 158

(8) Lansraux, G. 1953 Diffraction Instrumentale (Ed. de la Revue d'Optique, Paris) Chap I

(9) R. Fletcher, M.J.D. Powell, 1963, Computer Journal, Vol 6, ISS 2.

(10) I.S. Berezin, N.P. Zhidkov, 1965 "Computing Methods, Vol. I" Pergamon Press

(11) M. Born and E. Wolf "Principles of Optics" 2nd ed. (Pergamon Press)

(12) M. Francon "Modern Applications of Physical Optics" Interscience Publishers

(13) Watson, G.N. "Theory of Bessel's Functions" Cambridge University Press, Chap VII

(14) Allen, E.E. 1956 M.T.A.C. Note 169, Vol 10.

(15) M. Francon, 1966 "Optical Interferometry" Chap V. Academic Press.

(17) G. Lansraux, Cahiers de Physique, No 45, Septembre 1953.

(18) G. Lansraux, Unpublished work.

APPENDIX A

Distortion introduced in the image of a plane object formed by a thin lens when the object is not perpendicular to the optical axis.

We introduce a cartesian co-ordinate system having its origin at the optical center O of a thin lens L, the x-axis coinciding with the optical axis. A linear object of length 2ℓ is centered on the optical axis and tilted to it at an angle θ. Let x_o be the abscissa of the center Q of this object, and x_o' the abscissa of the image point Q'. The image of the object formed by the lens will not be linear; however, if the lengths of the object and image are small compared to x_o and x_o' resp., then the curvature of the image will be small; furthermore, if the depth of focus of the lens is sufficiently large, then it is possible to record by means of a flat photographic plate, or observe by means of a travelling microscope, a linear image. (This was the case in our work, where no curvature of the image plane could be detected.) However, if the object is not perpendicular to the optical axis, this image will be distorted, as we shall now show.

Following the comments made above, we assume that the image is linear and tilted with respect to the optical axis at an angle θ'. See diagram below:

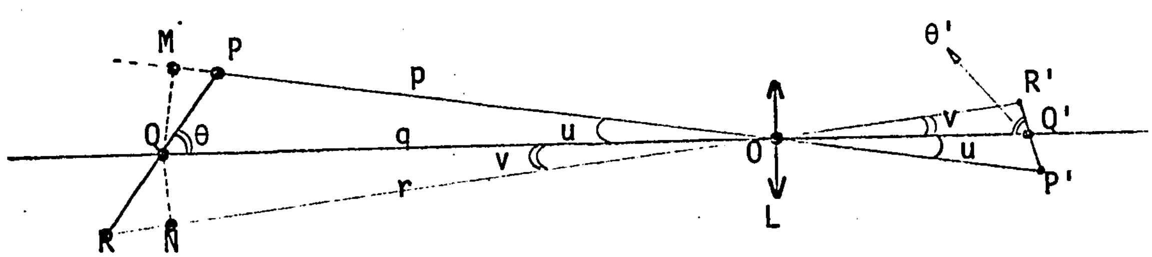

We have PQ = QR = ℓ. What are the corresponding lengths P'Q' and Q'R' ?

From the triangles PQO and P'Q'O, we have

$$\frac{\sin u}{PQ} = \frac{\sin\theta}{PO} \quad \text{and} \quad \frac{\sin u}{P'Q'} = \frac{\sin(\pi-\theta')}{P'O}$$

from which $P'Q' = PQ \, \frac{P'O}{PO} \, \frac{\sin\theta}{\sin\theta'}$

Since P and P' are conjugate points,

$$\frac{1}{PO} + \frac{1}{P'O} = \frac{1}{f} \qquad (f = \text{focal length of } L)$$

$$\frac{P'O}{PO} = \frac{f}{PO-f} \,. \qquad \text{Putting } PO \equiv p \text{ ,we have}$$

$$P'Q' = \ell \, \frac{f}{p-f} \, \frac{\sin\theta}{\sin\theta'}$$

Similarly, $Q'R' = \frac{\ell f}{r-f} \, \frac{\sin\theta}{\sin\theta'}$ with $r \equiv RO$.

Drawing QM and QN so that MO and NO are equal to q,

we have $p = q - PM \simeq q - \ell\cos\theta$

$r = q + RN \simeq q + \ell\cos\theta$

so that

$$P'Q' = \frac{f}{q-\ell\cos\theta-f} \, \frac{\sin\theta}{\sin\theta'} \, \ell \simeq \frac{f}{q-f} \, \frac{\sin\theta}{\sin\theta'} \, \ell \left(1 + \frac{\ell\cos\theta}{q-f}\right)$$

$$Q'R' = \frac{f}{q+\ell\cos\theta-f} \, \frac{\sin\theta}{\sin\theta'} \, \ell \simeq \frac{f}{q-f} \, \frac{\sin\theta}{\sin\theta'} \, \ell \left(1 - \frac{\ell\cos\theta}{q-f}\right)$$

Hence, the total length of the image, P'R', is

$\frac{2f}{q-f} \, \frac{\sin\theta\ell}{\sin\theta'}$.If θ and, hence, θ' are equal to $\pi/2$ (object and image perpendicular to the axis), there is no distortion: $P'Q' = Q'R' =$

$\frac{f\ell}{q-f} = \frac{Q'O}{QO}\,\ell$, as expected. If $\theta \neq \pi/2$, then distortion is introduced as follows:

(1) the image is uniformly contracted or expanded by the factor $\frac{\sin\theta}{\sin\theta'}$,

(2) to an object of length 2ℓ centered at Q corresponds an image whose center is shifted a distance

$$\Delta = \frac{f \sin\theta \cos\theta\, \ell^2}{(q - f)^2 \sin\theta'}$$

above or below the axis; note that Δ depends on ℓ .

For example, consider an object consisting of a series of concentric circles centered at Q, in the above diagram, and located in a plane perpendicular to the page and passing through the line PR; the image will consist of a series of distorted circles whose centers progressively move away from the optical axis (along P'R') as the radii of the circles increase. Also, the diameters of the circles measured along P'R' will differ from the corresponding diameters measured along an axis perpendicular to the page by a factor $\frac{\sin\theta}{\sin\theta'}$. However, if the diameters measured along P'R' are normalized and compared to the true diameters, no difference will be noted.

Thus, in the case of a flux selector negative, when comparing the measurements made on the photographic plate with the actual values in order to see if there is any distortion, one must:-

(1) calculate the actual diameters and the centers of the inner and outer edges of the rings, and check that there is no shift of the center.

(2) compare the actual diameters measured along one axis with those measured along an axis at 90° to that one.

(3) normalize the diameters and compare these with the theoretical values.

NOTE: In the above analysis, we have assumed that the lens was thin; however, all the equations used are equally valid for a compound lens, provided that object and image distances are referred to their respective nodal planes. Hence, the conclusions drawn from the above analysis are valid for our work.

APPENDIX B

Channelled spectrum formed by a collimated beam of white light reflected from a thin film bounded on one side by air and on the other by an opaque metallic coating.

Consider a collimated beam of light of wavelength λ incident at an angle θ on a uniform layer of refractive index n and thickness d, bounded on one side by air, and on the other by an opaque metallic layer having a reflection coefficient r_s ; let the phase change on reflection from the metal be ϕ_s (a function depending on λ, n, θ', and the state of polarization of the light beam). Assume the light beam to be polarized either parallel or perpendicular to the plane of incidence. Let the reflection coefficient of the medium be r_n (including phase term) for an air-medium reflection.

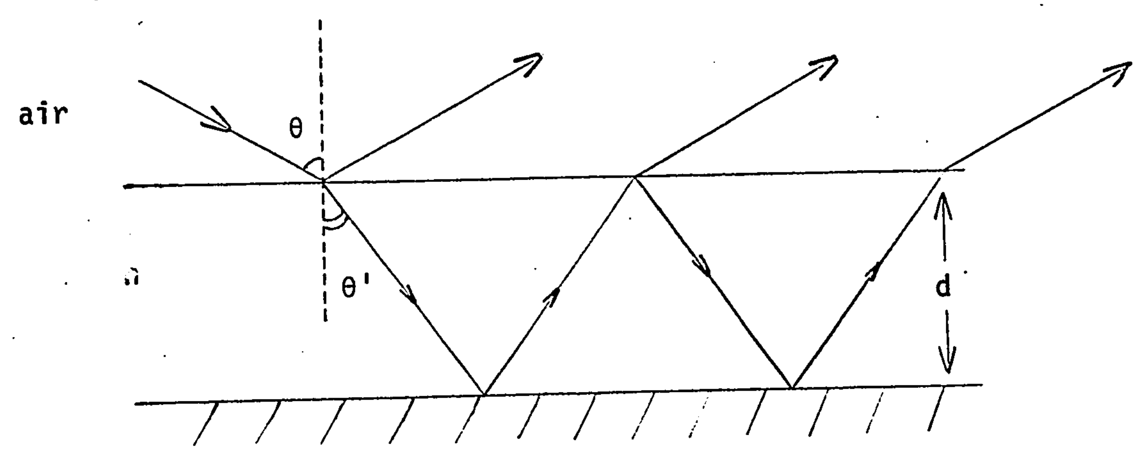

If A_i is the amplitude of the incident beam, then in the focal plane of a collecting lens, the reflected beam will have an amplitude A_r determined by summing the contributions of all the multiple reflections inside the layer. Thus we have

$$A_r = A_i\, r_n + A_i T r_s\, e^{i(\phi_s + \delta)} - A_i T r_s^2\, r_n\, e^{i(2\phi_s + 2\delta)}$$

$$+ A_i T\, r_s^3\, r_n^2\, e^{i3\phi_s+3\delta} - \ldots = A_i r_n + A_i T r_s\, e^{i(\phi_s+\delta)}[1-r_n r_s e^{i(\phi_s+\delta)} + \ldots]$$

where T = transmissivity of the film surface and δ = phase difference arising from the path difference between two successive reflections i.e., $\delta = 4\pi nd \cos\theta'/\lambda$

Assuming an infinite number of terms, we have

$$A_r = \frac{A_i\,[r_n + r_s\, e^{i(\phi_s+\delta)}]}{1 + r_n r_s\, e^{i(\phi_s+\delta)}}$$

where we have assumed no absorption by the medium, i.e., $T = 1 - r_n^2 = 1-R$ where R is the reflectivity of the medium n. Therefore, the intensity of the reflected beam is:

$$I_r = I_i\, \frac{(r_n + r_s)^2 - 4\, r_n\, r_s \sin^2 \left(\frac{\phi_s+\delta}{2}\right)}{(1 + r_n r_s)^2 - 4\, r_n r_s \sin^2 \left(\frac{\phi_s+\delta}{2}\right)} \qquad (1)$$

Now, if instead of a monochromatic beam, we have a beam of white light, and if the reflected beam is dispersed by a prism (or grating) and observed with a telescope, the spectrum will be crossed by dark bands, corresponding to wavelengths for which (1) is a minimum. In order to find the position of these minima (and the maxima) we write (1) as

$$I_r = I_i\, \frac{(a - b \sin^2 x)}{c - b \sin^2 x}$$

For a minimum or a maximum, $dI_r/dx = 0$ i.e., $\frac{(a-c)\, b \sin 2x}{(c-b \sin^2 x)^2} = 0$

Since the denominator cannot be equal to zero ($r_n r_s \neq 1$ in practice) we have that either a = c, or b = 0, or $x = \frac{m\pi}{2}$, m = 0, 1, 2, ...

The case a = c is impossible in practice since it requires both r_n and r_s to equal 1. The case b=o (i.e. r_n and/or r_s equal to zero) does not apply to the problem we are considering. When m is odd, we have $I_r = \frac{a - b}{c - b}$ and when m is even $I_r = a/c$. Which case corresponds to a maximum, and which to a minimum depends on the angle of incidence θ. If the latter is adjusted so that $a = 0$, i.e. $r_n = -r_s$, then odd values of m will correspond to maxima, and even m to minima; it is desirable to have $r_n = -r_s$ because the visibility of the fringes, defined as $V = \frac{I\ max - I\ min}{I\ max + I\ min}$, is unity in that case. In practice, this condition can be realized for only one wavelength, but if the medium n is not too dispersive, and if r_s does not vary too rapidly with wavelength, then one should be able to find a spectral region where the visibility of the fringes would be almost optimum. For metals having a relatively high reflectivity, the conditions above will be realized for a near-grazing angle of incidence on the medium. The positions of the minima are given by $\delta + \phi_s = 2\ m\pi \quad m = 0, 1, 2, \ldots$

i.e., $2nd\cos\theta' = (m - \phi_s')\lambda$ where $\phi_s' = \phi_s/2\pi$

Now, ϕ_s depends on n , θ' , λ, and the state of polarization of the light beam. Because of this latter dependence, the light beam has to be polarized either parallel or perpendicular to the plane of incidence in order to have fringes of good visibility; otherwise, if the beam is unpolarized, say, then the resulting fringes will consist of two sets of fringes: those corresponding to the parallel component, and those corresponding to the perpendicular component; since these two sets of fringes do not have their minima at the same wavelengths, the resulting fringes will have poor visibility.

APPENDIX C

IBM Computer Programs

The main programs which have been used to perform the calculations described in this thesis are listed on the following pages. The programs are listed in the order in which the associated calculations appear in the thesis. A small paragraph at the beginning of each program listing identifies the particular calculation performed by the program. The programs are written either in Fortran II (for the IBM 1620) or in Fortran IV (for the IBM 360).

N.B. The symbols > and < are to be interpreted as meaning = and + respectively.

```
C  PROGRAM TO DETERMINE THE PUPIL FUNCTION T(X,M) WHOSE CORRESPONDING
C  ENCIRCLED ENERGY CURVE IS THE BEST APPROXIMATION,IN THE LEAST SQUARE
C  SENSE, AND FOR A GIVEN DOMAIN OF W, TO THE ENVELOPE CURVE OF THE
C  ABSOLUTE MAXIMA OF ENCIRCLED ENERGY FACTORS  L.P. BOIVIN 8/3/68
      DOUBLE PRECISION W(16),P(5,5,16),PX(5,5),A(5),EMAX(16),X,DEL,AO,
     1 S,SO,SP,SMS,ALPHA,QN,QD
      DOUBLE PRECISION DABS,SIT(10,5),AIT(10,5),DER1,DER2,O
      M=1
      KK = 10
      NI=10
      L1 = KK-2
      L2 = KK-1
      L3 = KK
      READ(1,1) (W(I),I=1,M)
      READ(1,2) (((P(I,J,K),I=1,5),J=1,5),K=1,M)
      READ(1,3) ((PX(I,J),I=1,5),J=1,5)
      READ(1,4) (EMAX(I),I=1,M)
      READ(1,5) (A(I),I=1,5)
      X= .1DO0
      DO 50 JJ=1,NI
    7 DO 9 II=1,KK
      WRITE(3,21) II
C  RENVERSEMENT DE L'ORDRE DES ITERATIONS  VERSION 2
      DO 9 IJ=1,4
      I=6-IJ
C FIN
      NUM=0
      DEL= DABS(A(I)*X)
   10 AO=A(I)
      NUM=NUM + 1
      S=0.0D0
      QD = A(1)*A(1)*PX(1,1) + A(2)*A(2)*PX(2,2) + A(3)*A(3)*PX(3,3) +
     1A(4)*A(4)*PX(4,4) + A(5)*A(5)*PX(5,5) + 2.0D0*(A(1)*(A(2)*PX(1,2)
     2+ A(3)*PX(1,3) + A(4)*PX(1,4) + A(5)*PX(1,5)) + A(2)*(A(3)*PX(2,3)
     3 + A(4)*PX(2,4) + A(5)*PX(2,5)) + A(3)*(A(4)*PX(3,4) + A(5)*PX(3,
     4 5)) + A(4)*A(5)*PX(4,5))
      DO 32 L=1,M
      QN= A(1)*A(1)*P(1,1,L) + A(2)*A(2)*P(2,2,L) + A(3)*A(3)*P(3,3,L) +
     1 A(4)*A(4)*P(4,4,L) + A(5)*A(5)*P(5,5,L) + 2.0D0*(A(1)*(A(2)*P(1,
     2 2,L) + A(3)*P(1,3,L) + A(4)*P(1,4,L) + A(5)*P(1,5,L)) + A(2)*(
     3 A(3)*P(2,3,L) + A(4)*P(2,4,L) + A(5)*P(2,5,L)) + A(3)*(A(4)*P(3,
     4 4,L) + A(5)*P(3,5,L)) + A(4)*A(5)*P(4,5,L))
   32 S # S &(EMAX%L< - QN/QD )*(EMAX(L) - QN/QD)
      SO=S
      A(I) = AO + DEL
      S=0.0D0
      QD = A(1)*A(1)*PX(1,1) + A(2)*A(2)*PX(2,2) + A(3)*A(3)*PX(3,3) +
     1A(4)*A(4)*PX(4,4) + A(5)*A(5)*PX(5,5) + 2.0D0*(A(1)*(A(2)*PX(1,2)
     2+ A(3)*PX(1,3) + A(4)*PX(1,4) + A(5)*PX(1,5)) + A(2)*(A(3)*PX(2,3)
     3 + A(4)*PX(2,4) + A(5)*PX(2,5)) + A(3)*(A(4)*PX(3,4) + A(5)*PX(3,
     4 5)) + A(4)*A(5)*PX(4,5))
      DO 33 L=1,M
      QN= A(1)*A(1)*P(1,1,L) + A(2)*A(2)*P(2,2,L) + A(3)*A(3)*P(3,3,L) +
     1 A(4)*A(4)*P(4,4,L) + A(5)*A(5)*P(5,5,L) + 2.0D0*(A(1)*(A(2)*P(1,
     2 2,L) + A(3)*P(1,3,L) + A(4)*P(1,4,L) + A(5)*P(1,5,L)) + A(2)*(
     3 A(3)*P(2,3,L) + A(4)*P(2,4,L) + A(5)*P(2,5,L)) + A(3)*(A(4)*P(3,
     4 4,L) + A(5)*P(3,5,L)) + A(4)*A(5)*P(4,5,L))
   33 S # S &(EMAX%L< - QN/QD )*(EMAX(L) - QN/QD)
```

```
      SP=S
      A(I) = AO - DEL
      S=0.0D0
      QD = A(1)*A(1)*PX(1,1) + A(2)*A(2)*PX(2,2) + A(3)*A(3)*PX(3,3) +
     1A(4)*A(4)*PX(4,4) + A(5)*A(5)*PX(5,5) + 2.0D0*(A(1)*(A(2)*PX(1,2)
     2+ A(3)*PX(1,3) + A(4)*PX(1,4) + A(5)*PX(1,5)) + A(2)*(A(3)*PX(2,3)
     3 + A(4)*PX(2,4) + A(5)*PX(2,5)) + A(3)*(A(4)*PX(3,4) + A(5)*PX(3,
     4 5)) + A(4)*A(5)*PX(4,5))
      DO 34 L=1,M
      QN= A(1)*A(1)*P(1,1,L) + A(2)*A(2)*P(2,2,L) + A(3)*A(3)*P(3,3,L) +
     1 A(4)*A(4)*P(4,4,L) + A(5)*A(5)*P(5,5,L) + 2.0D0*(A(1)*(A(2)*P(1,
     2 2,L) + A(3)*P(1,3,L) + A(4)*P(1,4,L) + A(5)*P(1,5,L)) + A(2)*(
     3 A(3)*P(2,3,L) + A(4)*P(2,4,L) + A(5)*P(2,5,L)) + A(3)*(A(4)*P(3,
     4 4,L) + A(5)*P(3,5,L)) + A(4)*A(5)*P(4,5,L))
   34 S # S &(EMAX%L< - QN/QD )*(EMAX(L) - QN/QD)
      SMS=S
      ALPHA = (SP - 2.0D0*SO + SMS)/(2.0D0*DEL*DEL)
      IF(ALPHA) 11,11,12
   11 IF(SP - SMS) 13,13,14
   13 A(I) = AO + 3.0D0*DEL
      GO TO 10
   14 A(I) = AO - 3.0D0*DEL
      GO TO 10
   12 A(I) = AO - (SP-SMS)/(4.0D0*DEL*ALPHA)
      IF(DABS(A(I) - AO) - .1D-05 )  15,16,16
   16 IF(DABS(A(I) -AO) - 2.0D0*DEL) 17,17,18
   17 DEL = DEL*.2D0
      GO TO 10
   18 GO TO 10
   15 S=0.0D0
      QD = A(1)*A(1)*PX(1,1) + A(2)*A(2)*PX(2,2) + A(3)*A(3)*PX(3,3) +
     1A(4)*A(4)*PX(4,4) + A(5)*A(5)*PX(5,5) + 2.0D0*(A(1)*(A(2)*PX(1,2)
     2+ A(3)*PX(1,3) + A(4)*PX(1,4) + A(5)*PX(1,5)) + A(2)*(A(3)*PX(2,3)
     3 + A(4)*PX(2,4) + A(5)*PX(2,5)) + A(3)*(A(4)*PX(3,4) + A(5)*PX(3,
     4 5)) + A(4)*A(5)*PX(4,5))
      DO 35 L=1,M
      QN= A(1)*A(1)*P(1,1,L) + A(2)*A(2)*P(2,2,L) + A(3)*A(3)*P(3,3,L) +
     1 A(4)*A(4)*P(4,4,L) + A(5)*A(5)*P(5,5,L) + 2.0D0*(A(1)*(A(2)*P(1,
     2 2,L) + A(3)*P(1,3,L) + A(4)*P(1,4,L) + A(5)*P(1,5,L)) + A(2)*(
     3 A(3)*P(2,3,L) + A(4)*P(2,4,L) + A(5)*P(2,5,L)) + A(3)*(A(4)*P(3,
     4 4,L) + A(5)*P(3,5,L)) + A(4)*A(5)*P(4,5,L))
   35 S # S &(EMAX%L< - QN/QD )*(EMAX(L) - QN/QD)
      SIT(II,I) = S
      AIT(II,I) = A(I)
    9 WRITE(3,20)I, NUM,S,A(I)
      DO 50 J=1,5
   50 A(J) = .5D0*(AIT(L1,J) + AIT(L3,J))-.5D0*(SIT(L3,J) -SIT(L1,J))/((
     1 SIT(L3,J) - SIT(L2,J))/(AIT(L3,J) - AIT(L2,J)) - (SIT(L2,J) -
     2 SIT(L1,J))/(AIT(L2,J) - AIT(L1,J)))
    1 FORMAT(5F16.8)
    2 FORMAT(18X,D24.16)
    3 FORMAT(13X,D22.16)
    4 FORMAT(2D25.16)
    5 FORMAT(5D16.8)
    6 FORMAT('1 VALUES OF W ARE ' //5F10.2/// ' INITIAL VALUES OF A(I)
     1 ARE '//5D16.8////' INITIAL VALUE OF S IS '//D22.16 /////)
   21 FORMAT(/////' ITERATION # ' I2////)
   20 FORMAT(' I= ' I2, '   NUM. OF ITER.= 'I3,' VALUE OF S = 'D22.16,
```

```
1 ' VALUE OF A(I) = ' D16.8)
 STOP
 END
```

```
C   PROGRAM TO DETERMINE T(X,M) USING THE IBM DFMFP LIBRARY SUBROUTINE
C   L.P. BOIVIN 10/6/68
        EXTERNAL ENERG
        DOUBLE PRECISION P(5,5,20),PX(5,5),A(5),S,F,GRAD(5),ENERG,W(10),
       1 H(30)
        DOUBLE PRECISION EMAX(20)
        COMMON P,PX
        COMMON EMAX
        COMMON M
        M>10
        READ(1,1) ( W(I),I>1,M)
        READ(1,2) (((P(I,J,K),I>1,5),J>1,5),K>1,M)
        READ(1,3) ((PX(I,J),I>1,5),J>1,5)
        READ(1,4) (EMAX(I),I>1,M)
      4 FORMAT(2D25.16)
C   AJUSTEMENT DES COEFFICIENTS
        DO 44 J>1,5
        S> J
     44 A(J) > A(J)/S
C FIN
        N>5
        EPS > .1E-10
        LIMIT > 400
        EST> .4300
        WRITE(3,24) ( W(I),I>1,M)
        WRITE(3,25) ( A(I),I>1,5)
     24 FORMAT(:1 W(I) SONT : //(5F16.8)///)
     25 FORMAT(: INITIAL VALUES OF COEFFICIENTS ARE://5D16.8///)
        LIMIT> 200
        DO 9 K>1,8
        READ(1,5) (A(I),I>1,5)
        LIMIT > LIMIT < 25
        CALL DFMFP(ENERG,N,A,F,GRAD,EST,EPS,LIMIT,IER,H)
        WRITE(3,7) A,F,GRAD,IER
        WRITE(2,10) A
     10 FORMAT(5D16.8)
      9 CONTINUE
      7 FORMAT(///: COEFFICIENTS A SONT :// 5D16.8/// : VALEUR DE S : //
       1 D22.16///: GRADIENT : // 5D16.8///: PARAMETRE D ERREUR ://I2///)
      1 FORMAT(5F16.8)
      2 FORMAT(18X,D24.16)
      3 FORMAT(13X,D22.16)
      5 FORMAT(5D16.8)
        STOP
        END
```

```
C                                                                       D
C     ..................................................................D
C                                                                       D
C        SUBROUTINE DFMFP                                               D
C                                                                       D
C        PURPOSE                                                        D
C           TO FIND A LOCAL MINIMUM OF A FUNCTION OF SEVERAL VARIABLES  D
C           BY THE METHOD OF FLETCHER AND POWELL                        D
C                                                                       D
C        USAGE                                                          D
C           CALL DFMFP(FUNCT,N,X,F,G,EST,EPS,LIMIT,IER,H)               D
C                                                                       D
C        DESCRIPTION OF PARAMETERS                                      D
C           FUNCT  - USER-WRITTEN SUBROUTINE CONCERNING THE FUNCTION TO D
C                    BE MINIMIZED. IT MUST BE OF THE FORM               D
C                    SUBROUTINE FUNCT(N,ARG,VAL,GRAD)                   D
C                    AND MUST SERVE THE FOLLOWING PURPOSE               D
C                    FOR EACH N-DIMENSIONAL ARGUMENT VECTOR  ARG,       D
C                    FUNCTION VALUE AND GRADIENT VECTOR MUST BE COMPUTEDD
C                    AND, ON RETURN, STORED IN VAL AND GRAD RESPECTIVELYD
C                    ARG,VAL AND GRAD MUST BE OF DOUBLE PRECISION.      D
C           N      - NUMBER OF VARIABLES                                D
C           X      - VECTOR OF DIMENSION N CONTAINING THE INITIAL       D
C                    ARGUMENT WHERE THE ITERATION STARTS. ON RETURN,    D
C                    X HOLDS THE ARGUMENT CORRESPONDING TO THE          D
C                    COMPUTED MINIMUM FUNCTION VALUE                    D
C                    DOUBLE PRECISION VECTOR.                           D
C           F      - SINGLE VARIABLE CONTAINING THE MINIMUM FUNCTION    D
C                    VALUE ON RETURN, I.E. F=F(X).                      D
C                    DOUBLE PRECISION VARIABLE.                         D
C           G      - VECTOR OF DIMENSION N CONTAINING THE GRADIENT      D
C                    VECTOR CORRESPONDING TO THE MINIMUM ON RETURN,     D
C                    I.E. G=G(X).                                       D
C                    DOUBLE PRECISION VECTOR.                           D
C           EST    - IS AN ESTIMATE OF THE MINIMUM FUNCTION VALUE.      D
C                    SINGLE PRECISION VARIABLE.                         D
C           EPS    - TESTVALUE REPRESENTING THE EXPECTED ABSOLUTE ERROR.D
C                    A REASONABLE CHOICE IS 10**(-16), I.E.             D
C                    SOMEWHAT GREATER THAN 10**(-D), WHERE D IS THE     D
C                    NUMBER OF SIGNIFICANT DIGITS IN FLOATING POINT     D
C                    REPRESENTATION.                                    D
C                    SINGLE PRECISION VARIABLE.                         D
C           LIMIT  - MAXIMUM NUMBER OF ITERATIONS.                      D
C           IER    - ERROR PARAMETER                                    D
C                    IER = 0 MEANS CONVERGENCE WAS OBTAINED             D
C                    IER = 1 MEANS NO CONVERGENCE IN LIMIT ITERATIONS   D
C                    IER =-1 MEANS ERRORS IN GRADIENT CALCULATION       D
C                    IER = 2 MEANS LINEAR SEARCH TECHNIQUE INDICATES    D
C                    IT IS LIKELY THAT THERE EXISTS NO MINIMUM.         D
C           H      - WORKING STORAGE OF DIMENSION N*(N+7)/2.            D
C                    DOUBLE PRECISION ARRAY.                            D
C                                                                       D
C                                                                       D
C        REMARKS                                                        D
C            I) THE SUBROUTINE NAME REPLACING THE DUMMY ARGUMENT  FUNCT D
C               MUST BE DECLARED AS EXTERNAL IN THE CALLING PROGRAM.    D
C           II) IER IS SET TO 2 IF , STEPPING IN ONE OF THE COMPUTED    D
C               DIRECTIONS, THE FUNCTION WILL NEVER INCREASE WITHIN     D
C               A TOLERABLE RANGE OF ARGUMENT.                          D
C               IER = 2 MAY OCCUR ALSO IF THE INTERVAL WHERE F          D
```

```
C                    INCREASES IS SMALL AND THE INITIAL ARGUMENT WAS               DI
C                    RELATIVELY FAR AWAY FROM THE MINIMUM SUCH THAT THE            DI
C                    MINIMUM WAS OVERLEAPED. THIS IS DUE TO THE SEARCH             DI
C                    TECHNIQUE WHICH DOUBLES THE STEPSIZE UNTIL A POINT            D
C                    IS FOUND WHERE THE FUNCTION INCREASES.                        D
C                                                                                  D
C             SUBROUTINES AND FUNCTION SUBPROGRAMS REQUIRED                        D
C                FUNCT                                                             D
C                                                                                  D
C             METHOD                                                               DFM
C                THE METHOD IS DESCRIBED IN THE FOLLOWING ARTICLE                  DFM
C                R. FLETCHER AND M.J.D. POWELL, A RAPID DESCENT METHOD FOR         DFM
C                MINIMIZATION,                                                     DFM
C                COMPUTER JOURNAL VOL.6, ISS. 2, 1963, PP.163-168.                 DFM
C                                                                                  DFM
C                                                                                  DFM
C     ..................................................................          DFM
C                                                                                  DFM
      SUBROUTINE DFMFP(FUNCT,N,X,F,G,EST,EPS,LIMIT,IER,H)                          DFM
C                                                                                  DFM
C        DIMENSIONED DUMMY VARIABLES                                               DFM
      DIMENSION H(30),X(5),G(5)
      DOUBLE PRECISION X,F,FX,FY,OLDF,HNRM,GNRM,H,G,DX,DY,ALFA,DALFA,              DFM
     1AMBDA,T,Z,W                                                                  DFM
C                                                                                  DFM
C        COMPUTE FUNCTION VALUE AND GRADIENT VECTOR FOR INITIAL ARGUMENT           DFM
      CALL FUNCT(N,X,F,G)                                                          DFM
C                                                                                  DFM
C        RESET ITERATION COUNTER AND GENERATE IDENTITY MATRIX                      DFM
      IER=0                                                                        DFM
      KOUNT=0                                                                      DFM
      N2=N+N                                                                       DFM
      N3=N2+N                                                                      DFM
      N31=N3+1                                                                     DFM
    1 K=N31                                                                        DF
      DO 4 J=1,N                                                                   DFM
      H(K)=1.D0                                                                    DFM
      NJ=N-J                                                                       DFM
      IF(NJ)5,5,2                                                                  DFM
    2 DO 3 L=1,NJ                                                                  DFM
      KL=K+L                                                                       DFM
    3 H(KL)=0.D0                                                                   DFM
    4 K=KL+1                                                                       DFM
C                                                                                  DFM
C        START ITERATION LOOP                                                      DFM
    5 KOUNT=KOUNT +1                                                               DFM
C                                                                                  DFM
C        SAVE FUNCTION VALUE, ARGUMENT VECTOR AND GRADIENT VECTOR                  DFM
      OLDF=F                                                                       DFM
      DO 9 J=1,N                                                                   DFM
      K=N+J                                                                        DFM
      H(K)=G(J)                                                                    DFM
      K=K+N                                                                        DFM
      H(K)=X(J)                                                                    DFM
C                                                                                  DFM
C        DETERMINE DIRECTION VECTOR H                                              DFM
      K=J+N3                                                                       DFM
      T=0.D0                                                                       DFM
      DO 8 L=1,N                                                                   DFM
      T=T-G(L)*H(K)
```

```
      IF(L-J)6,7,7                                                      DFM
    6 K=K+N-L                                                           DFM
      GO TO 8                                                           DFM
    7 K=K+1                                                             DFM
    8 CONTINUE                                                          DFM
    9 H(J)=T                                                            DFM
C                                                                       DFM
C        CHECK WHETHER FUNCTION WILL DECREASE STEPPING ALONG H.         DFM
      DY=0.D0                                                           DFM
      HNRM=0.D0                                                         DFM
      GNRM=0.D0                                                         DFM
C                                                                       DFM
C        CALCULATE DIRECTIONAL DERIVATIVE AND TESTVALUES FOR DIRECTION  DFM
C        VECTOR H AND GRADIENT VECTOR G.                                DFM
      DO 10 J=1,N                                                       DFM
      HNRM=HNRM+DABS(H(J))                                              DFM
      GNRM=GNRM+DABS(G(J))                                              DFM
   10 DY=DY+H(J)*G(J)                                                   DFM
C                                                                       DFM
C        REPEAT SEARCH IN DIRECTION OF STEEPEST DESCENT IF DIRECTIONAL  DFM
C        DERIVATIVE APPEARS TO BE POSITIVE OR ZERO.                     DFM
      IF(DY)11,51,51                                                    DFM
C                                                                       DFM
C        REPEAT SEARCH IN DIRECTION OF STEEPEST DESCENT IF DIRECTION    DFM
C        VECTOR H IS SMALL COMPARED TO GRADIENT VECTOR G.               DFM
   11 IF(HNRM/GNRM-EPS)51,51,12                                         DFM
C                                                                       DFM
C        SEARCH MINIMUM ALONG DIRECTION H                               DFM
C                                                                       DFM
C        SEARCH ALONG H FOR POSITIVE DIRECTIONAL DERIVATIVE             DFM
   12 FY=F                                                              DFM
      ALFA=2.D0*(EST-F)/DY                                              DFM
      AMBDA=1.D0                                                        DFM
C                                                                       DFM
C        USE ESTIMATE FOR STEPSIZE ONLY IF IT IS POSITIVE AND LESS THAN DFM
C        1. OTHERWISE TAKE 1. AS STEPSIZE                               DFM
      IF(ALFA)15,15,13                                                  DFM
   13 IF(ALFA-AMBDA)14,15,15                                            DFM
   14 AMBDA=ALFA                                                        DFM
   15 ALFA=0.D0                                                         DFM
C                                                                       DFM
C        SAVE FUNCTION AND DERIVATIVE VALUES FOR OLD ARGUMENT           DFM
   16 FX=FY                                                             DFM
      DX=DY                                                             DFM
C                                                                       DFM
C        STEP ARGUMENT ALONG H                                          DFM
      DO 17 I=1,N                                                       DFM
   17 X(I)=X(I)+AMBDA*H(I)                                              DFM
C                                                                       DFM
C        COMPUTE FUNCTION VALUE AND GRADIENT FOR NEW ARGUMENT           DFM
      CALL FUNCT(N,X,F,G)                                               DFM
      FY=F                                                              DFM
C                                                                       DFM
C        COMPUTE DIRECTIONAL DERIVATIVE DY FOR NEW ARGUMENT.  TERMINATE DFM
C        SEARCH, IF DY IS POSITIVE. IF DY IS ZERO THE MINIMUM IS FOUND  DFM
C                                                                       DFM
      DY=0.D0                                                           DFM
      DO 18 I=1,N                                                       DFM
   18 DY=DY+G(I)*H(I)                                                   DFM
      IF(DY)19,36,22                                                    DFM
```

```
C                                                                       DFM
C      TERMINATE SEARCH ALSO IF THE FUNCTION VALUE INDICATES THAT       DFM
C      A MINIMUM HAS BEEN PASSED                                        DFM
   19 IF(FY-FX)20,22,22                                                 DFM
C                                                                       DFM
C      REPEAT SEARCH AND DOUBLE STEPSIZE FOR FURTHER SEARCHES           DFM
   20 AMBDA=AMBDA+ALFA                                                  DFM
      ALFA=AMBDA                                                        DFM
C      END OF SEARCH LOOP                                               DFM
C                                                                       DFM
C      TERMINATE IF THE CHANGE IN ARGUMENT GETS VERY LARGE              DFM
      IF(HNRM*AMBDA-1.D10)16,16,21                                      DFM
C                                                                       DFM
C      LINEAR SEARCH TECHNIQUE INDICATES THAT NO MINIMUM EXISTS         DFM
   21 IER=2                                                             DFM
      RETURN                                                            DFM
C                                                                       DFM
C      INTERPOLATE CUBICALLY IN THE INTERVAL DEFINED BY THE SEARCH      DFM
C      ABOVE AND COMPUTE THE ARGUMENT X FOR WHICH THE INTERPOLATION     DFM
C      POLYNOMIAL IS MINIMIZED                                          DFM
   22 T=0.D0                                                            DFM
   23 IF(AMBDA)24,36,24                                                 DFM
   24 Z=3.D0*(FX-FY)/AMBDA+DX+DY                                        DFM
      ALFA=DMAX1(DABS(Z),DABS(DX),DABS(DY))                             DFM
      DALFA=Z/ALFA                                                      DFM
      DALFA=DALFA*DALFA-DX/ALFA*DY/ALFA                                 DFM
      IF(DALFA)51,25,25                                                 DFM
   25 W=ALFA*DSQRT(DALFA)                                               DFM
      ALFA=(DY+W-Z)*AMBDA/(DY+2.D0*W-DX)                                DFM
      DO 26 I=1,N                                                       DFM
   26 X(I)=X(I)+(T-ALFA)*H(I)                                           DFM
C                                                                       DFM
C      TERMINATE, IF THE VALUE OF THE ACTUAL FUNCTION AT X IS LESS      DFM
C      THAN THE FUNCTION VALUES AT THE INTERVAL ENDS. OTHERWISE REDUCEDFM
C      THE INTERVAL BY CHOOSING ONE END-POINT EQUAL TO X AND REPEAT     DFM
C      THE INTERPOLATION. WHICH END-POINT IS CHOOSEN DEPENDS ON THE     DFM
C      VALUE OF THE FUNCTION AND ITS GRADIENT AT X                      DFM
C                                                                       DFM
      CALL FUNCT(N,X,F,G)                                               DFM
      IF(F-FX)27,27,28                                                  DFM
   27 IF(F-FY)36,36,28                                                  DFM
   28 DALFA=0.D0                                                        DFM
      DO 29 I=1,N                                                       DFM
   29 DALFA=DALFA+G(I)*H(I)                                             DFM
      IF(DALFA)30,33,33                                                 DFM
   30 IF(F-FX)32,31,33                                                  DFM
   31 IF(DX-DALFA)32,36,32                                              DFM
   32 FX=F                                                              DFM
      DX=DALFA                                                          DFM
      T=ALFA                                                            DFM
      AMBDA=ALFA                                                        DFM
      GO TO 23                                                          DFM
   33 IF(FY-F)35,34,35                                                  DFM
   34 IF(DY-DALFA)35,36,35                                              DFM
   35 FY=F                                                              DFM
      DY=DALFA                                                          DFM
      AMBDA=AMBDA-ALFA                                                  DFM
      GO TO 22                                                          DFM
C
```

```
C        COMPUTE DIFFERENCE VECTORS OF ARGUMENT AND GRADIENT FROM         DFM
C        TWO CONSECUTIVE ITERATIONS                                       DFM
   36 DO 37 J=1,N                                                         DFM
      K=N+J                                                               DFM
      H(K)=G(J)-H(K)                                                      DFM
      K=N+K                                                               DFM
   37 H(K)=X(J)-H(K)                                                      DFM
C                                                                         DFM
C        TERMINATE, IF FUNCTION HAS NOT DECREASED DURING LAST ITERATION   DFM
      IF(OLDF-F+EPS)51,38,38                                              DFM
C                                                                         DFM
C        TEST LENGTH OF ARGUMENT DIFFERENCE VECTOR AND DIRECTION VECTOR   DFM
C        IF AT LEAST N ITERATIONS HAVE BEEN EXECUTED. TERMINATE, IF       DFM
C        BOTH ARE LESS THAN  EPS                                          DFM
   38 IER=0                                                               DFM
      IF(KOUNT-N)42,39,39                                                 DFM
   39 T=0.D0                                                              DFM
      Z=0.D0                                                              DFM
      DO 40 J=1,N                                                         DFM
      K=N+J                                                               DFM
      W=H(K)                                                              DFM
      K=K+N                                                               DFM
      T=T+DABS(H(K))                                                      DFM
   40 Z=Z+W*H(K)                                                          DFM
      IF(HNRM-EPS)41,41,42                                                DFM
   41 IF(T-EPS)56,56,42                                                   DFM
C                                                                         DFM
C        TERMINATE, IF NUMBER OF ITERATIONS WOULD EXCEED  LIMIT           DFM
   42 IF(KOUNT-LIMIT)43,50,50                                             DFM
C                                                                         DFM
C        PREPARE UPDATING OF MATRIX H                                     DFM
   43 ALFA=0.D0                                                           DFM
      DO 47 J=1,N                                                         DFM
      K=J+N3                                                              DFM
      W=0.D0                                                              DFM
      DO 46 L=1,N                                                         DFM
      KL=N+L                                                              DFM
      W=W+H(KL)*H(K)                                                      DFM
      IF(L-J)44,45,45                                                     DFM
   44 K=K+N-L                                                             DFM
      GO TO 46                                                            DFM
   45 K=K+1                                                               DFM
   46 CONTINUE                                                            DFM
      K=N+J                                                               DFM
      ALFA=ALFA+W*H(K)                                                    DFM
   47 H(J)=W                                                              DFM
C                                                                         DFM
C        REPEAT SEARCH IN DIRECTION OF STEEPEST DESCENT IF RESULTS        DFM
C        ARE NOT SATISFACTORY                                             DFM
      IF(Z*ALFA)48,1,48                                                   DFM
C                                                                         DFM
C        UPDATE MATRIX H                                                  DFM
   48 K=N31                                                               DFM
      DO 49 L=1,N                                                         DFM
      KL=N2+L                                                             DFM
      DO 49 J=L,N                                                         DFM
      NJ=N2+J                                                             DFM
      H(K)=H(K)+H(KL)*H(NJ)/Z-H(L)*H(J)/ALFA                              DFM
   49 K=K+1
```

```
      GO TO 5                                                          DFM
C        END OF ITERATION LOOP                                         DFM
C                                                                      DFM
C        NO CONVERGENCE AFTER  LIMIT  ITERATIONS                       DFM
   50 IER=1                                                            DFM
      RETURN                                                           DFM
C                                                                      DFM
C        RESTORE OLD VALUES OF FUNCTION AND ARGUMENTS                  DFM
   51 DO 52 J=1,N                                                      DFM
      K=N2+J                                                           DFM
   52 X(J)=H(K)                                                        DFM
      CALL FUNCT(N,X,F,G)                                              DFM
C                                                                      DFM
C        REPEAT SEARCH IN DIRECTION OF STEEPEST DESCENT IF DERIVATIVE  DFM
C        FAILS TO BE SUFFICIENTLY SMALL                                DFM
      IF(GNRM-EPS)55,55,53                                             DFM
C                                                                      DFM
C        TEST FOR REPEATED FAILURE OF ITERATION                        DFM
   53 IF(IER)56,54,54                                                  DFM
   54 IER=-1                                                           DFM
      GOTO 1                                                           DFM
   55 IER=0                                                            DFM
   56 RETURN                                                           DFM
      END                                                              DFM
C     SUBROUTINE TO CALCULATE S> SUM(EMAX(W)-E(W)))**2 AND GRAD S
C     L.P. BOIVIN  14/6/68
      SUBROUTINE ENERG(N,A,VAL,GRAD)
      DOUBLE PRECISION QD,GRAD(5),VAL,QN,E,P(5,5,20),PX(5,5),A(5)
      DOUBLE PRECISION EMAX(20),S
      COMMON P,PX
      COMMON EMAX
      COMMON M
      QD > A(1)*A(1)*PX(1,1) < A(2)*A(2)*PX(2,2) < A(3)*A(3)*PX(3,3) <
     1A(4)*A(4)*PX(4,4) < A(5)*A(5)*PX(5,5) < 2.0D0*(A(1)*(A(2)*PX(1,2)
     2< A(3)*PX(1,3) < A(4)*PX(1,4) < A(5)*PX(1,5)) < A(2)*(A(3)*PX(2,3)
     3 < A(4)*PX(2,4) < A(5)*PX(2,5)) < A(3)*(A(4)*PX(3,4) < A(5)*PX(3,
     4 5)) < A(4)*A(5)*PX(4,5))
      DO 1 I>1,N
    1 GRAD(I) > 0.0D0
      VAL>0.0D0
      DO 2 L>1,M
      QN> A(1)*A(1)*P(1,1,L) < A(2)*A(2)*P(2,2,L) < A(3)*A(3)*P(3,3,L) <
     1 A(4)*A(4)*P(4,4,L) < A(5)*A(5)*P(5,5,L) < 2.0D0*(A(1)*(A(2)*P(1,
     2 2,L) < A(3)*P(1,3,L) < A(4)*P(1,4,L) < A(5)*P(1,5,L)) < A(2)*(
     3 A(3)*P(2,3,L) < A(4)*P(2,4,L) < A(5)*P(2,5,L)) < A(3)*(A(4)*P(3,
     4 4,L) < A(5)*P(3,5,L)) < A(4)*A(5)*P(4,5,L))
      E> QN/QD
      S> EMAX(L) - E
      VAL > VAL < S*S
      DO 2 I>1,N
    2 GRAD(I) > GRAD(I)-4.0D0*S*(A(1)*(P(1,I,L)-E*PX(1,I)) < A(2)*(
     1 P(2,I,L)-E*PX(2,I))<A(3)*(P(3,I,L)-E*PX(3,I))<A(4)*(P(4,I,L)-
     2 E*PX(4,I))<A(5)*(P(5,I,L)-E*PX(5,I)))/QD
      RETURN
      END
```

```
C   PROGRAM TO CALCULATE THE DIFFRACTION PATTERN FORMED BY AN ARBITRARY
C   COMPLEX PUPIL FUNCTION T(X) HAVING ROTATIONAL SYMMETRY ABOUT THE
C   OPTICAL AXIS    L.P. BOIVIN   28/12/67
C   REVISE 2/3/69
      DOUBLE PRECISION  T,ARG,DCOS,DSIN,BES,C(99),Z(99),D(99),E(99),
     1 SS(801),GAM(801),U,S,A,B,H,X,FI,PHI,DSQRT
      DOUBLE PRECISION  RL(801),COMP(801)
      DOUBLE PRECISION  DD(50)
      T(W)>(((-.11608768D-01*(1.0D0-W*W)-.21279474D<00)*(1.0D0-W*W)<
     1 .51883221D<00)*(1.0D0-W*W)<.45994938D<00)*(1.0D0-W*W)<
     2 .24562193D<00
      ARG(W)> W - W
      N>24
      M>801
      READ(1,1) (I,Z(I),C(I),I>1,N)
    1 FORMAT(I10,2E20.9 )
      READ(1,6)
      DO 2 I>1,N
      D(I)>(Z(I) < 1.0D0 )*T((Z(I)<1.0D0)/2.0D0)
      U>ARG((Z(I)<1.0D0)/2.0D0)
      E(I)>D(I)*DSIN(U)
    2 D(I)>D(I)*DCOS(U)
      S>0.0D0
      DO 3 J>1,M
      A>0.0D0
      B>0.0D0
      DO 4  K>1,N
      X>S*(Z(K) < 1.0D0) /2.0D0
      IF(X-3.0D0) 10,10,11
   10 U>(X/3.0D0)*(X/3.0D0)
      BES>  (((((U*.0002100 -.0039444 )*U<.0444479 )*U-.3163866 )*U<
     11.2656208)*U-2.2499997)*U<1.0
      GO TO 20
   11 U>3.0D0/X
      FI=(((((<.00014476*U-.00072805)*U<.00137237)*U-.00009512)*U-
     1.00552740)*U-.00000077)*U<.79788456
      PHI=(((((.00013558*U-.00029333)*U-.00054125)*U<.00262573)*U-
     1 .00003954)*U-.04166397)*(-U) <.78539816
      BES>FI*DCOS(X - PHI)/DSQRT(X)
   20 U>C(K)*BES
      A>A<D(K)*U
    4 B>B<E(K)*U
      RL(J)> A
      COMP(J)> B
      GAM(J)>RL(J)*RL(J) < COMP(J)*COMP(J)
      SS(J)>S
    3 S>S<.5D0
      DO 21 J>1,N
   21 DD(J) > ( Z(J) < 1.0D0 )*T((Z(J) < 1.0D0 )/2.0D0)
      H > 0.0D0
      DO 50  I>1,N
   50 H > H < DD(I)*C(I)
      DO 5 I>1,M
      RL(I) > RL(I)/H
       COMP(I) > COMP(I)/H
    5 GAM(I) > DSQRT(GAM(I))/H
      WRITE(2,6)
      WRITE(2,62)
   62 FORMAT(//)
```

```
      WRITE(2,9) ( SS(J),GAM(J), J>1,M )
    9 FORMAT(5(F8.1,F8.5))
      WRITE(3,61)
   61 FORMAT(:1        : )
      WRITE(3,7)
    7 FORMAT(//:                                DIFFRACTION PATTERN CORRESPONDING
     1TO : ///)
      WRITE(3,12)
   12 FORMAT(16X,:W:,11X,:AR:,11X,:AI:,11X,:A:,14X,:W:,11X,:AR:,11X,
     1 :AI:,11X,:A: ///)
      WRITE(3,13) (SS(I),RL(I), COMP(I),GAM(I),I>1,M)
   13 FORMAT(14X,F5.1,5X,F8.5,5X,F8.5,5X,F8.5,9X,F5.1,5X,F8.5,5X,F8.5,
     1 5X,F8.5 )
      WRITE(2,15)
      WRITE(2,14) (RL(J),COMP(J),J>1,M)
    6 FORMAT(:                                                         :)
   15 FORMAT(////)
   14 FORMAT( 10F8.5 )
      STOP
      END
```

```
C   SUBROUTINE TO CALCULATE JO(X)
      DOUBLE PRECISION FUNCTION BESO(X)
      DOUBLE PRECISION X,U,FI,PHI,DCOS,DSQRT,BESO
      IF(X-3.0DO) 10,10,11
   10 U>(X/3.0DO)*(X/3.0DO)
      BESO>  ((((((U*.0002100 -.0039444 )*U<.0444479 )*U-.3163866 )*U<
     11.2656208)*U-2.2499997)*U<1.0000000000
      GO TO 20
   11 U>3.0DO/X
      FI=((((((<.00014476*U-.00072805)*U<.00137237)*U-.00009512)*U-
     1.00552740)*U-.00000077)*U<.79788456
      PHI=(((((.00013558*U-.00029333)*U-.00054125)*U<.00262573)*U-
     1 .00003954)*U-.04166397)*(-U) <.78539816
      BESO>FI*DCOS(X - PHI)/DSQRT(X)
   20 RETURN
      END
C   SUBROUTINE TO CALCULATE J1(X)
      DOUBLE PRECISION FUNCTION BES1(X)
      DOUBLE PRECISION X,U,FI,PHI,DSIN,DSQRT,BES1
      IF(X - 3.0DO )  10,10,11
   10 U>(X/3.0DO)*(X/3.0DO)
      BES1=((((((U*.00001109-.00031761)*U+.00443319)*U-.03954289)*U+
     1.21093573)*U-.56249985)*U+.5DO)*X
      GO TO 20
   11 U> 3.0DO/X
      FI=(((((-.00020033*U+.00113653)*U-.00249511)*U+.00017105)*U+
     1.01659667)*U+.00000156)*U+.79788456
      PHI=(((((.00029166*U-.00079824)*U-.00074348)*U+.00637879)*U-
     1 .00005650)*U-.12499612)*U+.78539816
      BES1 > FI*DSIN(X - PHI)/DSQRT(X)
   20 RETURN
      END
C   PROGRAM TO CALCULATE THE ENCIRCLED ENERGY FACTOR ,FOR VARIOUS VALUES
C   OF  W , ASSOCIATED WITH AN ARBITRARY COMPLEX PUPIL HAVING ROTATIONAL
C   SYMMETRY ABOUT THE OPTICAL AXIS   L.P. BOIVIN   10/5/68
      DOUBLE PRECISION T,ARG,DCOS,Z1(64),Z2(64),C1(64),C2(64),ET,E,W,
     1 BESO,BES1
      DIMENSION ENERG(51),WW(51)
      N>24
      M>64
      READ(1,9)  (Z1(I),C1(I),I>1,N)
    9 FORMAT(2F20.15)
      READ(1,1)  (I,Z2(I),C2(I),I>1,M)
      READ(1,6)
      ET>0.0DO
      WRITE(3,6)
      WRITE(3,7)
      DO 2  I>1,N
    2 ET>ET < C1(I)*(.5DO*Z1(I) < .5DO)*T(.5DO*Z1(I) < .5DO)**2
      W>-.5DO
      DO 3  I>1,51
      W>W<.5DO
      E > 0.0DO
      DO 4  J>1,N
      DO 4  K>1,M
    4 E > E < C1(J)*C2(K)*(.5DO*Z1(J)<.5DO)*(.5DO*Z2(K)<.5DO)*T(
     1 .5DO*Z1(J)<.5DO)*T(.5DO*Z2(K)<.5DO)*DCOS(ARG(.5DO*Z1(J)<.5DO) -
     2 ARG(.5DO*Z2(K)<.5DO))*((.5DO*Z1(J)<.5DO)*BESO(W*(.5DO*Z2(K)<.5DO
     3 ))*BES1(W*(.5DO*Z1(J)<.5DO))-(.5DO*Z2(K)<.5DO)*BESO(W*(.5DO*Z1(J)
```

```
    4 <.5DO))*BES1(W*(.5DO*Z2(K) < .5DO )))/((.5DO*Z1(J)<.5DO)**2 -
    5 (.5DO*Z2(K) < .5DO)**2)
      E> .5DO*W*E/ET
      WW(I) > W
      ENERG(I) > E
   3  WRITE(3,5) W,E
      WRITE(2,6)
      WRITE(2,71)  ( WW(I),ENERG(I), I > 1,51 )
  71  FORMAT(5( F8.1,F8.5 ))
   1  FORMAT(I10,2E20.9)
   6  FORMAT(:                                                          :)
   7  FORMAT(///: FACTEUR D ENERGIE ENCERCLEE : ////)
   5  FORMAT(: W> : F6.1,10X,: E > : D16.8  ///)
      STOP
      END
```

```
C   PROGRAM TO CALCULATE  THE MTF CORRESPONDING TO AN ARBITRARY COMPLEX
C   PUPIL HAVING ROTATIONAL SYMMETRY ABOUT THE OPTICAL AXIS L.P. BOIVIN
      DOUBLE PRECISION C(96),Z(96),T,A,R,U,S1,S2,P,SNOR(41),ARG,FRE(41),
     1 W,DSQRT,H,DCOS,DSIN,Q,TC
      T(W)=(((-.116087680-01*(1.0D0-W*W)-.21279474D+00)*(1.0D0-W*W)+
     1 .51883221D+00)*(1.0D0-W*W)+.45994938D+00)*(1.0D0-W*W)+
     2 .24562193D+00
      TC(Q,W) =  (Q-1.0D0)*T(W)*DCOS(ARG(W)) + (2.0D0 - Q)*T(W)*DSIN(
     1 ARG(W))
      N = 64
      READ(1,1)  (I,Z(I),C(I),I=1,N)
    1 FORMAT(I10,2E20.9)
      READ(1,6)
      A=0.0D0
      K=40
      DO 2 I=1,K
      S1=0.0D0
      DO 3  J=1,N
      R=(2.0D0-A)*Z(J)/4.0D0 + (2.0D0+A)/4.0D0
      DO 3 M=1,2
      Q=M
      P= (Z(J)  + 1.0D0)*TC(Q,R)
      S2=0.0D0
      DO 4 L=1,N
      U=(2.0D0*R-A)*Z(L)/(4.0D0*R) + (2.0D0*R+A)/(4.0D0*R)
    4 S2=S2+(TC(Q,DSQRT(R*R+A*A-2.0D0*A*R*U))/DSQRT(1.0D0-U*U))*C(L)
    3 S1=S1 + C(J)*P*S2
      FRE(I)=A
      SNOR(I)=S1*(2.0D0-A)*(2.0D0-A)
    2 A = A + .5D-01
      H=SNOR(1)
      DO 10 I=1,K
   10 SNOR(I)=SNOR(I)/H
      K=K+1
      FRE(K)=2.0D0
      SNOR(K)=0.0D0
      WRITE(3,5)
    5 FORMAT('1 OPTICAL FREQUENCY RESPONSE OF PUPIL T(X**2) '//
     1' FUNCTION T(X**2) = ' //)
      WRITE(3,6)
      WRITE(3,7)
      WRITE(3,8) (FRE(I),SNOR(I),I=1,K)
      WRITE(2,6)
    6 FORMAT('
     1             ')
      WRITE(2,9)  ( FRE(I),SNOR(I),I=1,K)
    9 FORMAT(5( F8.2,F8.5))
    7 FORMAT(///'     SPA. FREQ.                        RESPONSE '///)
    8 FORMAT(6X,F5.2,20X,F12.8//)
      STOP
      END
```

```
C   PROGRAM TO CALCULATE DIFFRACTION PATTERN ASSOCIATED WITH AMPLITUDE
C   FILTER HAVING AMPLITUDE TRANSMISSION T(X) = SUM(A(K)*(1-X**2)**(K-1))
C   AND K =1,N
C L.P. BOIVIN  3/6/66      MODIFIED FOR /360  8/12/66
      DOUBLE PRECISION A(10),GAM(800),B(11),W(800),X,C,P,D,Y,U,FI,PHI,
     1 DCOS,DSIN,V
      N=10
      L>800
      X>0.0D0
      A(1)> 0.24562193D<00
      A(2)> 0.45994938D<00
      A(3)> 0.51883221D<00
      A(4)>-0.21279474D<00
      A(5)>-0.116087680-01
      A(6)> 0.0D0
      A(7)> 0.0D0
      A(8)> 0.0D0
      A(9)> 0.0D0
      A(10)> 0.0D0
      WRITE(3,5) A
      C>0.0D0
      DO 1  I=1,N
      P=I
    1 C=C+A(I)/P
      A(1)>A(1)*2.0D0
      D>2.0D0
      DO 2 I=2,N
      P=I-1
      D>D*P*2.0D0
    2 A(I)=A(I)*D
      DO 100  I=1,L
      X>X < .5D0
      Y>1.0D0/X
      W(I)=X
      IF(X-3.)  880,880,881
  880 U>(X/3.0D0)**2
      B(1)= ((((((U*.0002100 -.0039444 )*U+.0444479 )*U-.3163866 )*U+
     11.2656208)*U-2.2499997)*U+1.0D0
      B(2)=((((((U*.00001109-.00031761)*U+.00443319)*U-.03954289)*U+
     1.21093573)*U-.56249985)*U+.5D0)*X
      GO TO 20
  881 U>3.0D0/X
      FI=((((((+.00014476*U-.00072805)*U+.00137237)*U-.00009512)*U-
     1.00552740)*U-.00000077)*U+.79788456
      PHI=(((((.00013558*U-.00029333)*U-.00054125)*U+.00262573)*U-
     1 .00003954)*U-.04166397)*(-U) +.78539816
      B(1)=X**(-.5D0)*FI*DCOS(X-PHI)
      FI=(((((-.00020033*U+.00113653)*U-.00249511)*U+.00017105)*U+
     1.01659667)*U+.00000156)*U+.79788456
      PHI=(((((.00029166*U-.00079824)*U-.00074348)*U+.00637879)*U-
     1 .00005650)*U-.12499612)*U+.78539816
      B(2)=X**(-.5D0)*FI*DSIN(X-PHI)
   20 V>2.0D0/X
      B(3)=V*B(2)-B(1)
      B(4)=V*B(3)*2.D0-B(2)
      B(5)=V*B(4)*3.0D0-B(3)
      B(6)=V*B(5)*4.0D0-B(4)
      B(7)=V*B(6)*5.0D0-B(5)
      B(8)=V*B(7)*6.0D0-B(6)
```

```
      B(9)=V*B(8)*7.0D0-B(7)
      B(10)=V*B(9)*8.0D0-B(8)
      B(11)=V*B(10)*9.0D0-B(9)
  100 GAM(I)=(((((((((((B(11)*A(10)*Y+B(10)*A(9))*Y+B(9)*A(8))*Y+B(8)*
     1A(7))*Y+B(7)*A(6))*Y+B(6)*A(5))*Y+B(5)*A(4))*Y+B(4)*A(3))*Y+B(3)*
     2A(2))*Y+B(2)*A(1))*Y)/C
      WRITE(3,3) (W(I),GAM(I),I>1,L)
      WRITE(2,4) (W(I),GAM(I),I>1,L)
    3 FORMAT(3(9H   W(I)= F8.1,11H   GAM(I)= F12.8)//)
    4 FORMAT(5(F8.1,F8.5))
    5 FORMAT(//////120H ****************************  DIFFRACTION  PATTE
     1RN  PRODUCED  BY  AMPLITUDE  FILTER  T(X)  ***********************
     2*****//////32H     COEFFICIENTS  OF  T(X)  ARE ///10F12.8///)
      STOP
      END
```

```
C       PROGRAM TO CALCULATE DIFFRACTION PATTERN  ASSOCIATED WITH FLUX
C       SELECTOR. GAMMA=2SIGMA(RNP*J1(W*RNP)-RN*J1(W*RN) )/ (W*UN)
C       L.P. BOIVIN  18/10/65      CONVERTED TO /360 E LEVEL 17/11/66
        DOUBLE PRECISION R(100),RP(100),GAM(800),W(800),WO,DEL,UN,C,X,U,
       1BES,QQ,FI,PHI,VV,DSIN,DSQRT
        READ(1,1) N
        READ(1,10)
      1 FORMAT(I4)
     10 FORMAT(:                                                      :)
        READ(1,4) WO,DEL,L
      4 FORMAT(2F20.10,I4)
        READ(1,5) (R(I),RP(I),I>1,N)
      5 FORMAT(4F12.8)
        WRITE(3,10)
        WRITE(3,6) N
      6 FORMAT(///4H N> I4///)
        WRITE(3,7) (R(I),RP(I),I>1,N)
      7 FORMAT(: R(I)> :, F12.8,:            RP(I)> :,F12.8)
        WRITE(3,10)
        WRITE(3,8)
      8 FORMAT(: DIFFRACTION PATTERN (AMPLITUDE > GAM(I) ; RADIUS> W(I)):
       1///)
        UN>0.0D0
        DO 50 K=1,N
     50 UN>UN<RP(K)*RP(K)-R(K)*R(K)
        DO 300 I=1,L
        C=I
        W(I)=WO + DEL*C
        GAM(I)>0.0D0
        DO  200  J=1,N
        X=W(I)*RP(J)
        IF(X-3.0D0)  880,880,881
    880 U>(X/3.0D0)*(X/3.0D0)
        BES=((((((U*.00001109-.00031761)*U+.00443319)*U-.03954289)*U+
       1.21093573)*U-.56249985)*U+.5D0)*X
        QQ=RP(J)*BES
        GO TO 882
    881 U>3.0D0/X
        FI=(((((-.00020033*U+.00113653)*U-.00249511)*U+.00017105)*U+
       1.01659667)*U+.00000156)*U+.79788456
        PHI=(((((.00029166*U-.00079824)*U-.00074348)*U+.00637879)*U-
       1 .00005650)*U-.12499612)*U+.78539816
        BES> FI*DSIN(X-PHI)/DSQRT(X)
        QQ=RP(J)*BES
    882 X=W(I)*R(J)
        IF(X-3.0D0) 883,883,884
    883 U>(X/3.0D0)*(X/3.0D0)
        BES=((((((U*.00001109-.00031761)*U+.00443319)*U-.03954289)*U+
       1.21093573)*U-.56249985)*U+.5D0)*X
        VV=R(J)*BES
        GO TO 200
    884 U>3.0D0/X
        FI=(((((-.00020033*U+.00113653)*U-.00249511)*U+.00017105)*U+
       1.01659667)*U+.00000156)*U+.79788456
        PHI=(((((.00029166*U-.00079824)*U-.00074348)*U+.00637879)*U-
       1 .00005650)*U-.12499612)*U+.78539816
        BES> FI*DSIN(X-PHI)/DSQRT(X)
        VV=R(J)*BES
    200 GAM(I)=GAM(I)+QQ-VV
```

```
      GAM(I)>2.0D0*GAM(I)/(W(I)*UN)
  300 WRITE(3,3) W(I),GAM(I)
    3 FORMAT(  4H W= F7.2,6H GAM= F15.11)
      WRITE(2,301) (W(I),GAM(I),I>1,L)
  301 FORMAT(  5(F8.1,F8.5))
      STOP
      END
```

```
C   SUBROUTINE TO CALCULATE BESSELS  FUNCTION JN(X) FOR ANY INTEGRAL
C   ORDER N AND FOR ARGUMENT X UP TO 30   L.P. BOIVIN
      EPS=.0000000001
      AA=N
      BB=X/2.
      FAC=1.
      DO 111  I=1,N
      CC=I
  111 FAC=FAC*CC
      DD=BB**AA/FAC
      EE=-BB**2
      BE=1.
      UK=1.
      HH=1.
  222 GG=AA+HH
      RR=EE/(GG*HH)
      UK=UK*RR
      BE=BE+UK
      Z=ABSF(UK*DD)
      IF(Z-EPS) 444,444,333
  333 HH=HH+1.
      GOTO 222
  444 BESSEC=BE*DD
      RETURN
      END
C   SUBROUTINE TO CALCULATE  J1(X) FOR LARGE ARGUMENTS USING AN
C   ASYMPTOTIC EXPANSION
      FUNCTION BESIAC(X)
      EPS=.000000001
      PI=3.1415926536
      AM=(2./(PI*X))**.5
      B=X-.75*PI
      C=B/(2.*PI)
      K=C
      CP=K
      ARG=2.*PI*(C-CP)
      CO=COSF(ARG)
      SI=SINF(ARG)
      P=1.
      UP=1.
      D=-.5/(8.*X)**2
      EM=0.0
    1 RR=D*(4.-(4.*EM+1.)**2)*(4.-(4.*EM+3.)**2)/((EM+1.)*(2.*EM+1.))
      IF(ABSF(RR)-1.)  7,7,3
    7 UP=UP*RR
      P=P+UP
      IF(ABSF(UP)-EPS)  3,3,2
    2 EM=EM+1.
      GO TO 1
    3 Q=3./(8.*X)
      UQ=Q
      EM=0.0
    4 RR=D*(4.-(4.*EM+5.)**2)*(4.-(4.*EM+3.)**2)/((2.*EM+3.)*(EM+1.))
      IF(ABSF(RR)-1.)  8,8,6
    8 UQ=UQ*RR
      Q=Q+UQ
      IF(ABSF(UQ)-EPS) 6,6,5
    5 EM=EM+1.
      GO TO 4
```

```
 6 BESIAC=AM*(P*CO-Q*SI)
   RETURN
   END
```

```
C   PROGRAM TO CALCULATE FLUX SELECTOR 1B-A4-H  L.P. BOIVIN 24/7/66
      DOUBLE PRECISION  XP(100),R(100),RP(100),P,C,Q,V,U,HO,T,SIGMAC
      SIGMAC(W)>((((.65714397D-02*(1.0D0-W*W)-.17078728D<00)*(1.0D0-W*W)
     1 <.54121266D<00)*(1.0D0-W*W)<.62853524D<00)*(1.0D0-W*W)<
     2 .56750857D<00)*(1.0D0-W*W)
      N>50
      P=N
      READ(1,11)
   11 FORMAT( :                                                         :)
      R(1)>0.0D0
      C>(SIGMAC(0.0D0)-.5D0*SIGMAC(1.0D0/P)-.5D0*SIGMAC(2.D0/P))
     1 /(.5D0*((1.D0/P)*(1.D0/P) < (2.D0/P)*(2.D0/P)))
      C>1.D0/C
      RP(1)>DSQRT(C*(SIGMAC(0.0D0)-SIGMAC(1.0D0/P)))
      XP(1)>1.0D0/P
      DO 1  I=2,N
      Q=I
      XP(I)=Q/P
      V>.5D0*C*(SIGMAC(XP(I-1))-SIGMAC(XP(I)))
      U>(XP(I-1)*XP(I-1) < XP(I)*XP(I))/2.D0
      R(I)>DSQRT(U-V)
    1 RP(I)>DSQRT(U<V)
      HO>1.0D0/RP(N)
      T>0.0D0
      DO 2  I=1,N
      R(I)=R(I)*HO
      RP(I)=RP(I)*HO
    2 T>T < RP(I)*RP(I) - R(I)*R(I)
      WRITE(3,3)
    3 FORMAT(31H150 RING FLUX SELECTOR 1B-A4-H )
      WRITE(3,11)
      WRITE(3,4) T
    4 FORMAT(///4H T= F12.8 ///)
      WRITE(3,10) C
   10 FORMAT(///4H C= F12.8 ///)
      WRITE(3,5) (XP(I),I=1,N)
    5 FORMAT(7H XP(I)= //(5F12.8))
      WRITE(3,6) (R(I),RP(I),I=1,N)
    6 FORMAT(///(7H R(I)= F12.8,8H RP(I)= F12.8//))
      WRITE(2,3)
      WRITE(2,11)
      WRITE(2,7)T
    7 FORMAT(4H T=  F12.8)
      WRITE(2,8) (XP(I),I=1,N)
    8 FORMAT(5F12.8)
      WRITE(2,9) R(1),RP(2),(R(I),RP(I),I=3,N)
    9 FORMAT(4F12.8)
      STOP
      END
```

```
C  PROGRAM TO CALCULATE FLUX SELECTOR TYPE 1A-B4-H
C  L.P. BOIVIN  16/6/66
      DIMENSION R(11),RP(11),XP(11)
      PRINT 4
      N=10
      P=N
      XP(1)=1./(2.*P)
      XP(2)=3./(2.*P)
      R(1)=0.0
      A=SIGMAC(0.0)-SIGMAC(XP(1))
      B=SIGMAC(XP(1))-SIGMAC(XP(2))
      C=(A+.5*B-((A+.5*B)**2-.25*B**2)**.5)/(12.5*B**2)
       PRINT 10 ,C
   10 FORMAT(4H C= F12.8)
      RP(1)=(C*A)**.5
      DO 1 I=2,N
      Q=I
      XP(I)=(2.*Q-1.)/(2.*P)
      A=(Q-1.)/P
      B=P*C*(SIGMAC(XP(I-1))-SIGMAC(XP(I)))/(4.*(Q-1.))
      R(I)=A-B
    1 RP(I)=A+B
      RP(N+1)=1.
      XP(N+1)=1.
      R(N+1)=(1.-C*(SIGMAC(XP(N))-SIGMAC(XP(N+1))))**.5
      L=N+1
      PRINT 5,XP
    5 FORMAT(5H XP= 10F6.2)
      PRINT 2 ,(R(I),RP(I),I=1,L)
    2 FORMAT(//7H R(I)= F12.8,13H        RP(I)= F12.8)
      PUNCH 3 ,(R(I),RP(I),I=1,L)
    3 FORMAT(4F12.8)
    4 FORMAT(27H FLUX SELECTOR TYPE 1A-B4-H )
      CALL EXIT
      END
```

```
      FUNCTION SIGMAC(X)
      U>1.D0 - X*X
      SIGMAC=((((((((.0000002921371948*U+.0000019769951693)*U+
     1.0000328807324978)*U+.0003170420516771)*U+.0024171393275471)*U+
     2   .0133428400277380)*U+.0503250095615250)*U+.1179666235914349)*U
     3   +.1464164266043177)*U+.0682471471167938)*U
      RETURN
      END
      FUNCTION TORRAC(X)
      U=1.-X**2
      TORRAC= ((((((((.000000265579*U**2-.000000292137*U+.000001779296*U
     1-.000001976995)*U+.000029227318*U-.000032880732)*U+.000277411795*U
     2-.000317042052)*U+.002071833709*U-.002417139328)*U+.011119033356*U
     3-.013342840028)*U+.040260007649*U-.050325009562)*U+.088474967694*U
     4-.117966623591)*U+.097610951069*U-.146416426604)*U+.034123573558*U
      TORRAC=(TORRAC-.068247147117)*U
      RETURN
      END
C   PROGRAM TO CALCULATE A FLUX SELECTOR OF THE TYPE  2-... ,GIVEN THE
C   ZONE DIVISIONS  L.P. BOIVIN  1/11/65
C     MODIFIED  VERSION  (FASTER)  13/1/66
      DIMENSION A(10),X(102),R(100),RP(100)
      DIMENSION NN(3)
      DIMENSION DELRN(100)
      READ 11, NN
   11 FORMAT(I4)
      DO 10 L=1,3
      N=NN(L)
      PRINT 102 ,N
  102 FORMAT(////4H N= I4 ///)
      PUNCH 101 ,N
  101 FORMAT(4H N= I4 )
      KK=N-1
C   GENERATION OF VALUES OF X(I)
      X(1)=0.0
      X(N+1)=1.
      P=N
      DO 28 K=1,KK
      Q=K
   28 X(K+1)=Q/P
C   END OF GENERATION OF VALUES OF X(I)
      K=N+1
      PRINT 61
   61 FORMAT(//12H VALUES OF X //)
      PRINT 6,(X(I),I=1,K)
    6 FORMAT(6H X(I)=//(5F16.8))
      PRINT 7
    7 FORMAT(//33H VALUES OF R AND RP(HOMOTHETISED)  //)
      C=(TORRAC(X(2))-TORRAC(0.0))/(SIGMAC(0.0)-SIGMAC(X(2)))**2
      DO 2 I=1,N
      T=TORRAC(X(I+1))-TORRAC(X(I))
      U=SIGMAC(X(I))-SIGMAC(X(I+1))
      T=T/U
      U=C*U
      IF(T-U)  700,701,701
  700 R(I)=(U-T)**.5
      PRINT 702,I
  702 FORMAT(//41H R**2 IS NEGAT. TAKE ABSOLUTE VALUE   I= I4 //)
      GO TO 2
```

```
701 R(I)=(T-U)**.5
  2 RP(I)=(T+U)**.5
    RA=1./RP(N)
    DO 3 I=1,N
    R(I)=R(I)*RA
    RP(I)=RP(I)*RA
  3 PRINT 4,I,R(I),RP(I)
  4 FORMAT(4H I= I2,8H R(I) = F12.8,9H RP(I) = F12.8   )
    PUNCH 29 ,( R(I),RP(I),I=1,N)
 29 FORMAT(4F12.8)
    PRINT 30
 30 FORMAT(///27H WIDTH OF TRANSPARENT RINGS    ///)
    DO 10 I=1,N
    DELRN(I)=RP(I)-R(I)
 10 PRINT 12,I,DELRN(I)
 12 FORMAT(4H I= I3,8H DELRN= F16.8)
    CALL EXIT
    END
```

```
      FUNCTION SIGMA(X)
      DIMENSION A(10)
      COMMONA
      U=1.-X**2
      UK=U
      SIGMA> A(1)*U
      DO 1000 K=2,10
      UK=UK*U
      Z=K
 1000 SIGMA>SIGMA < A(K)*UK/Z
      RETURN
      END
C   PROGRAM TO CALCULATE A FLUX SELECTOR OF THE TYPE 2-C2-H
C   PART 1  SCANNING PROGRAM  L.P. BOIVIN  7/10/65
C   PRELIMINARY  PROGRAM  (N MAX. = 100 )
      DIMENSION A(10),XP(100)
      COMMON A
      READ1,N,M,ALO,R,A
    1 FORMAT(2I2,2F10.7/(5E16.8))
      EPS=.00001
      MP=N-2
      Q=N
      PRINT2,N
    2 FORMAT(5H  N=  I3)
      DO 100 J=1,M
      PJ=J
      AL=ALO+PJ*R
      XP(1)=1./Q**AL
      W=(SIGMA(0.0)-SIGMA(XP(1)))/XP(1)
      DO 50 I=1,MP
      DPI=W*XP(I)-SIGMA(XP(I))
      IF(DPI)  9,14,14
    9 XP(I+1)=XP(I)
      DEL=.1*W*EXPF(2.635*XP(I)**2)
   21 B=DPI+W*XP(I+1)+SIGMA(XP(I+1))
   20 XP(I+1)=XP(I+1)+DEL
      BP=DPI + W*XP(I+1) + SIGMA(XP(I+1))
      IF(ABSF(BP)-EPS)  50,50,180
  180 V=B*BP
      IF(V) 17,50,18
   18 IF(DPI+W*XP(I+1)) 19,14,14
   19 IF(XP(I+1)-1.) 21,14,14
   17 XP(I+1)=XP(I+1)-DEL
      DEL=.1*DEL
      GO TO 20
   14 L=I+1
      PRINT 15,AL,W,L
   15 FORMAT(6H  AL= F10.7, 4H W=  E16.8,16H NO SOLUTION I=  I3)
      GO TO 100
   50 CONTINUE
   51 WN=(SIGMA(XP(N-1))-SIGMA(1.))/(1.+XP(N-1))
      XP(N)=1.
      PERD=(W-WN)/W
      PRINT 52, AL,W,WN,PERD,(XP(I),I=1,N)
   52 FORMAT(6H  AL= F10.7,4H W= E16.8,5H WN= E16.8,6H PERD=E16.8/
     18H  XP(I)=/(1H 5E16.8)//)
  100 CONTINUE
      CALL EXIT
      END
```

```
C     PROGRAM TO CALCULATE A FLUX SELECTOR OF THE TYPE 2-C2-H
C     PART 2   CONVERGING   PROGRAM   L.P. BOIVIN   10/1/66
      DIMENSION XP(101),AL(16),R(100),RP(100),DIF(15),U(16),V(16)
      N=10
      EPS=.00000001
      NP=N-2
      Q=N
      AL(1)=1.2379
      AL(2)=1.23873
      PRINT 1,N
    1 FORMAT(5H N=  I3 ///)
      DO 2  J=1,15
      NUM=J
      XP(1)=1./Q**AL(J)
      ALPHA=AL(J)
      S=TORRAC(XP(1))-TORRAC(0.0)
      T=SIGMAC(0.0)-SIGMAC(XP(1))
      RP(1)=SQRTF(2.*S/T)
      R(1)=0.0
      W=RP(1)
      C=S/T**2
      DO 3 I=1,MP
      IF(I-1)  4,4,5
    4 DEL=XP(1)/10.
      GO TO 6
    5 DEL=(XP(I)-XP(I-1))/10.
    6 XP(I+1)=XP(I)+DEL
      X1=XP(I)
      W1=0.0
      X2=XP(I+1)
    9 S=TORRAC(XP(I+1))-TORRAC(XP(I))
      T=SIGMAC(XP(I))-SIGMAC(XP(I+1))
      S=S/T
      T=C*T
      R(I+1)=(S-T)**.5
      RP(I+1)=(S+T)**.5
      W2=RP(I+1)-R(I+1)
      IF(W2-W) 7,3,8
    7 XP(I+1)=XP(I+1)+DEL
      IF(XP(I+1)-1.) 11,11,12
   11 W1=W2
      X1=X2
      X2=XP(I+1)
      GO TO 9
   12 PRINT 24,I,AL(J),W
   24 FORMAT(//17H NO SOLUTION  I= I3,8H ALPHA= F15.8,4H W= F15.8  //)
       GO TO 50
    8 U(1)=X1
      U(2)=X2
      V(1)=W1-W
      V(2)=W2-W
      DO 16 L=2,15
      U(L+1)=(U(L-1)*V(L)-U(L)*V(L-1))/(V(L)-V(L-1))
      XP(I+1)=U(L+1)
      S=TORRAC(XP(I+1))-TORRAC(XP(I))
      T=SIGMAC(XP(I))-SIGMAC(XP(I+1))
      S=S/T
      T=C*T
      R(I+1)=(S-T)**.5
```

```
      RP(I+1)=(S+T)**.5
      V(L+1)=RP(I+1)-R(I+1)-W
      IF(ABSF(V(L+1))-EPS)  3,3,16
   16 CONTINUE
    3 CONTINUE
      XP(N)=1.
      S=TORRAC(XP(N))-TORRAC(XP(N-1))
      T=SIGMAC(XP(N-1))-SIGMAC(XP(N))
      S=S/T
      T=C*T
      R(N)=(S-T)**.5
      RP(N)=(S+T)**.5
      WN=RP(N)-R(N)
      DIF(J)=WN-W
      PRINT 30,AL(J),DIF(J)
   30 FORMAT(5H AL= F20.10,6H DIF= F20.10)
      IF(ABSF(DIF(J))-EPS)  20,20,21
   21 IF(J-1)  2,2,23
   23 AL(J+1)=(AL(J-1)*DIF(J)-AL(J)*DIF(J-1))/(DIF(J)-DIF(J-1))
    2 CONTINUE
   20 PRINT 27 ,NUM
   27 FORMAT(//29H NUMBER OF ITER. FOR ALPHA = I2 //)
      PRINT 28
   28 FORMAT(///12H SOLUTION IS ///)
      PRINT 29,ALPHA,W,(XP(I),I=1,N)
   29 FORMAT(8H ALPHA= F15.8,4H W= F15.8//8H XP(I)= /(5F24.8)///)
      HOF=1./RP(N)
      DO 25 K=1,N
      R(K)=R(K)*HOF
      RP(K)=RP(K)*HOF
      DELRN=RP(K)-R(K)
   25 PRINT 26,K,R(K),RP(K),DELRN
   26 FORMAT(4H I= I3,4H R= F10.8,14H           RP= F10.8,
     117H           DELRN= F10.8 //)
   50 CALL EXIT
      END
```

```
C   PROGRAM TO CALCULATE A FLUX SELECTOR OF THE TYPE 2-PX2-H
C   PART 1  SCANNING PROGRAM  L.P. BOIVIN  13/12/65
      DIMENSION ALPHA(10),R(10),RP(10),XP(10),THE(10),M(10)
      DIMENSION U(20),TE(20),W(6),A(10)
      N=10
      READ 1,(ALPHA(I),I=2,N)
    1 FORMAT(5F16.8)
      L = 8
      WO=34.
      XP(N)=1.
      DEL=1.
      BETA=3.8317060
      EPS=.00000001
      DO 500 I=1,L
       P=I-1
      W(I)=WO+DEL*P
      PRINT 2,W(I)
    2 FORMAT(4H W=  F5.1   //)
      R(1)=0.0
      RP(1)=BETA/W(I)
      XP(1)=RP(1)
      DO 505 K=1,20
      M(1)=K
      U(K)=XP(1)
      Q=TORRAC(XP(1))-TORRAC(0.0)
      S=SIGMAC(0.0)-SIGMAC(XP(1))
      B=RP(1)**2-2.*Q/S
      TE(K)=B
      IF(ABSF(B)-EPS)  506,506,507
  507 IF(K-1) 508,508,509
  508 P=N
      XP(1)=RP(1)*(1.+.1/P**2)
      GO TO 505
  509 XP(1)=(TE(K)*U(K-1)-TE(K-1)*U(K))/(TE(K)-TE(K-1))
  505 CONTINUE
  506 PRINT 510,M(1),B
  510 FORMAT(16H NO. OF ITER. = I2, 4H B= F20.10  //)
      C=Q/S**2
      KP=N-1
      DO 300 J=2,KP
      XP(J)=2.*ALPHA(J)/W(I) -XP(J-1)
      DO 330 K=1,20
      M(J)=K
      U(K)=XP(J)
      Q=TORRAC(XP(J))-TORRAC(XP(J-1))
      S=SIGMAC(XP(J-1))-SIGMAC(XP(J))
      Q=Q/S
      S=C*S
      IF(Q-S)   700,701,701
  700 PRINT 702 ,J, K, XP(J),XP(J-1)
  702 FORMAT(  ///25H NO SOLUTION R**2 -VE J= I4,4H K= I4,8H XP(J)=
     1F23.8,8H X(J)=  F23.8 ///)
      GO TO 500
  701 R(J)=(Q-S)**.5
      RP(J)=(Q+S)**.5
      TES=W(I)*RP(J)
      IF(TES-20.)  197,197,198
  197 QQ=RP(J)*BESSEC(1,TES)
      GO TO 600
```

```
198 QQ=RP(J)*BESIAC(TES)
600 TES=W(I)*R(J)
    IF(TES-20.)  601,601,602
601 VV=R(J)*BESSEC(1,TES)
    GO TO 603
602 VV=R(J)*BESIAC(TES)
603 THE(J)=QQ-VV
    TE(K)=THE(J)
199 IF(ABSF(THE(J))-EPS)  300,300,302
302 IF(K-1)  331,331,332
331 XP(J)=XP(J)*EXPF(THE(J))
    GO TO 330
332 XP(J)=(TE(K)*U(K-1)-TE(K-1)*U(K))/(TE(K)-TE(K-1))
330 CONTINUE
300 CONTINUE
    Q=TORRAC(XP(N))-TORRAC(XP(N-1))
    S=SIGMAC(XP(N-1))-SIGMAC(XP(N))
    Q=Q/S
    S=C*S
    R(N)=(Q-S)**.5
    RP(N)=(Q+S)**.5
    TES=W(I)*RP(N)
    IF(TES-20.)  350,350,351
350 QQ=RP(N)*BESSEC(1,TES)
    GO TO 605
351 QQ=RP(N)*BESIAC(TES)
605 TES=W(I)*R(N)
    IF(TES-20.) 606,606,607
606 VV=R(N)*BESSEC(1,TES)
    GO TO 608
607 VV=R(N)*BESIAC(TES)
608 THEN=QQ-VV
352 PRINT 401 ,(M(J),J=2,KP)
401 FORMAT(/// 15H NO. OF ITER. = / 10I5 ///)
    PRINT 400,(XP(J),J=1,N),(R(J),J=1,N),(RP(J),J=1,N),(THE(J),J=2,KP)
   1 ,THEN
400 FORMAT(8H XP(I)= //2(1H 5F23.8/)//8H R(I)=  //2(1H 5F23.8/)//
   18H RP(I)= //2(1H 5F23.8/)//10H THETA(I)=  //2(1H 4F23.15/)//
   210H THETAN = F24.15//)
500 CONTINUE
    CALL EXIT
    END
```

```
C   PROGRAM TO CALCULATE A FLUX SELECTOR OF THE TYPE 2-PX2-H
C   PART 2  CONVERGING PROGRAM   L.P. BOIVIN   13/12/65
      DIMENSION U(20),TE(20),A(10),THEN(6),W(7)
      DIMENSION R(10),RP(10),XP(10),THE(10),M(10)
      N=10
      BETA=3.8317060
      W(1)=40.220
      W(2)=40.225
      READ 14,(XP(I),I=2,N)
   14 FORMAT(5F10.8)
      EPS=.00000001
      DO 500 I=1,6
      PRINT 2,W(I)
      R(1)=0.0
      RP(1)=BETA/W(I)
      XP(1)=RP(1)
      DO 505 K=1,20
      M(1)=K
      U(K)=XP(1)
      Q=TORRAC(XP(1))-TORRAC(0.0)
      S=SIGMAC(0.0)-SIGMAC(XP(1))
      B=RP(1)**2-2.*Q/S
      TE(K)=B
      IF(ABSF(B)-EPS)  506,506,507
  507 IF(K-1) 508,508,509
  508 P=N
      XP(1)=RP(1)*(1.+.1/P**2)
      GO TO 505
  509 XP(1)=(TE(K)*U(K-1)-TE(K-1)*U(K))/(TE(K)-TE(K-1))
  505 CONTINUE
  506 PRINT 510,M(1),B
  510 FORMAT(16H NO. OF ITER. = I2, 4H B= F20.10  //)
      C=Q/S**2
      KP=N-1
      DO 300 J=2,KP
      DO 330 K=1,20
      M(J)=K
      U(K)=XP(J)
      Q=TORRAC(XP(J))-TORRAC(XP(J-1))
      S=SIGMAC(XP(J-1))-SIGMAC(XP(J))
      Q=Q/S
      S=C*S
      R(J)=(Q-S)**.5
      RP(J)=(Q+S)**.5
      TES=W(I)*RP(J)
      IF(TES-20.)  197,197,198
  197 QQ=RP(J)*BESSEC(1,TES)
      GO TO 888
  198 QQ=RP(J)*BESIAC(TES)
  888 TES=W(I)*R(J)
      IF(TES-20.) 890,890,891
  890 VV=R(J)*BESSEC(1,TES)
      GO TO 199
  891 VV=R(J)*BESIAC(TES)
  199 THE(J)=QQ-VV
      TE(K)=THE(J)
      IF(ABSF(THE(J))-EPS)   300,300,302
  302 IF(K-1)   331,331,332
  331 XP(J)=XP(J)*EXPF(THE(J))
```

```
      GO TO 330
  332 XP(J)=(TE(K)*U(K-1)-TE(K-1)*U(K))/(TE(K)-TE(K-1))
  330 CONTINUE
  300 CONTINUE
      Q=TORRAC(XP(N))-TORRAC(XP(N-1))
      S=SIGMAC(XP(N-1))-SIGMAC(XP(N))
      Q=Q/S
      S=C*S
      R(N)=(Q-S)**.5
      RP(N)=(Q+S)**.5
      TES=W(I)*RP(N)
      IF(TES-20.)  350,350,351
  350 QQ=RP(N)*BESSEC(1,TES)
      GO TO 892
  351 QQ=RP(N)*BESIAC(TES)
  892 TES=W(I)*R(N)
      IF(TES-20.) 893,893,894
  893 VV=R(N)*BESSEC(1,TES)
      GO TO 352
  894 VV=R(N)*BESIAC(TES)
  352 THEN(I)=QQ-VV
      THE(N)=THEN(I)
      PRINT 401 ,(M(J),J=2,KP)
  401 FORMAT(/// 15H NO. OF  ITER. = / 10I5 ///)
      PRINT 400,(THE(J),J=2,KP),THEN(I)
  400 FORMAT(10H THETA(I)= //1H 4F23.15/1H 4F23.15//10H THETAN = F24.15
     1///)
      WFIN=W(I)
      IF(ABSF(THEN(I))-EPS)  380,380,381
  381 IF(I-2)  370,372,372
  370 GO TO 500
  372 W(I+1)=(THEN(I)*W(I-1)-THEN(I-1)*W(I))/(THEN(I)-THEN(I-1))
  500 CONTINUE
  380 THE(1)=0.0
      PRINT 389
  389 FORMAT(//12H SOLUTION IS  //)
      PRINT 390,WFIN,(XP(J),J=1,N),(R(J),RP(J),THE(J),J=1,N)
  390 FORMAT(////4H W= F14.8//7H XP(I)= /2(1H 5F23.8/)//(4H R= F23.8,
     1 10H     RP=  F23.8,12H      THETA=    F23.15))
      PUNCH 391 , ( R(I),RP(I) ,I=1,N)
  391 FORMAT(4F12.8)
    2 FORMAT(4H W=  F20.8  //)
      CALL EXIT
      END
```

```
C   PROGRAM TO CALCULATE THE POSITIONS AND VALUES OF THE EXTREMA OF
C   AMPLITUDE IN A DIFFRACTION PATTERN.INPUT DATA= AMPLITUDE IN DIFF
C   PATTERN AT W=.5 INTERVALS . USES PARABOLIC INTERPOLATION L.P. BOIVIN
C   24/6/69
      DOUBLE PRECISION A(650),W(650),AE(150),WE(150),PA,PB,PC,DEL1,DEL2
      M=650
    1 READ(1,2)
      READ(1,3) (W(I),A(I),I=1,650)
    2 FORMAT(  '                                        ')
    3 FORMAT(5(F8.1,F8.5))
      WRITE(2,4)
      WRITE(2,2)
      WRITE(3,5)
      WRITE(3,2)
      K=1
      M=M-1
      DO 12 I=2,M
      DEL1= A(I) - A(I-1)
      DEL2= A(I+1) - A(I)
      T=DEL1*DEL2
      IF(T) 11,15,12
   15 IF(DEL1) 11,12,11
   11 K=K+1
      PA= 2.0DO*(DEL2 - DEL1)
      PB= 2.0DO*(A(I)-A(I-1)) - 2.0DO*(DEL2-DEL1)*(W(I)+W(I-1))
      WE(K-1)= -.5DO*PB/PA
      PC=A(I) - PA*W(I)*W(I) - PB*W(I)
      AE(K-1)= PA*WE(K-1)*WE(K-1) +PB*WE(K-1) + PC
   12 CONTINUE
      NN=K-1
      WRITE(2,13) (I,WE(I),AE(I),I=1,NN)
   13 FORMAT(4(I4,F8.3,F8.5))
      WRITE(3,14) (I,WE(I),AE(I),I=1,NN)
   14 FORMAT(//' N= ' I4,10X,' W EXT. = ' F8.3,10X,' A EXT. = 'F8.5)
    4 FORMAT(////)
    5 FORMAT('1       ')
      GO TO 1
  100 STOP
      END
```

```
C  RAY TRACING OF LIGHT RAYS INCIDENT  ON A GLASS CONE(AXICON) AT
C  VARIOUS ANGLES AND ORIGINATING  FROM A POINT SOURCE LOCATED AT
C  VARIOUS POSITIONS ON THE AXIS OF THE AXICON  PARAMETERS ARE APEX
C  ANGLE  AND DIAMETER OF AXICON, AND DISTANCE OF POINT SOURCE FROM THE
C  AXICON      L.P. BOIVIN   9/11/65
      DIMENSION R(11),THE(11),AL(5),Z(4),X(11),Y(11),H(1)
      READ 1,AL,Z
    1 FORMAT(5F5.1/4F6.1)
      H(1)=4.
      REF=1.517
      DO 8 I=1,5
      PRINT 3,AL(I)
    3 FORMAT(//// 8H ALPHA= F5.1   5H DEG. ////)
      PUNCH 31,AL(I)
   31 FORMAT(8H ALPHA=   F5.1 5H DEG. )
      AL(I)=AL(I)/57.2958
      DO 8 J=1,1
      PRINT 5,H(J)
    5 FORMAT(///5H  H= F10.6 4H CM. ///)
      DO 8 K=1,4
      PRINT 7,Z(K)
    7 FORMAT(//  6H   Z= F6.1 4H CM.  //)
      PUNCH 71,Z(K)
   71 FORMAT(6H   Z= F6.1 4H CM. )
      DEL=(ATANF(H(J)/Z(K)))/10.
      DO  12  N=1,11
      P=N-1
      THE(N)=P*DEL
      SI=SINF(THE(N))
      D=SINF(AL(I))
      E=COSF(AL(I))
      SI2=D*SQRTF(1.-(SI/REF)**2)-E*SI/REF
   10 A=Z(K)*SI/COSF(THE(N))
      B=H(J)-A
      COTA=E/D
      C=SI/SQRTF(REF**2-SI**2)
      X(N)=B/(COTA+C)
      IF(THE(N))  14,15,14
   15 Y(N)=0.0
      GO TO 16
   14 Y(N)=A+B/(1.+COTA/C)
   16 TAN3=REF*SI2/SQRTF(1.-(REF*SI2)**2)
      TANA=1./COTA
      TA3MA=(TAN3-TANA)/(1.+TAN3*TANA)
      R(N)=Y(N)+(Z(K)+X(N))*TA3MA
      PUNCH 91,X(N),Y(N),R(N)
   91 FORMAT(3F12.8)
      THETA=THE(N)*57.2958
   12 PRINT9,THETA,X(N),Y(N),R(N)
    8 CONTINUE
    9 FORMAT(11H    THETA= F12.8 5H DEG.,7H     X= F12.8,7H     Y= F12.8,
     17H    R= F12.8)
      CALL EXIT
      END
```

```
C     PROGRAM TO DETERMINE FOCAL POSITION OF VIRTUAL RING PRODUCED
C     BY AXICON, AND FOCAL DISPERSION , GIVEN RAY TRACING DATA , AND
C     APPROXIMATE FOCAL POSITION  L.P. BOIVIN    16/11/65
      DIMENSION  Y(20),AL(9),Z(9,1),N(9,1),UO(9,1),DEL(9,1),XI(9,1,11),
     1YI(9,1,11),R(9,1,11)
      READ 1,AL
    1 FORMAT(9F5.1)
      READ 2,((Z(I,J),UO(I,J),DEL(I,J),J=1,1),I=1,9)
    2 FORMAT(3F10.4)
       READ 3,N
    3 FORMAT(9I4)
      DO 7 I=1,9
      DO 7 J=1,1
      MM=N(I,J)
      DO 7 K=1,MM
    7 READ 4,XI(I,J,K),YI(I,J,K),R(I,J,K)
    4 FORMAT(3F12.8)
      DO 69 I=1,9
      PRINT 5,AL(I)
    5 FORMAT(///8H ALPHA=    F5.1 5H DEG.///)
      DO 69 J=1,1
      PRINT 6,Z(I,J)
    6 FORMAT(//6H    Z= F10.1//)
      DO 69 M=1,12
      IF(M-11)61,61,62
   62 PRINT 63
   63 FORMAT(//12H CHECK POINT  //)
      U=0.0
      GO TO 65
   61 P=M-1
      U=UO(I,J)
      U=U+P*DEL(I,J)
   65 NN=N(I,J)
      DO 30 K=1,NN
   30 Y(K)=YI(I,J,K)+((YI(I,J,K)-R(I,J,K))/(Z(I,J)+XI(I,J,K)))*(U-
     1 (Z(I,J)+XI(I,J,K)))
      BIGY=Y(1)
      DO 32 K=2,NN
      IF(BIGY-Y(K))  34,32,32
   34 BIGY=Y(K)
   32 CONTINUE
      DIMENSION TEMP(11)
      DO 100   K=1,NN
  100 TEMP(K)=50.-Y(K)
      BIGT=TEMP(1)
      DO 320   K=2,NN
      IF(BIGT-TEMP(K))  340,320,320
  340 BIGT=TEMP(K)
  320 CONTINUE
      SMALY=50.-BIGT
      CENT=(SMALY+BIGY)/2.
      DISP=BIGY-SMALY
      DISP=DISP*10.
      IF(M-11)  66,66,67
   66 PRINT20,U,CENT,DISP
   20 FORMAT(8H      U= F10.4 4H CM.,17H    MEAN RADIUS = F12.8 4H CM.,
     115H   DISPERSION= F12.8 4H MM.)
      GO TO 69
   67 PRINT 68,U,BIGY,SMALY
```

```
68 FORMAT(8H      U= F12.8 4H CM./13H      BIG R =   F12.8 4H CM. ,
  116H      SMALL R =  F12.8 4H CM.  //)
69 CONTINUE
   CALL  EXIT
   END
```

```
C   PROGRAM TO CALCULATE DIFFRACTION PATTERN ASSOCIATED WITH A FLUX
C   SELECTOR IN WHICH ONE OR MORE OPAQUE RINGS HAVE BEEN DELETED(= MADE
C   TRANSPARENT) USES AS INPUT DATA TRANSMISSION FACTOR , RING RADII,
C   AND DIFFRACTION PATTERN OF ORIGINAL FLUX SELECTOR    L.P. BOIVIN
C   19/11/66
      DOUBLE PRECISION RO(15),RPO(15),W(800),GAMO(800),T,TP,BES,X,U,QQ,
     1FI,PHI,DSIN,VV,D,SUM,DSQRT
      DIMENSION GAMD(800),DIF(800)
      L>650
      KI>9
      KK>9
      READ(1,1)
    1 FORMAT(:
     1              :)
      READ(1,10)T
   10 FORMAT(F12.8)
      READ(1,2) (W(I),GAMO(I),I=1,L)
    2 FORMAT(5(F8.1,F8.5))
      READ(1,3) (RO(I),RPO(I),I>1,KK)
    3 FORMAT(4F12.8)
      DO 23  K>KI,KK
      ND>K
      TP=T
      DO 4 I=1,ND
    4 TP=TP+RPO(I)*RPO(I)-RO(I)*RO(I)
      D=T/TP
      DO 5 I=1,L
      SUM=0.0D0
      DO 6 J=1,ND
      X=W(I)*RPO(J)
      IF(X-3.0D0) 880,880,881
  880 U=(X/3.0D0)*(X/3.0D0)
      BES=((((((U*.00001109-.00031761)*U+.00443319)*U-.03954289)*U+
     1.21093573)*U-.56249985)*U+.5D0)*X
      QQ=RPO(J)*BES
      GO TO 882
  881 U=3.0D0/X
      FI=(((((-.00020033*U+.00113653)*U-.00249511)*U+.00017105)*U+
     1.01659667)*U+.00000156)*U+.79788456
      PHI=(((((.00029166*U-.00079824)*U-.00074348)*U+.00637879)*U-
     1 .00005650)*U-.12499612)*U+.78539816
      BES=FI*DSIN(X-PHI)/DSQRT(X)
      QQ=RPO(J)*BES
  882 X>W(I)*RO(J)
      IF(X-3.0D0) 883,883,884
  883 U>(X/3.0D0)*(X/3.0D0)
      BES=((((((U*.00001109-.00031761)*U+.00443319)*U-.03954289)*U+
     1.21093573)*U-.56249985)*U+.5D0)*X
      VV>RO(J)*BES
      GO TO 6
  884 U>3.0D0/X
      FI=(((((-.00020033*U+.00113653)*U-.00249511)*U+.00017105)*U+
     1.01659667)*U+.00000156)*U+.79788456
      PHI=(((((.00029166*U-.00079824)*U-.00074348)*U+.00637879)*U-
     1 .00005650)*U-.12499612)*U+.78539816
      BES>FI*DSIN(X-PHI)/DSQRT(X)
      VV>RO(J)*BES
    6 SUM>SUM<QQ-VV
    5 GAMD(I)>D*GAMO(I)<2.0D0*SUM/(W(I)*TP)
```

```
      WRITE(3,11)
   11 FORMAT(:1DIFFRACTION PATTERN FOR: ://)
      WRITE(3,1)
      WRITE(3,12) ND
   12 FORMAT(: IN WHICH THE :,I2,: FIRST OPAQUE RINGS HAVE BEEN DELETED:
     1 ///)
      WRITE(3,13) (W(I),GAMD(I),I>1,L)
   13 FORMAT(: W(I)> :,F8.1,10X,:GAM(I)> :,F8.5)
      WRITE(2,1)
      WRITE(2,7) (W(I),GAMD(I),I>1,L)
    7 FORMAT(5(F8.1,F8.5))
      WRITE(3,21)
   21 FORMAT(42H1DIFFERENCES DIF(I)= /GAMO(I)/ - /GAMD(I)/    ////)
      DO 20 I=1,L
      DIF(I)>DABS(GAMO(I))-ABS(GAMD(I))
   20 WRITE(3,22) W(I),DIF(I)
   22 FORMAT(7H W(I)=  F7.2,10X,8HDIF(I)= F9.6  //)
   23 CONTINUE
      STOP
      END
```

ERRATA

(1) page 2 : the 19^{th} line from the top should read "... in this thesis to complete Lansraux's work..."

(2) page 37 ; the 6^{th} line from the top should read:

$$"\ldots \left[\frac{1}{x}\frac{d}{dx}\right]^k J_o(x) = (-1)^k \frac{J_k(x)}{x^k} \ldots"$$

(3) page 37 ; in equation A4-8b, the constant C has been placed in front of the second term instead of the first term,as it should have according to A4-8a. However,C being an undetermined constant, the change of position is equivalent to a redefinition of C (i.e., C is re-defined as its reciprocal), and,hence,in no way affects the results.

(4) page 40 ; the 5^{th} line from the top should read "... to multiply the integrand ..."

(5) page 46 ; in the 12^{th} line from the top, we should have "... $M = 1/\sum k_p$ ..."

(6) page 86 ; the fourth line should read "...image to lift off..."